Modelling the Dynamics of Mass Capture

by

Timothy John Lahey

A thesis
presented to the University of Waterloo
in fulfillment of the
thesis requirement for the degree of
Doctor of Philosophy
in
Systems Design Engineering

Waterloo, Ontario, Canada, 2013

I hereby declare that I am the sole author of this thesis. This is a true copy of the thesis, including any required final revisions, as accepted by my examiners.

I understand that my thesis may be made electronically available to the public.

Abstract

This thesis presents an approach to modelling dynamic mass capture which is applied to a number of system models. The models range from a simple 2D Euler-Bernoulli beam with point masses for the end-effector and target to a 3D Timoshenko beam model (including torsion) with rigid bodies for the end-effector and target. In addition, new models for torsion, as well as software to derive the finite element equations from first principles were developed to support the modelling. Results of the models are compared to a simple experiment as done by Ben Rhody. Investigations of offset capture are done by simulation to show why one would consider using a 3D model that includes torsion.

These problems have relevance to both terrestrial robots and to space based robotic systems such as the manipulators on the International Space Station capturing payloads such as the SpaceX Dragon capsule. One could increase production in an industrial environment if industrial robots could pick up items without having to establish a zero relative velocity between the end effector and the item. To have a robot acquire its payload in this way would introduce system dynamics that could lead to the necessity of modelling a previously 'rigid' robot as flexible.

Acknowledgements

First and foremost, I'd like to thank my supervisor Glenn Heppler who provided valuable advice and assistance throughout this process. I'd also like to thank Wayne Brodland for his guidance on several occasions. Lastly, I'd like to thank Kristine Meier without whom I'd likely never have finished this thesis.

Contents

List of Tables

List of Figures

CHAPTER

1 Introduction

This thesis details a project to model the dynamics of mass capture by a robotic link. Contained in this thesis is an overview of previous related work and a discussion of the theory and implementation various models of mass capture. In particular, this thesis contains models where the end effector and target are modelled as a particle mass as well as models where they are modelled as rigid bodies. The robot is modelled as a single flexible link driven by a motor at its base (see Figure 1.1). The flexible link is modelled alternatively by a 2D Euler-Bernoulli beam, a 2D Timoshenko beam, and a 3D Timoshenko beam (including torsion). The simplified model of a particle mass target/end-effector (and a 2D Euler-Bernoulli beam) is consistent with the model analysed by Kövecses *et al.* [3, 4] and the models from this thesis are compared with their simplified model.

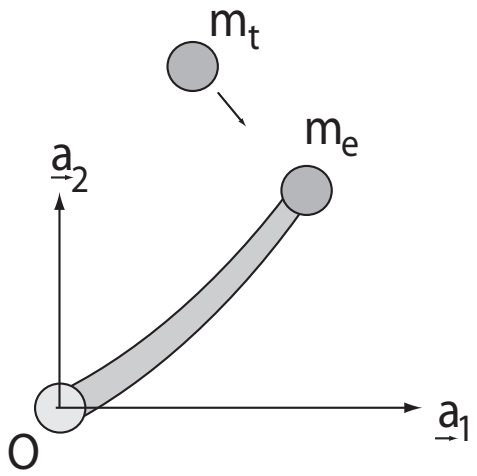

Figure 1.1: Simplified Model of Mass Capture

1.1 Previous Work

The problem of having a flexible robot linkage acquire a moving payload, shall be referred to as "dynamic mass capture", and can be broken down into several sub-classes as follows.
Class I: a stationary linkage with a payload attached subjected to a non-plastic impact;
Class II: a stationary linkage with an end effector that captures a moving mass particle (plastic impact);
Class III: a moving linkage with an end effector that captures a moving mass particle (known trajectories);
Class IV: a stationary linkage with an end effector that captures a translating rigid body (plastic impact);
Class V: a moving linkage with an end effector that captures a translating rigid body (plastic impact);
Class VI: a stationary linkage with an end effector that captures a translating and spinning rigid body (plastic impact);
Class VII: a moving linkage with an end effector that captures a translating and spinning rigid body (plastic impact);
Class VIII: the capture of a translating and spinning rigid body which has moving internal parts (*e.g.*, momentum wheels).

These problems have relevance to both terrestrial robots and to space based robotic systems such as the manipulators on the International Space Station. While the space applications are relatively high profile the terrestrial applications have significant economic implications. If industrial robots could pick up items without having to establish a zero relative velocity between the end effector and the item, cycle time could be reduced. To have a robot acquire its payload in this way would introduce system dynamics that could lead to the necessity of modelling a previously 'rigid' robot as flexible.

The flexibility in robotic members has long been a topic of interest and the problem that is the focus of this thesis has received attention [5]–[6]. It has most frequently been modelled by using Bernoulli-Euler beam theory [7], but the Timoshenko beam theory has better modelling fidelity in vibrations problems, especially for the higher modes [8].

To model the various cases of dynamic mass capture the impact dynamics of flexible beams must be examined. Many dynamicists have investigated the flexible beam impact problem for simply supported beams impacted in the centre [9, 10], but the proposed research requires that the tip impact of a chain of flexible beams, connected by flexible joints which also have friction and inertia must be studied. There has been work on the transverse elastic impact at the tip of a two link rigid-flexible configuration [11], on the axial impact of a single link [12, 13, 14], on the elastic impact on general rigid multibody systems [15, 16], on

the transverse elastic impact of single links [17, 18], and on the transverse plastic impact of single links [19]. None of the cited references consider structural damping or anything but ideal frictionless joints. Additional work related directly to spacecraft has also been reported [5, 20, 6].

Chapnik *et al.* [21, 22] examined the impact of a sphere and a rotating flexible beam with a tip mass, where the impact occurs at the tip mass (Class I). Of all the sphere-beam impact research, these papers are closest to the work done in this thesis.

To date, there has been little work specifically on the dynamics of mass capture for classes II and III. Rhody [1] has done some work on the dynamics and control of class II problems using a modal analysis approach and modelling the capture as a instantaneous impulsive force. A series of papers done by Kövecses, Fenton, and Cleghorn [23, 24, 25, 3, 26, 27, 4] cover class II and class III problems. They consistently use Jourdain's Variational Principle [28] in the form Bahar [29] outlines for use in impulsive problems. Kövecses *et al.*'s initial papers [23, 24] focus on geometric performance metrics to illustrate the effect of the impact on a robotic manipulator. Their next paper [25] presented the basic form of the dynamic equations before and after capture as well as presenting a set of equations to relate the two systems. In 1998, they presented a paper [3] that illustrates some of the details of constructing the set of equations relating the pre- and post-capture systems for a single flexible link with a tip mass. As mentioned earlier, this is the same system that is analysed in this thesis. They also present simulation studies for their method for this case in a later paper [26] in addition to a two-link flexible manipulator. Their paper [27] extends their earlier work on performance metrics using results from their later papers. In 2003, Kövecses and Cleghorn [4] published a new paper which created a larger framework for their analysis which allowed them to get the constraint impulses due to the capture process.

Note that while one might use a system identification approach to tackle this problem for an existing system, that lacks the flexibility of an analytical approach which allows one to predict the effect of different changes. This is useful in the design of the system (*e.g.*, a motor controller) and in testing different capture scenarios.

1.2 Layout of this document

Chapter 2 discusses the modelling of torsion in the beam, including a new model that uses fewer assumptions than existing models. Chapter 3 presents the work, kinetic and potential energy of the system for different models of the beam, target and end-effector. Chapter 4 presents a new mixed symbolic-numeric method to derive and solve equations of motion. Chapter 5 develops the theory and relations that link the pre-capture and post-capture systems. Chapter 6 discusses the method used to determine the system damping matrix.

Chapter 7 contains the discussion of the experimental apparatus, setup, and the experimental and simulation results. Lastly, Chapter 8 presents a summary of the results, conclusions and suggestions for future work.

CHAPTER

2 Beam Torsion Modelling

To completely model the dynamics of the beam, we need to take into account the fact that the beam can twist about its axis, which we refer to as torsion. For the purposes of the thesis, we will confine ourselves to beams of constant cross-section.

2.1 Overview

To justify the inclusion of torsion, let us look at the different possible ways torsion can arise for the beams studied herein. We will look at torsion due to an eccentric end-effector, eccentric target, or simply non-zero angular momentum. The first two are very similar and the eccentricity can arise from either an offset centre of mass or a non-principal inertia matrix.

Eccentric End-Effector

Consider a frame located with its origin at the end of the beam ($x = L$) on the neutral axis, and when the beam is undeformed is aligned with the origin frame $\mathcal{F}_b$. We will refer to this as frame C, and denote it as $\mathcal{F}_c$. The frame of reference located at the centre of mass of the end-effector is frame D, and is denoted as $\mathcal{F}_d$. These are shown in Figure 2.1. To determine the effect of the end-effector on the beam, we need to transform the inertia from about the end-effector centre of mass frame $\mathcal{F}_d$ to the beam-fixed frame $\mathcal{F}_c$. Note that no transformation of the momentum is needed since the velocity of end-effector in the beam-fixed frame is simply the velocity of the end of the beam. The vector from $\mathcal{F}_c$ to $\mathcal{F}_d$ we denote as

$$\underset{\sim}{r}_d = \underset{\sim}{\mathcal{F}}_c^T \begin{bmatrix} r_{dx} \\ r_{dy} \\ r_{dz} \end{bmatrix} \tag{2.1}$$

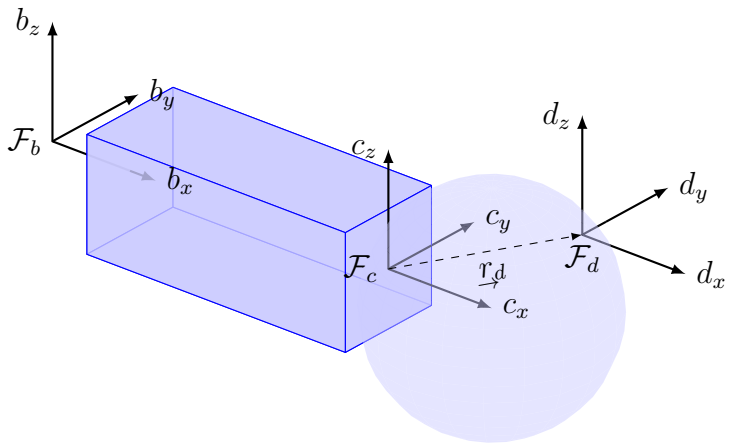

Figure 2.1: End-Effector Reference Frames

where $\underset{\rightarrow}{\mathcal{F}}_c$ is defined as,

$$\underset{\rightarrow}{\mathcal{F}}_c = \begin{bmatrix} \underset{\rightarrow}{c}_x \\ \underset{\rightarrow}{c}_y \\ \underset{\rightarrow}{c}_z \end{bmatrix} \tag{2.2}$$

The general parallel axis theorem [30] gives,

$$\mathbf{I}_c = \mathbf{I}_d + m_e \begin{bmatrix} (r_{dy}^2 + r_{dz}^2) & -r_{dx}r_{dy} & -r_{dx}r_{dz} \\ -r_{dx}r_{dy} & (r_{dx}^2 + r_{dz}^2) & -r_{dy}r_{dz} \\ -r_{dx}r_{dz} & -r_{dy}r_{dz} & (r_{dx}^2 + r_{dy}^2) \end{bmatrix} \tag{2.3}$$

where m_e is the mass of the end-effector, $\mathbf{I}_d$ is the inertia matrix about the centre of mass in $\mathcal{F}_d$. This assumes that $\mathcal{F}_c$ and $\mathcal{F}_d$ are not rotated with respect to each other. The case where they are is effectively the same as the eccentric capture case dealt with below.

Now that the inertia is known, it is straightforward to calculate the angular momentum.

$$\underset{\rightarrow}{h} = \mathbf{I}_c \, \underset{\rightarrow}{\omega}_e \tag{2.4}$$

where $\underset{\rightarrow}{h}$ is the angular momentum vector, and $\underset{\rightarrow}{\omega}_e$ is the angular velocity of the beam at $x = L$ (also the angular velocity of the end-effector),

$$\underset{\rightarrow}{\omega}_e = \underset{\rightarrow}{\mathcal{F}}_c^T \begin{bmatrix} \dot{\theta}_{xL} \\ \dot{\psi}_{yL} \\ \dot{\psi}_{zL} \end{bmatrix} \tag{2.5}$$

where $\dot{\theta}_{xL}$ is the rotation about the x-axis in the $\mathcal{F}_c$ frame, $\dot{\psi}_{yL}$ the rotation about the y-axis in $\mathcal{F}_c$, and $\dot{\psi}_{zL}$ the rotation about the z-axis in $\mathcal{F}_c$. Therefore, the $\mathcal{F}_c x$-coordinate angular

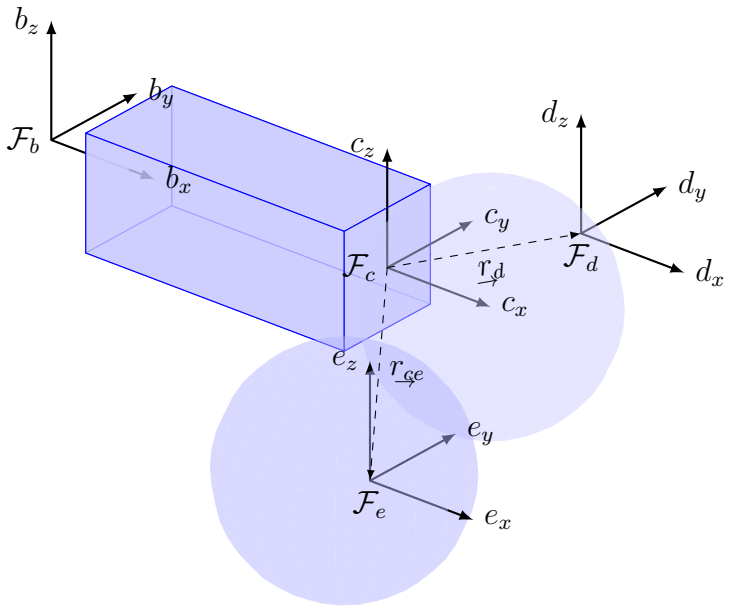

Figure 2.2: Post-Capture Target and End-Effector Reference Frames

momentum is,

$$h_{xL} = (I_{dxx} + m_e(r_{dy}^2 + r_{dz}^2))\dot{\theta}_{xL} - (I_{dxy} + r_{dx}r_{dy})\dot{\psi}_{yL} - (I_{dxz} + r_{dx}r_{dz})\dot{\psi}_{zL} \tag{2.6}$$

The centre of mass of the end-effector will be some distance past the end of the beam, so $r_{dx} \neq 0$. If the centre of mass is not on the neutral axis at least one of r_{dy} and r_{dz} will be non-zero. In that case, even if $\dot{\theta}_{xL} = 0$, there will be a non-zero torsional angular momentum. Alternatively, if the inertia of the end-effector about its centre of mass is non-principal (*i.e.*, I_{dxy} or $I_{dxz} \neq 0$) the centre of mass could be on the neutral axis and still create non-zero torsional angular momentum.

Eccentric Capture

In addition to the frames previously mentioned now we introduce an additional frame E, denoted as $\mathcal{F}_e$, located at the centre of mass of the target. Once captured, the target contributes its mass and inertia to the system so the same effects as the end-effector can be caused by the target in the post-capture case. This situation is shown in Figure 2.2. Transforming the target velocities from the target frame $\mathcal{F}_e$ to the beam fixed frame $\underrightarrow{\mathcal{F}}_c$, we use the vector from $\underrightarrow{\mathcal{F}}_c$ to $\underrightarrow{\mathcal{F}}_e$,

$$\underrightarrow{r}_{ce} = \underrightarrow{\mathcal{F}}_c^T \begin{bmatrix} r_{ex} \\ r_{ey} \\ r_{ez} \end{bmatrix} \tag{2.7}$$

As before, we have the general parallel axis theorem for the translation to $\underrightarrow{\mathscr{F}}_b$.

$$\mathbf{I}_{ct} = \mathbf{I}_e + m_t \begin{bmatrix} (r_{ey}^2 + r_{ez}^2) & -r_{ex}r_{ey} & -r_{ex}r_{ez} \\ -r_{ex}r_{ey} & (r_{ex}^2 + r_{ez}^2) & -r_{ey}r_{ez} \\ -r_{ex}r_{ez} & -r_{ey}r_{ez} & (r_{ex}^2 + r_{ey}^2) \end{bmatrix} \tag{2.8}$$

In general, the capture may have the two frames rotated with respect to one another. So, after the translation we need to perform a rotational transformation on the matrix [30],

$$\mathbf{I}_c = \mathbf{R}_{ce}\mathbf{I}_{et}\mathbf{R}_{ce}^T \tag{2.9}$$

where $\mathbf{R}_{ce}$ is the rotation matrix needed to rotate $\underrightarrow{\mathscr{F}}_e$ to $\underrightarrow{\mathscr{F}}_c$. This is dependent upon the orientation at capture, so in general the target's inertia matrix will be non-principal.

Since in the post-capture case, the target is part of the same rigid-body system as the end-effector, we can consider that the target's velocity at the end of the beam is the same as the end-effector, we have the same situation as Equation (2.6), just with the inertia as given in Equation (2.9). In this case, unless both the target and end-effector are specially designed, the target's centre of mass will be offset in at least one of the y or z directions. Therefore, even without rotation of the frames, there will be some torsional angular momentum due to the target's capture.

2.2 Traditional Torsion Models

Pure torsion models of beams can be broken into two kinds, uniform torsion where the beam in unrestrained,(where the same rate of twist occurs throughout the beam [31]) and non-uniform torsion where an end is restrained.

Uniform Torsion

For uniform torsion, the two most prevalent models are those of St. Venant [31] and Timoshenko [32, 33]. Timoshenko's model derives the equations of motion through differential forces and moments acting on a section of the beam. This approach isn't suitable for use with variational principles. Since both the capture equations and finite element models herein are derived using these, Timoshenko's model isn't useful for our purposes.

St. Venant's model is based on assuming the form of the displacements. Consider the cross-section shown in Figure 2.3. Let point P be located by a vector $\underrightarrow{r}_P$,

$$\underrightarrow{r}_P = \underrightarrow{\mathscr{F}}_a^T \begin{bmatrix} x \\ y \\ z \end{bmatrix} \tag{2.10}$$

and is moved to point P' due to a rotation of the cross-section through an angle θ. The vector to P', $\underset{\sim}{r}_{P'}$ is therefore,

$$\underset{\sim}{r}_{P'} = \underset{\sim}{\mathscr{F}}_a^T \begin{bmatrix} x \\ y+v \\ z+w \end{bmatrix} \tag{2.11}$$

The resulting displacement vector $\underset{\sim}{u}$ is,

$$\underset{\sim}{u} = \underset{\sim}{r}_{P'} - \underset{\sim}{r}_P = \underset{\sim}{\mathscr{F}}_a^T \begin{bmatrix} 0 \\ v \\ w \end{bmatrix} \tag{2.12}$$

Assuming the angle of rotation is small, we can write the displacements as

$$v = -\theta z \tag{2.13}$$
$$w = \theta y \tag{2.14}$$

For a beam of constant cross-section, we have $\theta = \alpha x$, where α is the angle of twist per unit length of the beam and x is the distance along the beam axis. We assume the displacements due to warping (*i.e.,* axial displacements) are of the form $u = \alpha\phi(y,z)$ where ϕ is a function of y and z and is called the *warping function.* This leads to the following formulas for the displacements of the beam.

$$u = \alpha\phi(y,z) \tag{2.15}$$
$$v = -\alpha xz \tag{2.16}$$
$$w = \alpha xy \tag{2.17}$$

St. Venant further assumes that all the normal stresses are zero. This combined with the displacement assumptions are used to derive the equations of motion/equilibrium. Complete details are described in Appendix A.1.

Non-Uniform Torsion

While there is an extension to Timoshenko's model for torsion that allows for non-uniform torsion [32], for our purposes it suffers from the same difficulty that the uniform model does. This also excludes the various coupled bending-torsion models that are based upon Timoshenko's torsion model [34, 35, 36, 37, 38, 39].

Reissner proposed models for non-uniform torsion [40] which are modifications to the uniform torsion St. Venant model (see [31]) in that he assumes the in-plane deflections are strictly due to rotation and he modifies how the warping is handled. In the first model, he

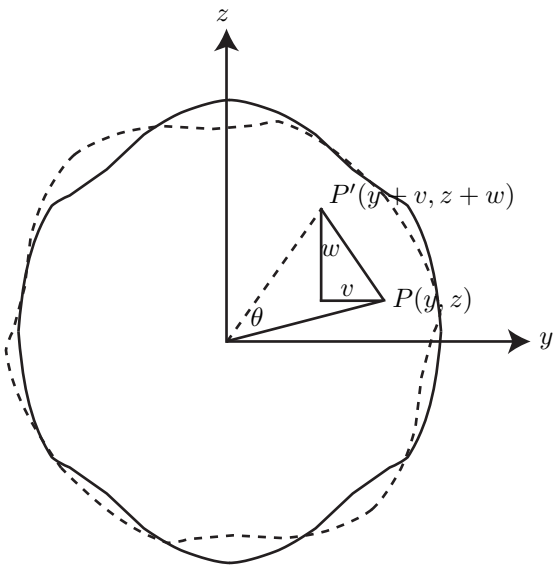

Figure 2.3: Arbitrary Cross-Section

assumes a form for the axial deflection. In the second model, he instead assumes a form for the axial stress. The axial stress form is mainly useful if one uses Reissner's Variational Principle which uses a variation with respect to stresses and strains, but poses some difficulties if one is to take variations with respect to other quantities.

Note that in both models, he assumes that the in-plane normal stresses (σ_{yy} and σ_{zz}) on a cross-section are zero which implicitly assumes that Poisson effects are negligible. In addition by assuming the in-plane deflections are strictly due to rotation the in-plane shear τ_{yz} is zero.

The notation used herein is slightly different from the notation in Reissner's paper mainly because while Reissner oriented the z axis along the length of the beam, here we align the x axis along the length.

While Reissner's original models were static, the model that assumes a form for the axial deflection was extended for dynamic problems by Barr [41] and later Ritchie and Leevers [42, 43]. For this reason, along with the problems of the axial stress form, we will consider the dynamic version of Reissner's axial deflection form.

In the dynamic version of Reissner's axial deflection form, we assume the deflection takes the form,

$$u(x,y,z,t) = \phi(y,z)\psi(x,t) \tag{2.18}$$

$$v(x,y,z,t) = -\theta(x,t)z \tag{2.19}$$

$$w(x,y,z,t) = \theta(x,t)y \tag{2.20}$$

So, the main difference to St. Venant torsion is the replacement of the rate of twist with the independent variable $\psi(x,t)$. If we follow Barr's approach [41], we find that the equations of motion are,

$$\rho P\ddot{\psi} = EP\psi_{,xx} - G(K\psi + L_c\theta_{,x}) \tag{2.21}$$

$$\rho J_g\ddot{\theta} = G(J_g\theta_{,xx} + L_c\psi_{,x}) \tag{2.22}$$

where the constants are (see Appendix C for their calculation),

$$P = \int_A \phi(y,z)^2 \mathrm{d}A \tag{2.23}$$

$$K = \int_A \left(\phi_{,y}(y,z)^2 + \phi_{,z}(y,z)^2\right) \mathrm{d}A \tag{2.24}$$

$$L_c = \int_A \left(\phi_{,z}(y,z)\,y - \phi_{,y}(y,z)z\right) \mathrm{d}A \tag{2.25}$$

$$J_g = \int_A (y^2+z^2) \mathrm{d}A \tag{2.26}$$

where $\mathrm{d}A = \mathrm{d}y\,\mathrm{d}z$, which is consistent with Ritchie and Leevers [42]. This is subject to the boundary conditions on a constrained end,

$$\psi = \theta = 0 \tag{2.27}$$

and using Ritchie and Leevers condition on a free end (since it is a simpler but equivalent form to Barr) in a consistent notation,

$$\psi_{,x} = 0 \tag{2.28}$$

$$T = G(J_g\theta_{,x} + L_c\psi) = 0 \tag{2.29}$$

where T is the transmitted torque at the free end. At this point, it's possible to decouple the equations, turning them into fourth order PDEs. However, both Barr and Ritchie and Leevers oversimplify their solution for θ (and don't solve for ψ) by assuming that the time modes are cosine functions. Barr compounds the problem by assuming the spatial modes are cosine functions as well; This assumption violates his boundary conditions at the constrained end.

Martinez and Ségura [44] use a static torsion model that is an extension of Reissner torsion. In it they add an additional warping term to u so it becomes (keeping notation consistent with the chapter),

$$u(x,y,z) = \psi(x)\phi(y,z) + \eta_x(x,y,z) \tag{2.30}$$

where $\eta_x(x,y,z)$ is,

$$\eta_x(x,y,z) = f(x)g(y,z) \tag{2.31}$$

This means we would need to solve for both warping functions ϕ and g.

Other Torsion Models

There are some simplified torsion models for use in coupled bending-torsion models [45, 46, 47, 48, 49, 50], but the models aren't suitable for our particular problem because of their modelling approach. The models [45, 47, 48, 50] start directly with a differential equation which makes them unsuitable for use in a variational approach. Eslimy-Isfanany *et al.* [46] uses a modal analysis approach which is also unsuitable for using in the variational equations. Fischera *et al.* [49] also appear to use a modal analysis approach, but are vague on the specific details of the system model. The coupled bending-torsion model by Klinkel and Govindjee [51] is similar to traditional St. Venant/Reissner torsion models, but it assumes that the warping doesn't depend upon the axial coordinate. Given the boundary conditions, this would not properly model non-uniform torsion.

2.3 Torsion Model Analysis

In the traditional analysis of a beam in torsion (*e.g.,* [31, 40]), the deflections are assumed to be of the form

$$u = u(x,y,z,t) \tag{2.32}$$
$$v = -\theta(x,t)z \tag{2.33}$$
$$w = \theta(x,t)y \tag{2.34}$$

(see Figure 2.3) where it is assumed that $\theta(x,t)$ is small. The shear strains, given in Equations (2.32)–(2.34), are

$$\gamma_{yz} = \frac{\partial v}{\partial z} + \frac{\partial w}{\partial y} = 0 \tag{2.35}$$
$$\gamma_{zx} = \frac{\partial u}{\partial z} + \frac{\partial w}{\partial x} = u_{,z}(x,y,z,t) + y\theta_{,x}(x,t) \tag{2.36}$$
$$\gamma_{xy} = \frac{\partial u}{\partial y} + \frac{\partial v}{\partial x} = u_{,y}(x,y,z,t) - z\theta_{,x}(x,t) \tag{2.37}$$

The corresponding shear stresses are,

$$\tau_{yz} = G\gamma_{yz} = 0 \tag{2.38}$$
$$\tau_{zx} = G\gamma_{zx} = G\left(u_{,z}(x,y,z,t) + y\theta_{,x}(x,t)\right) \tag{2.39}$$
$$\tau_{xy} = G\gamma_{xy} = G\left(u_{,y}(x,y,z,t) - z\theta_{,x}(x,t)\right) \tag{2.40}$$

and the normal strains are given by,

$$\epsilon_{xx} = \frac{\partial u}{\partial x} = u_{,x}(x,y,z,t) \tag{2.41}$$

$$\epsilon_{yy} = \frac{\partial v}{\partial y} = 0 \tag{2.42}$$

$$\epsilon_{zz} = \frac{\partial w}{\partial z} = 0 \tag{2.43}$$

Note that the axial strain is non-zero. Assuming a linear elastic material, relating the normal strains to the normal stresses yields

$$\epsilon_{xx} = \frac{1}{E}\left(\sigma_{xx} - \nu\left(\sigma_{yy} + \sigma_{zz}\right)\right) \tag{2.44}$$

$$\epsilon_{yy} = \frac{1}{E}\left(\sigma_{yy} - \nu\left(\sigma_{xx} + \sigma_{zz}\right)\right) \tag{2.45}$$

$$\epsilon_{zz} = \frac{1}{E}\left(\sigma_{zz} - \nu\left(\sigma_{xx} + \sigma_{yy}\right)\right) \tag{2.46}$$

which, after substitution of the normal strains from Equations (2.41)–(2.43) and solving, lead to,

$$\sigma_{xx} = \frac{E(\nu-1)}{(1+\nu)(2\nu-1)} u_{,x}(x,y,z,t) \tag{2.47}$$

$$\sigma_{yy} = -\frac{E\nu}{(1+\nu)(2\nu-1)} u_{,x}(x,y,z,t) \tag{2.48}$$

$$\sigma_{zz} = -\frac{E\nu}{(1+\nu)(2\nu-1)} u_{,x}(x,y,z,t) \tag{2.49}$$

Note that the in-plane axial stresses are dependent upon the axial displacement map. The standard assumptions made regarding the stresses are [31],

$$\sigma_{yy} = 0 \tag{2.50}$$

$$\sigma_{zz} = 0 \tag{2.51}$$

$$\tau_{yz} = 0 \tag{2.52}$$

We can see that the assumption of Equation (2.52) is satisfied as shown in Equation (2.38). In the uniform torsion case, we have

$$u_{,x}(x,y,z,t) = \phi(y,z)\theta_{,xx}(x,t) \tag{2.53}$$

In the static case (*i.e.*, $\theta_{,xx}(x,t) = \theta_{,xx}(x)$) all the normal stresses are zero since the angle of twist varies linearly throughout the beam and the remaining assumptions are satisfied. However, this is not true in the non-uniform case. For example, using the Reissner torsion approximation given in Equation (2.18) we get,

$$u_{,x}(x,y,z,t) = \phi(y,z)\psi_{,x}(x,t) \tag{2.54}$$

and $\psi_{,x}(x,t)$ is not zero. So, the stress assumptions from Equations (2.50) and (2.51) and the displacement assumptions as given in Equations (2.32)–(2.34) are inconsistent. For them to be consistent, $\psi(x,t)$ would have to be linear in x.

It might be possible for the stress assumptions in Equations (2.50)– (2.52) to be satisfied using Martinez and Ségura's model, but that would impose the constraint,

$$\psi_{,x}(x)\phi(y,z) = -f_{,x}(x)g(y,z) \tag{2.55}$$

It would likely not be satisfied without explicit application of the constraint.

Since the first model isn't consistent with the assumptions for non-uniform torsion and the second requires the application of the constraint from Equation (2.55), we need to consider other possibilities.

2.4 New Models for Torsion

Since we have two contradictory sets of assumptions in the non-uniform torsion case, we will consider two possible models, each only using one set of assumptions.

Assumed Displacement Model

For simplicity we will restrict ourselves to beams of constant cross-section. Therefore, we assume that each cross-section is warped in the same way and we will use Reissner's axial displacement map as given in (2.18). The torsional strain energy of a beam can be represented as (assuming Equations (2.32)–(2.34)),

$$U = \frac{1}{2}\int_V \left(\sigma_{xx}\epsilon_{xx} + \tau_{xy}\gamma_{xy} + \tau_{zx}\gamma_{zx}\right) \mathrm{d}V \tag{2.56}$$

and after substitution of the stresses (Equations (2.39), (2.40), and (2.47)) and strains (Equations (2.36), (2.37), and (2.41)), along with the definition of $u_{,x}$ as given in Equation (2.54),

$$\begin{aligned} U = \frac{1}{2}\int_V \frac{E(\nu-1)}{(1+\nu)(2\nu-1)}\phi(y,z)^2\psi_{,x}(x,t)^2 + G\left(\phi_{,y}(y,z)\psi(x,t) - z\theta_{,x}(x,t)\right)^2 \\ + G\left(\phi_{,z}(y,z)\psi(x,t) + y\theta_{,x}(x,t)\right)^2 \mathrm{d}V \end{aligned} \tag{2.57}$$

which we can simplify by introducing the constants P, K, and L, from Barr's analysis (Equations (2.23)–(2.24)) and the constant,

$$\eta = \frac{(\nu-1)}{(1+\nu)(2\nu-1)} \tag{2.58}$$

This results in

$$U = \frac{1}{2}\int_0^L E\eta P\psi_{,x}(x,t)^2 + G\left(K\psi(x,t)^2 + 2L_c\theta_{,x}(x,t)\psi(x,t) + J_g\theta_{,x}(x,t)^2\right)\mathrm{d}x \tag{2.59}$$

The torsional kinetic energy is,

$$T_{xt} = \frac{1}{2}\int_V \rho\left(\dot{u}^2 + \dot{v}^2 + \dot{w}^2\right)\mathrm{d}V \tag{2.60}$$

and after substitution of the assumed displacements we get,

$$T_{xt} = \frac{1}{2}\int_V \rho\left(\phi(y,z)^2\dot{\psi}(x,t)^2 + (z^2+y^2)\dot{\theta}(x,t)^2\right)\mathrm{d}V \tag{2.61}$$

Then using the constants defined above this becomes

$$T_{xt} = \frac{1}{2}\int_0^L \rho\left(P\dot{\psi}(x,t)^2 + J_g\dot{\theta}(x,t)^2\right)\mathrm{d}x \tag{2.62}$$

Hamilton's action integral $\mathscr{A}$ is [52],

$$\mathscr{A} = \int_{t_1}^{t_2}\mathscr{L}\mathrm{d}t = \int_{t_1}^{t_2} T - U\mathrm{d}t \tag{2.63}$$

where T is defined in Equation (2.62) (as T_{xt}) and U is defined in Equation (2.59) so the action integral becomes,

$$\begin{aligned}\mathscr{A} = \frac{1}{2}\int_{t1}^{t2}\int_0^L &\left[\rho\left(P\dot{\psi}(x,t)^2 + J_g\dot{\theta}(x,t)^2\right) - E\eta P\psi_{,x}(x,t)^2\right.\\ &\left. - G\left(K\psi(x,t)^2 + 2L_c\theta_{,x}(x,t)\psi(x,t) + J_g\theta_{,x}(x,t)^2\right)\right]\mathrm{d}x\mathrm{d}t\end{aligned} \tag{2.64}$$

Taking the variation of Equation (2.64) with respect to $\theta(x,t)$ gives,

$$\delta\mathscr{A}_1 = \int_{t1}^{t2}\int_0^L \left[\rho J_g\dot{\theta}(x,t)\delta\dot{\theta} - G\left(L_c\psi(x,t) + J_g\theta_{,x}(x,t)\right)\delta\theta_{,x}\right]\mathrm{d}x\mathrm{d}t = 0 \tag{2.65}$$

Subsequent integration of Equation (2.65) by parts gives,

$$\begin{aligned}&\int_0^L \rho J_g\dot{\theta}(x,t)\delta\theta\mathrm{d}x\Big|_{t1}^{t2} - \int_{t1}^{t2} G\left(L_c\psi(x,t) + J_g\theta_{,x}(x,t)\right)\delta\theta\mathrm{d}t\Big|_0^L\\ &-\int_{t1}^{t2}\int_0^L \left[\rho J_g\ddot{\theta}(x,t) - G\left(L_c\psi_{,x}(x,t) + J_g\theta_{,xx}(x,t)\right)\right]\delta\theta\mathrm{d}x\mathrm{d}t = 0\end{aligned} \tag{2.66}$$

The variation of Equation (2.64) with respect to $\psi(x,t)$ gives

$$\delta\mathscr{A}_2 = \int_{t1}^{t2}\int_0^L \left[\rho P\dot{\psi}(x,t)\delta\dot{\psi} - E\eta P\psi_{,x}(x,t)\delta\psi_{,x} - G\left(K\psi + L_c\theta_{,x}\right)\delta\psi\right]\mathrm{d}x\mathrm{d}t = 0 \tag{2.67}$$

and integration of this by parts yields

$$\int_0^L \rho P\dot{\psi}(x,t)\delta\psi \mathrm{d}x\Big|_{t1}^{t2} - \int_{t1}^{t2} E\eta P\psi_{,x}(x,t)\delta\psi \mathrm{d}t\Big|_0^L \\ -\int_{t1}^{t2}\int_0^L \left[\rho P\ddot{\psi}(x,t) - E\eta P\psi_{,xx}(x,t) + G\left(K\psi + L_c\theta_{,x}\right)\right]\delta\psi \mathrm{d}x\mathrm{d}t = 0 \tag{2.68}$$

From Equation (2.66) and (2.68) the equations of motion are found to be,

$$\rho J_g\ddot{\theta}(x,t) - G\left(L_c\psi_{,x}(x,t) + J_g\theta_{,xx}(x,t)\right) = 0 \tag{2.69}$$

$$\rho P\ddot{\psi}(x,t) - E\eta P\psi_{,xx}(x,t) + G\left(K\psi + L_c\theta_{,x}\right) = 0 \tag{2.70}$$

subject to the following initial and boundary conditions,

$$\int_0^L \rho P\dot{\psi}(x,t)\delta\psi \mathrm{d}x\Big|_{t1}^{t2} = 0 \tag{2.71}$$

$$\int_0^L \rho J_g\dot{\theta}(x,t)\delta\theta \mathrm{d}x\Big|_{t1}^{t2} = 0 \tag{2.72}$$

$$\int_{t1}^{t2} G\left(L_c\psi(x,t) + J_g\theta_{,x}(x,t)\right)\delta\theta \mathrm{d}t\Big|_0^L = 0 \tag{2.73}$$

$$\int_{t1}^{t2} E\eta P\psi_{,x}(x,t)\delta\psi \mathrm{d}t\Big|_0^L = 0 \tag{2.74}$$

Aside from the addition of η from Equation (2.58), these equations of motion (and boundary conditions) are consistent with the Reissner model in Equations (2.21) and (2.22). If we set ν to zero in η, the equations reduce to the dynamic Reissner equations.

Note that this model has the same problem as the Reissner model described in Appendix A.2, in that we can't consider that ϕ is independent. Therefore, we will use the St. Venant warping function (as derived in Appendix A.1). For other cases, one could use a numerical approximation to the St. Venant warping function [53] or use a different warping function [54, 55, 56] that is simpler to calculate.

Assumed Stress Model

If instead of assuming the displacements, we use the stress assumptions given in Equations (2.50) and (2.51) we can get a new model for torsion (see Appendix A.3 for details). The governing equations for this model are,

$$\rho\ddot{u} - (E-2G\nu)u_{,xx} - G(u_{,yy}+u_{,zz}) = 0 \tag{2.75}$$

$$\rho\ddot{v} - G\left(v_{,xx} + v_{,zz} + (1-\frac{1}{\nu})v_{,yy}\right) = 0 \tag{2.76}$$

$$\rho\ddot{w} - G\left(w_{,xx} + w_{,yy} + (1-\frac{1}{\nu})w_{,zz}\right) = 0 \tag{2.77}$$

The boundary conditions arising from the variations are,

$$\int_{t_1}^{t_2}\int_A E u_{,x}\delta u \,\mathrm{d}A\mathrm{d}t\Big|_0^L = 0 \tag{2.78}$$

$$\int_{t_1}^{t_2}\int_S G\left[\left(v_{,x}+u_{,y}\right)n_y+\left(w_{,x}+u_{,z}\right)n_z\right]\delta u\,\mathrm{d}S\mathrm{d}t = 0 \tag{2.79}$$

$$\int_{t_1}^{t_2}\int_S G[(u_{,y}+v_{,x})n_x+(v_{,z}+w_{,y})n_z]\,\delta v\,\mathrm{d}S\mathrm{d}t = 0 \tag{2.80}$$

$$\int_{t_1}^{t_2}\int_S G[(u_{,z}+w_{,x})n_x+(v_{,z}+w_{,y})n_y]\,\delta w\,\mathrm{d}S\mathrm{d}t = 0 \tag{2.81}$$

and the initial conditions are,

$$\int_V \rho\ddot{u}\,\delta u\mathrm{d}V\Big|_{t_1}^{t_2} = 0 \tag{2.82}$$

$$\int_V \rho\ddot{v}\,\delta v\mathrm{d}V\Big|_{t_1}^{t_2} = 0 \tag{2.83}$$

$$\int_V \rho\ddot{w}\delta w\mathrm{d}V\Big|_{t_1}^{t_2} = 0 \tag{2.84}$$

with the additional constraints due to Poisson effects of,

$$v_{,y}(x,y,z,t) = -\nu\, u_{,x}(x,y,z,t) \tag{2.85}$$

$$w_{,z}(x,y,z,t) = -\nu\, u_{,x}(x,y,z,t) \tag{2.86}$$

The governing equations themselves aren't difficult to solve for the general solution. However, finding the solutions that meet both the boundary conditions and the Poisson constraints, make an analytical solution extremely difficult. This would make working with it difficult and as such won't be used in the rest of the thesis.

CHAPTER

3 System Work, Kinetic, and Potential Energy

In this chapter we examine the kinetic and potential energy of the system for different beam and target models. Starting with the work and kinetic energy of the motor (since it is independent of the beam model), then the target models, followed by the beam models, and lastly, the end-effector models.

For the target and end-effector, we consider a point mass model, a 2D rigid body model, and a 3D rigid body model. For the beam, we consider 2D Euler-Bernoulli and Timoshenko beam models, as well as a 3D Timoshenko beam model including torsion. The 2D models are based upon the system shown in Figure 3.1.

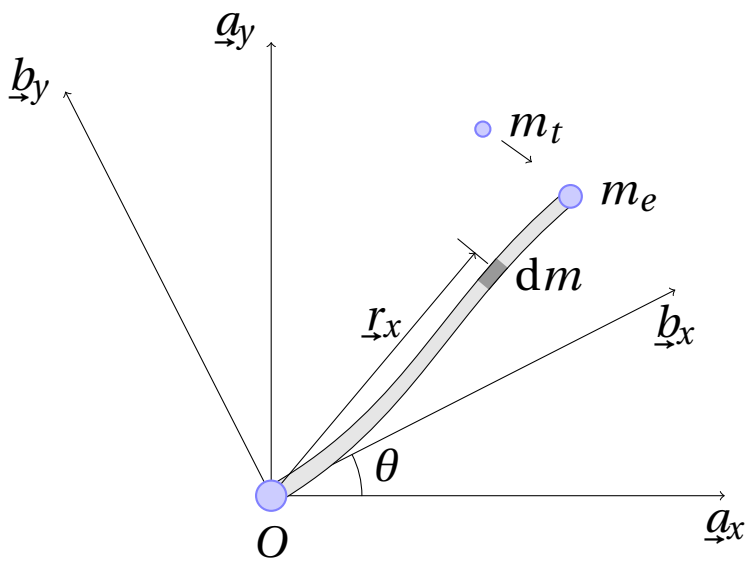

Figure 3.1: 2D System Model

3.1 Motor Work and Kinetic Energy

The kinetic energy of the motor is given by

$$T_m = \frac{1}{2} J_m \dot{\theta}^2 \tag{3.1}$$

where J_m is the rotary inertia of the motor. The work done by the motor due to the generated moment is,

$$W = \int_a^b M(\theta) \mathrm{d}\theta \tag{3.2}$$

where $M(\theta)$ is the generated moment of the motor.

3.2 Target Energy

This is the pre-capture target model. In the post capture case, the target is treated the same as the end-effector.

Point Mass Model

The kinetic energy of a particle is,

$$T_p = \frac{1}{2} m \underset{\sim}{v} \cdot \underset{\sim}{v} \tag{3.3}$$

and the inertial velocity of the target is given by

$$\underset{\sim}{v}_t = \underset{\rightarrow}{\mathscr{F}}_a^T \begin{bmatrix} \dot{x}_t \\ \dot{y}_t \\ 0 \end{bmatrix} \tag{3.4}$$

Hence, the kinetic energy of the target is

$$T_t = \frac{1}{2} m_t \left(\dot{x}_t^2 + \dot{y}_t^2 \right) \tag{3.5}$$

where m_t is the mass of the target.

2D Rigid Body Model

The translational kinetic energy is the same as the point mass model, so we only need to add the rotational kinetic energy. The angular velocity is,

$$\underset{\sim}{\omega}_t(t) = \underset{\rightarrow}{\mathscr{F}}_a^T \begin{bmatrix} 0 \\ 0 \\ \dot{\gamma}(t) \end{bmatrix} \tag{3.6}$$

For both this model and the 3D rigid body model, it is assumed that the rotation is about an axis that passes through the centre of mass. The rotational kinetic energy of a general rigid body is,

$$T_{rot} = \frac{1}{2} \underset{\rightarrow}{\omega}^T \mathbf{J} \underset{\rightarrow}{\omega} \tag{3.7}$$

where **J** is the inertia matrix for the body. For the target in this case, we assume that **J** is principal and only the (3,3) component (J_t) contributes to the kinetic energy. After substitution $\mathbf{J}_t$ and of $\underset{\rightarrow}{\omega}_t(t)$ for $\underset{\rightarrow}{\omega}$ in Equation (3.7), the rotational kinetic energy of the target is,

$$T_{tr} = \frac{1}{2} J_t \dot{\gamma}(t)^2 \tag{3.8}$$

Therefore, the kinetic energy a 2D rigid body target is,

$$T_t = \frac{1}{2} \left(m_t \left(\dot{x}_t^2 + \dot{y}_t^2 \right) + J_t \dot{\gamma}(t)^2 \right) \tag{3.9}$$

3D Rigid Body Model

The translational kinetic energy has an additional component due to the additional of a z-coordinate velocity, which results in,

$$T_t = \frac{1}{2} m_t \left(\dot{x}_t^2 + \dot{y}_t^2 + \dot{z}_t^2 \right) \tag{3.10}$$

The angular velocity is,

$$\underset{\rightarrow}{\omega}_t(t) = \underset{\rightarrow}{\mathscr{F}}_a^T \begin{bmatrix} \dot{\alpha}(t) \\ \dot{\beta}(t) \\ \dot{\gamma}(t) \end{bmatrix} \tag{3.11}$$

The rotational kinetic energy of a rigid body is as stated in Equation (3.7). For the target in this case, we use the general inertia matrix,

$$\mathbf{J}_t = \begin{bmatrix} J_{txx} & J_{txy} & J_{txz} \\ J_{txy} & J_{tyy} & J_{tyz} \\ J_{txz} & J_{tyz} & J_{tzz} \end{bmatrix} \tag{3.12}$$

Resulting in the rotational kinetic energy of the target as,

$$T_{tr} = \frac{1}{2} \left(\dot{\alpha}^2 J_{txx} + \dot{\beta}^2 J_{tyy} + \dot{\gamma}^2 J_{tzz} + 2\dot{\alpha}\dot{\beta} J_{txy} + 2\dot{\alpha}\dot{\gamma} J_{txz} + 2\dot{\beta}\dot{\gamma} J_{tyz} \right) \tag{3.13}$$

Therefore, the total kinetic energy of a 3D rigid body target is,

$$\begin{aligned} T_t = & \frac{1}{2} \left(m_t \left(\dot{x}_t^2 + \dot{y}_t^2 + \dot{z}_t^2 \right) + \dot{\alpha}^2 J_{txx} + \dot{\beta}^2 J_{tyy} + \dot{\gamma}^2 J_{tzz} \right. \\ & \left. + 2\dot{\alpha}\dot{\beta} J_{txy} + 2\dot{\alpha}\dot{\gamma} J_{txz} + 2\dot{\beta}\dot{\gamma} J_{tyz} \right) \end{aligned} \tag{3.14}$$

3.3 Beam Energy

2D Euler-Bernoulli Beam

The position of a small differential element of the beam (see Figure 3.1) with a volume of $A\mathrm{d}x$ is given by

$$\underset{\rightarrow}{r}_x = \underset{\rightarrow}{\mathscr{F}}_b^T \begin{bmatrix} x - y\overline{v}' \\ y + \overline{v} \\ 0 \end{bmatrix} \tag{3.15}$$

where $\overline{v} = \overline{v}(x,t)$ is the transverse deflection of the beam neutral axis and $\overline{v}'$ is the slope of that deflection. In this model, we are neglecting the axial extension of the beam. Transforming to the inertial frame

$$\underset{\rightarrow}{r}_x = \underset{\rightarrow}{\mathscr{F}}_a^T \mathbf{C}_{ab} \begin{bmatrix} x - y\overline{v}' \\ y + \overline{v} \\ z \end{bmatrix} \tag{3.16}$$

where $\mathbf{C}_{ab}$ is,

$$\mathbf{C}_{ab} = \begin{bmatrix} \cos\theta & -\sin\theta & 0 \\ \sin\theta & \cos\theta & 0 \\ 0 & 0 & 1 \end{bmatrix} \tag{3.17}$$

Therefore, the position vector in the inertial frame is,

$$\underset{\rightarrow}{r}_x = \underset{\rightarrow}{\mathscr{F}}_a^T \begin{bmatrix} (x - y\overline{v}')\cos\theta - (y + \overline{v})\sin\theta \\ +(x - y\overline{v}')\sin\theta + (y + \overline{v})\cos\theta \\ z \end{bmatrix} \tag{3.18}$$

Differentiating equation (3.18) with respect to time, we get the velocity of a differential element of the beam.

$$\underset{\rightarrow}{v}_x = \underset{\rightarrow}{\mathscr{F}}_a^T \begin{bmatrix} -\left(\dot{\overline{v}} + \dot{\theta}(x - y\overline{v}')\right)\sin\theta - \left(\dot{\theta}(y + \overline{v}) + y\dot{\overline{v}}'\right)\cos\theta \\ \left(\dot{\overline{v}} + \dot{\theta}(x - y\overline{v}')\right)\cos\theta - \left(\dot{\theta}(y + \overline{v}) + y\dot{\overline{v}}'\right)\sin\theta \\ 0 \end{bmatrix} \tag{3.19}$$

The kinetic energy of a flexible beam is given by

$$T_b = \frac{1}{2}\int_V \rho \underset{\rightarrow}{v} \cdot \underset{\rightarrow}{v}\,\mathrm{d}V \tag{3.20}$$

where ρ is the volume mass density. This can be reduced to

$$T_b = \frac{1}{2}\int_0^L \rho A \underset{\rightarrow}{v} \cdot \underset{\rightarrow}{v}\,\mathrm{d}x \tag{3.21}$$

substituting the differential beam element velocity derived in equation (3.19) we get the following expression for the kinetic energy of the beam.

$$T_b = \frac{1}{2}\int_0^L \rho A(x^2\dot{\theta}^2 + 2x\dot{\theta}\dot{\overline{v}} + \dot{\overline{v}}^2 + \dot{\theta}^2\overline{v}^2)\mathrm{d}x + \frac{1}{2}\int_0^L \rho I_{yy}(\dot{\overline{v}}'^2 + 2\dot{\overline{v}}'\dot{\theta} + \dot{\theta}^2(1+\overline{v}'^2))\mathrm{d}x \tag{3.22}$$

Since this is an Euler-Bernoulli beam, we will drop the $\overline{v}'$ terms (which arise from rotary inertia), resulting in,

$$T_b = \frac{1}{2}\int_0^L \rho A(x^2\dot{\theta}^2 + 2x\dot{\theta}\dot{\overline{v}} + \dot{\overline{v}}^2 + \dot{\theta}^2\overline{v}^2)\mathrm{d}x + \frac{1}{2}\int_0^L \rho I_{yy}\dot{\theta}^2\mathrm{d}x \tag{3.23}$$

The strain energy of the beam is given by

$$U = \frac{1}{2}\int_0^L EI_{yy}(\overline{v}'')^2\mathrm{d}x \tag{3.24}$$

where $\overline{v}''$ is the second derivative of $\overline{v}$ with respect to x.

2D Timoshenko Beam

The position of a differential element of the rotating beam is given by,

$$\underset{\sim}{r}_x = \underset{\sim}{\mathscr{F}}_b^T \begin{bmatrix} x + \overline{u} - y\psi_z \\ y + \overline{v} \\ z \end{bmatrix} \tag{3.25}$$

where $\overline{u} = \overline{u}(x,t)$, $\psi_z = \psi_z(x,t)$, and $\overline{v} = \overline{v}(x,t)$. In this formation, the axial extension of the neutral axis is included via $\overline{u}(x,t)$. Transforming to the inertial frame

$$\underset{\sim}{r}_x = \underset{\sim}{\mathscr{F}}_a^T \mathbf{C}_{ab} \begin{bmatrix} x + \overline{u} - y\psi_z \\ y + \overline{v} \\ z \end{bmatrix} \tag{3.26}$$

where $\mathbf{C}_{ab}$ is as given in Equation (3.17). The position of the differential element in the inertial frame is therefore,

$$\underset{\sim}{r}_x = \underset{\sim}{\mathscr{F}}_a^T \begin{bmatrix} (x + \overline{u} - y\psi_z)\cos\theta - (y + \overline{v})\sin\theta \\ (x + \overline{u} - y\psi_z)\sin\theta + (y + \overline{v})\cos\theta \\ z \end{bmatrix} \tag{3.27}$$

where $\theta = \theta(t)$. Differentiating this with respect to time, we get the inertial velocity for a differential element of the beam,

$$\underset{\sim}{v}_x = \underset{\sim}{\mathscr{F}}_a^T \begin{bmatrix} [\dot{\overline{u}} - y\dot{\psi}_z - \dot{\theta}(y + \overline{v})]\cos\theta - [\dot{\overline{v}} + \dot{\theta}(x + \overline{u} - y\psi_z)]\sin\theta \\ [\dot{\overline{v}} + \dot{\theta}(x + \overline{u} - y\psi_z)]\cos\theta + [\dot{\overline{u}} - \dot{\theta}(y + \overline{v}) - y\dot{\psi}_z]\sin\theta \\ 0 \end{bmatrix} \tag{3.28}$$

substituting this into Equation (3.20) and integrating over the cross-section, we get the kinetic energy of the beam,

$$T_b = \frac{1}{2}\int_0^L \rho A\left((\dot{\overline{v}} + \dot{\theta}(x+\overline{u}))^2 + (\dot{\overline{u}} - \dot{\theta}\overline{v})^2\right)\mathrm{d}x + \frac{1}{2}\int_0^L \rho I_{yy}\left((\dot{\theta}+\dot{\psi}_z)^2 + \dot{\theta}^2\psi_z^2\right)\mathrm{d}x \tag{3.29}$$

The strain energy of the beam is,

$$U = \frac{1}{2}\int_0^L (EI_{yy}\psi_z'^2 + \kappa^2 GA(\overline{v}' - \psi_z)^2 + EA\overline{u}'^2)\mathrm{d}x \tag{3.30}$$

3D Timoshenko Beam (with Torsion)

The position of a differential beam element in the rotating frame is given by,

$$\underset{\sim}{r}_x = \underset{\sim}{\mathscr{F}}_b^T \begin{bmatrix} x + \overline{u}(x,t) - yu_{pv}(x,t) - zu_{pw}(x,t) + \Phi(x,y,z,t) \\ y + \overline{v}(x,t) + V(x,y,z,t) \\ z + \overline{w}(x,t) + W(x,y,z,t) \end{bmatrix} \tag{3.31}$$

where $\overline{u}$, $\overline{v}$, and $\overline{w}$ are the deflections of the neutral axis, u_{pv} is the slope of the in-plane bending curve, u_{pw} is the slope of the out of plane bending curve, and the functions Φ, V, and W are general torsion functions. For Timoshenko beams, this becomes,

$$\underset{\sim}{r}_x = \underset{\sim}{\mathscr{F}}_b^T \begin{bmatrix} x + \overline{u}(x,t) - y\psi_z(x,t) - z\psi_y(x,t) + \Phi(x,y,z,t) \\ y + \overline{v}(x,t) + V(x,y,z,t) \\ z + \overline{w}(x,t) + W(x,y,z,t) \end{bmatrix} \tag{3.32}$$

Using the assumed displacement model from the last chapter, the torsion functions become,

$$\Phi(x,y,z,t) = \phi(y,z)\psi_x(x,t) \tag{3.33}$$

$$V(x,y,z,t) = -z\theta_x(,t) \tag{3.34}$$

$$W(x,y,z,t) = y\theta_x(x,t) \tag{3.35}$$

where θ_x is the torsion angle (about the x-axis) and ψ_x is used to prevent confusion with the bending angles. This results in the differential beam element position as,

$$\underset{\sim}{r}_x = \underset{\sim}{\mathscr{F}}_b^T \begin{bmatrix} x + \overline{u}(x,t) - y\psi_z(x,t) - z\psi_y(x,t) + \phi(y,z)\psi_x(x,t) \\ y + \overline{v}(x,t) - z\theta_x(x,t) \\ z + \overline{w}(x,t) + y\theta_x(x,t) \end{bmatrix} \tag{3.36}$$

In order to get the kinetic and strain energy of the beam, we will split the deflection into two contributions (in addition to the original position),

$$\underset{\sim}{r}_x = \underset{\sim}{\mathscr{F}}_b^T(\mathbf{r} + \mathbf{d}_b + \mathbf{d}_t) \tag{3.37}$$

where **r** (the original position of the differential beam element) is,

$$\mathbf{r} = \begin{bmatrix} x \\ y \\ z \end{bmatrix} \tag{3.38}$$

and $\mathbf{d}_b$ (the deflection due to extension and bending) is,

$$\mathbf{d}_b = \begin{bmatrix} \overline{u}(x,t) - y\psi_z(x,t) - z\psi_y(x,t) \\ \overline{v}(x,t) \\ \overline{w}(x,t) \end{bmatrix} \tag{3.39}$$

and $\mathbf{d}_t$ (the deflection due to torsion) is,

$$\mathbf{d}_t = \begin{bmatrix} \phi(y,z)\psi_x(x,t) \\ -z\theta_x(x,t) \\ y\theta_x(x,t) \end{bmatrix} \tag{3.40}$$

This split is done since we want Timoshenko's shear correction factor applied only to the shear contributions due to extension and bending. So, the inertial position for the extension and bending contribution is,

$$\underset{\rightarrow}{r}_{xb} = \underset{\rightarrow}{\mathscr{F}}_a^T \mathbf{C}_{ab} \begin{bmatrix} x + \overline{u}(x,t) - y\psi_z(x,t) - z\psi_y(x,t) \\ y + \overline{v}(x,t) \\ z + \overline{w}(x,t) \end{bmatrix} \tag{3.41}$$

and the torsion contribution is,

$$\underset{\rightarrow}{r}_{xt} = \underset{\rightarrow}{\mathscr{F}}_a^T \mathbf{C}_{ab} \begin{bmatrix} \phi(y,z)\psi_x(x,t) \\ -\theta_x(x,t)z \\ \theta_x(x,t)y \end{bmatrix} \tag{3.42}$$

which upon expansion the former becomes,

$$\underset{\rightarrow}{r}_{xb} = \underset{\rightarrow}{\mathscr{F}}_a^T \begin{bmatrix} (x + \overline{u} - y\psi_z + z\psi_y)\cos\theta - (y + \overline{v})\sin\theta \\ (x + \overline{u} + y\psi_z + z\psi_y)\sin\theta + (y + \overline{v})\cos\theta \\ z + \overline{w} \end{bmatrix} \tag{3.43}$$

and the latter becomes,

$$\underset{\rightarrow}{r}_{xt} = \underset{\rightarrow}{\mathscr{F}}_a^T \begin{bmatrix} \phi\psi_x\cos\theta + z\theta_x\sin\theta \\ \phi\psi_x\sin\theta - z\theta_x\cos\theta \\ y\theta_x \end{bmatrix} \tag{3.44}$$

Differentiating with respect to time for the bending and extension contributions,

$$\underset{\sim}{v}_{xb} = \underset{\sim}{\mathscr{F}}_a^T \begin{bmatrix} \left(\dot{\overline{u}} - \dot{\theta}(y+\overline{v}) - y\dot{\psi}_z - z\dot{\psi}_y\right)\cos\theta - \left(\dot{\theta}(x+\overline{u} - z\psi_y - y\psi_z) + \dot{\overline{v}}\right)\sin\theta \\ \left(\dot{\theta}(x+\overline{u} - z\psi_y - y\psi_z) + \dot{\overline{v}}\right)\cos\theta + \left(\dot{\overline{u}} - \dot{\theta}(y+\overline{v}) - y\dot{\psi}_z - z\dot{\psi}_y\right)\sin\theta \\ \dot{\overline{w}} \end{bmatrix} \tag{3.45}$$

and for the torsion contribution,

$$\underset{\sim}{v}_{xt} = \underset{\sim}{\mathscr{F}}_a^T \begin{bmatrix} \left(\phi\dot{\psi}_x + \dot{\theta}z\theta_x\right)\cos\theta - \left(\dot{\theta}\phi\psi_x - z\dot{\theta}_x\right)\sin\theta \\ \left(\dot{\theta}z\theta_x + \phi\dot{\psi}_x\right)\sin\theta + \left(\dot{\theta}\phi\psi_x - z\dot{\theta}_x\right)\cos\theta \\ y\dot{\theta}_x \end{bmatrix} \tag{3.46}$$

which after substituting into the beam energy equation given in Equation (3.20) and integrating over the cross-section yields,

$$\begin{aligned} T_{xb} = &\frac{1}{2}\int_0^L \rho A\left((\dot{\overline{v}} + \dot{\theta}(x+\overline{u}))^2 + (\dot{\overline{u}} - \dot{\theta}\overline{v})^2 + \dot{\overline{w}}^2\right)\mathrm{d}x \\ &+ \frac{1}{2}\int_0^L \rho\left(I_{yy}\left((\dot{\psi}_z + \dot{\theta})^2 + \dot{\theta}^2\psi_z^2\right) + I_{zz}(\dot{\psi}_y^2 + \dot{\theta}^2\psi_y^2)\right)\mathrm{d}x \end{aligned} \tag{3.47}$$

and the kinetic energy due to torsion is,

$$T_{xt} = \frac{1}{2}\int_0^L \rho\left(\dot{\theta}^2(P\psi_x^2 + I_{zz}\theta_x^2) + J_g\dot{\theta}_x^2 + P\dot{\psi}_x^2\right)\mathrm{d}x \tag{3.48}$$

Note that P is the integral as given in Equation (2.23). The total kinetic energy of the beam is the sum of these two,

$$T_b = T_{xb} + T_{xt} \tag{3.49}$$

For the strain energy of the beam due to torsion, we will use Equation (2.59), but with the additional assumption that $\nu \approx 0$ to stay consistent with the Timoshenko beam assumptions. This results in,

$$U_{xt} = \frac{1}{2}\int_0^L EP\psi_{,x}(x,t)^2 + G\left(K\psi(x,t)^2 + 2L_c\theta_{,x}(x,t)\psi(x,t) + J_g\theta_{,x}(x,t)^2\right)\mathrm{d}x \tag{3.50}$$

See Appendix C for the calculation of P, K, and L_c. For the bending and extension contribution to strain energy, we have the following strains,

$$\epsilon_{xx} = \frac{\partial u}{\partial x} = \frac{\partial\overline{u}}{\partial x} - y\frac{\partial\psi_z}{\partial x} - z\frac{\partial\psi_y}{\partial x} \tag{3.51}$$

$$\gamma_{xy} = \frac{\partial u}{\partial y} + \frac{\partial v}{\partial x} = \frac{\partial\overline{v}}{\partial x} - \frac{\partial\psi_z}{\partial x} \tag{3.52}$$

$$\gamma_{xz} = \frac{\partial u}{\partial z} + \frac{\partial w}{\partial x} = \frac{\partial\overline{w}}{\partial x} - \frac{\partial\psi_y}{\partial x} \tag{3.53}$$

The corresponding stresses are,

$$\sigma_{xx} = E\epsilon_{xx} \tag{3.54}$$
$$\tau_{xy} = \kappa^2 G\gamma_{xy} \tag{3.55}$$
$$\tau_{xz} = \kappa^2 G\gamma_{xz} \tag{3.56}$$

where κ^2 is the shear correction factor. The strain energy is,

$$U_{xb} = \frac{1}{2}\int_V \sigma_{xx}\epsilon_{xx} + \tau_{xy}\gamma_{xy} + \tau_{xz}\gamma_{xz}\mathrm{d}V \tag{3.57}$$
$$= \frac{1}{2}\int_V E\epsilon_{xx}^2 + \kappa^2 G\gamma_{xy}^2 + \kappa^2 G\gamma_{xz}\mathrm{d}V \tag{3.58}$$

Using the strain expressions, after integration over the cross-section, this becomes,

$$U_{xb} = \frac{1}{2}\int_0^L \Big(EA\overline{u}_{,x}^2 + EI_{yy}\psi_{z,x}^2 + EI_{zz}\psi_{y,x}^2 + \kappa^2 GA(\overline{v}_{,x} - \psi_z)^2 + \kappa^2 GA(\overline{w}_{,x} - \psi_y)^2 \Big)\,\mathrm{d}x \tag{3.59}$$

3.4 End-Effector Energy

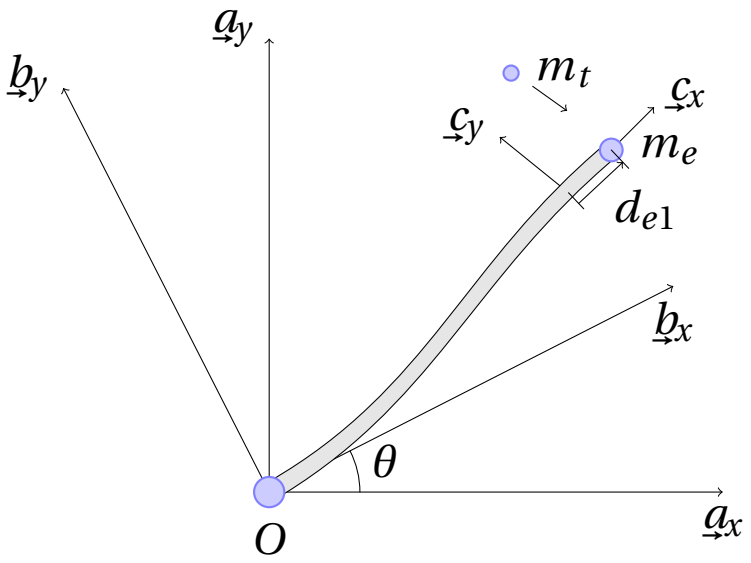

Figure 3.2: 2D System Model (with end-effector offset)

Point Mass (Euler-Bernoulli Beam)

The position of the end effector in the rotating frame (see Figure 3.2) is given by

$$\underset{\rightarrow}{r}_e = \underset{\rightarrow}{\mathscr{F}}_b^T \begin{bmatrix} L \\ \overline{v}_L \\ 0 \end{bmatrix} + \underset{\rightarrow}{\mathscr{F}}_c^T \begin{bmatrix} d_{e1} \\ 0 \\ 0 \end{bmatrix} \tag{3.60}$$

where d_{e1} is the offset of the point mass from the end of the beam. This assumes that the centre of mass (CoM) of the end-effector is located along the neutral axis of the beam. This is specified in a frame C fixed to the end of the beam. Note that in this particular case, we are assuming no extension of the beam. Transforming to the inertial frame,

$$\underset{\rightarrow}{r}_e = \underset{\rightarrow}{\mathscr{F}}_a^T \mathbf{C}_{ab} \left(\begin{bmatrix} L \\ \overline{v}_L \\ 0 \end{bmatrix} + \mathbf{C}_{bc} \begin{bmatrix} d_{e1} \\ 0 \\ 0 \end{bmatrix} \right) \tag{3.61}$$

where $\mathbf{C}_{bc}$ is the rotation matrix from frame C to frame B. $\mathbf{C}_{ab}$ is as before in Equation (3.17). Restated again,

$$\mathbf{C}_{ab} = \begin{bmatrix} \cos\theta & -\sin\theta & 0 \\ \sin\theta & \cos\theta & 0 \\ 0 & 0 & 1 \end{bmatrix} \tag{3.62}$$

and $\mathbf{C}_{bc}$ is the matrix due to infinitesimal rotation as given in Meirovitch [57] (p. 107),

$$\mathbf{C}_{bc} = \begin{bmatrix} 1 & -\Delta\theta_3 & \Delta\theta_2 \\ \Delta\theta_3 & 1 & -\Delta\theta_1 \\ -\Delta\theta_2 & \Delta\theta_1 & 1 \end{bmatrix} \tag{3.63}$$

where $\Delta\theta_i$ is the rotation of the frame C about axis i. In this case, only $\Delta\theta_3$ is non-zero giving,

$$\mathbf{C}_{bc} = \begin{bmatrix} 1 & -\overline{v}'_L & 0 \\ \overline{v}'_L & 1 & 0 \\ 0 & 0 & 1 \end{bmatrix} \tag{3.64}$$

Therefore, the position vector of the end effector centre of mass in the inertial frame is

$$\underset{\rightarrow}{r}_e = \underset{\rightarrow}{\mathscr{F}}_a^T \begin{bmatrix} (L+d_{e1})\cos\theta - (\overline{v}_L + \overline{v}'_L d_{e1})\sin\theta \\ (L+d_{e1})\sin\theta + (\overline{v}_L + \overline{v}'_L d_{e1})\cos\theta \\ 0 \end{bmatrix} \tag{3.65}$$

Differentiating this result with respect to time, we get the velocity of the end effector centre of mass,

$$\underset{\rightarrow}{v}_e = \underset{\rightarrow}{\mathscr{F}}_a^T \begin{bmatrix} -\dot{\theta}(\overline{v}_L + \overline{v}'_L d_{e1})\cos\theta - \left(\dot{\overline{v}}_L + d_{e1}\dot{\overline{v}}'_L + \dot{\theta}(L+d_{e1})\right)\sin\theta \\ \left(\dot{\overline{v}}_L + d_{e1}\dot{\overline{v}}'_L + \dot{\theta}(L+d_{e1})\right)\cos\theta - \dot{\theta}(\overline{v}_L + \overline{v}'_L d_{e1})\sin\theta \\ 0 \end{bmatrix} \tag{3.66}$$

Using this result in the equation for particle kinetic energy, Equation (3.3), we get,

$$T_e = \frac{1}{2} m_e \left((\dot{\overline{v}}_L + \dot{\overline{v}}'_L d_{e1}) + (L + d_{e1})\dot{\theta} \right)^2 + \frac{1}{2} m_e (\overline{v}_L + \overline{v}'_L d_{e1})^2 \dot{\theta}^2 \tag{3.67}$$

2D Rigid Body Model (Timoshenko Beam)

First, we define the position centre of mass of the end-effector in the beam frames as.

$$\underset{\sim}{r}_e = \underset{\rightarrow}{\mathscr{F}}_b^T \begin{bmatrix} L + \overline{u}_L \\ \overline{v}_L \\ 0 \end{bmatrix} + \underset{\rightarrow}{\mathscr{F}}_c^T \begin{bmatrix} d_{e1} \\ 0 \\ 0 \end{bmatrix} \tag{3.68}$$

Here d_{e1} is the offset of the end-effector centre of mass from the end of the beam (as shown in Figure 3.2). Note that this assumes that the centre of mass of the end-effector is located along the neutral axis of the beam. If we model the end-effector as a rigid body we also need the orientation of the body. Since this is easily defined in the inertial frame, it is stated in the inertial frame.

$$\underset{\sim}{\theta}_e = \underset{\rightarrow}{\mathscr{F}}_a^T \begin{bmatrix} 0 \\ 0 \\ \theta + \psi_{zL} \end{bmatrix} \tag{3.69}$$

Transforming the position vector to the inertial frame

$$\underset{\sim}{r}_e = \underset{\rightarrow}{\mathscr{F}}_a^T \mathbf{C}_{ab} \left(\begin{bmatrix} L + \overline{u}_L \\ \overline{v}_L \\ 0 \end{bmatrix} + \mathbf{C}_{bc} \begin{bmatrix} d_{e1} \\ 0 \\ 0 \end{bmatrix} \right) \tag{3.70}$$

where $\mathbf{C}_{ab}$ is as given in Equation (3.17) and $\mathbf{C}_{bc}$ is,

$$\mathbf{C}_{bc} = \begin{bmatrix} 1 & -\psi_{zL} & 0 \\ \psi_{zL} & 1 & 0 \\ 0 & 0 & 1 \end{bmatrix} \tag{3.71}$$

which results in,

$$\underset{\sim}{r}_e = \underset{\rightarrow}{\mathscr{F}}_a^T \begin{bmatrix} (L + d_{e1} + \overline{u}_L)\cos\theta - (\overline{v}_L + d_{e1}\psi_{zL})\sin\theta \\ (L + d_{e1} + \overline{u}_L)\sin\theta + (\overline{v}_L + d_{e1}\psi_{zL})\cos\theta \\ 0 \end{bmatrix} \tag{3.72}$$

Differentiating the end-effector position with respect to time, we get the end-effector velocity,

$$\underset{\sim}{v}_e = \underset{\rightarrow}{\mathscr{F}}_a^T \begin{bmatrix} -\left(\dot{\overline{v}}_L + (L + d_{e1} + \overline{u}_L)\dot{\theta} + \dot{\psi}_{zL} d_{e1}\right)\sin\theta + \left(\dot{\overline{u}}_L - \dot{\theta}(\overline{v}_L + \psi_{zL} d_{e1})\right)\cos\theta \\ \left(\dot{\overline{v}}_L + (L + d_{e1} + \overline{u}_L)\dot{\theta} + \dot{\psi}_{zL} d_{e1}\right)\cos\theta + \left(\dot{\overline{u}}_L - \dot{\theta}(\overline{v}_L + \psi_{zL} d_{e1})\right)\sin\theta \\ 0 \end{bmatrix} \tag{3.73}$$

and its corresponding angular velocity is,

$$\underset{\sim}{\omega}_e = \underset{\rightarrow}{\mathscr{F}}_a^T \begin{bmatrix} 0 \\ 0 \\ \dot{\theta} + \dot{\psi}_{zL} \end{bmatrix} \tag{3.74}$$

Substituting the velocity into Equation (3.3), we get the translational kinetic energy,

$$T_{te} = \frac{1}{2} m_e \left(\dot{\overline{v}}_L + (\overline{u}_L + L + d_{e1})\dot{\theta} + d_{e1}\dot{\psi}_{zL} \right)^2 + \frac{1}{2} m_e \left(\dot{\overline{u}}_L - (\overline{v}_L + d_{e1}\psi_{zL})\dot{\theta} \right)^2 \tag{3.75}$$

The inertia matrix for the end-effector is assumed to be of the form,

$$\mathbf{J}_e = \begin{bmatrix} J_1 & 0 & 0 \\ 0 & J_2 & 0 \\ 0 & 0 & J_e \end{bmatrix} \tag{3.76}$$

Using this and the angular velocity from Equation (3.74) in Equation (3.7),

$$T_{re} = \frac{1}{2} J_e (\dot{\theta} + \dot{\psi}_{zL})^2 \tag{3.77}$$

Therefore, the kinetic energy of the end-effector is of the form,

$$T_e = \frac{1}{2} m_e \left(\dot{\overline{v}}_L + (\overline{u}_L + L + d_{e1})\dot{\theta} + d_{e1}\dot{\psi}_{zL} \right)^2 + \frac{1}{2} m_e \left(\dot{\overline{u}}_L - (\overline{v}_L + d_{e1}\psi_{zL})\dot{\theta} \right)^2 + \frac{1}{2} J_e (\dot{\theta} + \dot{\psi}_{zL})^2 \tag{3.78}$$

3D Rigid Body Model (Timoshenko Beam with Torsion)

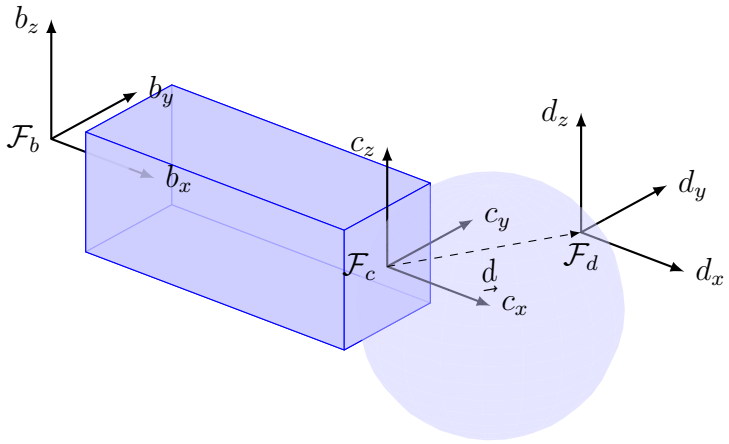

Figure 3.3: 3D end-effector offset

The frame of reference for the end-effector is located at the neutral axis of the beam (see Figure 3.3). So, the position of the end-effector's frame of reference can be found from Equation (3.36) when $x = L$ and both y and z are zero. This leads to,

$$\underset{\rightarrow}{r}_e = \underset{\rightarrow}{\mathscr{F}}_b^T \begin{bmatrix} L + \overline{u}_L \\ \overline{v}_L \\ \overline{w}_L \end{bmatrix} + \underset{\rightarrow}{\mathscr{F}}_c^T \begin{bmatrix} d_{e1} \\ d_{e2} \\ d_{d3} \end{bmatrix} \tag{3.79}$$

In this case, the end-effector has an offset of the vector $\underset{\rightarrow}{d}$ from the end of the beam. Note that torsion has no direct contribution to the position since the reference frame is at the neutral axis. However, it does affect the angular velocity of the end-effector. The position vector in the inertial frame is,

$$\underset{\rightarrow}{r}_e = \underset{\rightarrow}{\mathscr{F}}_a^T \mathbf{C}_{ab} \left(\begin{bmatrix} L + \overline{u}_L \\ \overline{v}_L \\ \overline{w}_L \end{bmatrix} + \mathbf{C}_{bc} \begin{bmatrix} d_{e1} \\ d_{e2} \\ d_{e3} \end{bmatrix} \right) \tag{3.80}$$

where $\mathbf{C}_{bc}$ is,

$$\mathbf{C}_{bc} = \begin{bmatrix} 1 & -\psi_{zL} & \psi_{yL} \\ \psi_{zL} & 1 & -\theta_{xL} \\ -\psi_{yL} & \theta_{xL} & 1 \end{bmatrix} \tag{3.81}$$

which results in,

$$\underset{\rightarrow}{r}_e = \underset{\rightarrow}{\mathscr{F}}_a^T \begin{bmatrix} (L + \overline{u}_L + d_{e1} - \psi_{zL} d_{e2} + \psi_{yL} d_{e3}) \cos\theta - (\overline{v}_L + d_{e2} + \psi_{zL} d_{e1} - \theta_{xL} d_{e3}) \sin\theta \\ (\overline{v}_L + d_{e2} + \psi_{zL} d_{e1} - \theta_{xL} d_{e3}) \cos\theta + (L + \overline{u}_L + d_{e1} - \psi_{zL} d_{e2} + \psi_{yL} d_{e3}) \sin\theta \\ \overline{w}_L + d_{e3} - \psi_{yL} d_{e1} + \theta_{xL} d_{e2} \end{bmatrix} \tag{3.82}$$

Differentiating with respect to time, we get the velocity of the end-effector in the inertial frame,

$$\begin{aligned} \underset{\rightarrow}{v}_e &= \underset{\rightarrow}{\mathscr{F}}_a^T \begin{bmatrix} \dot{\overline{u}}_L - \dot{\theta}(\overline{v}_L + d_{e2} + \psi_{zL} d_{e1} - \theta_{xL} d_{e3}) + \dot{\psi}_{yL} d_{e3} - \dot{\psi}_{zL} d_{e2} \\ -\left(\dot{\overline{v}}_L + \dot{\psi}_{zL} d_{e1} - \dot{\theta}_{xL} d_{e3} + \dot{\theta}(L + \overline{u}_L + d_{e1} - \psi_{zL} d_{e2} + \psi_{yL} d_{e3})\right) \\ 0 \end{bmatrix} \cos\theta \\ &+ \underset{\rightarrow}{\mathscr{F}}_a^T \begin{bmatrix} \dot{\overline{v}}_L + \dot{\psi}_{zL} d_{e1} - \dot{\theta}_{xL} d_{e3} + \dot{\theta}(L + \overline{u}_L + d_{e1} - \psi_{zL} d_{e2} + \psi_{yL} d_{e3}) \\ \dot{\overline{u}}_L - \dot{\theta}(\overline{v}_L + d_{e2} + \psi_{zL} d_{e1} - \theta_{xL} d_{e3}) + \dot{\psi}_{yL} d_{e3} - \dot{\psi}_{zL} d_{e2} \\ 0 \end{bmatrix} \sin\theta \\ &+ \begin{bmatrix} 0 \\ 0 \\ \dot{\overline{w}}_L - \dot{\psi}_{yL} d_{e1} + \dot{\theta}_{xL} d_{e2} \end{bmatrix} \end{aligned} \tag{3.83}$$

Which alternatively can be represented as,

$$\underset{\sim}{v}_e = \underset{\rightarrow}{\mathscr{F}}_a^T \begin{bmatrix} K_{ve1}\cos\theta - K_{ve2}\sin\theta \\ K_{ve2}\cos\theta + K_{ve1}\sin\theta \\ K_{ve3} \end{bmatrix} \tag{3.84}$$

where,

$$K_{ve1} = \dot{\overline{u}}_L - \dot{\theta}(\overline{v}_L + d_{e2} + \psi_{zL}d_{e1} - \theta_{xL}d_{e3}) + \dot{\psi}_{yL}d_{e3} - \dot{\psi}_{zL}d_{e2} \tag{3.85}$$

$$K_{ve2} = \dot{\overline{v}}_L + \dot{\psi}_{zL}d_{e1} - \dot{\theta}_{xL}d_{e3} + \dot{\theta}(L + \overline{u}_L + d_{e1} - \psi_{zL}d_{e2} + \psi_{yL}d_{e3}) \tag{3.86}$$

$$K_{ve3} = \dot{\overline{w}}_L - \dot{\psi}_{yL}d_{e1} + \dot{\theta}_{xL}d_{e2} \tag{3.87}$$

and the angular velocity is,

$$\underset{\sim}{\omega}_e = \underset{\rightarrow}{\mathscr{F}}_a^T \begin{bmatrix} \dot{\theta}_{xL} \\ \dot{\psi}_{yL} \\ \dot{\theta} + \dot{\psi}_{zL} \end{bmatrix} \tag{3.88}$$

In general, the end-effector has an inertia matrix of the form,

$$\mathbf{J}_e = \begin{bmatrix} J_{exx} & J_{exy} & J_{exz} \\ J_{exy} & J_{eyy} & J_{eyz} \\ J_{exz} & J_{eyz} & J_{ezz} \end{bmatrix} \tag{3.89}$$

which we can transform from the body-centric reference frame to the end of the beam using the formulas given in Chapter 2. Since the final product has the same form as given above, we will use this form to determine the rotational kinetic energy from Equation (3.7) viz.,

$$T_{re} = \frac{1}{2}(J_{exx}\dot{\theta}_{xL}^2 + J_{eyy}\dot{\psi}_{yL}^2 + J_{ezz}(\dot{\psi}_{yL} + \dot{\theta})^2) + \dot{\theta}_{xL}(J_{exy}\dot{\psi}_{yL} + J_{exz}(\dot{\theta} + \dot{\psi}_{zL})) + J_{eyz}\dot{\psi}_{yL}(\dot{\theta} + \dot{\psi}_{zL}) \tag{3.90}$$

Similarly, the translational kinetic energy is,

$$T_{te} = \frac{1}{2}m_e(K_{ve1}^2 + K_{ve2}^2 + K_{ve3}^2) \tag{3.91}$$

Now that the work, kinetic and strain energy is defined for each component in the system (and for each model) we can use these results in subsequent chapters in the variational principles to define the motion of the system (via Hamilton's Principle) and the capture equations (via Jourdain's Variational Principle).

CHAPTER

4 Mixed Symbolic-Numeric Finite Element Modelling

4.1 Introduction

In this chapter we are concerned with solving systems that can be derived through variational principles (*e.g.,* Hamilton's Principle) [58]. Therefore, we have equations of the following form to solve,

$$\delta \int_{t_0}^{t_1} L(\mathbf{q}, \mathbf{q}', t)\, \mathrm{d}t = 0 \tag{4.1}$$

where L (the Lagrangian) is a function of the column matrix $\mathbf{q}$, the variable t and possibly partial derivatives of $\mathbf{q}$. The solution to this problem is a system of Euler-Lagrange equations which take the form (assuming $L(\mathbf{q}, \mathbf{q}', t)$),

$$\frac{\partial}{\partial t}\left(\frac{\partial L}{\partial \dot{q}_i}\right) - \frac{\partial}{\partial x}\left(\frac{\partial L}{\partial q_i'}\right) - \frac{\partial L}{\partial q_i} = 0 \tag{4.2}$$

The difficulty with these partial differential equations (PDEs) is that they often have no known analytical solution. The standard approach to solving these PDEs is to use the Finite Element Method (FEM) to approximate the solution. For common PDEs there are standard finite element software packages that will solve these equations. However, for less common problems we must derive the system of equations that result from using the finite element method and then solve them (possibly with a standard package).

Symbolic techniques have been used in books [59, 60] to teach the finite element method but their use has been limited calculation of the stiffness matrix for specific elements and problems. Other work has been done on the derivation of optimized Fortran code using Macsyma [61, 62, 63, 64] for evaluation of the element stiffness matrix.They symbolically derive the strain-displacement relations and assume the stiffness matrix takes the form,

$$\mathbf{K} = \int_V \mathbf{B}^T \mathbf{D} \mathbf{B}\, \mathrm{d}V \tag{4.3}$$

where **B** is the strain-displacement matrix, **D** is the constitutive matrix, and the integral is over the volume V. The work by Beltzer also assumes this form of the stiffness matrix. This approach is fine if the forms of **B** and **D** for the specific problem are known but for more complex problems these need to be derived.

More general work by Amberg [65] relates to the development of a software package, "femLego", built upon Maple and Fortran. Their software begins with the specification of the weak form of the PDE and produces optimized Fortran code to solve the problem. However, the weak form of the PDE can be difficult to derive. Also, their formulation handles time domain solutions through finite differences and is limited in the types of elements and basis functions that can be used. These requirements limit the types of problems that can be solved.

Examining the previous work leads to the following goals for a new approach to the problem,

1. All work deriving the system of equations can be done using the software;
2. that there is no inherent limitation to the types of elements and basis functions that can be used;
3. static and dynamic problems are handled using the same approach.

4.2 Overview

The approach we are taking to derive and solve equations of the form given in Equation (4.1) is to divide the problem into two stages. First, we derive the equations valid for a single element in the finite element mesh using a symbolic computational approach. This is done using a Symbolic Finite Element Method (SFEM) package in Maple that we have developed. The second stage assembles the set of ODEs given these element matrices and a given mesh then solves the resulting system numerically. While a number of programming languages could be used for this task, Matlab is used because of its supporting facilities for numerical computation and analysis. This two stage approach uses the strengths of both symbolic and numeric computation.

An overview of the approach used to derive and solve the system equations is shown in Figure 4.1. The first step, defining the Lagrangian, is problem specific and can typically be handled using the standard Maple tools. The trial functions (*i.e.,* the approximations) used in the SFEM package are of the form,

$$f(x,t) = \sum_{i=1}^{n} \phi_i(x) q_i(t) \tag{4.4}$$

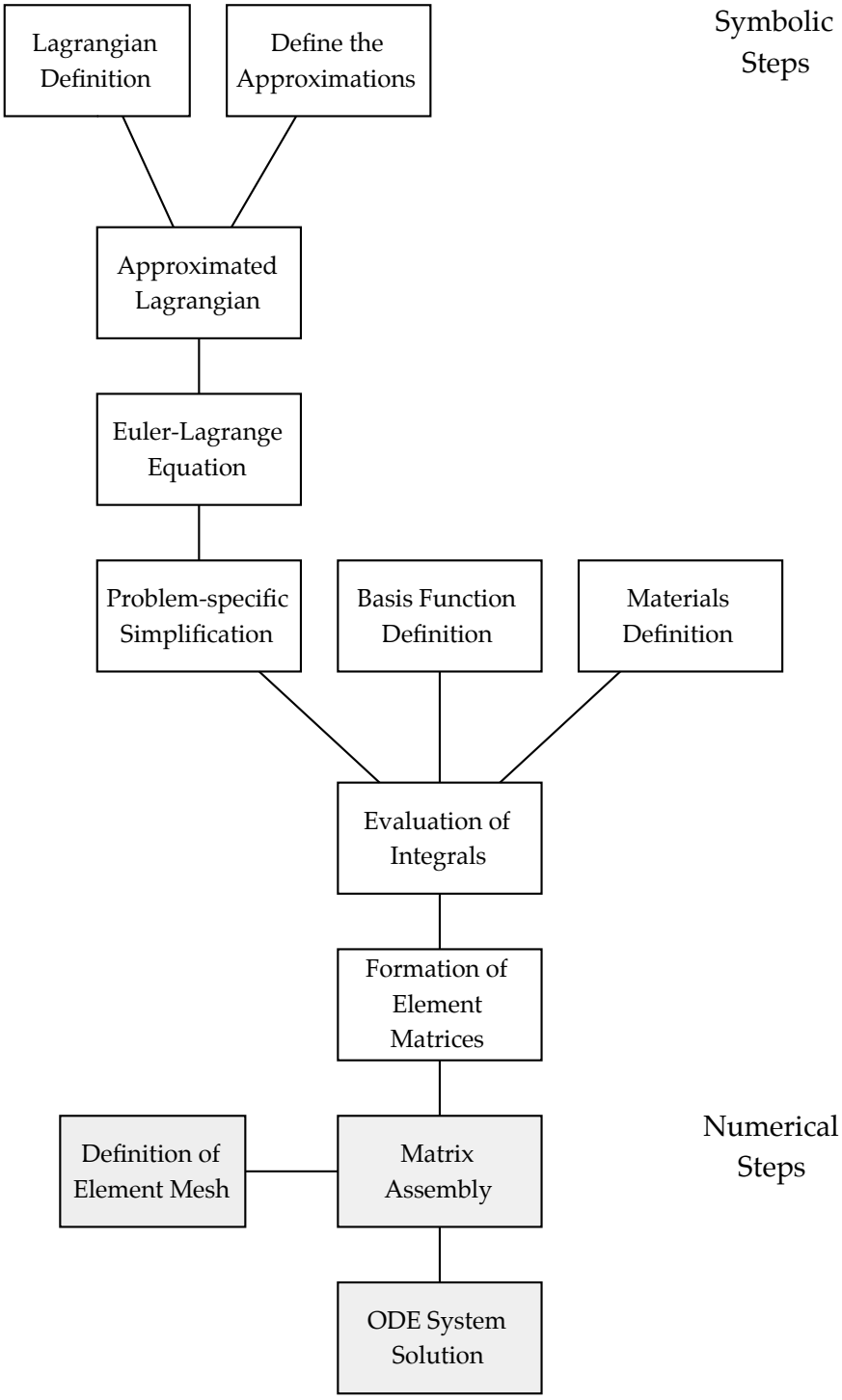

Figure 4.1: Element Matrix Calculation Process

where $\phi_i(x)$ are the basis functions and $q_i(t)$ are the nodal degrees-of-freedom (or nodal variables). Once the trial functions and Lagrangian are defined we substitute the trial functions into the Lagrangian L and calculate the Euler-Lagrange equations:

$$\frac{\mathrm{d}}{\mathrm{d}t}\left(\frac{\partial L}{\partial \dot{q}_i}\right) = \frac{\partial L}{\partial q_i} + Q_k \tag{4.5}$$

where Q_k are the generalized forces on the system. However, rather than calculating the complete equation we instead calculate the individual terms and return them separately since the left hand side leads to the mass matrix **M** while the right hand side leads to the stiffness matrix **K**. Typically, after the Euler-Lagrange equation has been calculated there are a number of simplifications that can be made.

The simplified results are combined with the definitions of the basis functions and the materials (as they may vary spatially) to evaluate the integrals in the system. Lastly, the element matrices are formed using the GenerateMatrix command from Maple's LinearAlgebra package.

Once the matrices are generated, we can use Maple's code generation features to generate optimized Matlab code which is output into separate functions for the mass and stiffness element matrices to be used in the assembly process.

4.3 Assembly of Full Matrices

Application of Boundary Conditions

To apply a forced boundary condition, there are two main techniques:

1. Removal of the degrees of freedom from the system;

2. Modify the system of equations to enforce the constraint.

Since the first approach is more computationally efficient it is used. Since the system has a pin joint at the hub, we will only consider the beam to be modelled as a cantilever beam in a rotating frame. So our boundary conditions at $x = 0$ require us to remove the rows and columns associate with the first node (for all element variables).

Augmentation of Matrices with Rotational DOF

Note that the governing equations of the system can be written in matrix form as:

$$\hat{\mathbf{M}}\ddot{\mathbf{q}} + \hat{\mathbf{K}}\mathbf{q} = \hat{\mathbf{F}} \tag{4.6}$$

where,

$$\hat{\mathbf{M}} = \begin{bmatrix} 0 & 0 \\ 0 & \mathbf{M} \end{bmatrix} + \begin{bmatrix} \hat{J} & \mathbf{t}^T \\ \mathbf{t} & 0 \end{bmatrix} + \mathbf{M}_e \tag{4.7}$$

$$\hat{\mathbf{K}} = \begin{bmatrix} 0 & 0 \\ 0 & \mathbf{K} \end{bmatrix} \tag{4.8}$$

$$\hat{\mathbf{F}} = \begin{bmatrix} M(\theta) \\ 0 \\ \cdots \\ 0 \end{bmatrix} \tag{4.9}$$

$$\mathbf{q} = \begin{bmatrix} \theta \\ \mathbf{d} \end{bmatrix} \tag{4.10}$$

Therefore, the augmentation of the stiffness matrix can be performed by the addition of a new row and column of all zeros. Augmentation of the mass matrix requires the calculation of $\hat{J}$ (the effective inertia of the hub), $\mathbf{t}$ which is the contribution of the beam inertia to the hub equation, and the matrix $\mathbf{M}_e$ which is the contribution of the end-effector's inertia to the system. Note that the material mass and stiffness matrices $\mathbf{M}$ and $\mathbf{K}$ that are used in these equations are the reduced DOF matrices resulting from the application of boundary conditions.

4.4 Newmark-Beta Solver

Bathe and Wilson [66] present a version of the Newmark-Beta method that does not require a prediction-correction step. The overview of the method as presented in Bathe and Wilson [66] is presented below. Starting with the following equations,

$$\dot{U}_{t+\Delta t} = \dot{U}_t + \left((1-\gamma)\ddot{U}_t + \gamma\ddot{U}_{t+\Delta t}\right)\Delta t \tag{4.11}$$

$$U_{t+\Delta t} = U_t + \dot{U}_t\Delta t + \left((\tfrac{1}{2}-\beta)\ddot{U}_t + \beta\ddot{U}_{t+\Delta t}\right)\Delta t \tag{4.12}$$

where β and γ are parameters that are chosen for accuracy and stability. Setting $\beta = \frac{1}{6}$ and $\gamma = \frac{1}{2}$ results in the linear acceleration method. Choosing $\beta = \frac{1}{4}$ and $\gamma = \frac{1}{2}$ results in an unconditionally stable scheme [66, 67] which uses a constant average acceleration. Note that

Bathe and Wilson [66] recommend these settings for good accuracy and stability. We also consider the equilibrium equations at time $t+\Delta t$,

$$\mathbf{M}\ddot{U}_{t+\Delta t} + \mathbf{C}\dot{U}_{t+\Delta t} + \mathbf{K}U_{t+\Delta t} = \mathbf{F}_{t+\Delta t} \tag{4.13}$$

In order to prevent the prediction-correction process, Bathe and Wilson [66] solve Equation (4.11) for $\ddot{U}_{t+\Delta t}$ in terms of $U_{t+\Delta t}$, and substitute the result into Equation (4.12). This results in equations for $\ddot{U}_{t+\Delta t}$ and $\dot{U}_{t+\Delta t}$ in terms of $U_{t+\Delta t}$ alone. These equations are then substituted into Equation (4.13) to solve for $U_{t+\Delta t}$. Then we can use the value of $U_{t+\Delta t}$ to calculate $\ddot{U}_{t+\Delta t}$ and $\dot{U}_{t+\Delta t}$.

According to Bathe and Wilson [66], to ensure unconditional stability for the damped system, the following constraints on the parameters in Equations (4.11) and (4.12) hold:

$$\gamma \geq \quad \tfrac{1}{2} \tag{4.14}$$

$$\beta \geq \quad \tfrac{1}{4}(\gamma + \tfrac{1}{2})^2 \tag{4.15}$$

In particular, we use the following values:

$$\gamma = \quad \tfrac{1}{2} \tag{4.16}$$

$$\beta = \quad \tfrac{1}{4} \tag{4.17}$$

This is also consistent with Heppler and Hansen [67] who state that

$$\gamma \geq \frac{1}{2} \qquad \beta \geq \frac{1}{2}\gamma \tag{4.18}$$

is unconditionally stable for the damped system. Note that in the system of equations that we are solving, none of our matrices depend upon time.

With this approach we can factorise the effective stiffness matrix once and only the effective load vector needs to change at each timestep.

4.5 Pure Torsion Convergence Test

To test whether this system properly represents a dynamic system, we consider the case of a fixed-free beam in pure torsion [68]. The natural frequency characteristic equation is [68],

$$\omega_n = \frac{(2n-1)\pi c}{2L} \tag{4.19}$$

$$c = \sqrt{\frac{G}{\rho}} \tag{4.20}$$

If we normalize the modes of the finite element model with respect to these equations, we get Figures 4.2 and 4.3. The first mode is nearly converged with just one element, but we can see that we converge to the analytical solutions to the first eight modes in less than 10 elements, so the finite element model can accurately represent this pure torsion model.

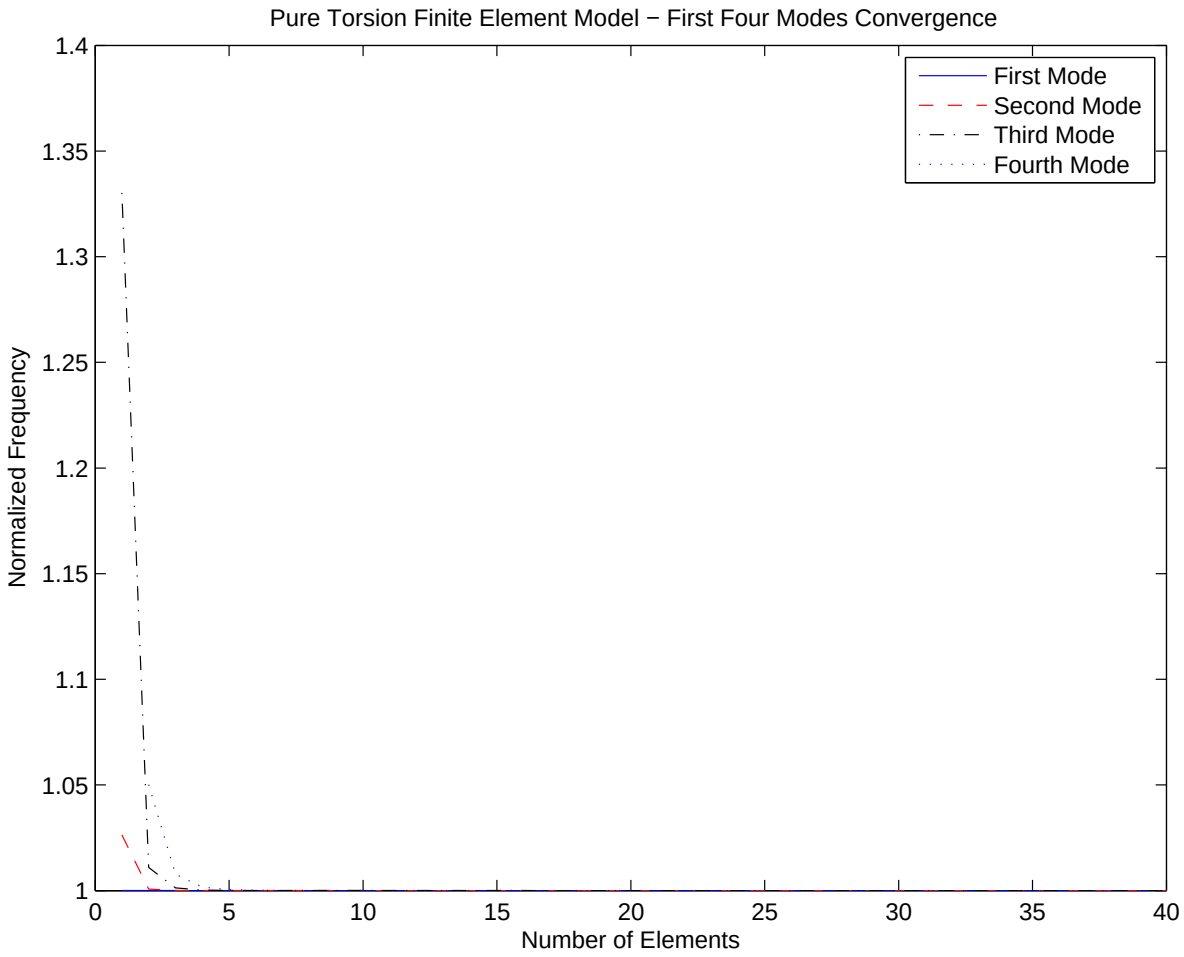

Figure 4.2: Pure Torsion Modes 1 through 4 Convergence

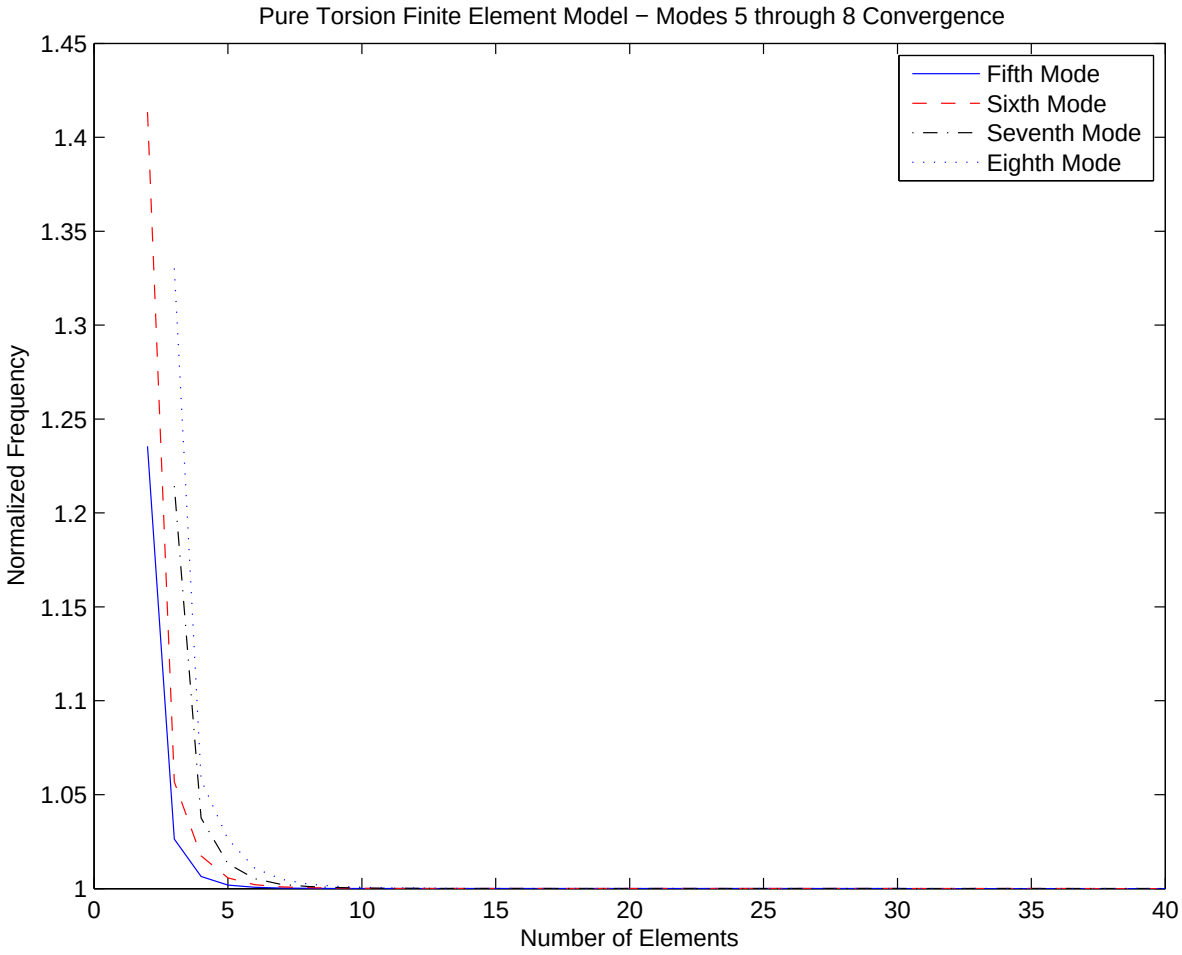

Figure 4.3: Pure Torsion Modes 5 through 8 Convergence

CHAPTER

5 Modelling the Capture Dynamics

This chapter presents the theory used in the analysis of the mass capture. First, the equations relating the pre- and post-impact velocities of a two particle system are presented. This is done to justify the modelling of a plastic impact as a set of constraints. Second, an overview of the variational theory of impact as presented in Bahar [29] is given. Next, we present a three step process to model the dynamics of mass capture. Finally, the variational theory of impact is applied to the system of interest.

5.1 Plastic Impact of Two Masses

Considering the impact of two smooth particles (Figure 5.1), the normal velocities before and after impact are related by [69]:

$$\underset{\rightarrow}{v}^{+}_{2n} - \underset{\rightarrow}{v}^{+}_{1n} = -e(\underset{\rightarrow}{v}^{-}_{2n} - \underset{\rightarrow}{v}^{-}_{1n}) \tag{5.1}$$

where e is the coefficient of restitution. Given that these are particles, Brach [69] also states that the tangential velocities are related by

$$\underset{\rightarrow}{v}^{+}_{1t} = \underset{\rightarrow}{v}^{+}_{2t} \tag{5.2}$$

Note that this is also true for rigid bodies with no sliding between the bodies. In the event of plastic impact, the coefficient of restitution is zero, therefore, Equation (5.1) becomes

$$\underset{\rightarrow}{v}^{+}_{2n} = \underset{\rightarrow}{v}^{+}_{1n} \tag{5.3}$$

Therefore, for plastic impacts, we can model the impact as a constraint upon the velocities of the particles. That is, after impact the velocities of the particles must be equal.

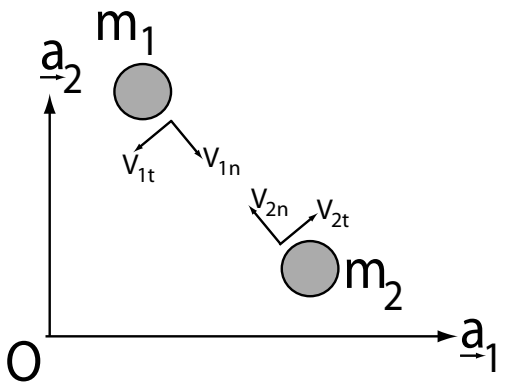

Figure 5.1: Two Particle Impact

5.2 Variational Methods for Mass Capture

From Bahar [29] the Jourdain Variational Principle (JVP) [28] is:

$$\sum_{i=1}^{n}\left[\frac{\mathrm{d}}{\mathrm{d}t}\left(\frac{\partial T}{\partial \dot{q}_i}\right)-\frac{\partial T}{\partial q_i}-Q_i\right]\delta\dot{q}_i=0 \tag{5.4}$$

where q_i is the i-coordinate of the system, T is the kinetic energy of the system, and Q_i is applied impulsive force i. Note that this formulation requires that both δq_i and δt be set equal to zero. Integrating Equation (5.4) with respect to time [29] (see also Appendix E) yields,

$$\sum_{i=1}^{n}\left[\Delta p_i-\hat{Q}_i\right]\delta\dot{q}_i=0 \tag{5.5}$$

where Δp_i is the increment in the generalised momentum:

$$\Delta p_i=(p_i)^{+}-(p_i)^{-} \tag{5.6}$$

between the pre-impact and post-impact states with $\hat{Q}_i$ being the generalised impulse. The generalised momentum p_i of the state is given by [29]:

$$p_i=\frac{\partial T}{\partial \dot{q}_i} \tag{5.7}$$

Therefore, Equation (5.5) can be written as

$$\sum_{i=1}^{n}\left[\frac{\partial T}{\partial \dot{q}_i}^{+}-\frac{\partial T}{\partial \dot{q}_i}^{-}-\hat{Q}_i\right]\delta\dot{q}_i=0 \tag{5.8}$$

The above analysis holds for "true" velocities. However, Bahar [29] shows that the above also holds when velocities are mapped to quasi-velocities[1]. This form is presented in Equation (5.9) below.

$$\sum_{j=1}^{k}\left[\frac{\partial T^{*}{}^{+}}{\partial \dot{\mathscr{Q}}_j}-\frac{\partial T^{*}{}^{-}}{\partial \dot{\mathscr{Q}}_j}-\hat{\Pi}_j\right]\delta\dot{\mathscr{Q}}_j=0 \tag{5.9}$$

where $\dot{\mathscr{Q}}_j$ are the quasi-velocities, $\frac{\partial T^*}{\partial \dot{\mathscr{Q}}_j}$ is the generalised quasi-momentum, and $\hat{\Pi}_j$ is the generalised quasi-impulse associated with the quasi-velocity $\dot{\mathscr{Q}}_j$.

Note that any velocity constraint can be modelled as an additional quasi-velocity. A plastic impact can be considered to be a set of velocity constraints as shown in Section 5.1. Therefore, we can embed the constraints into the problem by converting to quasi-velocities. This approach of constraint embedding differs from the approach done by Kövecses *et al.* [3].

Since each of the quasi-velocity variations are independent, either the variation or the term multiplying the variation must go to zero. The variations with respect to the constrained quasi-velocities will be zero since the quasi-velocity values are fixed via the constraints after impact and can be calculated before impact. Before, impact they will be defined by the initial pre-impact conditions and after impact the quasi-velocities are set to satisfy the constraint. However, the velocity variation with respect to the remaining quasi-velocities will not be zero. Therefore, Equation (5.9) will result in a set of $k-m$ (where m is the number of velocity constraints) equations of the form,

$$\frac{\partial T^{*}{}^{+}}{\partial \dot{\mathscr{Q}}_j}-\frac{\partial T^{*}{}^{-}}{\partial \dot{\mathscr{Q}}_j}-\hat{\Pi}_j=0, j\in\mathbf{A} \tag{5.10}$$

where **A** is the set of unconstrained quasi-velocities. These equations relate the post-impact velocities to the pre-impact velocities. It is important to note that this analysis assumes that the capture process occurs instantaneously.

5.3 Analysis Process for Mass Capture Problems

The analysis process for mass capture problems is as follows:

1. Solve the pre-capture system of equations until time t_1, the instant of impact/capture.
2. Use the final velocities from step 1 to determine post-capture velocities. This is done using the variational method presented above.

[1] A quasi-velocity is a "linear combination of the generalized velocities, but they are not necessarily derivatives of any coordinates and thus cannot always be integrated to generalized coordinates." [30] Examples of quasi-velocities are Euler angles and nonholonmic constraints. Since the capture contraints are nonholonomic we can model them as quasi-velocities.

3. Solve the post-capture system of equations using the post-capture velocity results from step 2 as initial conditions. Note that the position initial conditions are the same as the final position of step 1, since the analysis in step 2 assumes that the impact is instantaneous.

where the pre-capture and post-capture system of equations can be derived through traditional means (e.g., Hamilton's Principle). This analysis process is consistent with the approach taken by Kövecses *et al.* [27].

5.4 Capture Process Models

We will use the analysis process for different system models. The different models are:

1. A 2D Euler-Bernoulli beam (with no extension) and point masses for the target and the end-effector;

2. A 2D Timoshenko beam (including extension) and 2D rigid bodies for the target and the end-effector. It is assumed that the capture happens along the neutral axis of the beam;

3. A 3D Timoshenko beam and 3D rigid bodies for the target and the end-effector. The capture can happen anywhere.

Note that the 2D Euler-Bernoulli beam model included as a based of comparison with the work done by Kövecses *et al.* [3, 4]. This chapter will show the complete process for the last two cases and the results of the other first case. The details of the analysis for the first case are shown in Appendix F.

5.5 2D Euler-Bernoulli Beam (with Point Masses) System

Considering a 2D Euler-Bernoulli beam (as in section 3.3 and point mass end-effector (section 3.4) and target (section 3.2), we get the following capture equations (complete details of the

derivation are in Appendix F).

$$\dot{\overline{v}}_L^+ = \frac{m_e\left(\dot{\overline{v}}_L^- + (L+d_{e1})\dot{\theta}^- + d_{e1}\dot{\overline{v}}'^-_L\right) + m_t\left(\dot{y}_t^- \cos\theta_0 - \dot{x}_t^- \sin\theta_0\right) - (m_e+m_t)(L+d_{e1})\dot{\theta}^+}{2(m_t+m_e)} \tag{5.11}$$

$$\dot{\overline{v}}'^+_L = \frac{\dot{\overline{v}}_L^+}{d_{e1}} \tag{5.12}$$

$$\dot{\overline{v}}(x)^+ = \dot{\overline{v}}(x)^- - x(\dot{\theta}^- - \dot{\theta}^+) \tag{5.13}$$

$$\dot{\theta}^+ = \frac{\left(J_m + m_e(\overline{v}'_{L0}d_{e1} + \overline{v}_{L0})^2 + \int_0^L \rho\left(A\overline{v}_0(x)^2 + I_{yy}\right)\mathrm{d}x\right)\dot{\theta}^- - m_t(\overline{v}'_{L0}d_{e1} + \overline{v}_{L0})(\dot{x}_t^- \cos\theta_0 + \dot{y}_t^- \sin\theta_0)}{J_m + (m_e+m_t)(\overline{v}'_{L0}d_{e1} + \overline{v}_{L0})^2 + \int_0^L \rho\left(A\overline{v}_0(x)^2 + I_{yy}\right)\mathrm{d}x} \tag{5.14}$$

Note that in contrast to the work of Kövecses *et al.* [3, 4], this 2D Euler-Bernoulli beam model does not assume the end-effector is coincident with the end of the beam. Instead, we allow for an offset so the point mass can be placed at the centre of mass of the end-effector. Therefore, we have additional terms with $\overline{v}'_{L0}d_{e1}$ and $\dot{\overline{v}}'_L$. Also, our model includes beam inertia (I_{yy}) which is missing in theirs because their definition of an element of the beam is,

$$\underset{\rightarrow}{r}_{xK} = \underset{\rightarrow}{\mathscr{F}}_b^T \begin{bmatrix} x \\ v \\ 0 \end{bmatrix} \tag{5.15}$$

which is missing the y term in the second component as compared to Equation (3.15). The $\overline{v}'$ terms in Equation (3.15) are ignored in the kinetic energy of an Euler-Bernoulli beam so they don't affect the capture equations along the length. The only appear in the capture equations at the end of the beam due to the offset of the end-effector.

5.6 2D Timoshenko Beam (with Rigid Bodies) System

Now we will consider a model in between the other two models set out in section 5.4. Here, we have a 2D Timoshenko beam (as in section 3.3) and 2D rigid body end-effector (section 3.4) and target (section 3.2).

Post-capture velocity constraint

Since the capture is assumed to happen instantaneously, the position variables won't change. So, replacing the position variables (but not the velocities) with their values at the instant of

capture (time t_1),

$$\underset{\sim}{v}_e = \underset{\rightarrow}{\mathscr{F}}_a^T \begin{bmatrix} \left(\dot{\overline{u}}_L - \dot{\theta}(\overline{v}_{L0} + \psi_{zL0} d_{e1})\right)\cos\theta_0 - \left(\dot{\overline{v}}_L + (L + d_{e1} + \overline{u}_{L0})\dot{\theta} + \dot{\psi}_{zL} d_{e1}\right)\sin\theta_0 \\ \left(\dot{\overline{v}}_L + (L + d_{e1} + \overline{u}_{L0})\dot{\theta} + \dot{\psi}_{zL} d_{e1}\right)\cos\theta_0 + \left(\dot{\overline{u}}_L - \dot{\theta}(\overline{v}_{L0} + \psi_{zL0} d_{e1})\right)\sin\theta_0 \\ 0 \end{bmatrix} \quad (5.16)$$

$$\underset{\sim}{\omega}_e(t) = \underset{\rightarrow}{\mathscr{F}}_a^T \begin{bmatrix} 0 \\ 0 \\ \dot{\theta}(t) + \dot{\psi}_{zL}(t) \end{bmatrix} \quad (5.17)$$

$$\underset{\sim}{v}_t(t) = \underset{\rightarrow}{\mathscr{F}}_a^T \begin{bmatrix} \dot{x}_t(t) \\ \dot{y}_t(t) \\ 0 \end{bmatrix} \quad (5.18)$$

$$\underset{\sim}{\omega}_t(t) = \underset{\rightarrow}{\mathscr{F}}_a^T \begin{bmatrix} 0 \\ 0 \\ \dot{\gamma}(t) \end{bmatrix} \quad (5.19)$$

$$\underset{\sim}{v}_x = \underset{\rightarrow}{\mathscr{F}}_a^T \begin{bmatrix} [\dot{\overline{u}} - y\dot{\psi}_z + \dot{\theta}(y + \overline{v}_0)]\cos\theta_0 - [\dot{\overline{v}} - \dot{\theta}(x + \overline{u}_0 - y\psi_{z0})]\sin\theta_0 \\ [\dot{\overline{v}} - \dot{\theta}(x + \overline{u}_0 - y\psi_{z0})]\cos\theta_0 + [\dot{\overline{u}} - y\dot{\psi}_z + \dot{\theta}(y + \overline{v}_0)]\sin\theta_0 \\ 0 \end{bmatrix} \quad (5.20)$$

Modelling the capture process as a plastic collision, we get that the velocities before and after impact must be equivalent. Since we are modelling the end-effector and target as rigid bodies we equate both the translational and rotational velocities respectively. First, equating the translational velocities yields,

$$\dot{x}_t(t) = \left(\dot{\overline{u}}_L - \dot{\theta}(\overline{v}_{L0} + \psi_{zL0} d_{e1})\right)\cos\theta_0 - \left(\dot{\overline{v}}_L + (L + d_{e1} + \overline{u}_{L0})\dot{\theta} + \dot{\psi}_{zL} d_{e1}\right)\sin\theta_0 \quad (5.21)$$

$$\dot{y}_t(t) = \left(\dot{\overline{v}}_L + (L + d_{e1} + \overline{u}_{L0})\dot{\theta} + \dot{\psi}_{zL} d_{e1}\right)\cos\theta_0 + \left(\dot{\overline{u}}_L - \dot{\theta}(\overline{v}_{L0} + \psi_{zL0} d_{e1})\right)\sin\theta_0 \quad (5.22)$$

and equating the rotational velocities gives,

$$\dot{\gamma}(t) = \dot{\theta}(t) + \dot{\psi}_{zL}(t) \quad (5.23)$$

Rearraging these equations so that all terms are on the left-hand side, leads to

$$\dot{x}_t(t) + \left(\dot{\overline{v}}_L + (L + d_{e1} + \overline{u}_{L0})\dot{\theta} + \dot{\psi}_{zL} d_{e1}\right)\sin\theta_0 - \left(\dot{\overline{u}}_L - \dot{\theta}(\overline{v}_{L0} + \psi_{zL0} d_{e1})\right)\cos\theta_0 = 0 \quad (5.24)$$

$$\dot{y}_t(t) - \left(\dot{\overline{v}}_L + (L + d_{e1} + \overline{u}_{L0})\dot{\theta} + \dot{\psi}_{zL} d_{e1}\right)\cos\theta_0 + \left(\dot{\overline{u}}_L - \dot{\theta}(\overline{v}_{L0} + \psi_{zL0} d_{e1})\right)\sin\theta_0 = 0 \quad (5.25)$$

$$\dot{\gamma}(t) - \dot{\theta}(t) - \dot{\psi}_{zL}(t) = 0 \quad (5.26)$$

Quasi-velocities

We now convert each of the beam and end-effector velocity variables to quasi-velocities.

$$\dot{\mathscr{Q}}_1(t) = \dot{\psi}_z(x,t) \tag{5.27}$$
$$\dot{\mathscr{Q}}_2(t) = \dot{\psi}_{zL}(t) \tag{5.28}$$
$$\dot{\mathscr{Q}}_3(x,t) = \dot{\theta}(t) \tag{5.29}$$
$$\dot{\mathscr{Q}}_4(x,t) = \dot{\overline{u}}(x,t) \tag{5.30}$$
$$\dot{\mathscr{Q}}_5(x,t) = \dot{\overline{u}}_L(t) \tag{5.31}$$
$$\dot{\mathscr{Q}}_6(t) = \dot{\overline{v}}(x,t) \tag{5.32}$$
$$\dot{\mathscr{Q}}_7(t) = \dot{\overline{v}}_L(t) \tag{5.33}$$

There are three remaining quasi-velocities necessary to completely define the system. The three constraint equations (Equations (5.21) - (5.23)) are chosen to be the these three remaining quasi-velocities. So, substituting the quasi-velocity relations into the constraint equations, yields

$$\dot{x}_t(t) + \left(\dot{\mathscr{Q}}_7 + (L + d_{e1} + \overline{u}_{L0})\dot{\mathscr{Q}}_3 + \dot{\mathscr{Q}}_2 d_{e1}\right)\sin\theta_0 - \left(\dot{\mathscr{Q}}_5 - \dot{\mathscr{Q}}_3(\overline{v}_{L0} + \psi_{zL0} d_{e1})\right)\cos\theta_0 = 0 \tag{5.34}$$
$$\dot{y}_t(t) - \left(\dot{\mathscr{Q}}_7 + (L + d_{e1} + \overline{u}_{L0})\dot{\mathscr{Q}}_3 + \dot{\mathscr{Q}}_2 d_{e1}\right)\cos\theta_0 + \left(\dot{\mathscr{Q}}_5 - \dot{\mathscr{Q}}_3(\overline{v}_{L0} + \psi_{zL0} d_{e1})\right)\sin\theta_0 = 0 \tag{5.35}$$
$$\dot{\gamma}(t) - \dot{\mathscr{Q}}_3(t) - \dot{\mathscr{Q}}_2(t) = 0 \tag{5.36}$$

Now we equate the left-hand side of each equation to a quasi-velocity variable according to,

$$\dot{\mathscr{Q}}_8 = \dot{x}_t(t) + \left(\dot{\mathscr{Q}}_7 + (L + d_{e1} + \overline{u}_{L0})\dot{\mathscr{Q}}_3 + \dot{\mathscr{Q}}_2 d_{e1}\right)\sin\theta_0 - \left(\dot{\mathscr{Q}}_5 - \dot{\mathscr{Q}}_3(\overline{v}_{L0} + \psi_{zL0} d_{e1})\right)\cos\theta_0 \tag{5.37}$$
$$\dot{\mathscr{Q}}_9 = \dot{y}_t(t) - \left(\dot{\mathscr{Q}}_7 + (L + d_{e1} + \overline{u}_{L0})\dot{\mathscr{Q}}_3 + \dot{\mathscr{Q}}_2 d_{e1}\right)\cos\theta_0 + \left(\dot{\mathscr{Q}}_5 - \dot{\mathscr{Q}}_3(\overline{v}_{L0} + \psi_{zL0} d_{e1})\right)\sin\theta_0 \tag{5.38}$$
$$\dot{\mathscr{Q}}_{10} = \dot{\gamma} - \dot{\mathscr{Q}}_3 - \dot{\mathscr{Q}}_2 \tag{5.39}$$

Quasi-kinetic energy

To calculate the kinetic energy of the target it is necessary to rearrage the quasi-velocity expressions in terms of the original target velocity variables ($\dot{x}_t(t)$, $\dot{y}_t(t)$, $\dot{\gamma}(t)$). So, the new translational velocity expression is,

$$\underset{\sim}{v}_t(t) = \underset{\sim}{\mathscr{F}}_a^T \begin{bmatrix} \dot{\mathscr{Q}}_8 - \left(\dot{\mathscr{Q}}_7 + (L + d_{e1} + \overline{u}_{L0})\dot{\mathscr{Q}}_3 + \dot{\mathscr{Q}}_2 d_{e1}\right)\sin\theta_0 + \left(\dot{\mathscr{Q}}_5 - \dot{\mathscr{Q}}_3(\overline{v}_{L0} + \psi_{zL0} d_{e1})\right)\cos\theta_0 \\ \dot{\mathscr{Q}}_9 + \left(\dot{\mathscr{Q}}_7 + (L + d_{e1} + \overline{u}_{L0})\dot{\mathscr{Q}}_3 + \dot{\mathscr{Q}}_2 d_{e1}\right)\cos\theta_0 - \left(\dot{\mathscr{Q}}_5 - \dot{\mathscr{Q}}_3(\overline{v}_{L0} + \psi_{zL0} d_{e1})\right)\sin\theta_0 \\ 0 \end{bmatrix} \tag{5.40}$$

and the new angular velocity is,

$$\underset{\sim}{\omega}_e(t) = \underset{\sim}{\mathscr{F}}_a^T \begin{bmatrix} 0 \\ 0 \\ \dot{\mathscr{Q}}_{10}(t) + \dot{\mathscr{Q}}_3 + \dot{\mathscr{Q}}_2 \end{bmatrix} \tag{5.41}$$

The translational kinetic energy of a rigid body is,

$$T_{trans} = \frac{1}{2} m \underset{\rightarrow}{v} \cdot \underset{\rightarrow}{v} \tag{5.42}$$

For the target, this results in (for simplicity of form the variable dependence is left out),

$$T_{tt}^{*} = \frac{1}{2} m_t \left(\left(\dot{\mathscr{Q}}_8 - K_{tt1} \sin\theta_0 + K_{tt2} \cos\theta_0 \right)^2 + \left(\dot{\mathscr{Q}}_9 + K_{tt1} \cos\theta_0 - K_{tt2} \sin\theta_0 \right)^2 \right) \tag{5.43}$$

where,

$$K_{tt1} = \dot{\mathscr{Q}}_7 + (L + d_{e1} + \overline{u}_{L0}) \dot{\mathscr{Q}}_3 + \dot{\mathscr{Q}}_2 d_{e1} \tag{5.44}$$

$$K_{tt2} = \dot{\mathscr{Q}}_5 - \dot{\mathscr{Q}}_3 (\overline{v}_{L0} + \psi_{zL0} d_{e1}) \tag{5.45}$$

Similarly, the rotational kinetic energy of a rigid body is,

$$T_{rot} = \frac{1}{2} \underset{\rightarrow}{\omega} \mathbf{J} \underset{\rightarrow}{\omega} \tag{5.46}$$

where **J** is the inertia matrix for the body. For the target in this case, the inertia matrix can be stated as,

$$\mathbf{J} = \begin{bmatrix} J_{t1} & 0 & 0 \\ 0 & J_{t2} & 0 \\ 0 & 0 & J_t \end{bmatrix} \tag{5.47}$$

Resulting in the rotational quasi-kinetic energy of the target as,

$$T_{tr}^{*} = \frac{1}{2} J_t (\dot{\mathscr{Q}}_{10} + \dot{\mathscr{Q}}_3 + \dot{\mathscr{Q}}_2)^2 \tag{5.48}$$

The end-effector velocity using quasi-velocities is,

$$\underset{\rightarrow}{v}_e(t) = \underset{\rightarrow}{\mathscr{F}}_a^T \begin{bmatrix} \left(\left(\dot{\mathscr{Q}}_5 - \dot{\mathscr{Q}}_3 (\overline{v}_{L0} + \psi_{zL0} d_{e1}) \right) \cos\theta_0 - \dot{\mathscr{Q}}_7 + (L + d_{e1} + \overline{u}_{L0}) \dot{\mathscr{Q}}_3 + \dot{\mathscr{Q}}_2 d_{e1} \right) \sin\theta_0 \\ \left(\dot{\mathscr{Q}}_7 + (L + d_{e1} + \overline{u}_{L0}) \dot{\mathscr{Q}}_3 + \dot{\mathscr{Q}}_2 d_{e1} \right) \cos\theta_0 + \left(\dot{\mathscr{Q}}_5 - \dot{\mathscr{Q}}_3 (\overline{v}_{L0} + \psi_{zL0} d_{e1}) \right) \sin\theta_0 \\ 0 \end{bmatrix} \tag{5.49}$$

and its corresponding angular velocity is,

$$\underset{\rightarrow}{\omega}_e(t) = \underset{\rightarrow}{\mathscr{F}}_a^T \begin{bmatrix} 0 \\ 0 \\ \dot{\mathscr{Q}}_3(t) + \dot{\mathscr{Q}}_2(t) \end{bmatrix} \tag{5.50}$$

The inertia matrix for the end effector in this case is,

$$\mathbf{J} = \begin{bmatrix} J_{e1} & 0 & 0 \\ 0 & J_{e2} & 0 \\ 0 & 0 & J_e \end{bmatrix} \tag{5.51}$$

This results in the following expressions for the translational and rotational quasi-kinetic energies.

$$T_{et}^{*} = \frac{1}{2} m_e \left(\left(\dot{\mathscr{Q}}_7 + (L + d_{e1} + \overline{u}_{L0}) \dot{\mathscr{Q}}_3 + \dot{\mathscr{Q}}_2 d_{e1} \right)^2 + \left(\dot{\mathscr{Q}}_5 - \dot{\mathscr{Q}}_3 (\overline{v}_{L0} + \psi_{zL0} d_{e1}) \right)^2 \right) \tag{5.52}$$

$$T_{er}^{*} = \frac{1}{2} J_e (\dot{\mathscr{Q}}_3 + \dot{\mathscr{Q}}_2)^2 \tag{5.53}$$

The quasi-kinetic energy due to the flexibility of the beam is in general,

$$T_b = \frac{1}{2} \int_V \rho (\underset{\sim}{v}_b \cdot \underset{\sim}{v}_b) \mathrm{d}V \tag{5.54}$$

where ρ is the volume mass density. In this case, $\underset{\sim}{v}_b$ is given by,

$$\underset{\sim}{v}_b(x,t) = \underset{\rightarrow a}{\mathscr{F}}^T \begin{bmatrix} [\dot{\mathscr{Q}}_4 - y\dot{\mathscr{Q}}_1 + \dot{\mathscr{Q}}_3 (y + \overline{v}_0)] \cos\theta_0 - [\dot{\mathscr{Q}}_6 - \dot{\mathscr{Q}}_3 (x + \overline{u}_0 - y\psi_{z0})] \sin\theta_0 \\ [\dot{\mathscr{Q}}_6 - \dot{\mathscr{Q}}_3 (x + \overline{u}_0 - y\psi_{z0})] \cos\theta_0 + [\dot{\mathscr{Q}}_4 - y\dot{\mathscr{Q}}_1 + \dot{\mathscr{Q}}_3 (y + \overline{v}_0)] \sin\theta_0 \\ 0 \end{bmatrix} \tag{5.55}$$

Resulting in the following expression for the kinetic energy of the beam,

$$T_b^{*} = \frac{1}{2} \int_V \rho \left([\dot{\mathscr{Q}}_4 - y\dot{\mathscr{Q}}_1 + \dot{\mathscr{Q}}_3 (y + \overline{v}_0)]^2 + [\dot{\mathscr{Q}}_6 - \dot{\mathscr{Q}}_3 (x + \overline{u}_0 - y\psi_{z0})] \right) \mathrm{d}V \tag{5.56}$$

The kinetic energy of the motor is,

$$T_m^{*} = \frac{1}{2} J_m \dot{\mathscr{Q}}_3^2 \tag{5.57}$$

where J_m is the inertia of the motor. The total quasi-kinetic energy of the system is given by the sum of Equations (5.43), (5.48), (5.52), (5.53), (5.56), and (5.57).

Generalised Quasi-momenta

The quasi-momenta for the system can be found by differentiating the total quasi-kinetic energy of the system, as per

$$\frac{\partial T^*}{\partial \dot{\mathcal{Q}}_1} = \int_V \rho \left(y^2(\dot{\mathcal{Q}}_1 + \dot{\mathcal{Q}}_3) - y(\dot{\mathcal{Q}}_4 - \overline{v}_0 \dot{\mathcal{Q}}_3) \right) \mathrm{d}V \tag{5.58}$$

$$\begin{aligned} \frac{\partial T^*}{\partial \dot{\mathcal{Q}}_2} &= (m_e + m_t) d_{e1} \left(d_{e1}(\dot{\mathcal{Q}}_2 + \dot{\mathcal{Q}}_3) + \dot{\mathcal{Q}}_7 + (L + \overline{u}_{L0}) \dot{\mathcal{Q}}_3 \right) \\ &\quad + (J_t + J_e)(\dot{\mathcal{Q}}_2 + \dot{\mathcal{Q}}_3) + m_t d_{e1}(-\dot{\mathcal{Q}}_8 \sin\theta_0 + \dot{\mathcal{Q}}_9 \cos\theta_0) + J_t \dot{\mathcal{Q}}_{10} \end{aligned} \tag{5.59}$$

$$\begin{aligned} \frac{\partial T^*}{\partial \dot{\mathcal{Q}}_3} &= ((J_e + J_t) + (m_e + m_t) d_{e1}(L + \overline{u}_{L0} + d_{e1})) \dot{\mathcal{Q}}_2 + (J_m + J_e + J_t) \dot{\mathcal{Q}}_3 \\ &\quad + (m_e + m_t) \left(\left((L + \overline{u}_{L0} + d_{e1})^2 + (\overline{v}_{L0} + d_{e1} \psi_{zL0})^2 \right) \dot{\mathcal{Q}}_3 + (L + \overline{u}_{L0} + d_{e1}) \dot{\mathcal{Q}}_7 \right. \\ &\quad \left. + (\overline{v}_{L0} + d_{e1} \psi_{zL0}) \dot{\mathcal{Q}}_5 \right) - m_t \left((\overline{v}_{L0} + d_{e1} \psi_{zL0})(\dot{\mathcal{Q}}_8 \cos\theta_0 + \dot{\mathcal{Q}}_9 \sin\theta_0) \right. \\ &\quad \left. - (L + \overline{u}_{L0} + d_{e1})(-\dot{\mathcal{Q}}_8 \sin\theta_0 + \dot{\mathcal{Q}}_9 \cos\theta_0) \right) + J_t \dot{\mathcal{Q}}_{10} + \int_V \rho \left(-(y + \overline{v}_0) \dot{\mathcal{Q}}_4 \right. \\ &\quad \left. (x + \overline{u}_0 - y\psi_z) \dot{\mathcal{Q}}_6 + y(y + \overline{v}_0) \dot{\mathcal{Q}}_1 + \left((x + \overline{u}_0 - y\psi_z)^2 + (y + \overline{v}_0)^2 \right) \dot{\mathcal{Q}}_3 \right) \mathrm{d}V \end{aligned} \tag{5.60}$$

$$\frac{\partial T^*}{\partial \dot{\mathcal{Q}}_4} = \int_V \rho \left(-\overline{v}_0 \dot{\mathcal{Q}}_3 + \dot{\mathcal{Q}}_4 - y(\dot{\mathcal{Q}}_3 + \dot{\mathcal{Q}}_1) \right) \mathrm{d}V \tag{5.61}$$

$$\frac{\partial T^*}{\partial \dot{\mathcal{Q}}_5} = (m_e + m_t)(\dot{\mathcal{Q}}_5 - \dot{\mathcal{Q}}_3(\overline{v}_{L0} + d_{e1} \psi_{zL0}) + m_t(\dot{\mathcal{Q}}_8 \cos\theta_0 + \dot{\mathcal{Q}}_9 \sin\theta_0) \tag{5.62}$$

$$\frac{\partial T^*}{\partial \dot{\mathcal{Q}}_6} = \int_V \rho \left(\dot{\mathcal{Q}}_6 + (x + \overline{u}_0 - y\psi_{z0}) \dot{\mathcal{Q}}_3 \right) \mathrm{d}V \tag{5.63}$$

$$\frac{\partial T^*}{\partial \dot{\mathcal{Q}}_7} = (m_e + m_t)(\dot{\mathcal{Q}}_7 + \dot{\mathcal{Q}}_3(L + \overline{u}_{L0} + d_{e1}) + d_{e1} \dot{\mathcal{Q}}_2) + m_t(-\dot{\mathcal{Q}}_8 \sin\theta_0 + \dot{\mathcal{Q}}_9 \cos\theta_0) \tag{5.64}$$

Note that we don't need to calculate the quasi-momenta for the constraint quasi-variables since the variation associated with these quasi-momenta is zero (as stated in section 5.2).

Velocity Relations

The results from the previous section are used in the Jourdain Variational Principle (JVP) [29],

$$\sum_{i=1}^{10} \left(\frac{\partial T}{\partial \dot{\mathcal{Q}}_i}^{+} - \frac{\partial T}{\partial \dot{\mathcal{Q}}_i}^{-} \right) \delta \dot{\mathcal{Q}}_i = 0 \tag{5.65}$$

where the superscript + indicates the post-capture quasi-momentum, superscript − indicates the pre-capture quasi-momentum, and $\delta \dot{\mathcal{Q}}_i$ is the variation with respect to quasi-velocity i. The variation for $i = 8, 9, 10$ is zero since these quasi-velocities are constrained. Therefore, we have velocity relations for $i = 1..7$ as stated in the following equations. First, there is the velocity relation for the bending slope rate along the beam, $\dot{\psi}_z(x,t)$,

$$\int_V \rho y((y + \overline{v}_0)\dot{\theta}^+ - \dot{\overline{u}}(x)^+ + y\dot{\psi}_z(x)^+) \mathrm{d}V = \int_V \rho y((y + \overline{v}_0)\dot{\theta}^- - \dot{u}(x)^- + y\dot{\psi}_z(x)^-) \mathrm{d}V \tag{5.66}$$

Next, the velocity relation for the bending slope of the end of the beam $\dot{\psi}_{zL}(t)$,

$$\begin{aligned}&(m_e+m_t)d_{e1}\left(\dot{\overline{v}}_L^+ + d_{e1}\dot{\psi}_{zL}^+ + (L+\overline{u}_{L0}+d_{e1})\dot{\theta}^+\right) + (J_e+J_t)(\dot{\psi}_{zL}^+ + \dot{\theta}^+) = \\ &(m_e+m_t)d_{e1}\left(\dot{\overline{v}}_L^- + d_{e1}\dot{\psi}_{zL}^- + L + \overline{u}_{L0}+d_{e1})\dot{\theta}^-\right) + (J_t+J_e)(\dot{\psi}_{zL}^- + \dot{\theta}^-) \\ &+ m_t d_{e1}(-\dot{\mathcal{Q}}_8^- \sin\theta_0 + \dot{\mathcal{Q}}_9^- \cos\theta_0) + J_t\dot{\mathcal{Q}}_{10}^-\end{aligned} \tag{5.67}$$

The velocity relation for the angular velocity of the beam $\dot{\theta}(t)$.

$$\begin{aligned}&(m_e+m_t)\left(\left((L+\overline{u}_{L0}+d_{e1})^2 + (\overline{v}_{L0}+d_{e1}\psi_{zL0})^2\right)\dot{\theta}^+ - (\overline{v}_{L0}+d_{e1}\psi_{zL0})\dot{\overline{u}}_L^+\right. \\ &\left.+(L+\overline{u}_{L0}+d_{e1})(\dot{\overline{v}}_L^+ + d_{e1}\dot{\psi}_{zL}^+)\right) + (J_e+J_t)\dot{\psi}_{zL}^+ + (J_m+J_e+J_t)\dot{\theta}^+ \\ &+\int \rho\left(\left((x+\overline{u}_0-y\psi_z)^2 + (y+\overline{v}_0)^2\right)\dot{\theta}^+ - (y+\overline{v}_0)\dot{\overline{u}}^+ + (x+\overline{u}_0-y\psi_z)\dot{\overline{v}}^+ + y(y+\overline{v}_0)\dot{\psi}_z^+\right)\mathrm{d}V \\ &= (m_e+m_t)\left((L+\overline{u}_{L0}+d_{e1})^2 + (\overline{v}_{L0}+d_{e1}\psi_{zL0})^2\right)\dot{\theta}^- + (J_e+J_t)(\dot{\psi}_{zL}^- + \dot{\theta}^-) + J_m\dot{\theta}^- \\ &-(m_e+m_t)(\overline{v}_{L0}+d_{e1}\psi_{zL0})\dot{\overline{u}}_L^- + (m_e+m_t)d_{e1}(L+\overline{u}_{L0}+d_{e1})\dot{\psi}_{zL}^- + (m_e+m_t)(L+\overline{u}_{L0}+d_{e1})\dot{\overline{v}}_L^- \\ &+\int \rho(((x+\overline{u}_0-y\psi_z)^2 + (y+\overline{v}_0)^2)\dot{\theta}^- - (y+\overline{v}_0)\dot{\overline{u}}^- + (x+\overline{u}_0-y\psi_z)\dot{\overline{v}}^- + y(y+\overline{v}_0)\dot{\psi}_z^-)\mathrm{d}V \\ &-m_t(\overline{v}_{L0}+\psi_{zL0}d_{e1})(\dot{\mathcal{Q}}_8^-\cos\theta_0 + \dot{\mathcal{Q}}_9^-\sin\theta_0) + m_t(L+\overline{u}_{L0}+d_{e1})(\dot{\mathcal{Q}}_9^-\cos\theta_0 - \dot{\mathcal{Q}}_8^-\sin\theta_0) + J_t\dot{\mathcal{Q}}_{10}^-\end{aligned} \tag{5.68}$$

The velocity relation for the extension of the beam $\dot{\overline{u}}(x,t)$,

$$\int_V \rho\left(\dot{\overline{u}}(x)^+ - y\dot{\psi}^+ - (y+\overline{v}_0)\dot{\theta}^+\right)\,\mathrm{d}V = \int_V \rho\left(\dot{\overline{u}}(x)^- - y\dot{\psi}^- - (y+\overline{v}_0)\dot{\theta}^-\right)\,\mathrm{d}V \tag{5.69}$$

The velocity relation for the extension of the end of the beam $\dot{\overline{u}}_L(t)$,

$$\begin{aligned}(m_e+m_t)\left(\dot{\overline{u}}_L^+ - (\overline{v}_{L0}+\psi_{zL0}d_{e1})\dot{\theta}^+\right) =& (m_e+m_t)\left(\dot{\overline{u}}_L - (\overline{v}_{L0}+d_{e1}\psi_{zL0})\dot{\theta}^-\right) + m_t(\dot{\mathcal{Q}}_8^-\cos\theta_0 \\ &+ \dot{\mathcal{Q}}_9^-\sin\theta_0)\end{aligned} \tag{5.70}$$

The velocity relation for the transverse deflection of the beam $\dot{\overline{v}}(x,t)$,

$$\int \rho((x+\overline{u}_0-y\psi_{z0})\dot{\theta}^+ + \dot{\overline{v}}^+)\mathrm{d}V = \int \rho((x+\overline{u}_0-y\psi_{z0})\dot{\theta}^- + \dot{\overline{v}}(x)^-)\mathrm{d}V \tag{5.71}$$

and finally, the velocity relation for the transverse deflection of the end of the beam $\dot{\overline{v}}_L(t)$,

$$\begin{aligned}(m_e+m_t)(\dot{\overline{v}}_L^+ + d_{e1}\dot{\psi}_{zL}^+ + (L+\overline{u}_{L0}+d_{e1})\dot{\theta}^+) =& (m_e+m_t)(\dot{\overline{v}}_L^- + d_{e1}\dot{\psi}_{zL}^- + (L+\overline{u}_{L0}+d_{e1})\dot{\theta}^-) \\ &+ m_t(-\dot{\mathcal{Q}}_8^-\sin\theta_0 + \dot{\mathcal{Q}}_9^-\cos\theta_0)\end{aligned} \tag{5.72}$$

Now, we substitute the constraint equations in for $\dot{\mathscr{Q}}_8$, $\dot{\mathscr{Q}}_9$ and $\dot{\mathscr{Q}}_{10}$ into Equations (5.66)–(5.72). The bending slope along the beam is unchanged,

$$\int_V \rho y((y+\overline{v}_0)\dot{\theta}^+ - \dot{\overline{u}}(x)^+ + y\dot{\psi}_z(x)^+)\mathrm{d}V = \int_V \rho y((y+\overline{v}_0)\dot{\theta}^- - \dot{u}(x)^- + y\dot{\psi}_z(x)^-)\mathrm{d}V \tag{5.73}$$

and the bending slope at the end of the beam becomes,

$$\begin{aligned}
&(m_e+m_t)d_{e1}\left(\dot{\overline{v}}_L^+ + (L+\overline{u}_{L0}+d_{e1})\dot{\theta}^+ + d_{e1}\dot{\psi}_{zL}^+\right) + (J_e+J_t)(\dot{\psi}_{zL}^+ + \dot{\theta}^+) \\
&= m_e d_{e1}\left(\dot{\overline{v}}_L^- + d_{e1}\dot{\psi}_{zL}^- + (L+\overline{u}_{L0}+d_{e1})\dot{\theta}^-\right) + J_e(\dot{\psi}_{zL}^- + \dot{\theta}^-) + m_t d_{e1}(\dot{y}_t^-\cos\theta_0 - \dot{x}_t^-\sin\theta_0) + J_t\dot{\gamma}^-
\end{aligned} \tag{5.74}$$

The velocity relation for the angular velocity of the beam becomes,

$$\begin{aligned}
&(m_e+m_t)\Big(\big((L+\overline{u}_{L0}+d_{e1})^2 + (\overline{v}_{L0}+d_{e1}\psi_{zL0})^2\big)\dot{\theta}^+ + (\overline{v}_{L0}+d_{e1}\psi_{zL0})\dot{\overline{u}}_L^+ \\
&-(L+\overline{u}_{L0}+d_{e1})(\dot{\overline{v}}_L^+ + d_{e1}\dot{\psi}_{zL}^+)\Big) + (J_e+J_t)\dot{\psi}_{zL}^+ + (J_m+J_e+J_t)\dot{\theta}^+ \\
&+\int \rho\Big(\big((x+\overline{u}_0-y\psi_z)^2 + (y+\overline{v}_0)^2\big)\dot{\theta}^+ + (y+\overline{v}_0)\dot{\overline{u}}^+ - (x+\overline{u}_0-y\psi_z)\dot{\overline{v}}^+ - y(y+\overline{v}_0)\dot{\psi}_z^+\Big)\mathrm{d}V \\
&= m_e\big((L+\overline{u}_{L0}+d_{e1})^2 + (\overline{v}_{L0}+d_{e1}\psi_{zL0})^2\big)\dot{\theta}^- + J_e(\dot{\psi}_{zL}^- + \dot{\theta}^-) + J_m\dot{\theta}^- \\
&+ m_e(\overline{v}_{L0}+d_{e1}\psi_{zL0})\dot{\overline{u}}_L^- - m_e(L+\overline{u}_{L0}+d_{e1})\dot{\overline{v}}_L^- - m_e d_{e1}(L+\overline{u}_{L0}+d_{e1})\dot{\psi}_{zL}^- \\
&+\int \rho(((x+\overline{u}_0-y\psi_z)^2 + (y+\overline{v}_0)^2)\dot{\theta}^- + (y+\overline{v}_0)\dot{\overline{u}}^- - (x+\overline{u}_0-y\psi_z)\dot{\overline{v}}^- - y(y+\overline{v}_0)\dot{\psi}_z^-)\mathrm{d}V \\
&+ m_t(\overline{v}_{L0}+d_{e1}\psi_{zL0})(\dot{x}_t^-\cos\theta_0 - \dot{y}_t^-\sin\theta_0) - m_t(L+\overline{u}_{L0}+d_{e1})(\dot{x}_t^-\sin\theta_0 + \dot{y}_t^-\cos\theta_0) + J_t\dot{\gamma}^-
\end{aligned} \tag{5.75}$$

The velocity relation for the extension of the beam is unchanged as,

$$\int_V \rho\left(\dot{\overline{u}}(x)^+ - y\dot{\psi}^+ - (y+\overline{v}_0)\dot{\theta}^+\right)\mathrm{d}V = \int_V \rho\left(\dot{\overline{u}}(x)^- - y\dot{\psi}^- - (y+\overline{v}_0)\dot{\theta}^-\right)\mathrm{d}V \tag{5.76}$$

and the velocity relation for the extension of the end of the beam is,

$$(m_e+m_t)\left(\dot{\overline{u}}_L^+ - (\overline{v}_{L0}+d_{e1}\psi_{zL0})\dot{\theta}^+\right) = m_e\left(\dot{\overline{u}}_L^- - (\overline{v}_{L0}+d_{e1}\psi_{zL0})\dot{\theta}^-\right) + m_t(\dot{x}_t^-\cos\theta_0 + \dot{y}_t^-\sin\theta_0) \tag{5.77}$$

The transverse deflection velocity relation is unchanged,

$$\int \rho((x+\overline{u}_0-y\psi_{z0})\dot{\theta}^+ + \dot{\overline{v}}^+)\mathrm{d}V = \int \rho((x+\overline{u}_0-y\psi_{z0})\dot{\theta}^- + \dot{\overline{v}}(x)^-)\mathrm{d}V \tag{5.78}$$

but the transverse deflection velocity relation for the end of the beam becomes,

$$\begin{aligned}
(m_e+m_t)(\dot{\overline{v}}_L^+ + d_{e1}\dot{\psi}_{zL}^+ + (L+\overline{u}_{L0}+d_{e1})\dot{\theta}^+) = &m_e(\dot{\overline{v}}_L^- + d_{e1}\dot{\psi}_{zL}^- + (L+\overline{u}_{L0}+d_{e1})\dot{\theta}^-) \\
&+ m_t(\dot{y}_t^-\cos\theta_0 - \dot{x}_t^-\sin\theta_0)
\end{aligned} \tag{5.79}$$

Under the assumption that the x-axis corresponds to the centroidal axis of the beam we can simplify the integrals using,

$$\int\int \mathrm{d}y\mathrm{d}z = A(x) \tag{5.80}$$

$$\int\int y\mathrm{d}y\mathrm{d}z = 0 \tag{5.81}$$

$$\int\int y^2\mathrm{d}y\mathrm{d}z = I_{yy}(x) \tag{5.82}$$

which means the equations (5.73)–(5.79) become, respectively,

$$\int_0^L \rho I_{yy}(x)\left(\dot{\psi}_z^+ + \dot{\theta}^+\right)\mathrm{d}x = \int_0^L \rho I_{yy}(x)\left(\dot{\psi}_z^- + \dot{\theta}^-\right)\mathrm{d}x \tag{5.83}$$

$$\begin{aligned}&(m_e+m_t)d_{e1}\left(\dot{\overline{v}}_L^+ - (L+\overline{u}_{L0}+d_{e1})\dot{\theta}^+ + d_{e1}\dot{\psi}_{zL}^+\right) + (J_e+J_t)(\dot{\psi}_{zL}^+ + \dot{\theta}^+)\\ &= m_e d_{e1}\left(\dot{\overline{v}}_L^- + d_{e1}\dot{\psi}_{zL}^- - (L+\overline{u}_{L0}+d_{e1})\dot{\theta}^-\right) + J_e(\dot{\psi}_{zL}^- + \dot{\theta}^-) + m_t d_{e1}(\dot{x}_t^-\sin\theta_0 + \dot{y}_t^-\cos\theta_0) + J_t\dot{\gamma}^-\end{aligned} \tag{5.84}$$

$$\begin{aligned}&(m_e+m_t)\left(\left((L+\overline{u}_{L0}+d_{e1})^2 + (\overline{v}_{L0}+d_{e1}\psi_{zL0})^2\right)\dot{\theta}^+ + (\overline{v}_{L0}+d_{e1}\psi_{zL0})\dot{\overline{u}}_L^+\right.\\ &\left.+(L+\overline{u}_{L0}+d_{e1})(\dot{\overline{v}}_L^+ + d_{e1}\dot{\psi}_{zL}^+)\right) + (J_e+J_t)\dot{\psi}_{zL}^+ + (J_m+J_e+J_t)\dot{\theta}^+\\ &+\int_0^L \rho\left(A\left(((x+\overline{u}_0)^2+\overline{v}_0^2)\dot{\theta}^+ - \overline{v}_0\dot{\overline{u}}^+ + (x+\overline{u}_0)\dot{\overline{v}}^+\right) + I_{yy}\left((1+\psi_{z0}^2)\dot{\theta}^+ + \dot{\psi}^+\right)\right)\mathrm{d}x\\ &= m_e\left(L+\overline{u}_{L0}+d_{e1}\right)^2 + (\overline{v}_{L0}+d_{e1}\psi_{zL0})^2\left)\dot{\theta}^- + J_e(\dot{\psi}_{zL}^- + \dot{\theta}^-) + J_m\dot{\theta}^-\right.\\ &+ m_e(\overline{v}_{L0}+d_{e1}\psi_{zL0})\dot{\overline{u}}_L^- - m_e(L+\overline{u}_{L0}+d_{e1})\dot{\overline{v}}_L^- + m_e d_{e1}(L+\overline{u}_{L0}+d_{e1})\dot{\psi}_{zL}^-\\ &+\int_0^L \rho\left(A\left(((x+\overline{u}_0)^2+\overline{v}_0^2)\dot{\theta}^- - \overline{v}_0\dot{\overline{u}}^- + (x+\overline{u}_0)\dot{\overline{v}}^-\right) + I_{yy}\left((1+\psi_{z0}^2)\dot{\theta}^- + \dot{\psi}^-\right)\right)\mathrm{d}x\\ &- m_t(\overline{v}_{L0}+d_{e1}\psi_{zL0})(\dot{x}_t^-\cos\theta_0 + \dot{y}_t^-\sin\theta_0) + m_t(L+\overline{u}_{L0}+d_{e1})(\dot{y}_t^-\cos\theta_0 - \dot{x}_t^-\sin\theta_0) + J_t\dot{\gamma}^-\end{aligned} \tag{5.85}$$

$$\int_0^L \rho A(x)\left(\dot{\overline{u}}(x)^+ - \overline{v}_0(x)\dot{\theta}^+\right)\mathrm{d}x = \int_0^L \rho A(x)\left(\dot{\overline{u}}(x)^- - \overline{v}_0(x)\dot{\theta}^-\right)\mathrm{d}x \tag{5.86}$$

$$(m_e+m_t)\left(\dot{\overline{u}}_L^+ - (\overline{v}_{L0}+d_{e1}\psi_{zL0})\dot{\theta}^+\right) = m_e\left(\dot{\overline{u}}_L^- - (\overline{v}_{L0}+d_{e1}\psi_{zL0})\dot{\theta}^-\right) + m_t(\dot{x}_t^-\cos\theta_0 - \dot{y}_t^-\sin\theta_0) \tag{5.87}$$

$$\int_0^L \rho A(x)\left(\dot{\overline{v}}(x)^+ + (x+\overline{u}_0(x))\dot{\theta}^+\right)\mathrm{d}x = \int_0^L \rho A(x)\left(\dot{\overline{v}}(x)^- + (x+\overline{u}_0(x))\dot{\theta}^-\right)\mathrm{d}x \tag{5.88}$$

$$(m_e+m_t)(\dot{\overline{v}}_L^+ + d_{e1}\dot{\psi}_{zL}^+ + (L+\overline{u}_{L0}+d_{e1})\dot{\theta}^+) = m_e(\dot{\overline{v}}_L^- + d_{e1}\dot{\psi}_{zL}^- + (L+\overline{u}_{L0}+d_{e1})\dot{\theta}^-) + m_t(\dot{y}_t^- \cos\theta_0 - \dot{x}_t^- \sin\theta_0) \tag{5.89}$$

Leaving aside Equation (5.85) for the moment, we will simplify the remaining equations. Note that because the integrals are over the same domain and range, we will simply equate the integrands where appropriate,

$$\dot{\psi}(x)^+ = \dot{\psi}(x)^- - \dot{\theta}^+ + \dot{\theta}^- \tag{5.90}$$

$$\begin{aligned}\dot{\psi}_{zL}^+ = {} & \frac{m_e d_{e1}\left(\dot{\overline{v}}_L^- + d_{e1}\dot{\psi}_{zL}^- - (L+\overline{u}_{L0}+d_{e1})\dot{\theta}^-\right) + J_e(\dot{\psi}_{zL}^- + \dot{\theta}^-) + J_t\dot{\gamma}^-}{(m_e+m_t)d_{e1}^2 + (J_e+J_t)} \\ & + \frac{m_t d_{e1}(\dot{x}_t^- \sin\theta_0 + \dot{y}_t^- \cos\theta_0) - (J_e+J_t)\dot{\theta}^+}{(m_e+m_t)d_{e1}^2 + (J_e+J_t)} \\ & - \frac{(m_e+m_t)d_{e1}\left(\dot{\overline{v}}_L^+ + (L+\overline{u}_{L0}+d_{e1})\dot{\theta}^+\right)}{(m_e+m_t)d_{e1}^2 + (J_e+J_t)}\end{aligned} \tag{5.91}$$

$$\dot{\overline{u}}(x)^+ = \dot{\overline{u}}(x)^- - \overline{v}_0(x)(\dot{\theta}^+ - \dot{\theta}^-) \tag{5.92}$$

$$\begin{aligned}\dot{\overline{u}}_L^+ = {} & \frac{m_e\left(\dot{\overline{u}}_L^- - (\overline{v}_{L0}+d_{e1}\psi_{zL0})\dot{\theta}^-\right) + m_t(\dot{x}_t^- \cos\theta_0 + \dot{y}_t^- \sin\theta_0)}{m_e+m_t} \\ & + (\overline{v}_{L0}+d_{e1}\psi_{zL0})\dot{\theta}^+\end{aligned} \tag{5.93}$$

$$\dot{\overline{v}}(x)^+ = \dot{\overline{v}}(x)^- + (x+\overline{u}_0(x))(\dot{\theta}^- - \dot{\theta}^+) \tag{5.94}$$

$$\begin{aligned}\dot{\overline{v}}_L^+ = {} & \frac{m_e(\dot{\overline{v}}_L^- + d_{e1}\dot{\psi}_{zL}^- + (L+\overline{u}_{L0}+d_{e1})\dot{\theta}^-) + m_t(\dot{y}_t^- \cos\theta_0 - \dot{x}_t^- \sin\theta_0)}{(m_e+m_t)} \\ & - (d_{e1}\dot{\psi}_{zL}^+ + (L+\overline{u}_{L0}+d_{e1})\dot{\theta}^+)\end{aligned} \tag{5.95}$$

After substituting these results into Equation (5.85) and simplifying, we find that

$$\dot{\theta}^+ = \dot{\theta}^- \tag{5.96}$$

which means the final set of equations (5.90)–(5.96) can be written as,

$$\dot{\psi}_z(x)^+ = \dot{\psi}_z(x)^- \tag{5.97}$$

$$\dot{\psi}^+_{zL} = \frac{J_t(\dot{\gamma}^- - \dot{\theta}^-) + J_e\dot{\psi}^-_{zL}}{J_t + J_e} \tag{5.98}$$

$$\dot{\overline{u}}(x)^+ = \dot{\overline{u}}(x)^- \tag{5.99}$$

$$\dot{\overline{u}}^+_L = \frac{m_t\left(\dot{x}_t^- \cos\theta + \dot{y}_t^- \sin\theta + (\overline{v}_L + d_{e1}\psi_{zL})\dot{\theta}^-\right) + m_e\dot{\overline{u}}^-_L}{m_t + m_e} \tag{5.100}$$

$$\dot{\overline{v}}(x)^+ = \dot{\overline{v}}(x)^- \tag{5.101}$$

$$\begin{aligned}\dot{\overline{v}}^+_L = {} & \frac{m_e\dot{\overline{v}}^-_L + m_t\left(\dot{y}_t^- \cos\theta - \dot{x}_t^- \sin\theta - \dot{\theta}^-(\overline{u}_L + L + d_{e1})\right)}{m_t + m_e} \\ & + \frac{d_{e1}J_t(\dot{\theta}^- - \dot{\gamma}^-)}{J_t + J_e} + \frac{d_{e1}\dot{\psi}^-_{zL}(m_eJ_t - m_tJ_e)}{(m_t + m_e)(J_t + J_e)}\end{aligned} \tag{5.102}$$

$$\dot{\theta}^+ = \dot{\theta}^- \tag{5.103}$$

From these we can note that only the tip velocities (Equations (5.98), (5.100), and (5.102)) are directly affected by the capture event. Also of importance is that the angular velocity changes are taken strictly by the rotation of the end-effector, not the beam. So in this case, we see the tip velocities updated and then the changes will propagate down the beam.

5.7 General Beam Capture

In this case, we are considering a 3D beam model (including torsion) and general rigid bodies for both the end-effector and target. The capture can happen at any point on the end-effector and target. Because of the torsion model, we do assume that the beam cross-section is constant along the beam.

Post-Capture Velocity Constraint

Modelling the capture process as a plastic collision, from Section 5.1 we get that the velocities at impact must be equivalent. Therefore, our velocity constraint is that after capture the target velocity and end effector velocities have to match. Since both the target and end-effector are rigid bodies, we assume that they contact at a minimum of one point post-capture and that the target and end-effector have the same velocity at that point.

The target velocity given in Equation (3.4) is for the centre of mass, not the point of contact. So, assuming a vector $\underrightarrow{r}_{tc}$ from the centre of mass to the point of contact, we need to

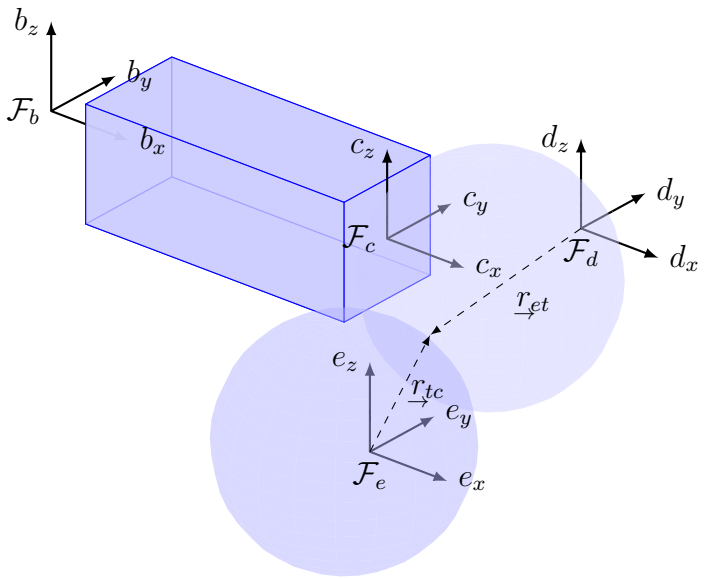

Figure 5.2: 3D Target Capture

add the additional velocity (see Figure 5.2),

$$\underset{\rightarrow}{v}_{tc}(t) = \underset{\rightarrow}{\omega}_t \times \underset{\rightarrow}{r}_{tc} \tag{5.104}$$

$$= \underset{\rightarrow}{\mathcal{F}}_a^T \begin{bmatrix} r_{tc3}\dot{\beta} \\ -r_{tc3}\dot{\alpha} \\ r_{tc2}\dot{\alpha} - r_{tc1}\dot{\beta} \end{bmatrix} \tag{5.105}$$

Therefore, the translational velocity at the point of contact is,

$$\underset{\rightarrow}{v}_c(t) = \underset{\rightarrow}{\mathcal{F}}_a^T \begin{bmatrix} \dot{x}_t + r_{tc3}\dot{\beta} \\ \dot{y}_t - r_{tc3}\dot{\alpha} \\ \dot{z}_t + r_{tc2}\dot{\alpha} - r_{tc1}\dot{\beta} \end{bmatrix} \tag{5.106}$$

The end-effector velocity is given in Equation (3.83), but we need the velocity at the point of contact. The velocity at the point of contact has an additional component from the offset of the contact point from the centre of mass, given by vector $\underset{\rightarrow}{r}_{et}$ (see Figure 5.2),

$$\underset{\rightarrow}{v}_{et}(t) = \underset{\rightarrow}{\omega}_e \times \underset{\rightarrow}{r}_{et} \tag{5.107}$$

$$= \underset{\rightarrow}{\mathcal{F}}_a^T \begin{bmatrix} -(\dot{\theta}+\dot{\psi}_{zL})\left((r_{et1}-\psi_{zL}r_{et2}+\psi_{yL}r_{et3})\sin\theta + (-\psi_{zL}r_{et1}-r_{et2}+\theta_{xL}r_{et3})\cos\theta\right) \\ (\dot{\theta}+\dot{\psi}_{zL})\left(-\psi_{zL}r_{et1}-r_{et2}+\theta_{xL}r_{et3})\sin\theta + (r_{et1}-\psi_{zL}r_{et2}+\psi_{yL}r_{et3})\cos\theta\right) \\ -\dot{\psi}_{yL}\left((r_{et1}-\psi_{zL}r_{et2}+\psi_{yL}r_{et3})\cos\theta + (\psi_{zL}r_{et1}+r_{et2}-\theta_{xL}r_{et3})\sin\theta\right) \end{bmatrix}$$
$$+ \begin{bmatrix} -\dot{\psi}_{yL}\left(\psi_{yL}r_{et1}-\theta_{xL}r_{et2}-r_{et3}\right) \\ \dot{\theta}_{xL}\left(\psi_{yL}r_{et1}-\theta_{xL}r_{et2}-r_{et3}\right) \\ \dot{\theta}_{xL}\left((\psi_{zL}r_{et1}+r_{et2}-\theta_{xL}r_{et3})\cos\theta + (r_{et1}-\psi_{zL}r_{et2}+\psi_{yL}r_{et3})\sin\theta\right) \end{bmatrix} \tag{5.108}$$

which we can write as,

$$\underset{\sim}{v}_{et}(t) = \begin{bmatrix} (\dot{\theta}+\dot{\psi}_{zL})(-K_{et1}\sin\theta + K_{et2}\cos\theta) - K_{et3}\dot{\psi}_{yL} \\ (\dot{\theta}+\dot{\psi}_{zL})(K_{et2}\sin\theta + K_{et1}\cos\theta) + K_{et3}\dot{\theta}_{xL} \\ \dot{\theta}_{xL}(-K_{et2}\cos\theta + K_{et1}\sin\theta) - \dot{\psi}_{yL}(K_{et1}\cos\theta - K_{et2}\sin\theta) \end{bmatrix} \tag{5.109}$$

where K_{et1}, K_{et2}, and K_{et3} are defined as,

$$K_{et1} = r_{et1} - \psi_{zL}r_{et2} + \psi_{yL}r_{et3} \tag{5.110}$$

$$K_{et2} = -\psi_{zL}r_{et1} - r_{et2} + \theta_{xL}r_{et3} \tag{5.111}$$

$$K_{et3} = \psi_{yL}r_{et1} - \theta_{xL}r_{et2} - r_{et3} \tag{5.112}$$

Note that during capture all of these are considered to be constant. The velocity at the point of contact is defined by,

$$\underset{\sim}{v}_{ec} = \underset{\sim}{v}_{e} + \underset{\sim}{v}_{et} \tag{5.113}$$

where $\underset{\sim}{v}_{e}$ is as defined in Equation (3.84). Therefore, The velocity of the end-effector at the contact point is,

$$\underset{\sim}{v}_{ec}(t) = \underset{\sim}{\mathscr{F}}_{a}^{T} \begin{bmatrix} \big(K_{ve1} + K_{et2}(\dot{\theta}+\dot{\psi}_{zL})\big)\cos\theta - \big(K_{ve2} + K_{et1}(\dot{\theta}+\dot{\psi}_{zL})\big)\sin\theta - K_{et3}\dot{\psi}_{yL} \\ \big(K_{ve2} + K_{et1}(\dot{\theta}+\dot{\psi}_{zL})\big)\cos\theta + \big(K_{ve1} + K_{et2}(\dot{\theta}+\dot{\psi}_{zL})\big)\sin\theta + K_{et3}\dot{\theta}_{xL} \\ K_{ve3} + \dot{\theta}_{xL}(-K_{et2}\cos\theta + K_{et1}\sin\theta) - \dot{\psi}_{yL}(K_{et1}\cos\theta + K_{et2}\sin\theta) \end{bmatrix} \tag{5.114}$$

In this equation, K_{ve1}, K_{ve2}, and K_{ve3} contain velocities and as such are not constant during capture which means we will need to redefine them in terms of quasi-velocities later. The velocities of the target and the end-effector at the point of contact are given in the inertial frame so we can subtract components to get the following constraints,

$$\begin{aligned} &\dot{x}_t + r_{tc3}\dot{\beta} + K_{et3}\dot{\psi}_{yL} - \big(K_{ve1} + K_{et2}(\dot{\theta}+\dot{\psi}_{zL})\big)\cos\theta \\ &+ \big(K_{ve2} + K_{et1}(\dot{\theta}+\dot{\psi}_{zL})\big)\sin\theta = 0 \end{aligned} \tag{5.115}$$

$$\begin{aligned} &\dot{y}_t - r_{tc3}\dot{\alpha} - K_{et3}\dot{\theta}_{xL} - \big(K_{ve2} + K_{et1}(\dot{\theta}+\dot{\psi}_{zL})\big)\cos\theta \\ &- \big(K_{ve1} + K_{et2}(\dot{\theta}+\dot{\psi}_{zL})\big)\sin\theta = 0 \end{aligned} \tag{5.116}$$

$$\begin{aligned} &\dot{z}_t + r_{tc2}\dot{\alpha} + r_{tc1}\dot{\beta} - K_{ve3} - \dot{\theta}_{xL}(-K_{et2}\cos\theta + K_{et1}\sin\theta) \\ &+\dot{\psi}_{yL}(K_{et1}\cos\theta + K_{et2}\sin\theta) = 0 \end{aligned} \tag{5.117}$$

Since we are considering the impact duration to be infinitesimal, all position variables can be replaced with their value at impact ($\theta(t) = \theta(t_1)$, $\overline{u}(L,t) = \overline{u}(L,t_1)$, $\overline{v}(L,t) = \overline{v}(L,t_1)$,

$\overline{w}(L,t) = \overline{w}(L,t_1)$) which we will denote as θ_0, $\overline{u}_{L0}$, $\overline{v}_{L0}$ and $\overline{w}_{L0}$ respectively.

$$\dot{x}_t + r_{tc3}\dot{\beta} + K_{et3}\dot{\psi}_{yL} - \left(K_{ve1} + K_{et2}(\dot{\theta} + \dot{\psi}_{zL})\right)\cos\theta_0$$
$$- \left(K_{ve2} + K_{et1}(\dot{\theta} + \dot{\psi}_{zL})\right)\sin\theta_0 = 0 \tag{5.118}$$
$$\dot{y}_t - r_{tc3}\dot{\alpha} - K_{et3}\dot{\theta}_{xL} - \left(K_{ve2} + K_{et1}(\dot{\theta} + \dot{\psi}_{zL})\right)\cos\theta_0$$
$$- \left(K_{ve1} + K_{et2}(\dot{\theta} + \dot{\psi}_{zL})\right)\sin\theta_0 = 0 \tag{5.119}$$
$$\dot{z}_t + r_{tc2}\dot{\alpha} + r_{tc1}\dot{\beta} - K_{ve3} - \dot{\theta}_{xL}(-K_{et2}\cos\theta_0 + K_{et1}\sin\theta_0)$$
$$+\dot{\psi}_{yL}(K_{et1}\cos\theta_0 + K_{et2}\sin\theta_0) = 0 \tag{5.120}$$

where K_{et1}, K_{et2}, K_{et3}, K_{ve1}, K_{ve2}, and K_{ve3} become,

$$K_{et1} = r_{et1} - \psi_{zL0}r_{et2} + \psi_{yL0}r_{et3} \tag{5.121}$$
$$K_{et2} = -\psi_{zL0}r_{et1} - r_{et2} + \theta_{xL0}r_{et3} \tag{5.122}$$
$$K_{et3} = \psi_{yL0}r_{et1} - \theta_{xL}r_{et2} - r_{et3} \tag{5.123}$$
$$K_{ve1} = \dot{\overline{u}}_L - \dot{\theta}(\overline{v}_{L0} + d_{e2} + \psi_{zL0}d_{e1} - \theta_{xL0}d_{e3}) + \dot{\psi}_{yL}d_{e3} - \dot{\psi}_{zL}d_{e2} \tag{5.124}$$
$$K_{ve2} = \dot{\overline{v}}_L + \dot{\psi}_{zL}d_{e1} - \dot{\theta}_{xL}d_{e3} + \dot{\theta}(L + \overline{u}_{L0} + d_{e1} - \psi_{zL0}d_{e2} + \psi_{yL0}d_{e3}) \tag{5.125}$$
$$K_{ve3} = \dot{\overline{w}}_L - \dot{\psi}_{yL}d_{e1} + \dot{\theta}_{xL}d_{e2} \tag{5.126}$$

Similarly, for the angular velocities,

$$\dot{\alpha}(t) - \dot{\theta}_{xL}(t) = 0 \tag{5.127}$$
$$\dot{\beta}(t) - \dot{\psi}_{yL}(t) = 0 \tag{5.128}$$
$$\dot{\gamma}(t) - \dot{\theta}(t) - \dot{\psi}_{zL}(t) = 0 \tag{5.129}$$

Quasi-Velocities

Representing each of the beam and end-effector velocity variables as quasi-velocities,

$$\dot{\mathcal{Q}}_1(x,t) = \dot{\psi}_x(x,t) \tag{5.130}$$
$$\dot{\mathcal{Q}}_2(x,t) = \dot{\psi}_y(x,t) \tag{5.131}$$
$$\dot{\mathcal{Q}}_3(t) = \dot{\psi}_{yL}(t) \tag{5.132}$$
$$\dot{\mathcal{Q}}_4(x,t) = \dot{\psi}_z(x,t) \tag{5.133}$$
$$\dot{\mathcal{Q}}_5(t) = \dot{\psi}_{zL}(t) \tag{5.134}$$
$$\dot{\mathcal{Q}}_6(t) = \dot{\theta}(t) \tag{5.135}$$
$$\dot{\mathcal{Q}}_7(x,t) = \dot{\theta}_x(x,t) \tag{5.136}$$
$$\dot{\mathcal{Q}}_8(x,t) = \dot{\overline{u}}(x,t) \tag{5.137}$$
$$\dot{\mathcal{Q}}_9(t) = \dot{\overline{u}}_L(t) \tag{5.138}$$
$$\dot{\mathcal{Q}}_{10}(x,t) = \dot{\overline{v}}(x,t) \tag{5.139}$$
$$\dot{\mathcal{Q}}_{11}(t) = \dot{\overline{v}}_L(t) \tag{5.140}$$
$$\dot{\mathcal{Q}}_{12}(x,t) = \dot{\overline{w}}(x,t) \tag{5.141}$$
$$\dot{\mathcal{Q}}_{13}(t) = \dot{\overline{w}}_L(t) \tag{5.142}$$
$$\dot{\mathcal{Q}}_{14}(t) = \dot{\theta}_{xL}(t) \tag{5.143}$$

There are six remaining quasi-velocities to completely define the system corresponding to the translation and rotation constraints. Starting with the translation constraints,

$$\begin{aligned}\dot{\mathcal{Q}}_{15} &= \dot{x}_t + r_{tc3}\dot{\beta} + K_{et3}\dot{\mathcal{Q}}_3 - \left(K_{ve1} + K_{et2}(\dot{\mathcal{Q}}_6 + \dot{\mathcal{Q}}_5)\right)\cos\theta_0 \\ &- \left(K_{ve2} + K_{et1}(\dot{\mathcal{Q}}_6 + \dot{\mathcal{Q}}_5)\right)\sin\theta_0 \end{aligned} \tag{5.144}$$
$$\begin{aligned}\dot{\mathcal{Q}}_{16} &= \dot{y}_t - r_{tc3}\dot{\alpha} - K_{et3}\dot{\mathcal{Q}}_{14} - \left(K_{ve2} + K_{et1}(\dot{\mathcal{Q}}_6 + \dot{\mathcal{Q}}_5)\right)\cos\theta_0 \\ &- \left(K_{ve1} + K_{et2}(\dot{\mathcal{Q}}_6 + \dot{\mathcal{Q}}_5)\right)\sin\theta_0 \end{aligned} \tag{5.145}$$
$$\begin{aligned}\dot{\mathcal{Q}}_{17} &= \dot{z}_t + r_{tc2}\dot{\alpha} + r_{tc1}\dot{\beta} - K_{ve3} - \dot{\mathcal{Q}}_{14}(-K_{et2}\cos\theta_0 + K_{et1}\sin\theta_0) \\ &+ \dot{\mathcal{Q}}_3(K_{et1}\cos\theta_0 + K_{et2}\sin\theta_0) \end{aligned} \tag{5.146}$$

where K_{ve1}, K_{ve2}, and K_{ve3} are now as follows,

$$K_{ve1} = \dot{\mathcal{Q}}_9 - \dot{\mathcal{Q}}_6(\overline{v}_{L0} + d_{e2} + \psi_{zL0}d_{e1} - \theta_{xL0}d_{e3}) + \dot{\mathcal{Q}}_3 d_{e3} - \dot{\mathcal{Q}}_5 d_{e2} \tag{5.147}$$
$$K_{ve2} = \dot{\mathcal{Q}}_{11} + \dot{\mathcal{Q}}_5 d_{e1} - \dot{\mathcal{Q}}_{14}d_{e3} + \dot{\mathcal{Q}}_6(L + \overline{u}_{L0} + d_{e1} - \psi_{zL0}d_{e2} + \psi_{yL0}d_{e3}) \tag{5.148}$$
$$K_{ve3} = \dot{\mathcal{Q}}_{13} - \dot{\mathcal{Q}}_3 d_{e1} + \dot{\mathcal{Q}}_{14}d_{e2} \tag{5.149}$$

and the rotation constraints,

$$\dot{\mathcal{Q}}_{18}(t) = \dot{\alpha}(t) - \dot{\theta}_{xL}(t) \tag{5.150}$$
$$\dot{\mathcal{Q}}_{19}(t) = \dot{\beta}(t) - \dot{\psi}_{yL}(t) \tag{5.151}$$
$$\dot{\mathcal{Q}}_{20}(t) = \dot{\gamma}(t) - \dot{\theta}(t) - \dot{\psi}_{zL}(t) \tag{5.152}$$

Substituting the quasi-velocities into the rotation constraints,

$$\dot{\mathcal{Q}}_{18}(t) = \dot{\alpha}(t) - \dot{\mathcal{Q}}_{14}(t) \tag{5.153}$$
$$\dot{\mathcal{Q}}_{19}(t) = \dot{\beta}(t) - \dot{\mathcal{Q}}_{3}(t) \tag{5.154}$$
$$\dot{\mathcal{Q}}_{20}(t) = \dot{\gamma}(t) - \dot{\mathcal{Q}}_{6}(t) - \dot{\mathcal{Q}}_{5}(t) \tag{5.155}$$

which can be re-arranged for the angular velocities gives,

$$\dot{\alpha}(t) = \dot{\mathcal{Q}}_{18}(t) + \dot{\mathcal{Q}}_{14}(t) \tag{5.156}$$
$$\dot{\beta}(t) = \dot{\mathcal{Q}}_{19}(t) + \dot{\mathcal{Q}}_{3}(t) \tag{5.157}$$
$$\dot{\gamma}(t) = \dot{\mathcal{Q}}_{20}(t) + \dot{\mathcal{Q}}_{6}(t) + \dot{\mathcal{Q}}_{5}(t) \tag{5.158}$$

Substituting these into Equations (5.144)–(5.146) we get the quasi-velocities for the translational constraints,

$$\dot{\mathcal{Q}}_{15} = \dot{x}_t + r_{tc3}(\dot{\mathcal{Q}}_{19} + \dot{\mathcal{Q}}_{3}) + K_{et3}\dot{\mathcal{Q}}_{3} - \left(K_{ve1} - K_{et2}(\dot{\mathcal{Q}}_{6} + \dot{\mathcal{Q}}_{5})\right)\cos\theta_0 - \left(K_{ve2} + K_{et1}(\dot{\mathcal{Q}}_{6} + \dot{\mathcal{Q}}_{5})\right)\sin\theta_0 \tag{5.159}$$
$$\dot{\mathcal{Q}}_{16} = \dot{y}_t - r_{tc3}(\dot{\mathcal{Q}}_{18} + \dot{\mathcal{Q}}_{14}) - K_{et3}\dot{\mathcal{Q}}_{14} - \left(K_{ve2} + K_{et1}(\dot{\mathcal{Q}}_{6} + \dot{\mathcal{Q}}_{5})\right)\cos\theta_0 - \left(K_{ve1} - K_{et2}(\dot{\mathcal{Q}}_{6} + \dot{\mathcal{Q}}_{5})\right)\sin\theta_0 \tag{5.160}$$
$$\dot{\mathcal{Q}}_{17} = \dot{z}_t + r_{tc2}(\dot{\mathcal{Q}}_{18} + \dot{\mathcal{Q}}_{14}) + r_{tc1}(\dot{\mathcal{Q}}_{19} + \dot{\mathcal{Q}}_{3}) - K_{ve3} - \dot{\mathcal{Q}}_{14}(-K_{et2}\cos\theta_0 - K_{et1}\sin\theta_0) + \dot{\mathcal{Q}}_{3}(K_{et1}\cos\theta_0 + K_{et2}\sin\theta_0) \tag{5.161}$$

and re-arranging for the target velocities,

$$\dot{x}_t = \dot{\mathcal{Q}}_{15} - r_{tc3}(\dot{\mathcal{Q}}_{19} + \dot{\mathcal{Q}}_{3}) - K_{et3}\dot{\mathcal{Q}}_{3} + \left(K_{ve1} + K_{et2}(\dot{\mathcal{Q}}_{6} + \dot{\mathcal{Q}}_{5})\right)\cos\theta_0 + \left(K_{ve2} + K_{et1}(\dot{\mathcal{Q}}_{6} + \dot{\mathcal{Q}}_{5})\right)\sin\theta_0 \tag{5.162}$$
$$\dot{y}_t = \dot{\mathcal{Q}}_{16} + r_{tc3}(\dot{\mathcal{Q}}_{18} + \dot{\mathcal{Q}}_{14}) + K_{et3}\dot{\mathcal{Q}}_{14} + \left(K_{ve2} + K_{et1}(\dot{\mathcal{Q}}_{6} + \dot{\mathcal{Q}}_{5})\right)\cos\theta_0 + \left(K_{ve1} - K_{et2}(\dot{\mathcal{Q}}_{6} + \dot{\mathcal{Q}}_{5})\right)\sin\theta_0 \tag{5.163}$$
$$\dot{z}_t = \dot{\mathcal{Q}}_{17} - r_{tc2}(\dot{\mathcal{Q}}_{18} + \dot{\mathcal{Q}}_{14}) - r_{tc1}(\dot{\mathcal{Q}}_{19} + \dot{\mathcal{Q}}_{3}) + K_{ve3} + \dot{\mathcal{Q}}_{14}(-K_{et2}\cos\theta_0 - K_{et1}\sin\theta_0) - \dot{\mathcal{Q}}_{3}(K_{et1}\cos\theta_0 + K_{et2}\sin\theta_0) \tag{5.164}$$

Quasi-Kinetic Energy

Starting with the kinetic energy of the motor, the kinetic energy in quasi-velocities (which we refer to as quasi-kinetic energy) is,

$$T_m^* = \frac{1}{2} J_m \dot{\mathcal{Q}}_6^2 \tag{5.165}$$

The quasi-kinetic energy of the beam due to bending is,

$$\begin{aligned} T_{xb}^* = &\frac{1}{2}\int_0^L \rho A(\dot{\mathcal{Q}}_8^2 + \dot{\mathcal{Q}}_{10}^2 + \dot{\mathcal{Q}}_{12}^2 + \dot{\mathcal{Q}}_6^2((x+\overline{u}_0)^2 + \overline{v}_0^2))\mathrm{d}x \\ &+ \frac{1}{2}\int_0^L \rho(I_{yy}(\dot{\mathcal{Q}}_6^2(1+\psi_{z0}^2)) + \dot{\mathcal{Q}}_4^2 - 2\dot{\mathcal{Q}}_6\dot{\mathcal{Q}}_4) + I_{zz}(\dot{\mathcal{Q}}_2^2 + \dot{\mathcal{Q}}_6^2\psi_{y0}))\mathrm{d}x \\ &- \int_0^L \rho A\dot{\mathcal{Q}}_6((x+\overline{u}_0)\dot{\mathcal{Q}}_{10} + \dot{\mathcal{Q}}_8\overline{v}_0)\mathrm{d}x \end{aligned} \tag{5.166}$$

and the quasi-kinetic energy due to torsion is,

$$T_{xt}^* = \frac{1}{2}\int_0^L \rho\left(\dot{\mathcal{Q}}_6^2(A\phi^2\psi_{x0}^2 + I_{zz}\theta_{x0}^2) + J_g\dot{\mathcal{Q}}_7^2 + A\phi^2\dot{\mathcal{Q}}_1^2\right)\mathrm{d}x \tag{5.167}$$

The rotational quasi-kinetic energy of the end-effector is,

$$T_{re}^* = \frac{1}{2}(J_{exx}\dot{\mathcal{Q}}_{14}^2 + J_{eyy}\dot{\mathcal{Q}}_3^2 + J_{ezz}(\dot{\mathcal{Q}}_3+\dot{\mathcal{Q}}_6)^2) + \dot{\mathcal{Q}}_{14}(J_{exy}\dot{\mathcal{Q}}_3 + J_{exz}(\dot{\mathcal{Q}}_6+\dot{\mathcal{Q}}_5)) + J_{eyz}\dot{\mathcal{Q}}_3(\dot{\mathcal{Q}}_6+\dot{\mathcal{Q}}_5) \tag{5.168}$$

and the translational quasi-kinetic energy of the end-effector is,

$$T_{te}^* = \frac{1}{2}m_e(K_{ve1}^2 + K_{ve2}^2 + K_{ve3}^2) \tag{5.169}$$

where K_{ve1}, K_{ve2}, and K_{ve3} are as given in Equations (5.147)–(5.149). As stated in Equation (3.14), the kinetic energy of the target is,

$$\begin{aligned} T_t^* = &\frac{1}{2}\left(m_t\left(\dot{x}_t^2 + \dot{y}_t^2 + \dot{z}_t^2\right) + \dot{\alpha}^2 J_{txx} + \dot{\beta}^2 J_{tyy} + \dot{\gamma}^2 J_{tzz}\right. \\ &\left. + 2\dot{\alpha}\dot{\beta}J_{txy} + 2\dot{\alpha}\dot{\gamma}J_{txz} + 2\dot{\beta}\dot{\gamma}J_{tyz}\right) \end{aligned} \tag{5.170}$$

but we use that $\dot{x}_t$, $\dot{y}_t$, and $\dot{z}_t$ are as given in Equations (5.162)–(5.164) and the angular velocities $\dot{\alpha}$, $\dot{\beta}$, and $\dot{\gamma}$ are as given in (5.156)–(5.158). The resulting equation is long and is omitted for brevity.

Derivation of System of Capture Equations

Since we have 14 independent quasi-velocities, upon applying the capture equation as given in Equation (5.9), we arrive at a set of 14 equations. However, the number of terms in a number of the equations makes writing them down difficult and unproductive. As a result, we derive a set of equations that we can solve numerically once the system parameters are known. This is done as follows,

1. Calculate the quasi-momenta terms as given in Equation (5.9) for the 14 independent quasi-velocities.

2. Evaluate the quasi-momenta at the times pre- and post-capture and substitute the results into Equation (5.9).

3. Evaluate the quasi-momenta for the constrained quasi-velocities associated with the target and substitute that into the results from step 2.

4. For equations with only integral terms, since both the domain and range of the integral is equal, one can equate the integrands and solve for q_i^+ in each equation. These equations arise from beam deflection velocities along the beam (but not the tip).

5. Substitute the known q_i^+ into the remaining equations as needed (which is just the hub angular velocity relation).

6. Convert the system of equations into a matrix system of the form,

$$\begin{bmatrix} q_1^+ \\ q_2^+ \\ \dots \\ q_n^+ \end{bmatrix} = \mathbf{K}_{vp} \begin{bmatrix} q_1^+ \\ q_2^+ \\ \dots \\ q_n^+ \end{bmatrix} + \mathbf{K}_{vm} \tag{5.171}$$

where $\mathbf{K}_{vp}$ is a $n \times n$ matrix and $\mathbf{K}_{vm}$ is a $n \times 1$ column matrix of known terms (arising mostly from the pre-capture velocities). Converting to this form is possible since the system is linear in q_i^+. I have unfortunately not been able to solve this system symbolically, but since both $\mathbf{K}_{vp}$ and $\mathbf{K}_{vm}$ can be computed once the system parameters are known, this can be solved numerically.

CHAPTER

6 Determination of System Damping

Using the exact viscous damping parameters as determined by Rhody [1] in our simulations results in an underestimation of the damping when simulations are compared to experiment. To improve the damping model, the damping parameters can be reset for the system requiring the same damping ratio of the first two elastic modes.

One way to calculate the damping ratios is to use the proportional damping relationship between the Rayleigh damping parameters, damping ratios, and natural frequencies as presented in Bathe and Wilson [66],

$$\xi_i = \frac{b_1 + \omega_i^2 b_2}{2\omega_i} \tag{6.1}$$

where ω_i is the frequency of the ith mode, b_1 is the mass damping coefficient, b_2 is the stiffness damping coefficent, and ξ_i is the damping ratio of the ith mode.

Once the damping ratios (ξ_1, ξ_2) have been calculated we can then calculate the damping coefficents for our discretisation by calculating the natural frequencies of our system, and solving the linear system to calculate the new damping coefficients. However, there is a more general approach which we will discuss in the rest of this chapter.

The natural frequencies of the first two modes for the experiment and Rhody's simulation are presented in Table 6.

Mode	Experiment	Rhody Simulation
1	11.9	12.4
2	38.3	35.6

Table 6.1: Natural Frequencies (Hz) [1]

One of the things we would like for the best model possible for a given system, is to have an accurate representation of the damping in a given system. To that end, we would like to

determine the damping matrix directly from experimental data. Adhikari [70, 71] describes techniques for fitting viscous damping models as well as non-viscous damping models to experimental data. This is effectively a generalization of Rayleigh damping. He notes that [70], "... any damping model can be fitted to reconstruct the measured set of poles and residues." This means that we can use a simple viscous damping model to represent what may be non-viscous damping.

The basic steps in this process are as follows [71]:

1. Determine Transfer Function(s) for the system. Ideally, one would determine the N transfer functions due to impulse excitations applied in a grid pattern to the system.
2. Obtain the undamped natural frequencies ω_j and modal damping factors ζ_j, for example, using the circle-fitting method [2]. See section 6.2 for details of the procedure.
3. Fit a function $\zeta = \hat{f}(\omega)$ which represents the variation of ζ_j with respect to ω_j for the range of frequency considered in the study.
4. Calculate the matrix $\mathbf{T} = \sqrt{\mathbf{M}^{-1}\mathbf{K}}$.
5. Obtain the damping matrix using $\hat{\mathbf{C}} = 2\mathbf{M}\mathbf{T}\hat{f}(\mathbf{T})$.

If one has multiple transfer functions, we obtain a damping sub-matrix for each mode following this approach and then assemble in the traditional finite element fashion.

From Rhody [1], we have experimental data for the rotation of the beam and the tip deflection, so we have two transfer functions excited by the same impulse (the capture of the target mass).

If we look at the structure of our matrices in block form we have,

$$\mathbf{M} = \begin{bmatrix} \mathbf{M}_1 & \mathbf{M}_2 \\ \mathbf{M}_3 & \mathbf{M}_4 \end{bmatrix}, \quad \mathbf{K} = \begin{bmatrix} 0 & 0 \\ 0 & \mathbf{K}_4 \end{bmatrix} \tag{6.2}$$

where $\mathbf{M}_1$ is a scalar quantity that multiplies $\ddot{\theta}$, $\mathbf{M}_4$ and $\mathbf{K}_4$ are the traditional beam mass and stiffness matrices (augmented for the addition of the end-effector) and $\mathbf{M}_2$ is a $1 \times n$ row matrix that couples the beam rotation to the elements. Also, we have,

$$\mathbf{M}_3 = \mathbf{M}_2^T \tag{6.3}$$

So, there is no stiffness matrix for the hub equation (since θ doesn't appear in the strain energy). This poses a problem in applying the approach advocated by Adhikari [71] given above, since the $\mathbf{T}$ matrix for that case can't be calculated (since the sub-matrix for the θ variable has no stiffness contribution). As such we will propose an alternate approach to determining the damping matrix.

6.1 A Coupled System Approach to Damping Modelling

Using the block matrices as given above along with the vector $\mathbf{q}$,

$$\mathbf{q} = \begin{bmatrix} \theta & \mathbf{d} \end{bmatrix}^T \tag{6.4}$$

where $\mathbf{d}$ is of the form,

$$\mathbf{d} = \begin{bmatrix} d_1 & \dots & d_n \end{bmatrix} \tag{6.5}$$

we have the general system of,

$$\mathbf{M}\ddot{\mathbf{q}} + \mathbf{C}\dot{\mathbf{q}} + \mathbf{K}\mathbf{q} = \mathbf{F} \tag{6.6}$$

where $\mathbf{F}$ is a vector of zeros for a freely rotating beam. We assume that the damping matrix takes the form,

$$\mathbf{C} = \begin{bmatrix} \mathbf{C}_1 & \mathbf{C}_2 \\ \mathbf{C}_3 & \mathbf{C}_4 \end{bmatrix} \tag{6.7}$$

where $\mathbf{C}_1$ is a scalar, $\mathbf{C}_2$ is a $1 \times n$ matrix, $\mathbf{C}_3 = \mathbf{C}_2^T$ and $\mathbf{C}_4$ is a $n \times n$ matrix. Breaking this system into two separate (but coupled) systems,

$$\mathbf{M}_1\ddot{\theta} + \mathbf{C}_1\dot{\theta} = -\mathbf{M}_2\ddot{\mathbf{d}} - \mathbf{C}_2\dot{\mathbf{d}} \tag{6.8}$$

$$\mathbf{M}_4\ddot{\mathbf{d}} + \mathbf{C}_4\dot{\mathbf{d}} + \mathbf{K}_4\mathbf{d} = -\mathbf{M}_3\ddot{\theta} - \mathbf{C}_3\dot{\theta} \tag{6.9}$$

So, we can think of the the right-hand side of each equation as the applied force to that system. For the second system, we can solve for $\mathbf{C}_4$ using Adhikari's approach and we can estimate $\mathbf{C}_3$ and $\mathbf{C}_1$ from the viscous damping model.

6.2 Determining Transfer Functions

To this end, we first determine the transfer function for the system. Consider the input-output relation in the time domain as,

$$y(t) = H(q)u(t) + v(t) \tag{6.10}$$

where $y(t)$ is the system output, $H(q)$ the model of system plant, $u(t)$ is the system input, and $v(t)$ is the noise in the measurement. The transfer function $H(\omega)$ can be estimated given $u(t)$ and $y(t)$ using an Empirical Transfer Function Estimate (ETFE) [72] which is implemented in the System Identification Toolbox in MATLAB with the **etfe** function. In particular, we leave the data unsmoothed and tell the function to estimate the transfer function at 50 000 points. The default is to use only 128 data points which provides poor resolution around the natural frequencies which is necessary for step 2 of the process.

If the input is due to the capture of a point mass, we can represent $u(t)$ as [1],

$$u(t) \approx m_t \dot{y}_t \delta_\Delta(t) \tag{6.11}$$

where m_t is the mass of the target, $\dot{y}_t$ is the velocity of the target at capture, and $\delta_\Delta(t)$ is the Dirac delta function. The system output $y(t)$ is the measured response of the system.

The Bode plot of the magnitude of the ETFE for the beam's tip deflection during one of the capture experiments is shown in Figure 6.1. We can note that there are prominent peaks near 0 Hz, just past 10 Hz and just short of 40 Hz. The first is the rigid body mode while the others are the first two elastic modes of the beam.

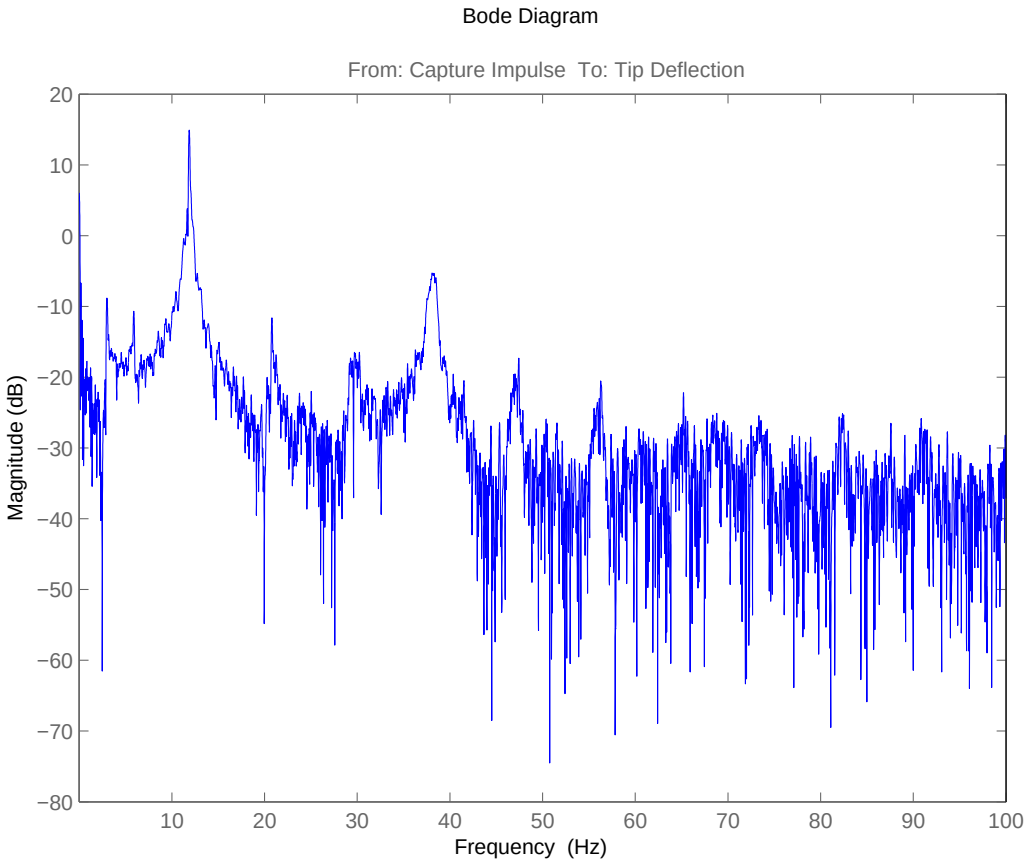

Figure 6.1: Empirical Transfer Function Estimate

Finding the Natural Frequency from a Transfer Function

We will use a fitting technique in the neighbourhood of a resonance known as a "circle-fit" as described by Ewins [2]. If the modes are weakly coupled, in the vicinity of of a resonance, we

assume that the behaviour of the system is dominated by a single mode. This means that we can write the magnitude of the response in the vicinity of the resonance as,

$$\alpha(\omega) = \frac{A_r}{\omega_r^2 - \omega^2 + \mathbf{i}\eta_r\omega_r^2} + B_r \tag{6.12}$$

where $\alpha(\omega)$ is the magnitude of the transfer function response at frequency ω, ω_r is the natural frequency of mode r, η_r is the damping constant of mode r, A_r is what Ewins calls the "modal constant" and B_r is the contribution of the other modes to the transfer function response. It is assumed that this is only weakly dependent or independent of frequency.

Ewins states that the effect or A_r is to scale the size of the circle and rotate it, so for the basic formula he gives is,

$$\alpha(\omega) = \frac{1}{\omega_r^2 - \omega^2 + \mathbf{i}\eta_r\omega_r^2} \tag{6.13}$$

Examining Ewins' modal circle (Figure 6.2), from geometry he gets,

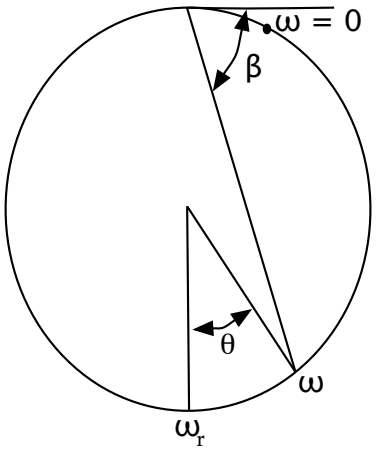

Figure 6.2: Modal Circle [2]

$$\tan\beta = \frac{\eta_r}{1 - \left(\frac{\omega}{\omega_r}\right)^2} \tag{6.14}$$

$$\tan(90^\circ - \beta) = \tan\frac{\theta}{2} = \frac{1 - \left(\frac{\omega}{\omega_r}\right)^2}{\eta_r} \tag{6.15}$$

which leads to,

$$\omega^2 = \omega_r^2\left(1 - \eta_r \tan\frac{\theta}{2}\right) \tag{6.16}$$

where θ is the angle between ω and ω_r on the modal circle. If we differentiate this with respect to θ,

$$\frac{\mathrm{d}\omega^2}{\mathrm{d}\theta} = -{\omega_r}^2\eta_r\frac{1}{2}\left(1 + \tan\left(\frac{\theta}{2}\right)^2\right) \tag{6.17}$$

Using the formula for $\tan\frac{\theta}{2}$ from earlier,

$$\frac{\mathrm{d}\omega^2}{\mathrm{d}\theta} = -{\omega_r}^2\eta_r\frac{1}{2}\left(1+\left(\frac{1-(\omega/\omega_r)^2}{\eta_r}\right)^2\right) \tag{6.18}$$

The reciprocal quantity $\frac{\mathrm{d}\theta}{\mathrm{d}\omega^2}$ is a measure of the rate at which the modal circle is swept out. This goes to a maximum at the natural frequency. We can see this by differentiating this expression with respect to ω and noticing that it goes to zero when $\omega^2 = \omega_r^2$. This gives us a means of locating the natural frequency once the modal circle is fit to the data.

Ewins [2] gives the following steps to calculate the natural frequency of the system.

1. Select the points to be used;
2. fit the circle to the data;
3. locate the natural frequency.

Once the natural frequency has been located we can estimate the damping constant η_r from,

$$\left.\frac{\mathrm{d}\theta}{\mathrm{d}\omega^2}\right|_{\omega=\omega_r} = \frac{-2}{\omega_r^2\eta_r} \tag{6.19}$$

Once we have η_r, we can get the standard damping ratio, ζ from,

$$\zeta = \frac{\eta_r}{2} \tag{6.20}$$

Ewins [2] gives a few recommendations on selecting the data points. The points chosen should not be largely influenced by other modes in the system, and should cover 270° of the circle, but less than 180° is common. But, no less than 6 points should be used.

So, to select the data points, we first find the frequency that gives the maximum amplitude. Next, we select all the data points within a window of $\Delta_\omega/2$ around the resonant frequency this can be done using the **fselect** routine of the System Identification MATLAB toolbox, where Δ_ω is a user selectable window width. Typically, this is some number much less than 1 Hz but will be dependent upon the resolution of $H(\omega)$. In our case, we choose the number of points based upon the quality of the fit. We choose the largest number of points that still gives a high quality fit.

The transfer function response will be in general a complex number, so we can generate a Nyquist plot of the transfer function using the System ID toolbox routine **nyquist**. We would like to generate a "best" fit circle to this data. To this end, we use the technique of Rorres and Romano [73] by defining the error of the fit as,

$$E(x_c, y_c, r) = \sum_{i=1}^{N}\left(\sqrt{(x_i-x_c)^2+(y_i-y_c)^2}-r\right)^2 \tag{6.21}$$

In our case, the x_i points are the real values of our response and the y_i points are the imaginary values of response. Differentiating this expression with respect to r and setting it equal to zero, we get this expression for the radius,

$$r = \frac{1}{N}\sum_{i=1}^{N}\sqrt{(x_i - x_c)^2 + (y_i - y_c)^2} \tag{6.22}$$

This means that the optimal radius can be found using an average of the distances to the center. We can substitute this into the error expression to get this function of two variables,

$$E(x_c, y_c) = \sum_{i=1}^{N}\left(\sqrt{(x_i - x_c)^2 + (y_i - y_c)^2} - \frac{1}{N}\sum_{i=1}^{N}\sqrt{(x_i - x_c)^2 + (y_i - y_c)^2}\right)^2 \tag{6.23}$$

This can be solved numerically in MATLAB using the function **fminsearch** that employs a Nelder-Mead simplex search which is how Rorres and Romano [73] minimize this equation. The only caveat is that an initial guess is needed. An initial guess of $(x_c, y_c) = (0,0)$ appears to be adequate. Now that the center point is known we can calculate the radius.

We would like to numerically approximate the sweep rate $\frac{d\theta}{d\omega^2}$. Since the frequencies are only known at the individual data points we will only work with them. First, begin by finding the angle of the data points using a polar coordinate system with its' origin at the center of the fitted circle.

$$\theta_i = \tan^{-1}\left(\frac{y_i - y_c}{x_i - x_c}\right) \tag{6.24}$$

Care must be taken in evaluating the arctangent as it is quadrant dependent. The sweep rate can now be evaluated using finite differences. Once we have calculated the differences, the frequency at which the maximum sweep rate occurs is the natural frequency.

We can see the result of this process for the first mode is shown in Figure 6.3. The corresponding plot for the second mode is shown in Figure 6.4 and the rigid body mode is shown in Figure 6.5. The centre frequency shown in these figures is the centre of the frequency window Δ_ω.

Performing a Nyquist plot, we can see that for the first mode (Figure 6.3), we have an excellent fit between the circle and the experimental response. Similarly, the second mode (Figure 6.4) doesn't fit quite as well over the entire frequency window, but it does still fit well near the natural frequency.

Note that the rigid body mode (Figure 6.5) is a poor fit (likely because this method isn't designed for rigid body modes), but we will use the damping estimate from this procedure to determine an initial estimate $\zeta = \hat{f}(\omega)$ for the beam.

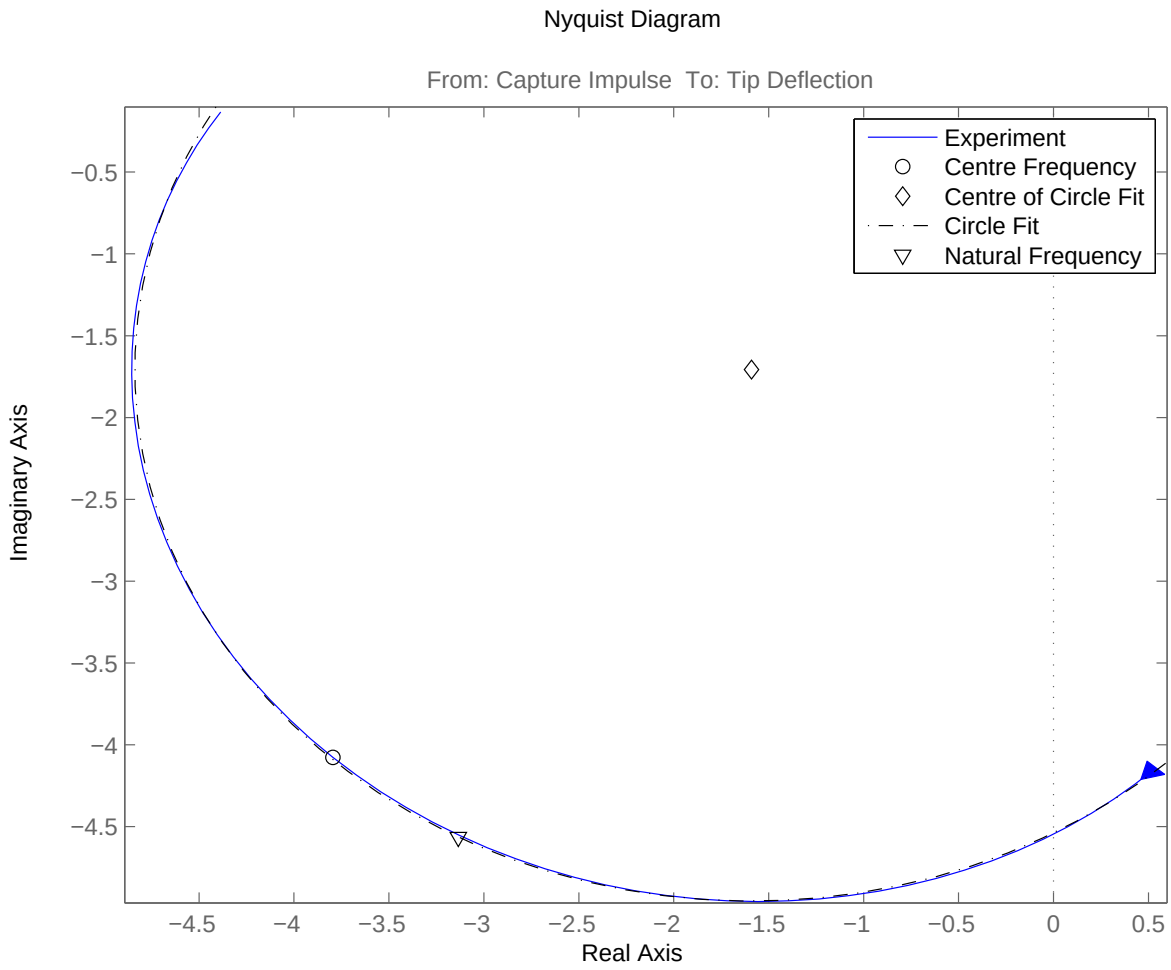

Figure 6.3: Circle Fit Approximation for the first mode

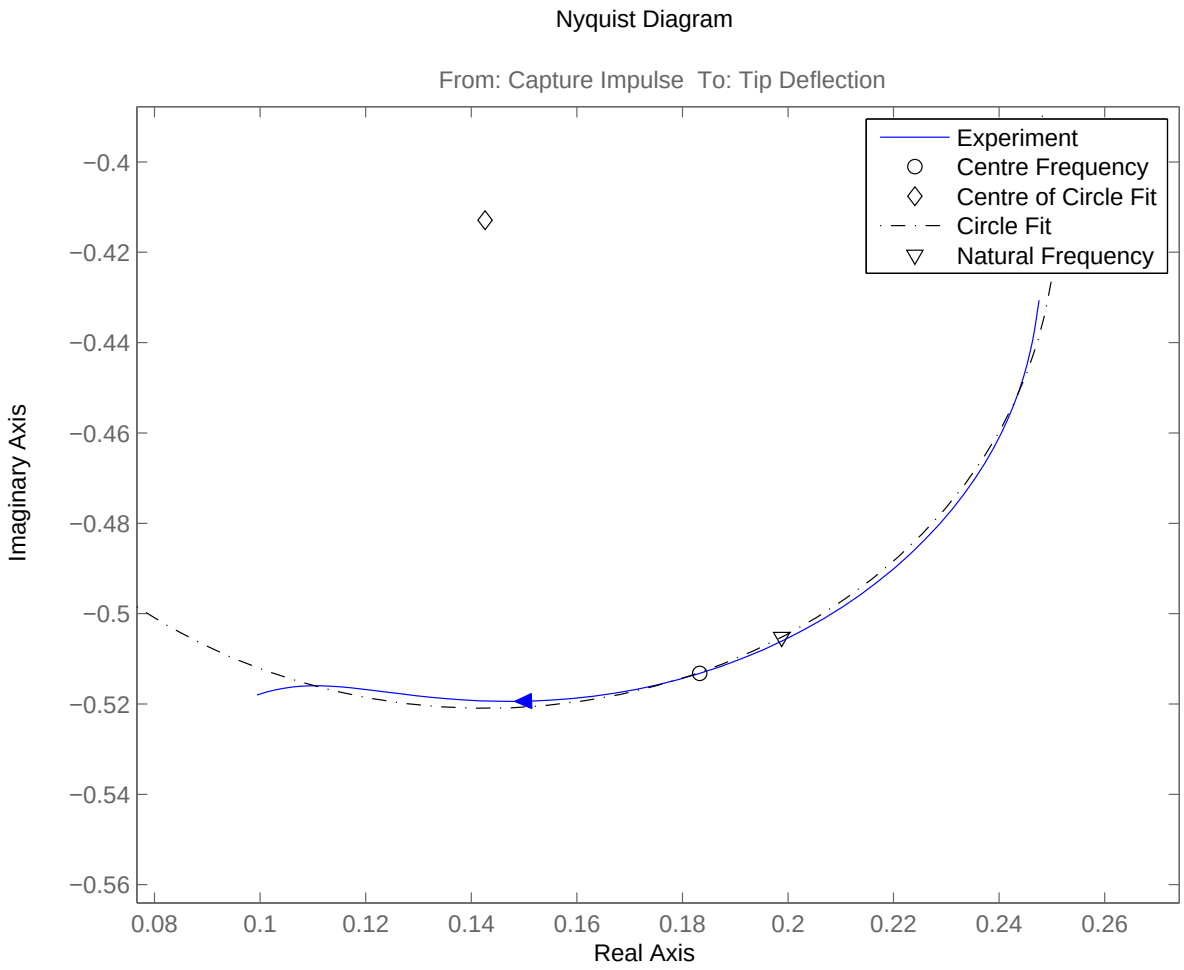

Figure 6.4: Circle Fit Approximation for the second mode

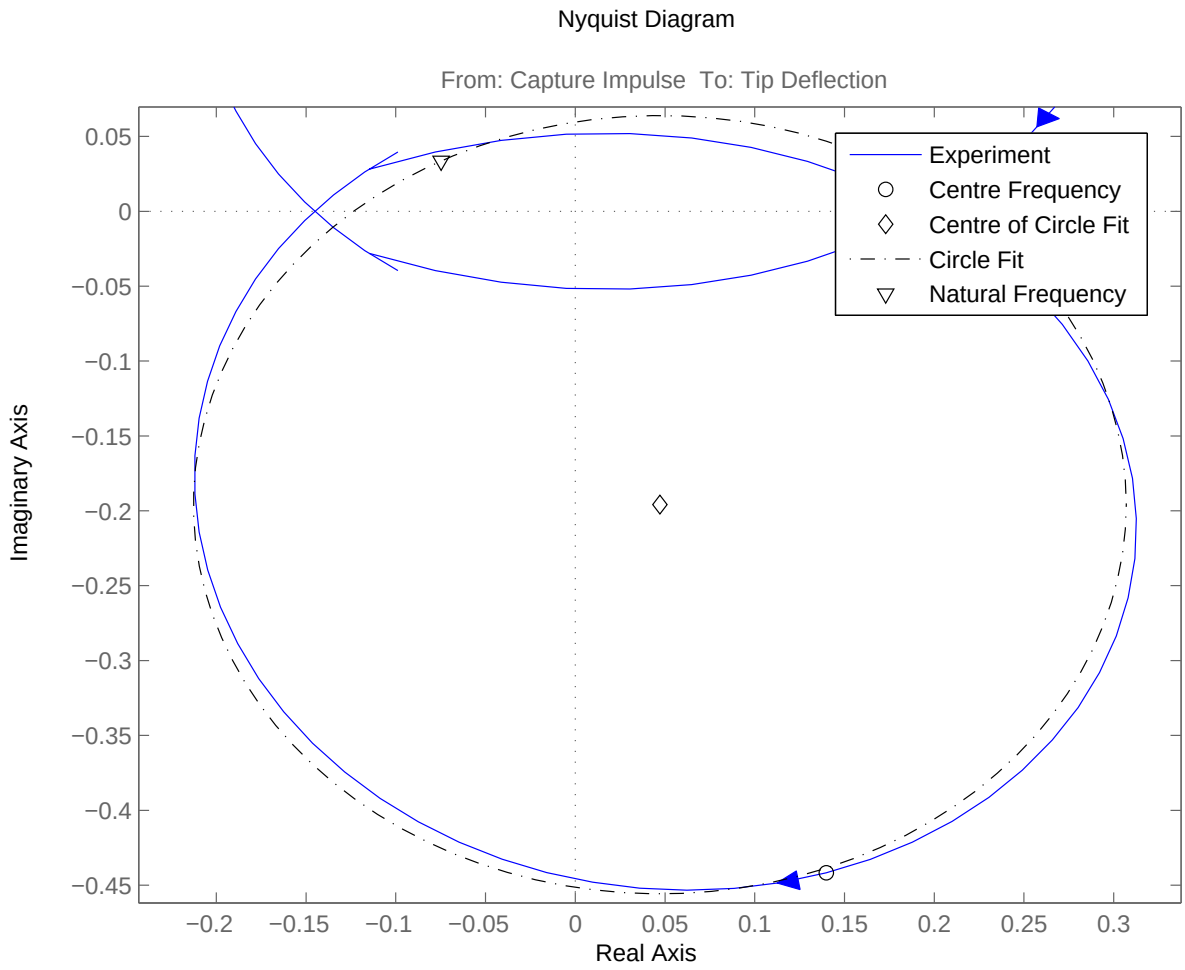

Figure 6.5: Circle Fit Approximation for the rigid body mode

6.3 Estimating $\zeta = \hat{f}(\omega)$

Following the procedure outlined in section 6.2, we have three data points, whereas we need a function $\hat{f}(\omega)$ that works for all ω. To that end, we fit functions to the data using non-linear least squares (implemented in MATLAB using **lsqcurvefit**). It solves the problem

$$\min_a \| F(a,\mathbf{x}) - \mathbf{y} \|_2 = \min_a \sum_i \left(F(a,x_i) - y_i\right)^2 \tag{6.25}$$

Based upon the shape of the data, we consider a couple of candidate functions $\hat{f}_i(\omega)$. The first is a sum of decaying exponentials (with an offset),

$$\hat{f}_1(\omega) = a_0 + \sum_{i=1}^{N} a_i e^{-b_i \omega} \tag{6.26}$$

The offset is to allow for the function to decay to a non-zero value. The second is an rational polynomial of the form,

$$\hat{f}_2(\omega) = \frac{a_0}{1 + \sum_{i=1}^{N} a_i \omega^i} \tag{6.27}$$

Considering two terms in each sum, we get the plot shown in Figure 6.6. The parameters for the functions $\hat{f}_1$ and $\hat{f}_2$ for this plot are shown in Table 6.3.

Approximation	a_0	a_1	a_2	b_1	b_2
$\hat{f}_1$	0.0026	0.1200	0.1200	0.3444	0.3444
$\hat{f}_2$	0.3834	5.2381	-0.0365	N/A	N/A

Table 6.2: Damping Model Parameters

We can see that both models provide good fits to the experimental damping calculated, although the polynomial continues well past the damping approximation to the rigid body mode as it approaches 0 Hz from above. The exponential approximation also allows for a more gradual changes between the rigid body mode and the first elastic mode. As a result, we will use the exponential approximation $\hat{f}_1(\omega)$ for our system.

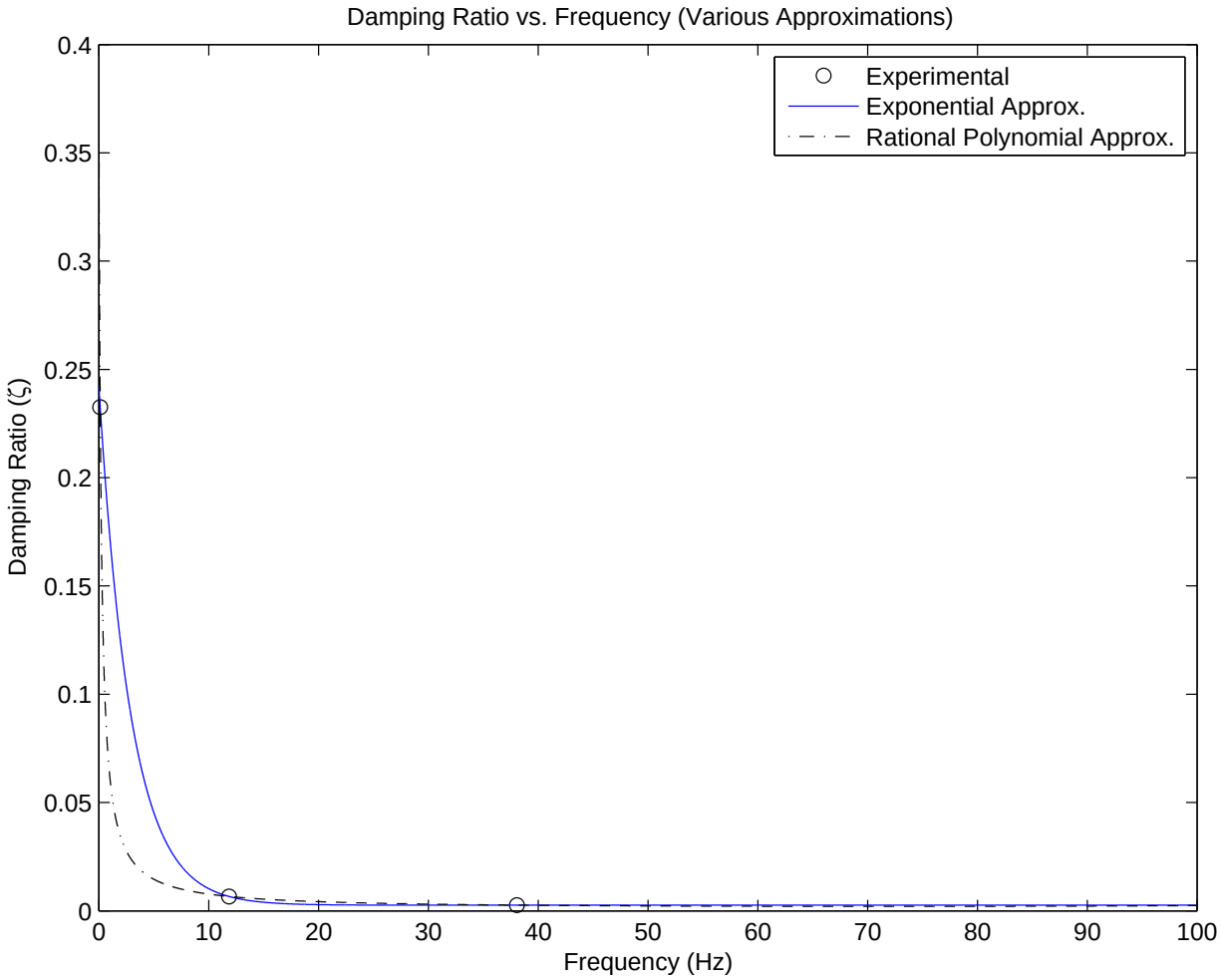

Figure 6.6: Damping vs. Frequency (Various Approximations)

6.4 Determining C through parameter identification

Recalling Equations (6.8) and (6.9),

$$\mathbf{M}_1\ddot{\theta} + \mathbf{C}_1\dot{\theta} = -\mathbf{M}_2\ddot{\mathbf{d}} - \mathbf{C}_2\dot{\mathbf{d}} \tag{6.28}$$

$$\mathbf{M}_4\ddot{\mathbf{d}} + \mathbf{C}_4\dot{\mathbf{d}} + \mathbf{K}_4\mathbf{d} = -\mathbf{M}_3\ddot{\theta} - \mathbf{C}_3\dot{\theta} \tag{6.29}$$

we can use a form of $\hat{\mathbf{C}}$ in place of $\mathbf{C}_4$, which gives us,

$$\mathbf{M}_1\ddot{\theta} + \mathbf{C}_1\dot{\theta} = -\mathbf{M}_2\ddot{\mathbf{d}} - \mathbf{C}_2\dot{\mathbf{d}} \tag{6.30}$$

$$\mathbf{M}_4\ddot{\mathbf{d}} + \mathbf{E}_4\hat{f}(\mathbf{T})\dot{\mathbf{d}} + \mathbf{K}_4\mathbf{d} = -\mathbf{M}_3\ddot{\theta} - \mathbf{C}_3\dot{\theta} \tag{6.31}$$

where,

$$\hat{f}_1(\omega) = a_0 + \sum_{i=1}^{N} a_i e^{-b_i\omega} \tag{6.32}$$

$$\mathbf{T} = \sqrt{\mathbf{M}_4^{-1}\mathbf{K}_4} \tag{6.33}$$

$$\mathbf{E}_4 = 2\mathbf{M}_4\mathbf{T} \tag{6.34}$$

which gives us an unknown scalar $\mathbf{C}_1$, a vector of unknowns $\mathbf{C}_3$ and a set of unknown parameters in $\hat{f}$. We use the estimate of $\hat{f}(\omega)$ we determined earlier as the initial guess and initially assume Rayleigh viscous damping for $\mathbf{C}_3$ using the same damping ratios as Rhody [1]. This is sufficient for an initial guess. We then consider scaling the resulting sub-matrices for inclusion in the final damping matrix $\mathbf{C}$.

Evaluation of T and $\hat{f}(\mathbf{T})$

While both $\mathbf{M}_4$ and $\mathbf{K}_4$ are symmetric matrices, the product,

$$\mathbf{T} = \sqrt{\mathbf{M}_4^{-1}\mathbf{K}_4} \tag{6.35}$$

in general will not be symmetric. As a result, there is no easy way to diagonalize $\mathbf{T}$ (which is a first step in the simplest method for evaluating functions of a matrix). As such other methods must be used. For calculating the square root of a matrix, we use the MATLAB function **sqrtm** [74, 75] for calculation of $\hat{f}(\mathbf{T})$. Because of our choice of $\hat{f}$ we have two different approaches to its evaluation. We can calculate the matrix function directly using the Davies and Higham's method [76] (implemented in MATLAB using **funm**) or we can calculate the matrix exponential [77, 78] for each exponential term (using **expm** in MATLAB). Since the latter allows us to easily add terms to the sum in $\hat{f}$, we will evaluate using **expm**. Note that matrix square root and matrix exponential functions in MATLAB do not support sparse matrices so the $\mathbf{M}_4^{-1}\mathbf{K}_4$ product must be converted to a full matrix.

It is left for future work to determine which of using **expm** or **funm** is more accurate and/or faster. In addition, since only the scalar in the exponential terms of $\hat{f}_1$ changes it may be possible to modify the algorithms to reuse results to speed computation. This is also left for future work.

For all models, given sufficient numbers of elements, the size of **T** (and therefore functions of it) will be too large to show in a reasonable manner in this thesis.

6.5 Summary

So, we have a modified version of Adhikari's approach [71] presented at the beginning of this chapter,

1. Determine Transfer Function(s) for the system using ETFE [72].
2. Obtain the undamped natural frequencies ω_j and modal damping factors ζ_j, using the circle-fitting method [2].
3. Fit a function $\zeta = \hat{f}(\omega)$ (in our case this is a sum of decaying exponentials).
4. Calculate the matrix $\mathbf{T} = \sqrt{\mathbf{M}_4^{-1}\mathbf{K}_4}$.
5. Obtain the damping matrix using $\hat{\mathbf{C}}_4 = 2\mathbf{M}_4\mathbf{T}\hat{f}(\mathbf{T})$.
6. Estimate $\mathbf{C}_1$ and $\mathbf{C}_3$ based upon Rayleigh viscous damping.
7. Scale $\mathbf{C}_1$, $\mathbf{C}_3$, and $\hat{\mathbf{C}}_4$ appropriately to match the experimental data.

CHAPTER

7 Experiment, Results, and Discussion

7.1 Overview of Experiment

To validate the model, we compare the results to experimental results obtained by Rhody [1]. One of his experiments consisted of a capture of a steel block by a beam initially at rest. This experimental setup is used to check our simulations.

The target mass was placed on a model railway car set on an inclined track. The car was released from rest, and the capture was performed by an electromagnet end effector at a specified distance down the track and the railway car continues under the beam until it hits the foam bumper. See Figure 7.1 for an overview of the experimental setup.

The experimental parameters related to the beam (including the motor and end-effector) are in Table 7.1 and the parameters of the target are in Table 7.1.

Parameter	Value
A, Cross-sectional Area of Beam	$3.175 \times 10^{-4}\,\mathrm{m}^2$
E, Young's Modulus	$6.5 \times 10^{10}\,\mathrm{Pa}$
I, Beam Moment of Inertia	$2.67 \times 10^{-10}\,\mathrm{m}^4$
J_e, End-Effector Inertia	$1.6 \times 10^{-3}\,\mathrm{kg \cdot m}^2$
J_m, Motor Inertia	$1.3233 \times 10^{-4}\,\mathrm{kg \cdot m}^2$
L, Effective Beam Length	$0.725\,\mathrm{m}$
b_1, Mass Damping Constant	$-2.85 \times 10^{-3}\,\mathrm{s}^{-1}$
b_2, Stiffness Damping Constant	$2.54 \times 10^{-5}\,\mathrm{s}$
d_{e1}, End-effector offset	$5.175 \times 10^{-2}\,\mathrm{m}$
m_e, End Effector Mass	$0.55\,\mathrm{kg}$
$\overline{m}$, Linear Mass Density of Beam	$0.874\,\mathrm{kg/m}$

Table 7.1: Beam Experimental Parameters [1]

There are a few parameters are needed that are not given in this table, but can be derived

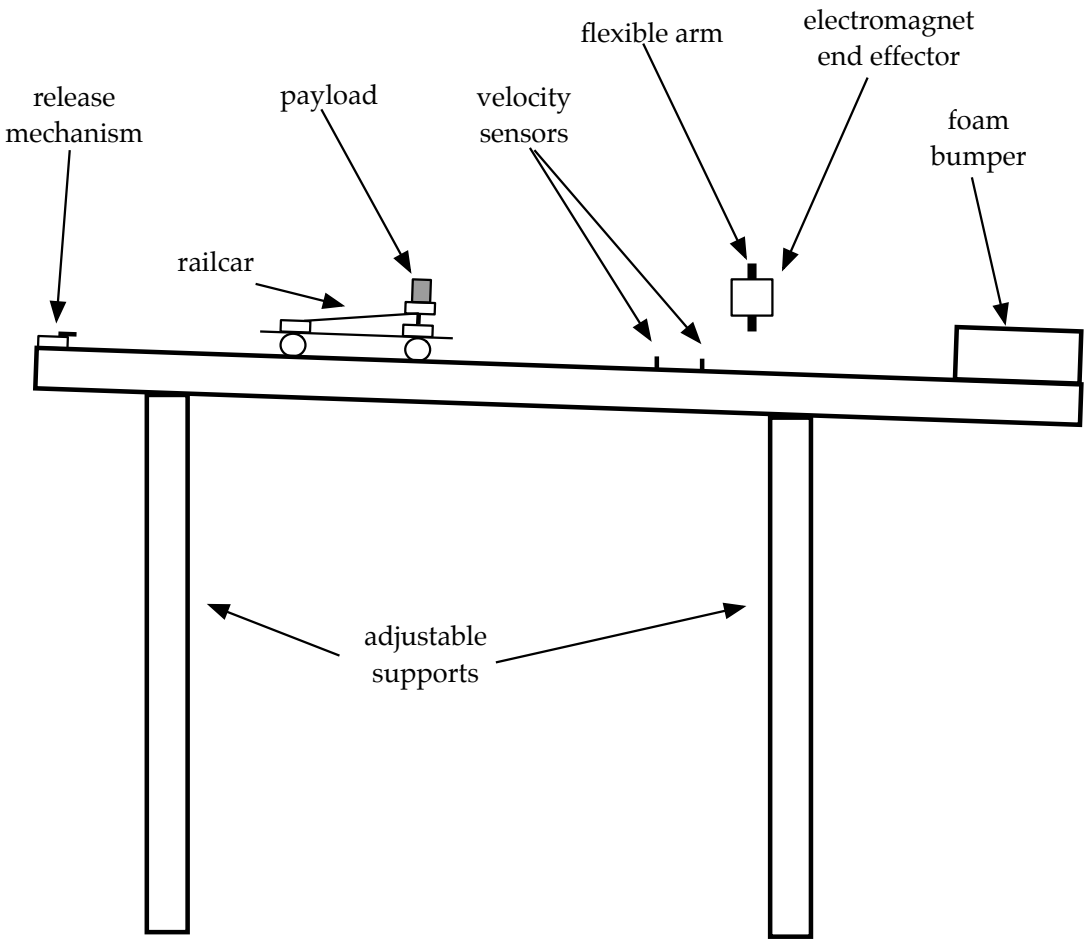

Figure 7.1: Experimental Setup - Side View [1]

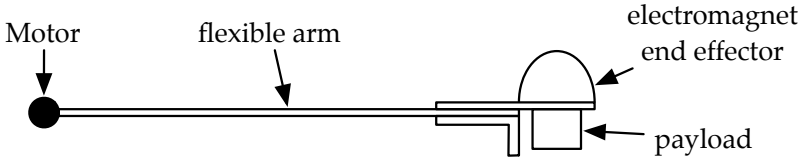

Figure 7.2: Experimental Setup - Beam Top View (Target Captured)

from this data, these are shown in Table 7.1.

Parameter	Calculation	Value
ρ, Mass Density of Beam	$\overline{m}/A$	$2.753 \times 10^3\ \mathrm{kg/m^3}$
a, Width of Beam	$\sqrt{12(I/A)}$	$3.18 \times 10^{-3}\ \mathrm{m}$
b, Height of Beam	A/a	$1.00 \times 10^{-1}\ \mathrm{m}$
a/b, Width/Height ratio	a/b	$3.18 \times 10^{-2}\ \mathrm{m}$

Table 7.2: Derived Experimental Parameters

Target Mass (kg)	Dimensions, $x \times y \times z$ (cm)	Inertia ($\mathrm{kg \cdot m^2}$)
0.5	$2.54 \times 3.81 \times 6.67$	1.72×10^{-3}

Table 7.3: Target Parameters [1]

7.2 Finite Element Models

For all of the models discussed in this chapter, a 20 element finite element approximation is used. The 2D Euler-Bernoulli Beam uses C^1 cubics to approximate $\overline{v}$ whereas the 2D and 3D Timoshenko beams use C^0 cubics for each system variable. This is done to prevent locking [79]. The element mesh is a 1D line with equally spaced elements with a single shared node between elements. See Figure 7.3 for an example 7 element mesh for the 2D Euler-Bernoulli beam. The mesh for the 3D cases is similar but each element contains two interior nodes as shown in Figure 7.5. Note that in all cases, since the beam itself is modelled as clamped at the hub, node 1 is fixed so those degrees of freedom (DoF) are removed from the system after the element assembly is complete.

The total number of degrees of freedom for each model is given in Table 7.2. Note that the first node is fixed and we have an additional degree of freedom from the rotation of the hub (θ) which is why there is an odd number of degrees of freedom.

Model	Nodes/Element	DoF/Node	Total Degrees of Freedom
2D Euler-Bernoulli	2	2	41
2D Timoshenko	4	3	181
3D Timoshenko	4	7	421

Table 7.4: System Degrees of Freedom

The C^1 cubic elements have two nodes and two degrees of freedom per node, as shown in Figure 7.4. The C^0 cubic elements have four nodes and three DoF per node (for the 2D

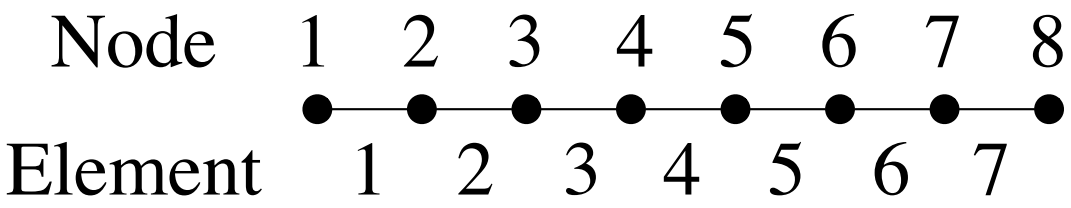

Figure 7.3: 2D Euler-Bernoulli Beam 7 Element Mesh

Figure 7.4: 2D Euler-Bernoulli C^1 Cubic Beam Element

Timoshenko case) and seven DoF per node (for the 3D Timoshenko case). See Figure 7.5 for an example of the structure of the C^0 cubic element in the 3D Timoshenko beam case.

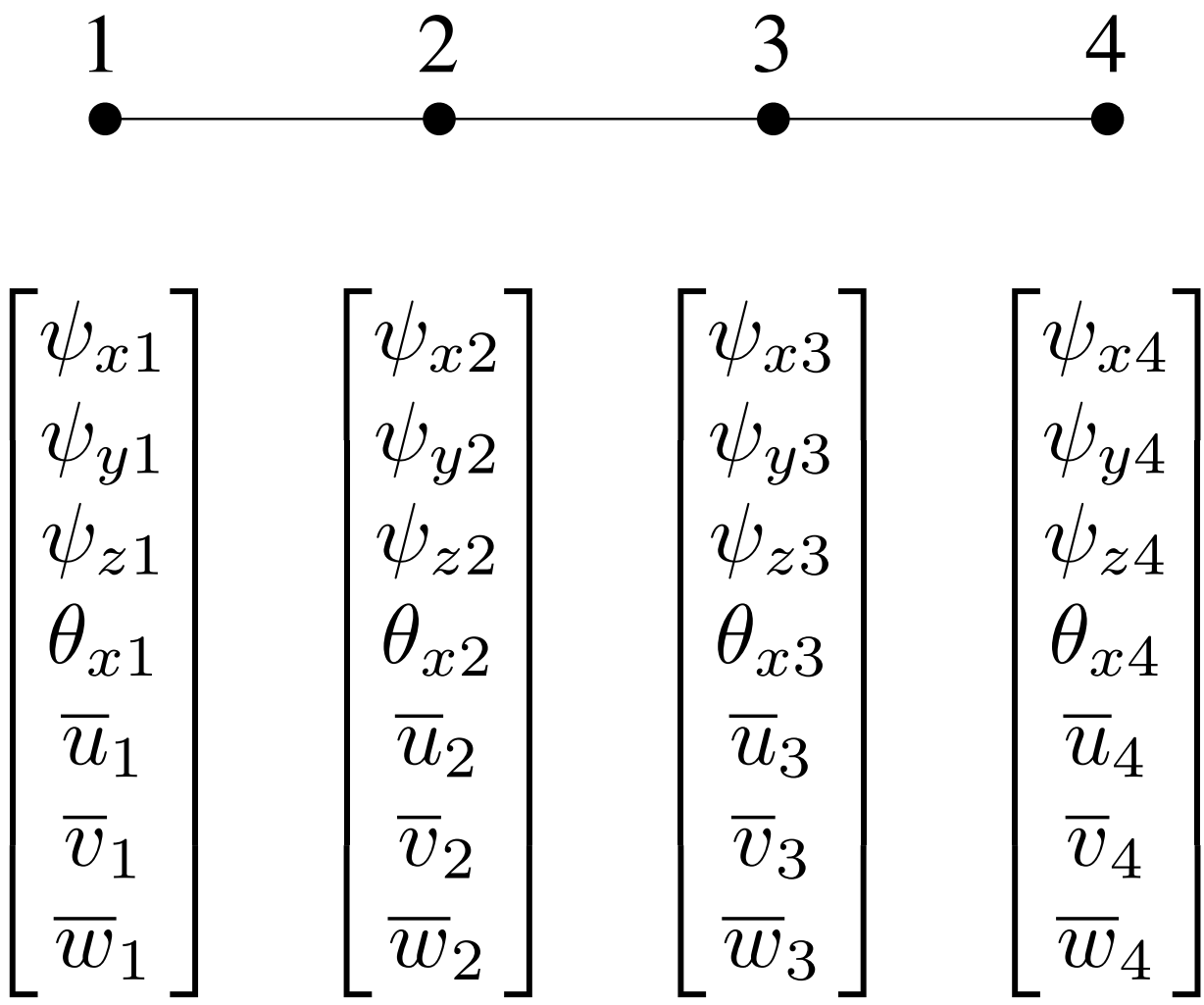

Figure 7.5: 3D Timoshenko C^0 Cubic Beam Element

7.3 Comparison of Natural Frequencies

Mode	2D Euler-Bernoulli Beam	2D Timoshenko Beam	3D Timoshenko Beam
1	12.26	11.20	11.20
2	46.74	36.38	13.06
3	103.06	77.57	36.38
4	178.03	142.13	57.65
5	266.10	225.02	77.57
6	368.71	321.06	138.94
7	497.72	438.73	142.13
8	657.86	587.57	225.02
9	847.87	753.91	280.07

Table 7.5: Mode Frequency Comparison (Hz)

Examining the 2D Euler-Bernoulli beam's elastic modes (all in-plane bending) shown in Table 7.3 they overestimate the natural frequencies shown in Table 6. The first mode is only slightly high, whereas the second mode is much higher than the experiment. In contrast, the Timoshenko beam models consistently underestimate the natural frequencies, but provide a better estimate of the second experimental mode. All of the 2D Timoshenko beam modes are in-plane bending except the final mode which is extension. The 3D Timoshenko beam modes not found in the experimental data are all out-of-plane modes (see Table 7.3).

Mode	Frequency Hz	Mode Type
1	11.20	In-Plane Bending
2	13.06	Torsion
3	36.38	In-Plane Bending
4	57.65	Out-of-Plane Bending
5	77.57	In-Plane Bending
6	138.94	Torsion
7	142.13	In-Plane Bending
8	225.02	In-Plane Bending
9	280.07	Torsion

Table 7.6: 3D Timoshenko Mode Types

If we normalize the frequencies based upon the frequencies for a 40 element beam, we can see that the first three modes of the 2D Euler-Bernoulli beam all converge within the first 10 elements as shown in Figure 7.6. The higher modes also converge quickly, but since the experimental data is all less than 100 Hz, only the first two modes are of interest.

Now, normalizing the frequencies for the 2D Timoshenko beam (with respect to the 40 element beam), we get Figures 7.7 and 7.8. For this beam, convergence occurs in roughly 5 elements.

Lastly, normalizing the frequencies for the 3D Timoshenko beam (with respect to the 40 element beam), we get Figures 7.9 and 7.10 which show convergence within 10 elements. The fourth elastic mode is not visible in Figure 7.9 because it converges very quickly and has nearly converged to start.

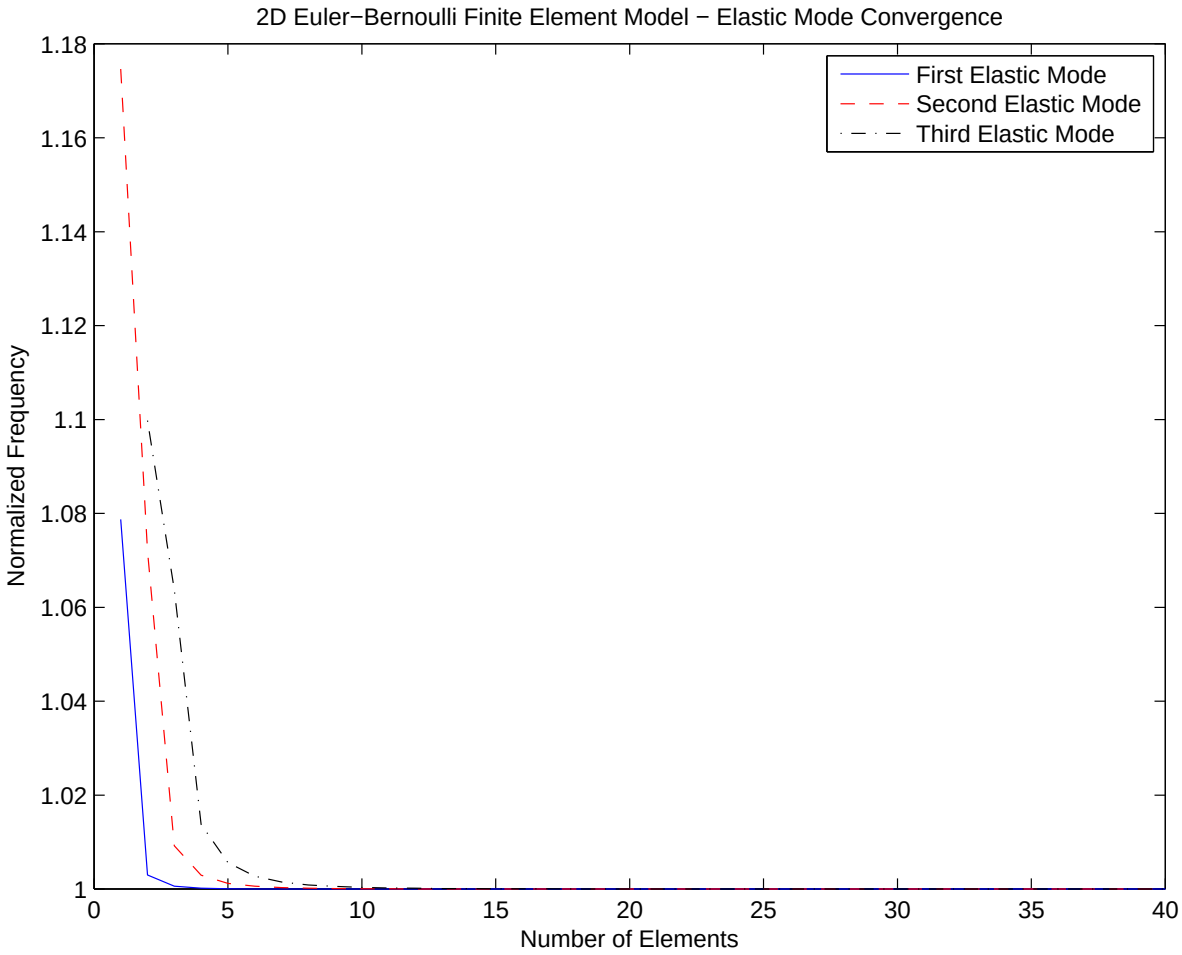

Figure 7.6: 2D Euler-Bernoulli Beam Elastic Mode Convergence

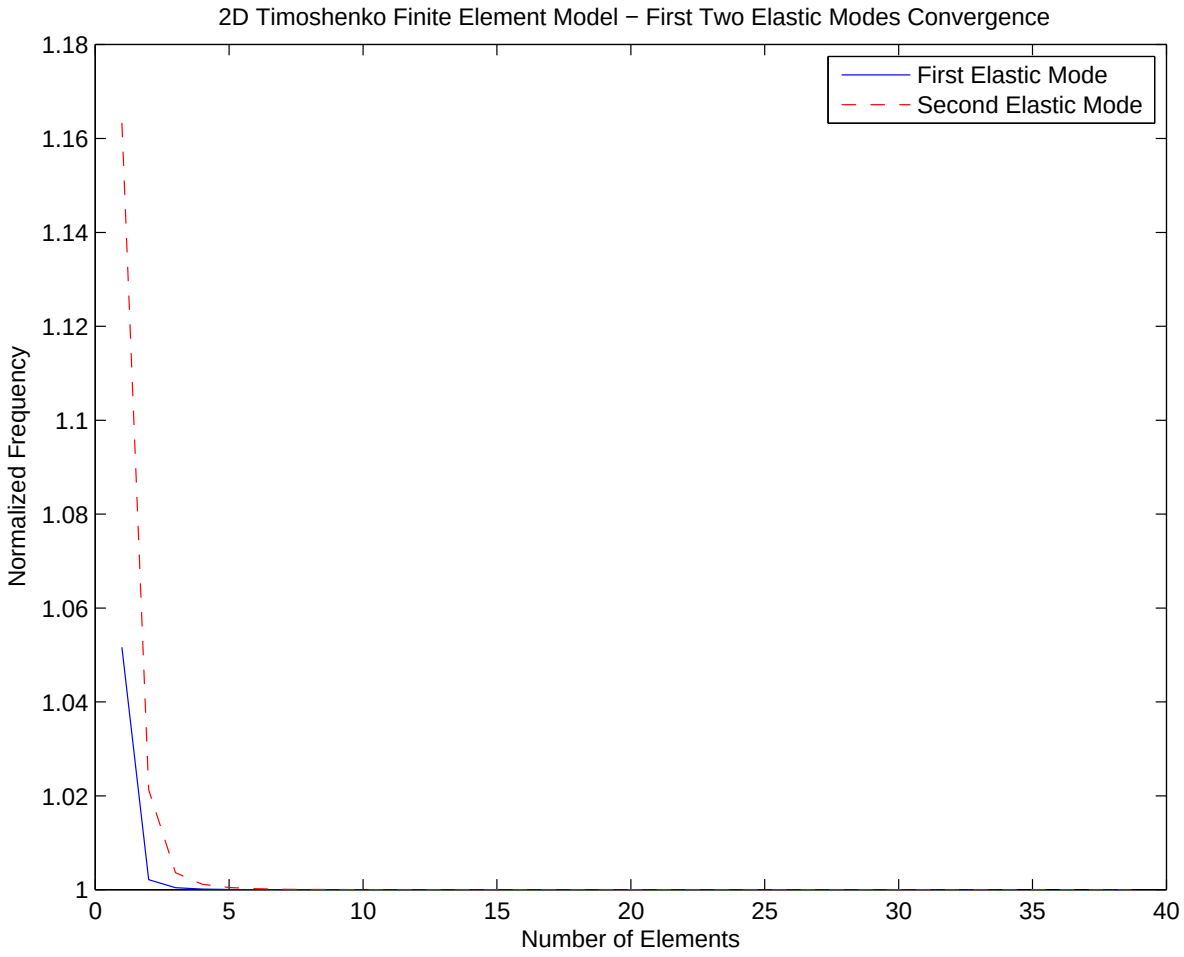

Figure 7.7: 2D Timoshenko Beam - First Two Elastic Mode Convergence

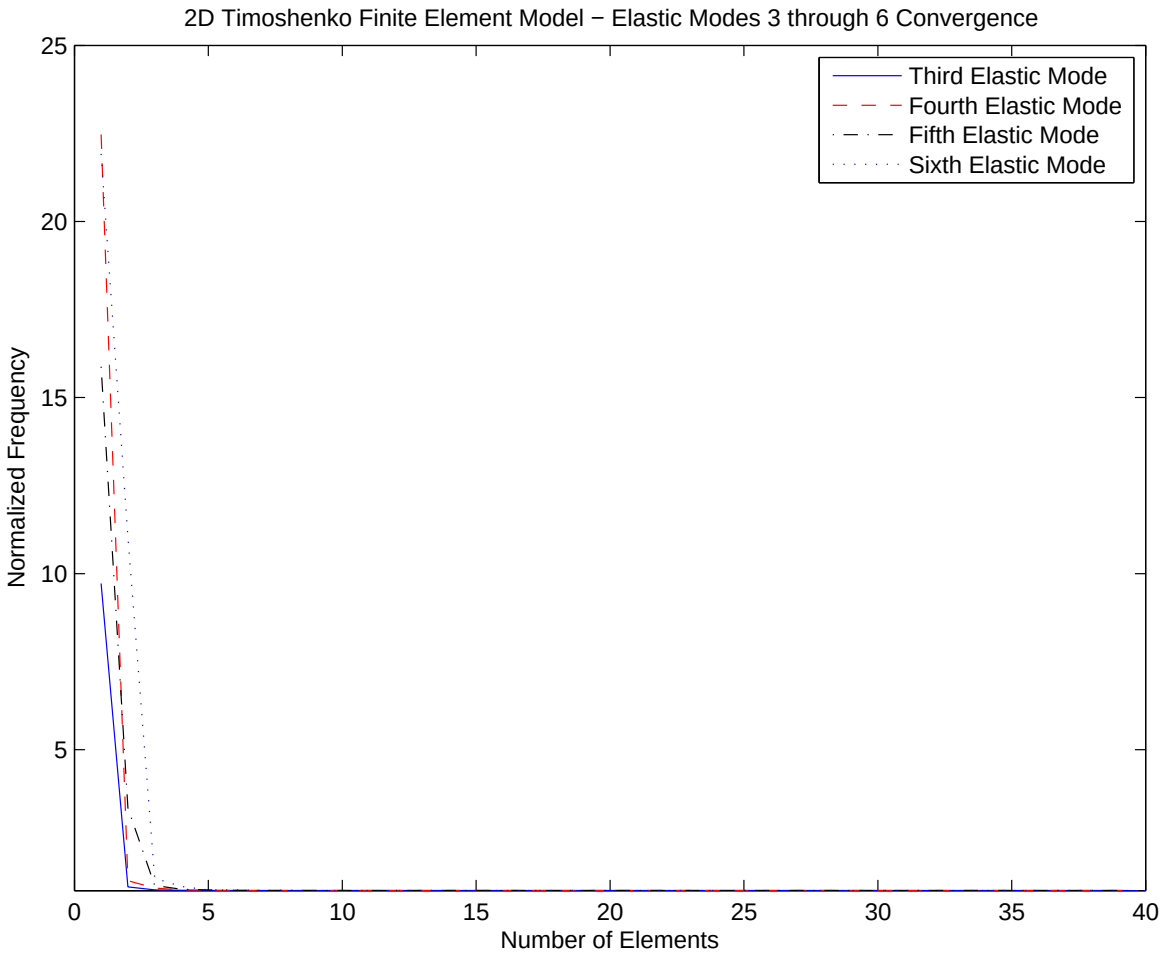

Figure 7.8: 2D Timoshenko Beam Elastic Modes 3 through 6 Convergence

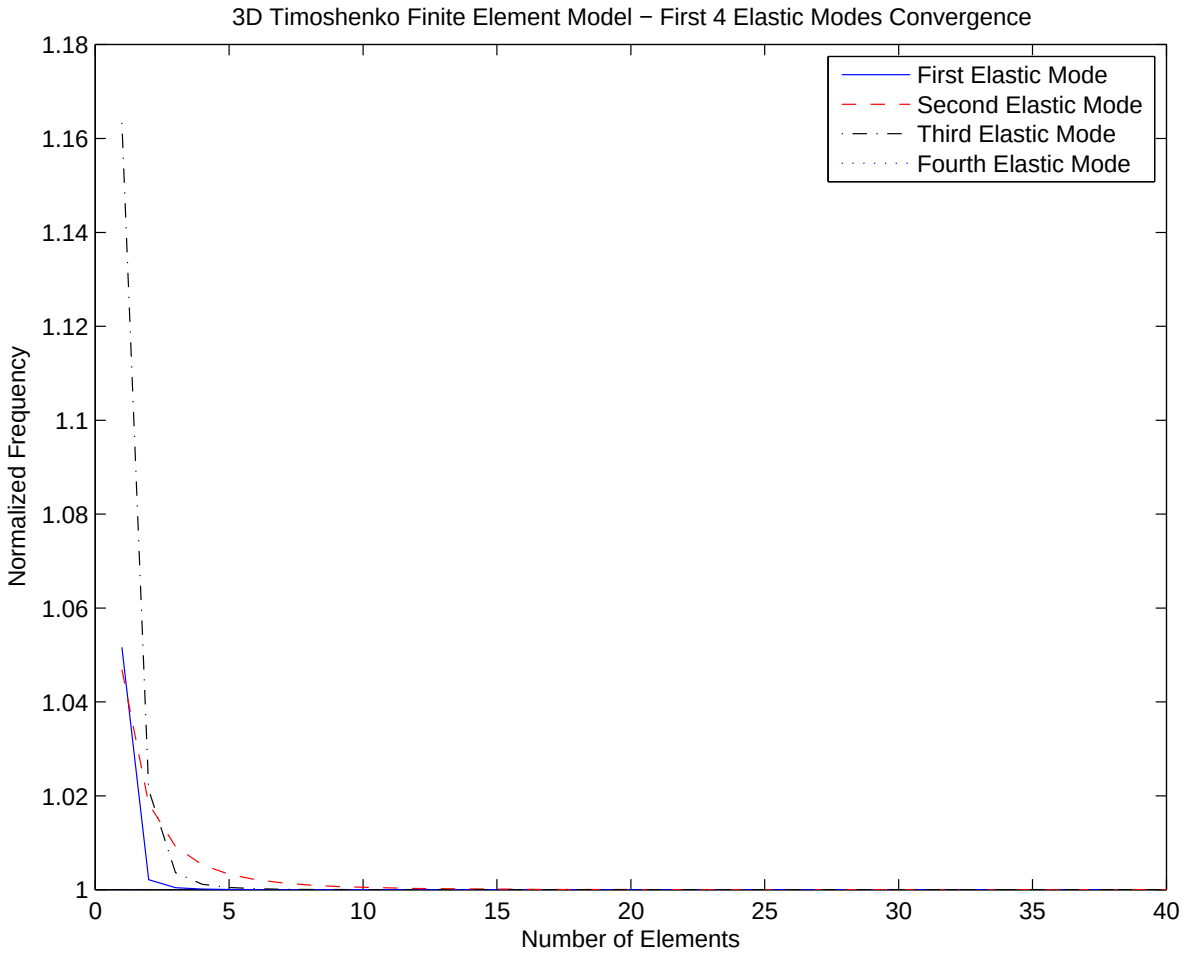

Figure 7.9: 3D Timoshenko Beam - First Four Elastic Modes Convergence

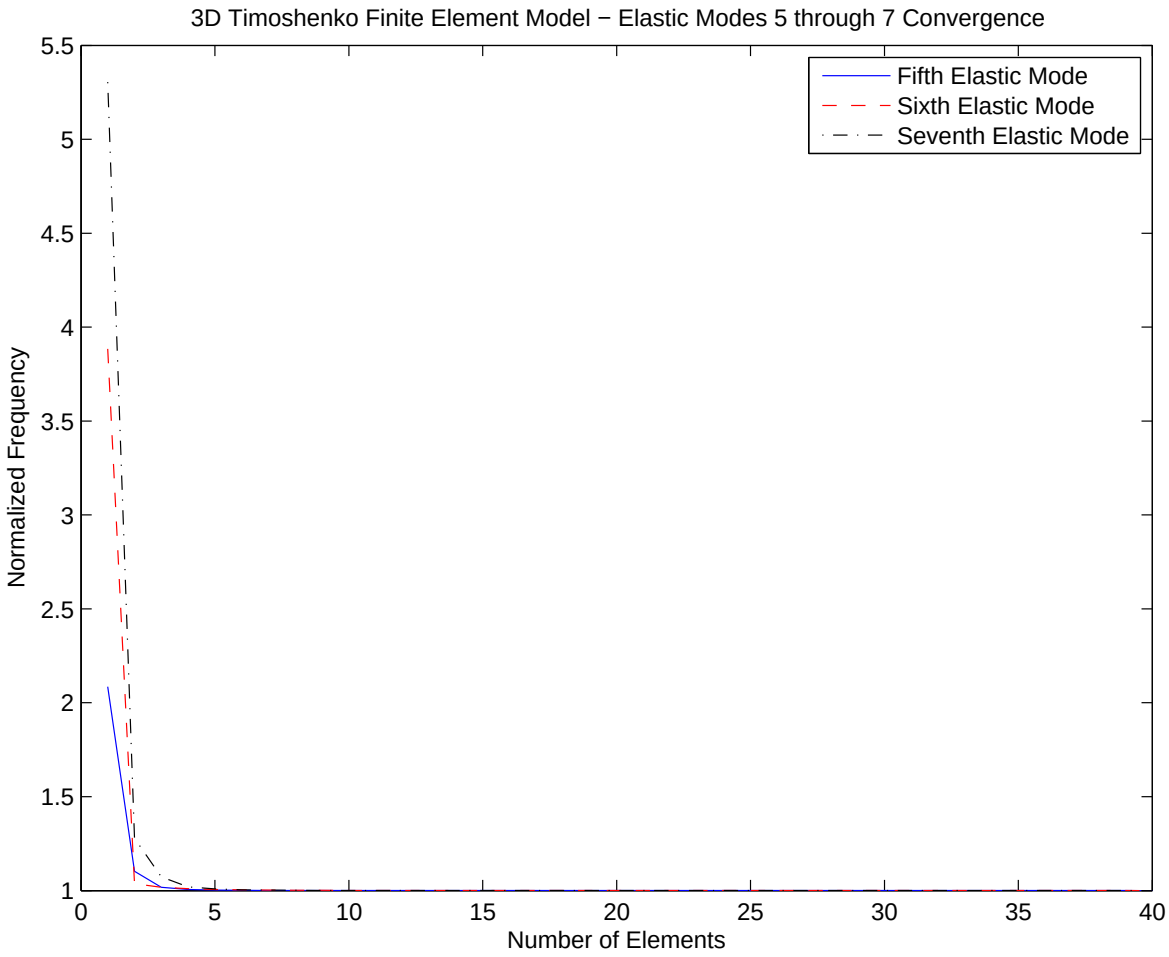

Figure 7.10: 3D Timoshenko Beam Elastic Modes 5 through 7 Convergence

7.4 2D Euler-Bernoulli Beam Results

As one can see from the tip deflection (Figures 7.11 and 7.12) the initial peak from the simulation is smaller (0.9×10^{-2} m vs. 1.55×10^{-2} m). Examining Figure 7.12 we can see the harmonic behaviour around 0.5 s-1.0 s is captured in the simulation.

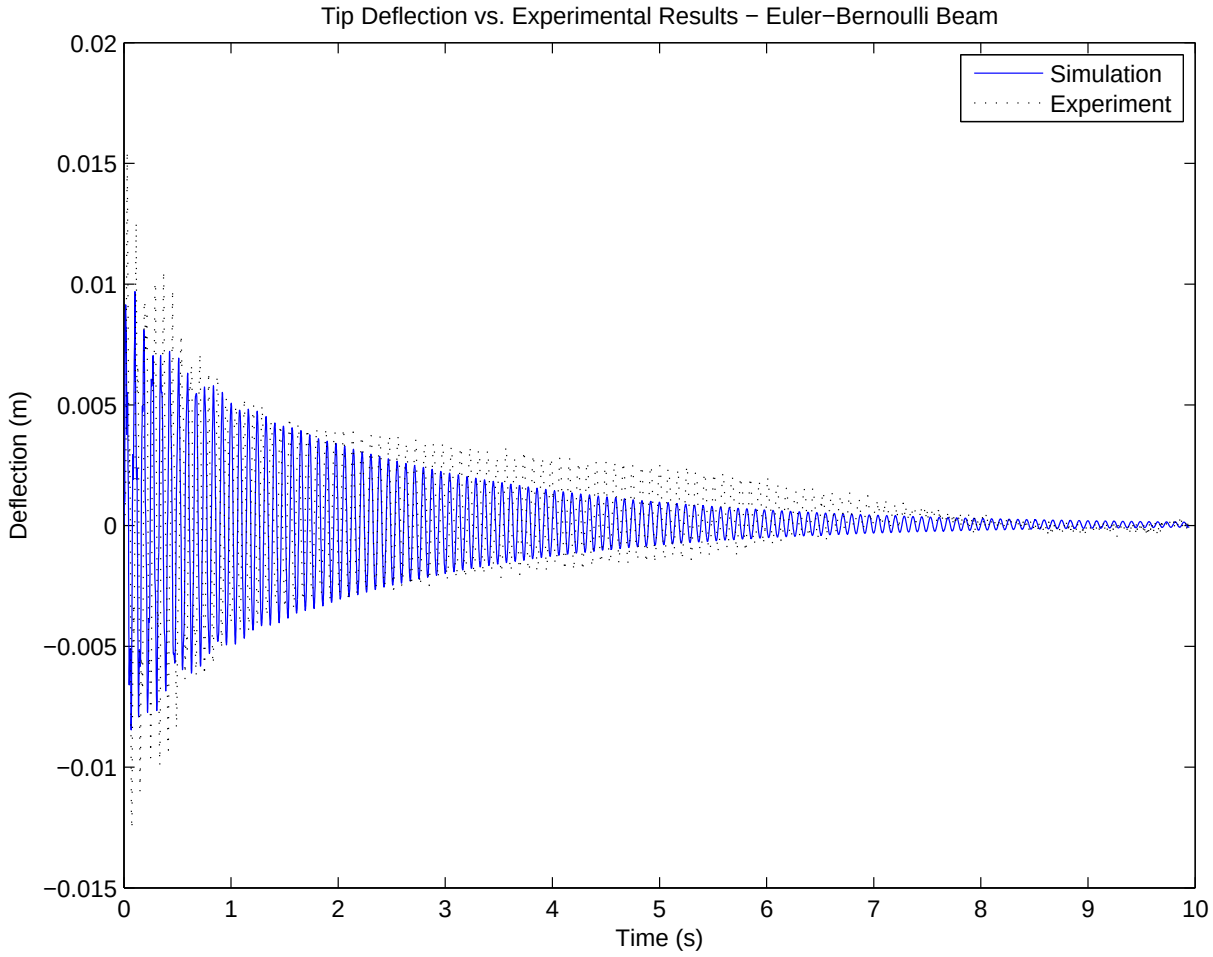

Figure 7.11: 2D Euler-Bernoulli Beam Tip Deflection vs. Experiment

Examining the FFTs of the simulation as compared to the experiment (Figure 7.13), we see that the simulation has a rigid body mode at 0 Hz and the first two elastic modes given in Table 7.3. As stated before, the first elastic mode is very close to experiment, but the second mode is quite a bit higher than the experimental mode.

Looking at the initial hub rotation (Figure 7.14) we can see that the hub is initially still for 0.015 s which is far longer than in the simulation. The wave speed for an Euler-Bernoulli beam is,

$$c = \sqrt{\frac{E}{\rho}} \tag{7.1}$$

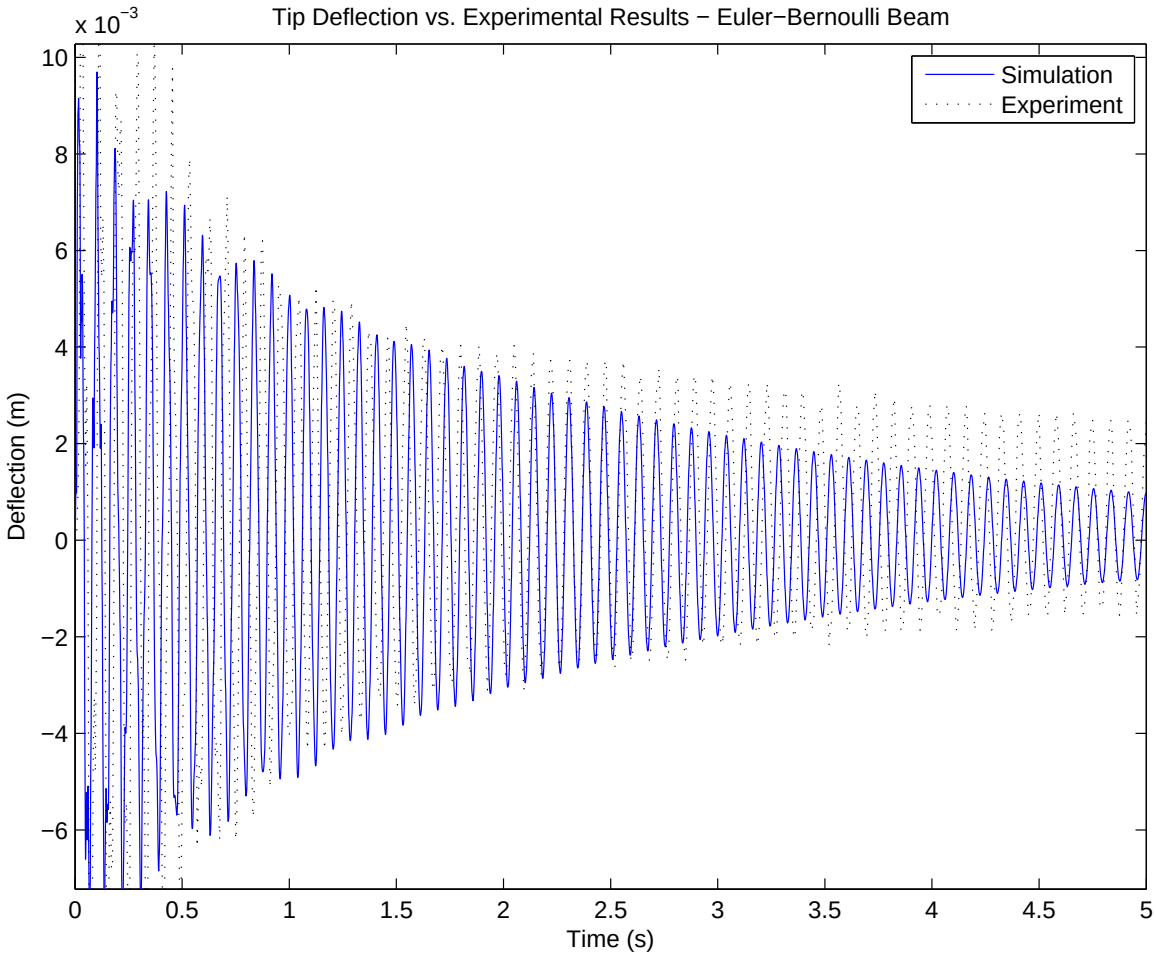

Figure 7.12: 2D Euler-Bernoulli Beam Tip Deflection vs. Experiment (initial 5s)

which leads to a time from the beam tip to the hub of 1.492×10^{-4} s. This is smaller than simulation step size and also the experimental sampling rate. So, the initial delay before the hub begins moving in the experiment is not due to the wave speed and is therefore likely due to static friction. The hub starts moving in the simulation immediately (in the negative direction) but the magnitudes are small enough that this is not apparent. Note that the simulation time step is smaller than the experiment's sampling rate so higher frequency behaviour can be seen in the simulation.

The hub rotation (Figure 7.15) levels off around 6 s. This is likely due to both friction and damping. Since the system model doesn't include friction, damping is increased to give similar behaviour, but it cannot reproduce it exactly. Looking at the initial 2.5 s, we see that while it drifts, we see that the simulation is reproducing the oscillatory behaviour of rotation.

If we consider minimal damping for the hub, we get behaviour as shown in Figures 7.17 and 7.18. We can see that we get relatively good correspondence for the first 3 s. This leads one to conclude that with smaller damping and the inclusion of friction, we would be able to

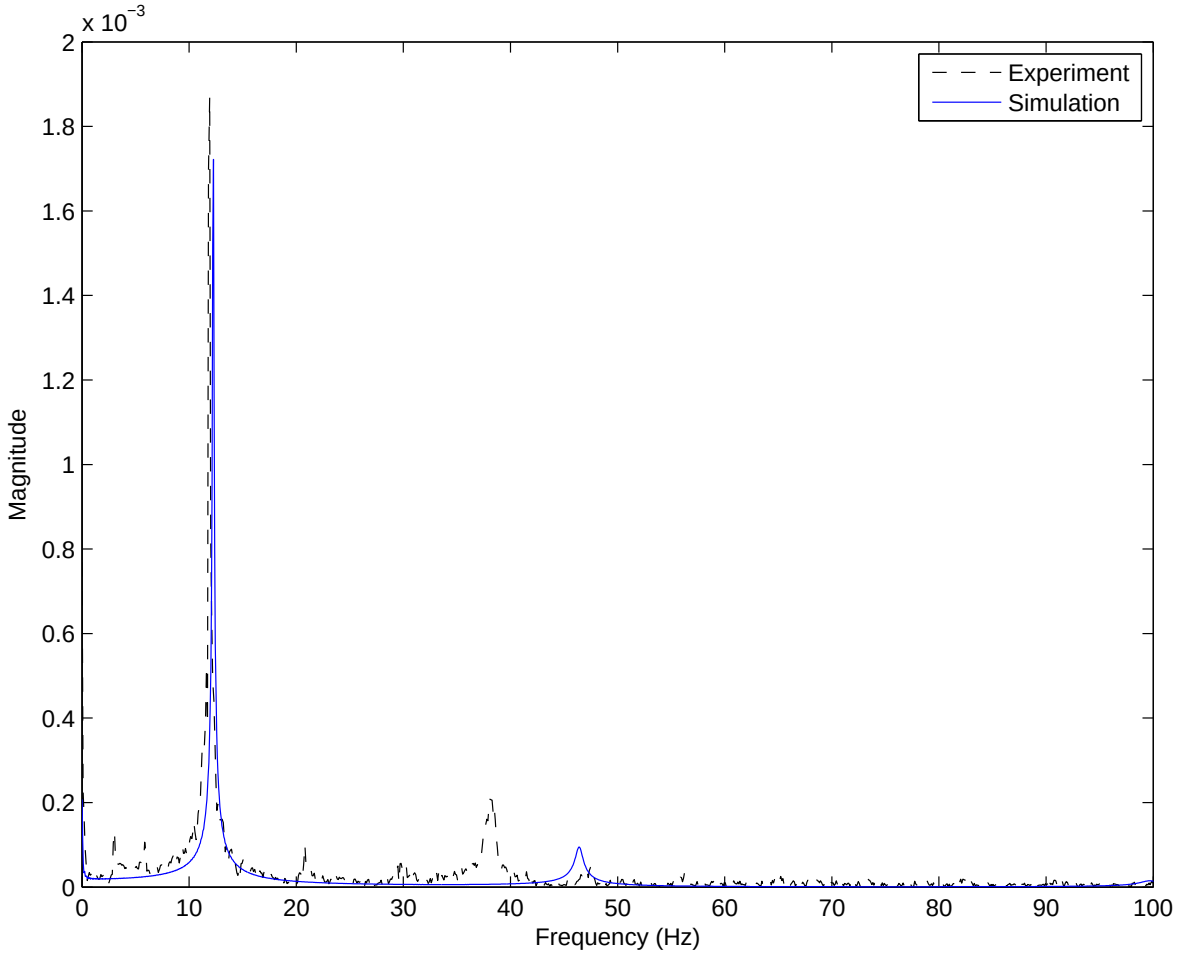

Figure 7.13: 2D Euler-Bernoulli Beam FFT Simulation vs. Experiment

improve the accuracy of the model.

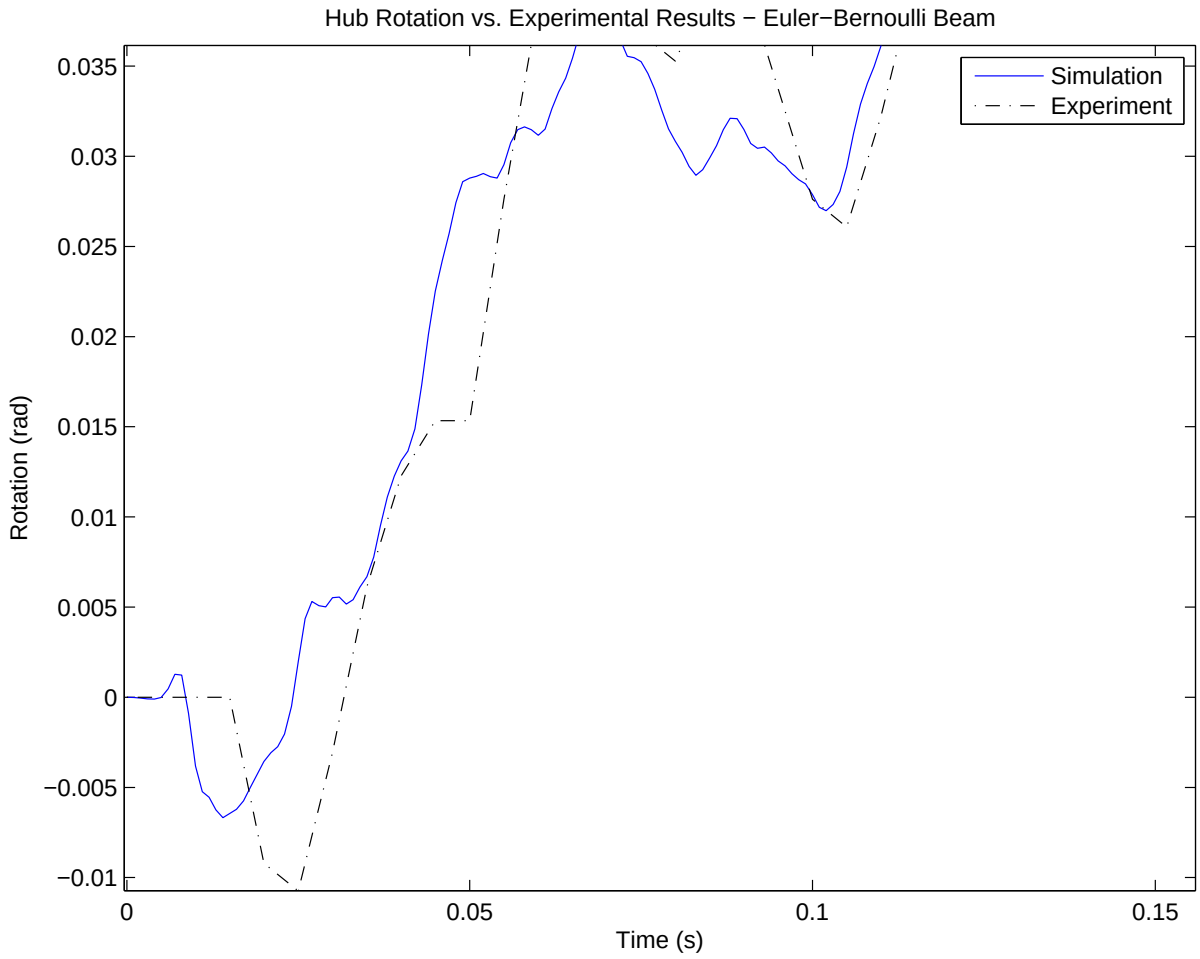

Figure 7.14: 2D Euler-Bernoulli Beam Hub Rotation vs. Experiment (initial 0.15s)

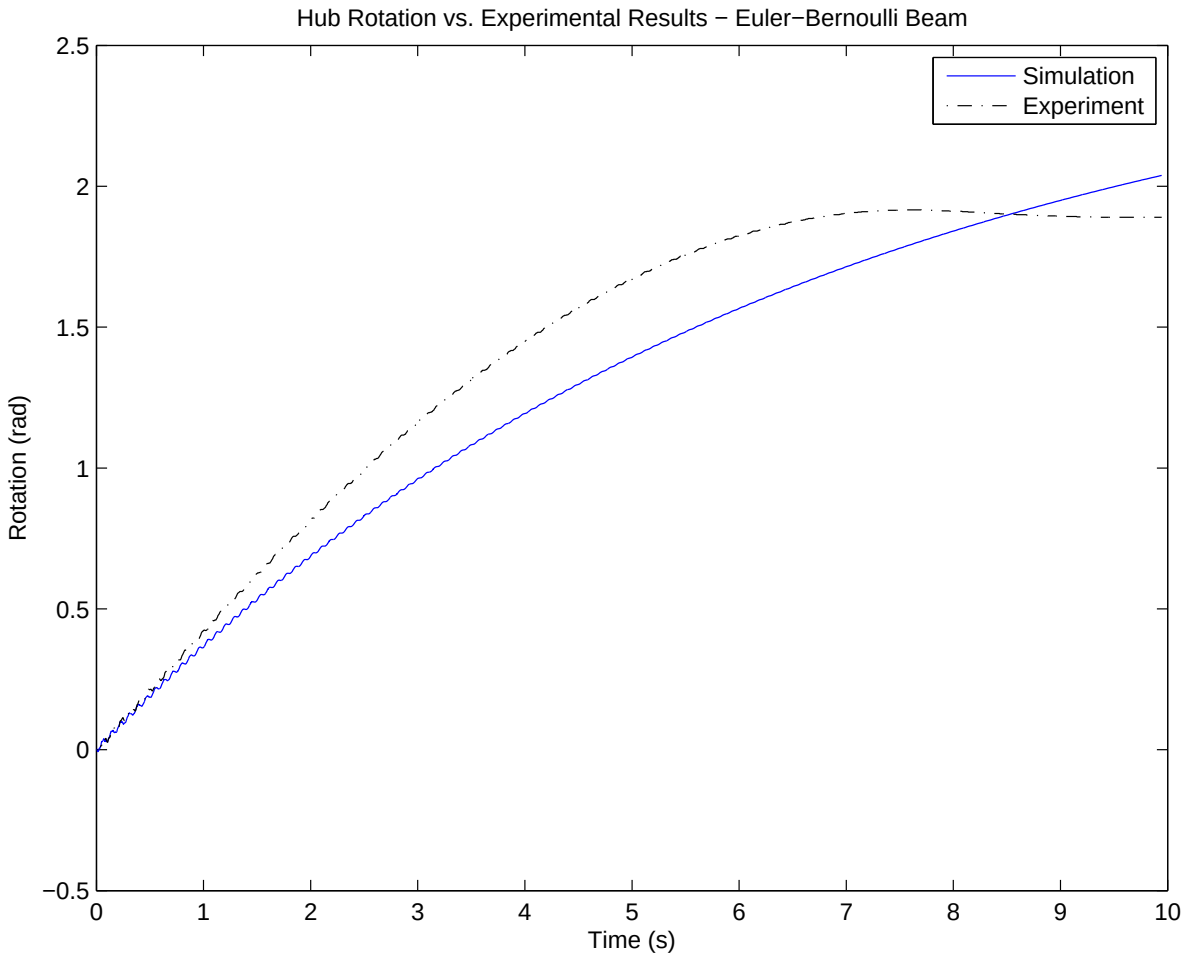

Figure 7.15: 2D Euler-Bernoulli Beam Hub Rotation vs. Experiment

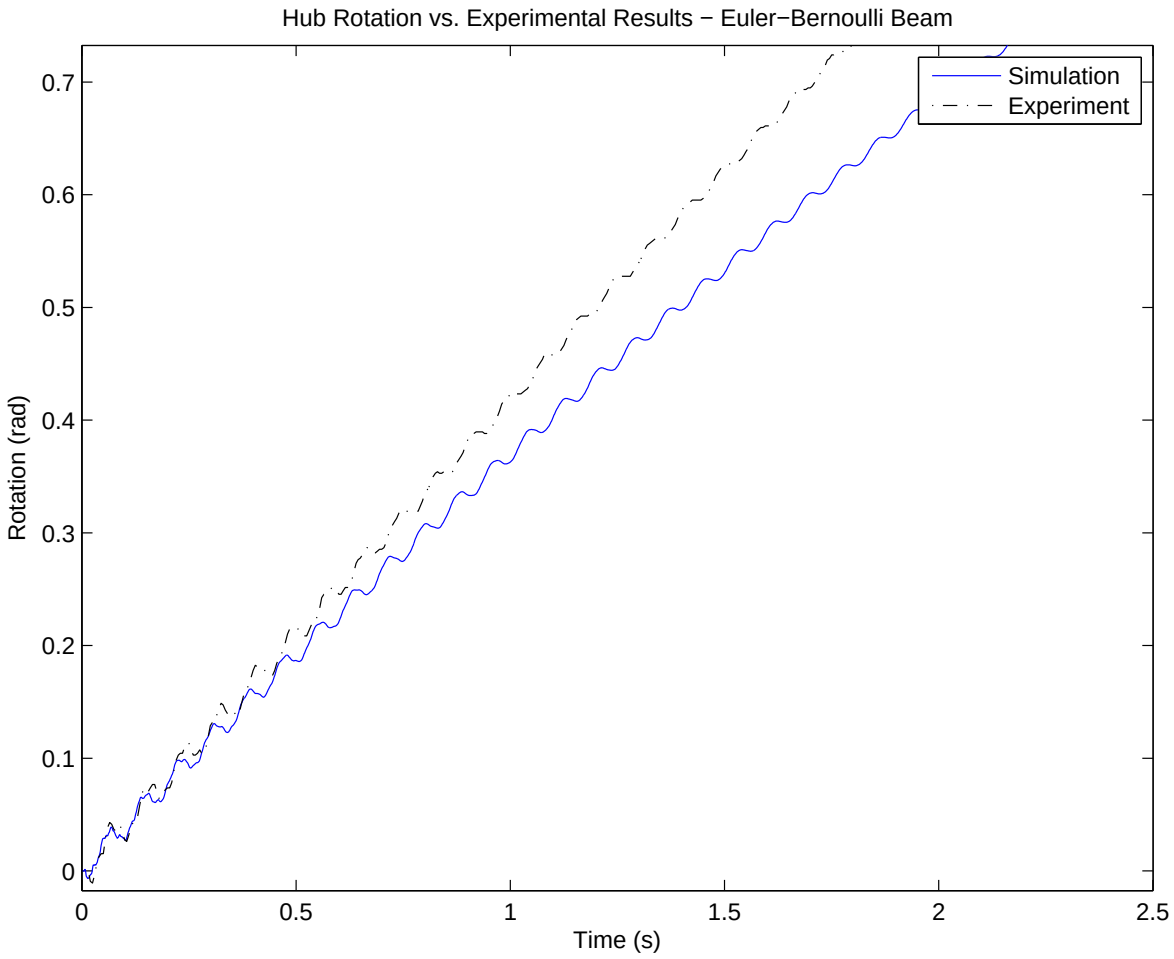

Figure 7.16: 2D Euler-Bernoulli Beam Hub Rotation vs. Experiment (initial 2.5s)

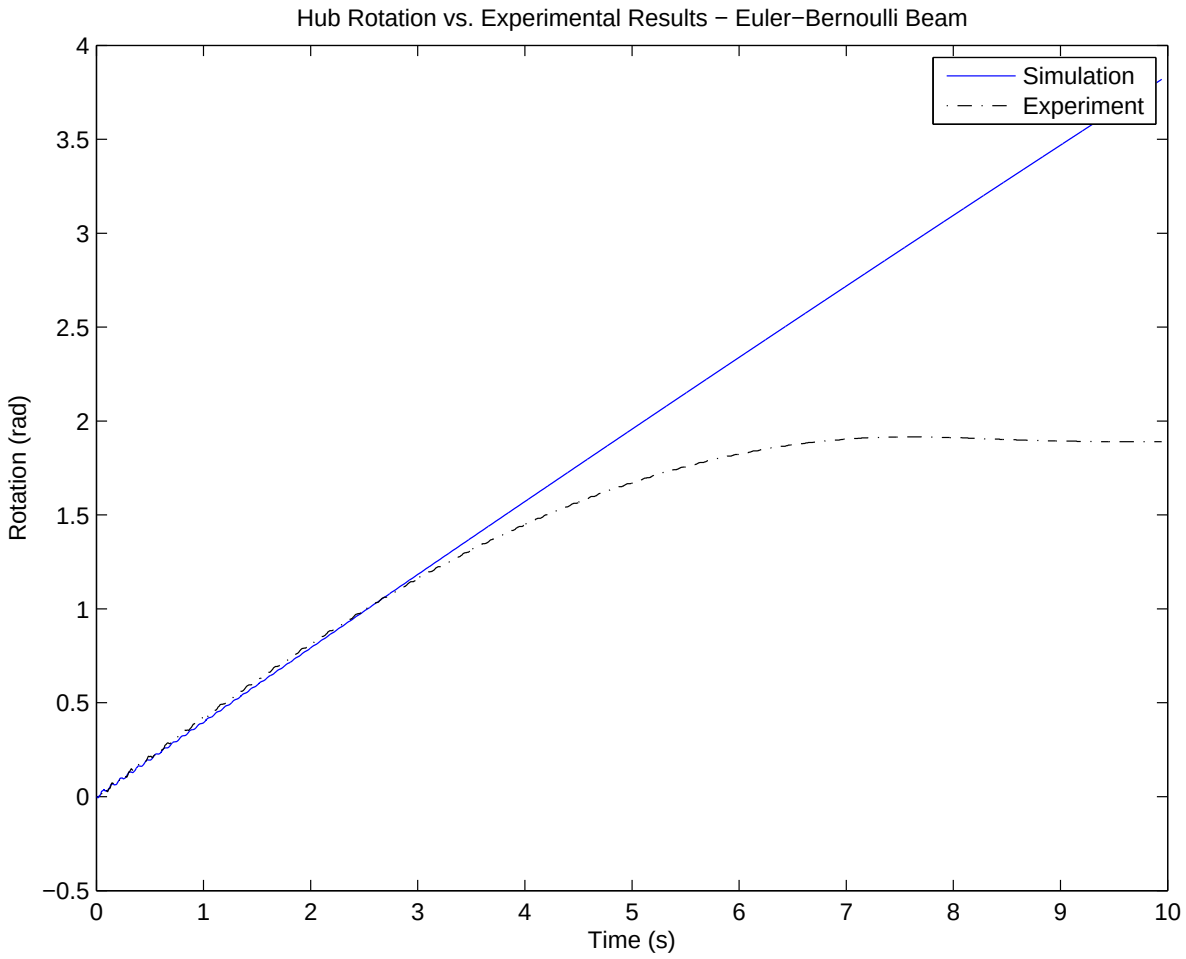

Figure 7.17: 2D Euler-Bernoulli Beam Hub Rotation (Minimal Damping)

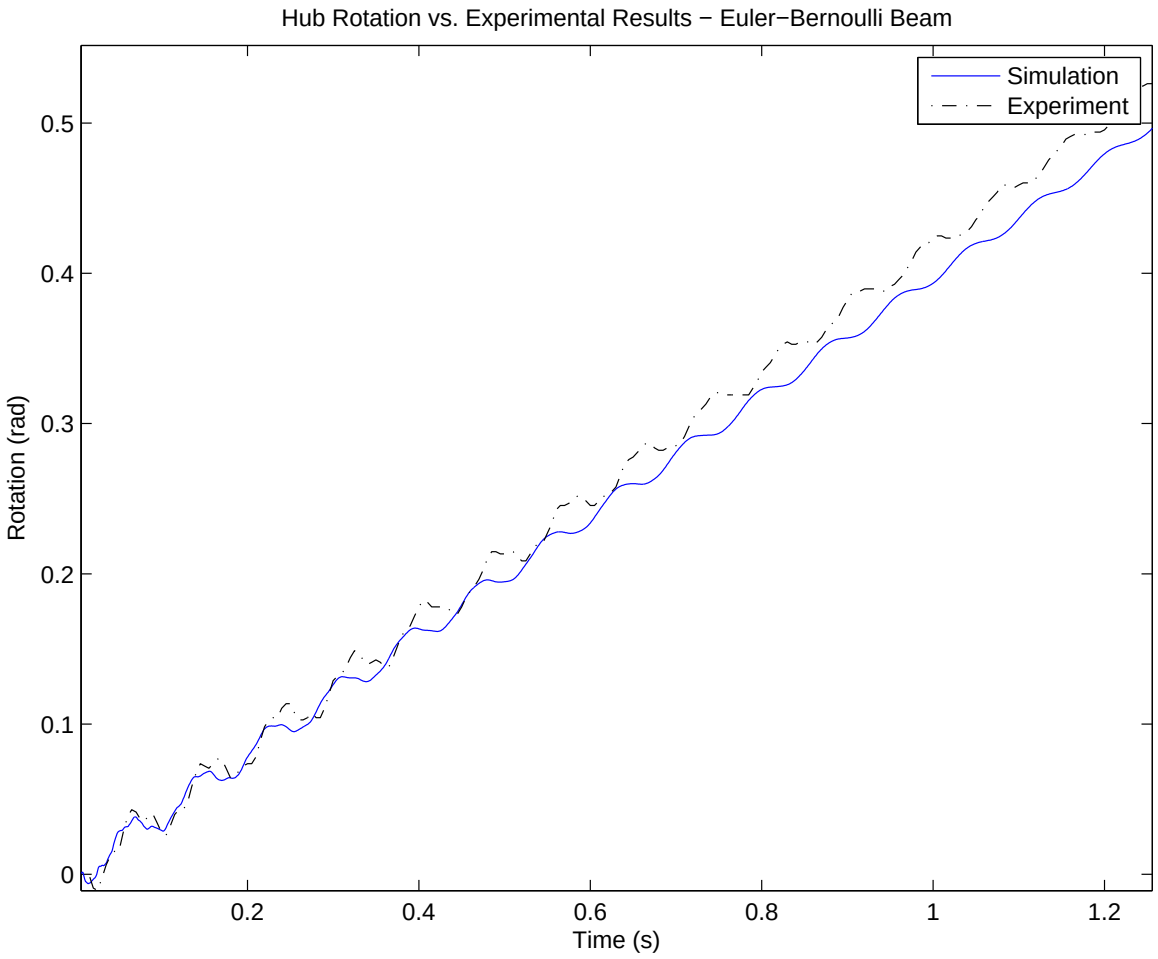

Figure 7.18: 2D Euler-Bernoulli Beam Hub Rotation (Minimal Damping - Initial 1.2s)

7.5 2D Timoshenko Beam Model Results

As with the Euler-Bernoulli beam model, the tip deflection (Figures 7.19 and 7.20) the initial peak from the simulation is smaller (0.85×10^{-2} m vs. 1.55×10^{-2} m). While this is smaller than in the Euler-Bernoulli model, that may be due to the choice of damping parameters.

Examining Figure 7.20 we can see the harmonic behaviour around 0.5 s-1.0 s is in the simulation, but with the chosen damping, it is nearly damped out. This is reflected in the FFT of the system as given in Figure 7.21, as the second elastic mode is nearly damped out, while the first elastic mode is close and we have a larger third elastic mode at 77 Hz.

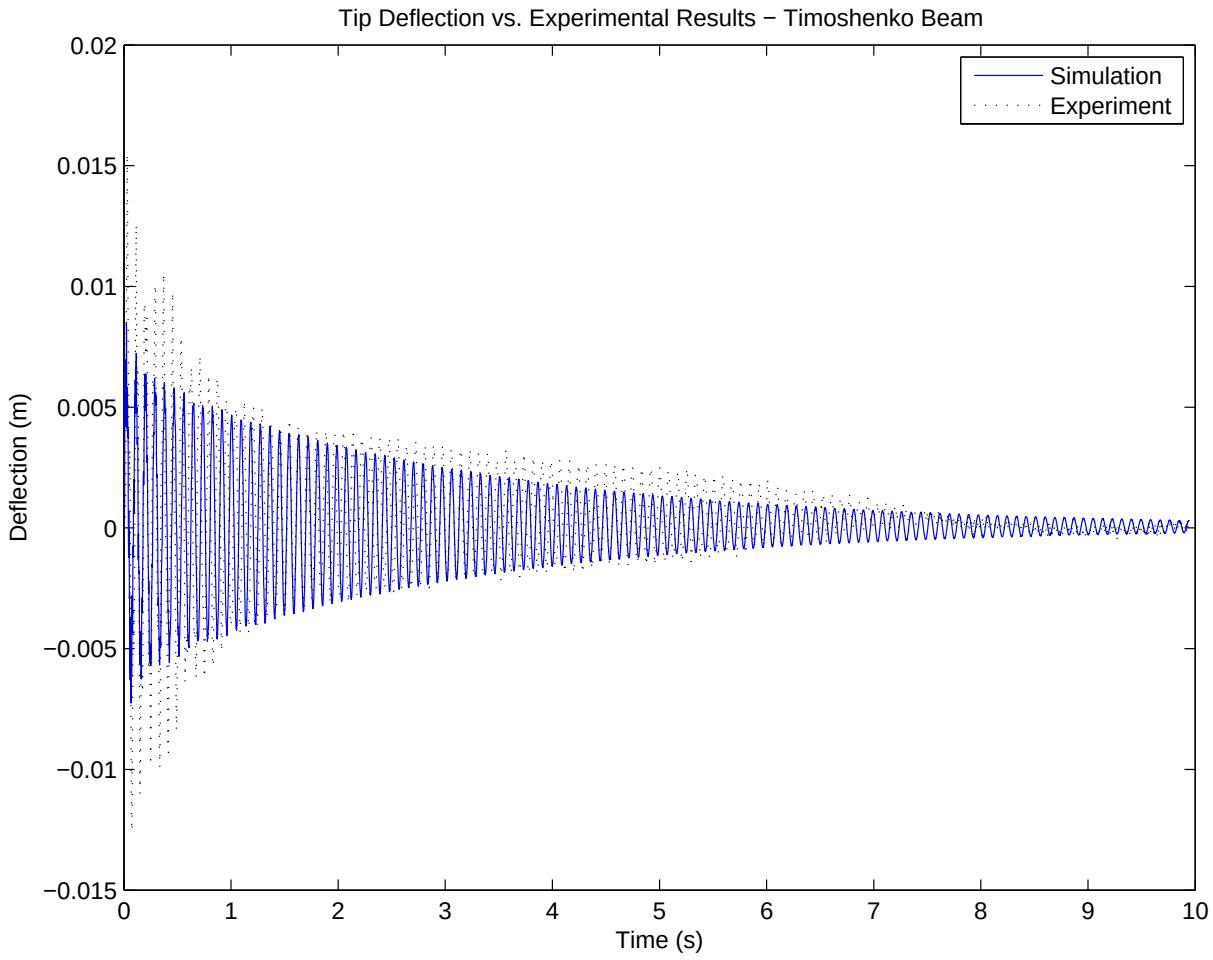

Figure 7.19: 2D Timoshenko Beam Tip Deflection vs. Experiment

The initial hub rotation (Figure 7.22) is very similar to the Euler-Bernoulli model. We see higher frequency behaviour in the simulation since the time step is higher than the experimental sampling rate.

The 2D Timoshenko beam model also can't reproduce the levelling off as shown in the experimental results (Figure 7.23), but it does fit the initial behaviour (once the initial still

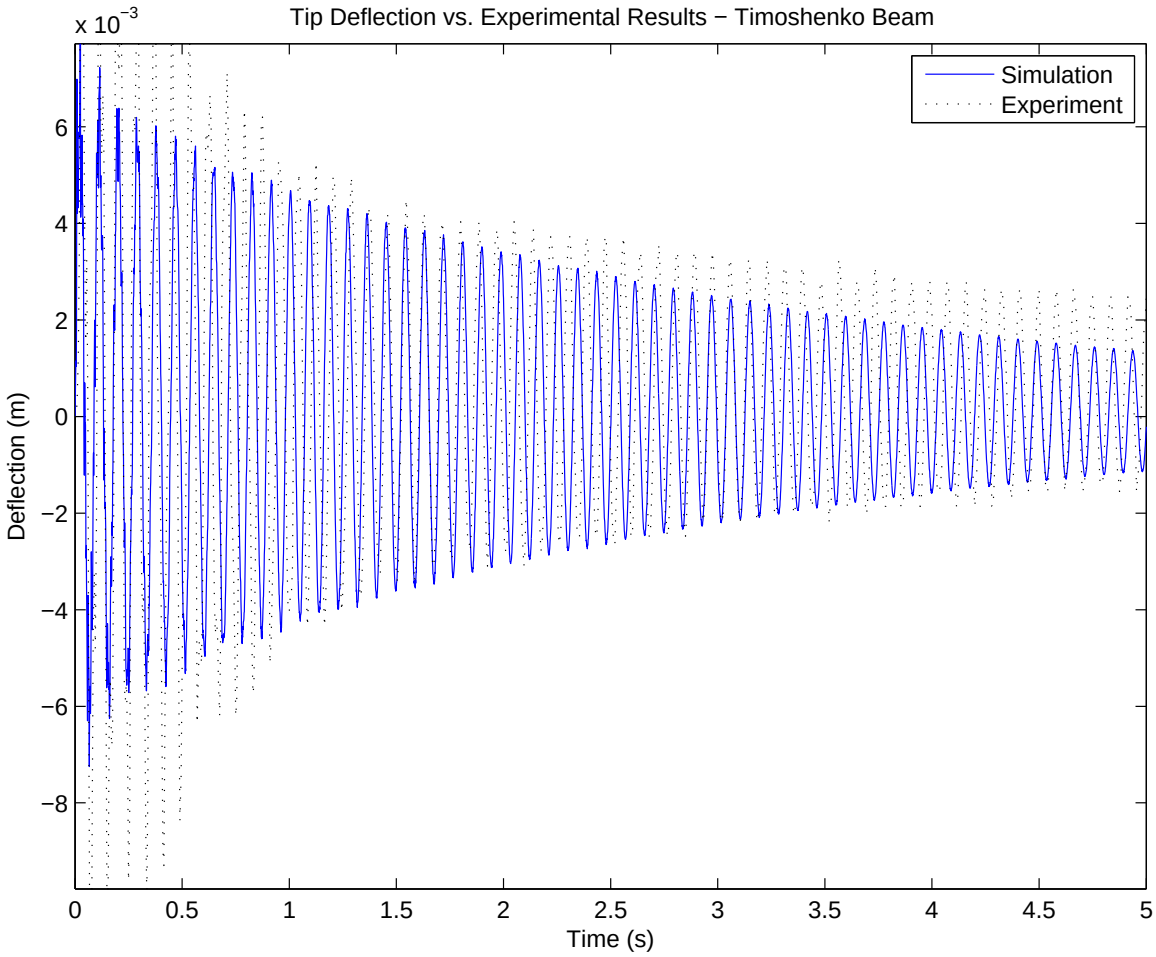

Figure 7.20: 2D Timoshenko Beam Tip Deflection vs. Experiment (initial 5s)

period is past). The initial 2.5 s (Figure 7.24) is reproduced fairly well aside from the drift (due to the increased damping).

If we consider minimal damping for the hub, we get behaviour as shown in Figures 7.25 and 7.26. The behaviour is reasonably accurate for the first 4 s. This also supports the conclusions from the 2D Euler-Bernoulli model that friction is necessary.

The axial deflection of the beam (Figure 7.27) is extremely small which lends one to conclude that axial deflection is not important to include in the model.

The rotation of the tip of the beam ψ_{zL} (Figure 7.28) is on the same order of magnitude as the tip deflection. However, rotation of the tip is in the Euler-Bernoulli as $\overline{v}'$ (but it is directly coupled to $\overline{v}$).

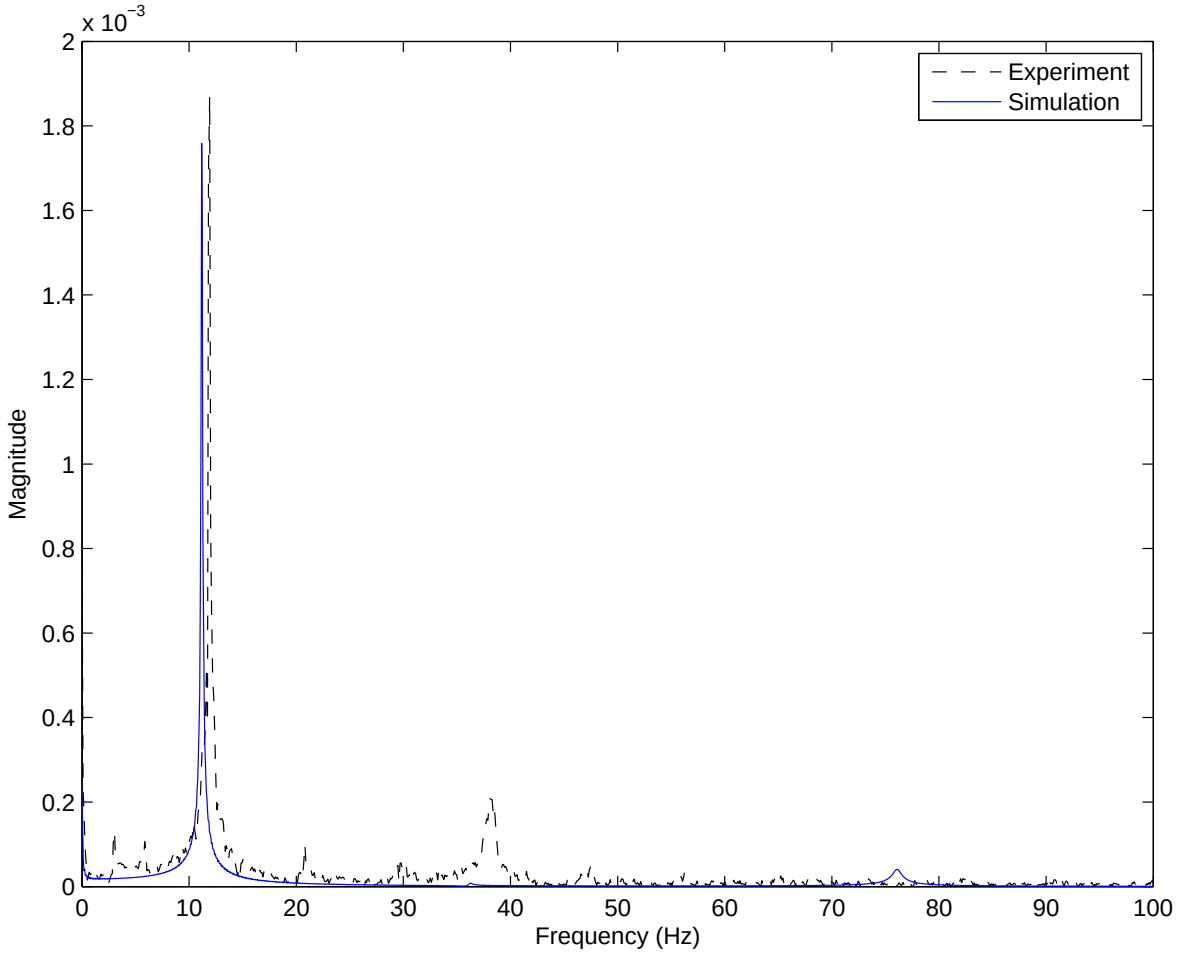

Figure 7.21: 2D Timoshenko Beam FFT Simulation vs. Experiment

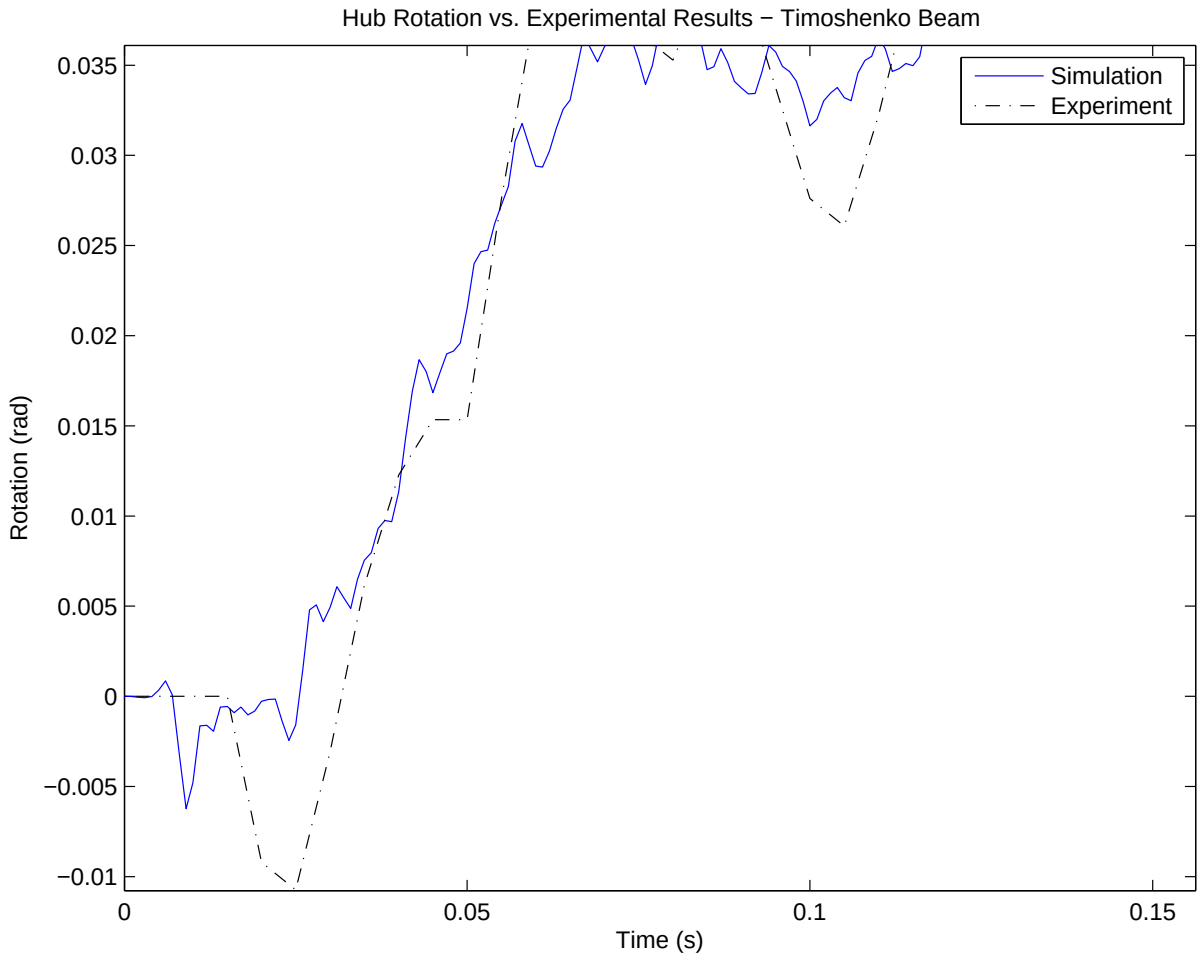

Figure 7.22: 2D Timoshenko Beam Hub Rotation vs. Experiment (initial 0.15s)

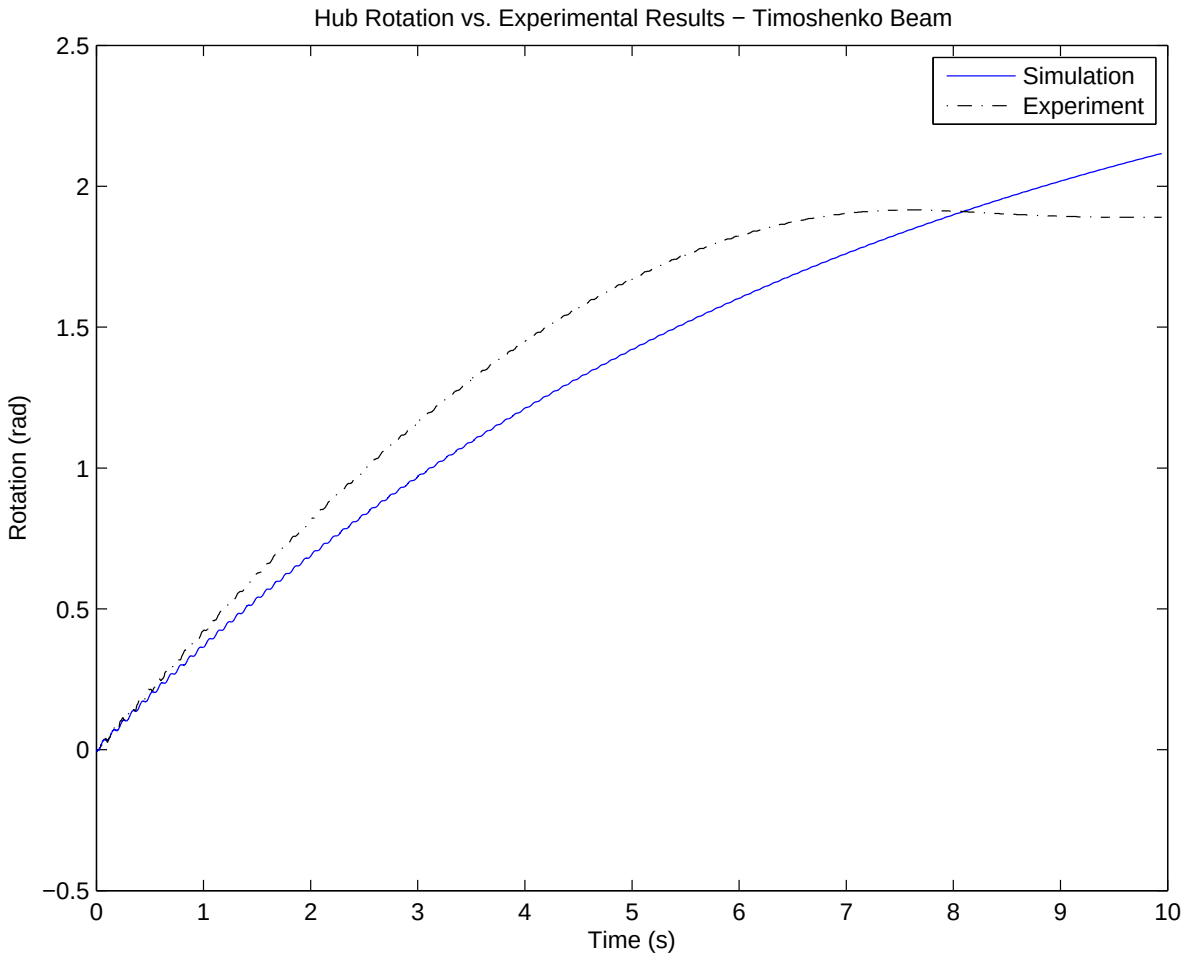

Figure 7.23: 2D Timoshenko Beam Hub Rotation vs. Experiment

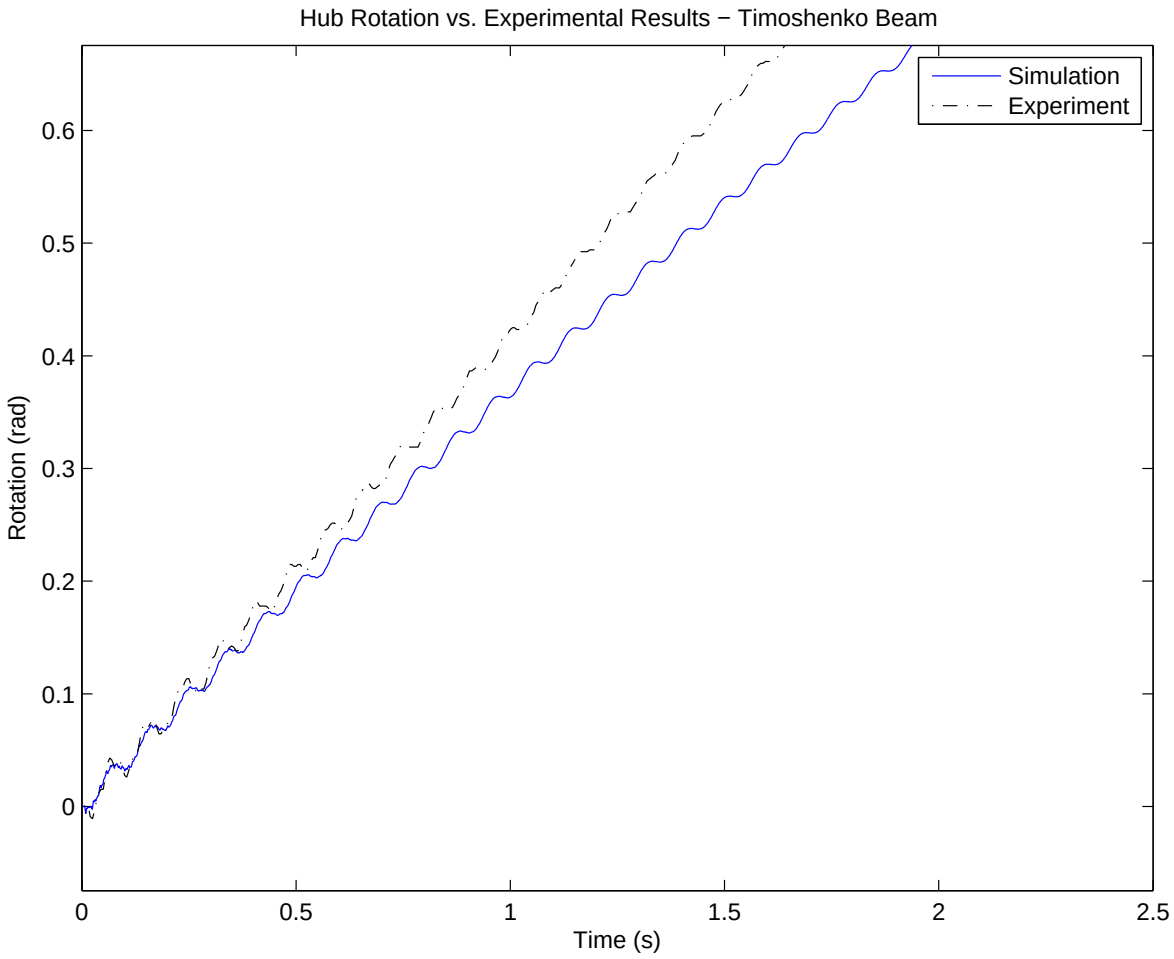

Figure 7.24: 2D Timoshenko Beam Hub Rotation vs. Experiment (initial 2.5s)

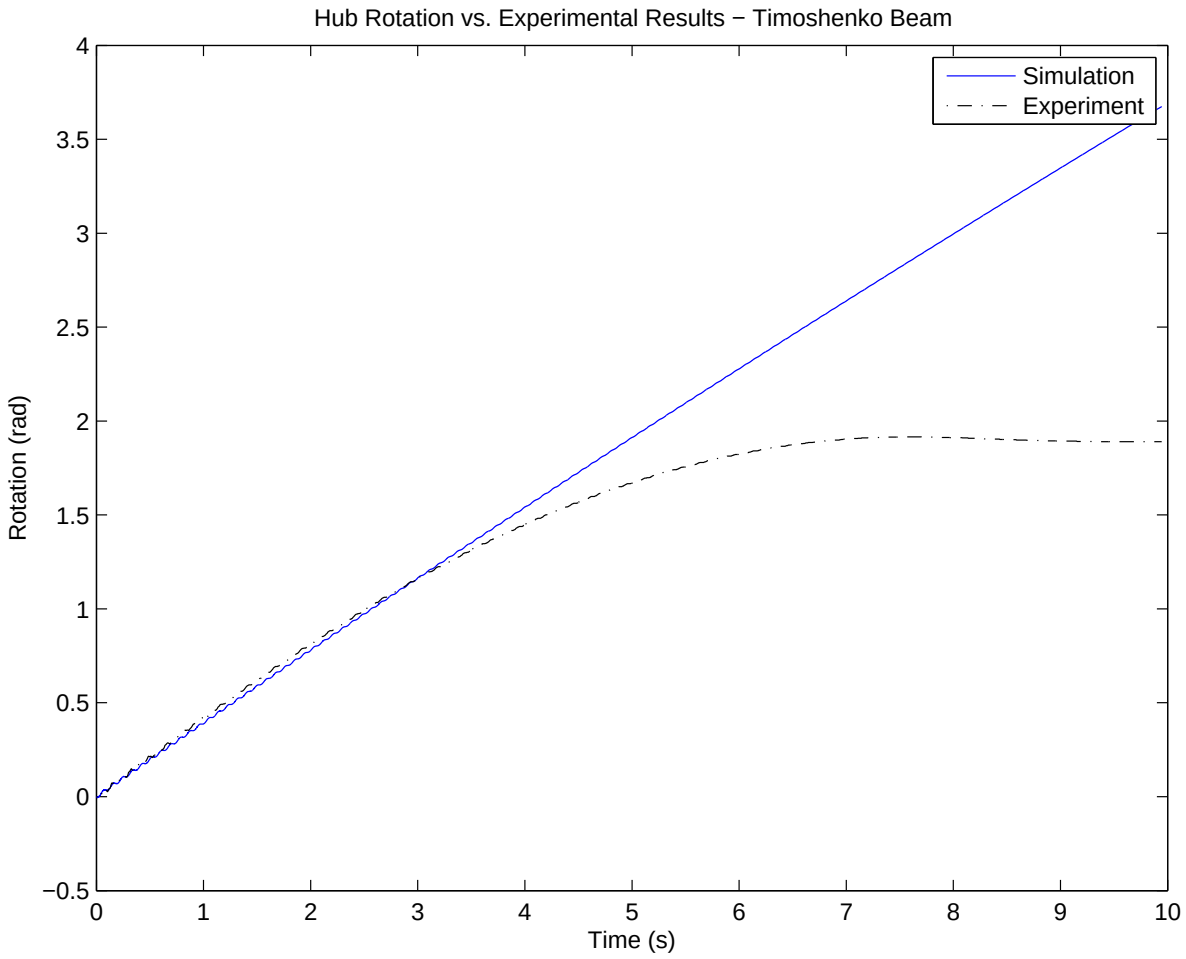

Figure 7.25: 2D Timoshenko Beam Hub Rotation (Minimal Damping)

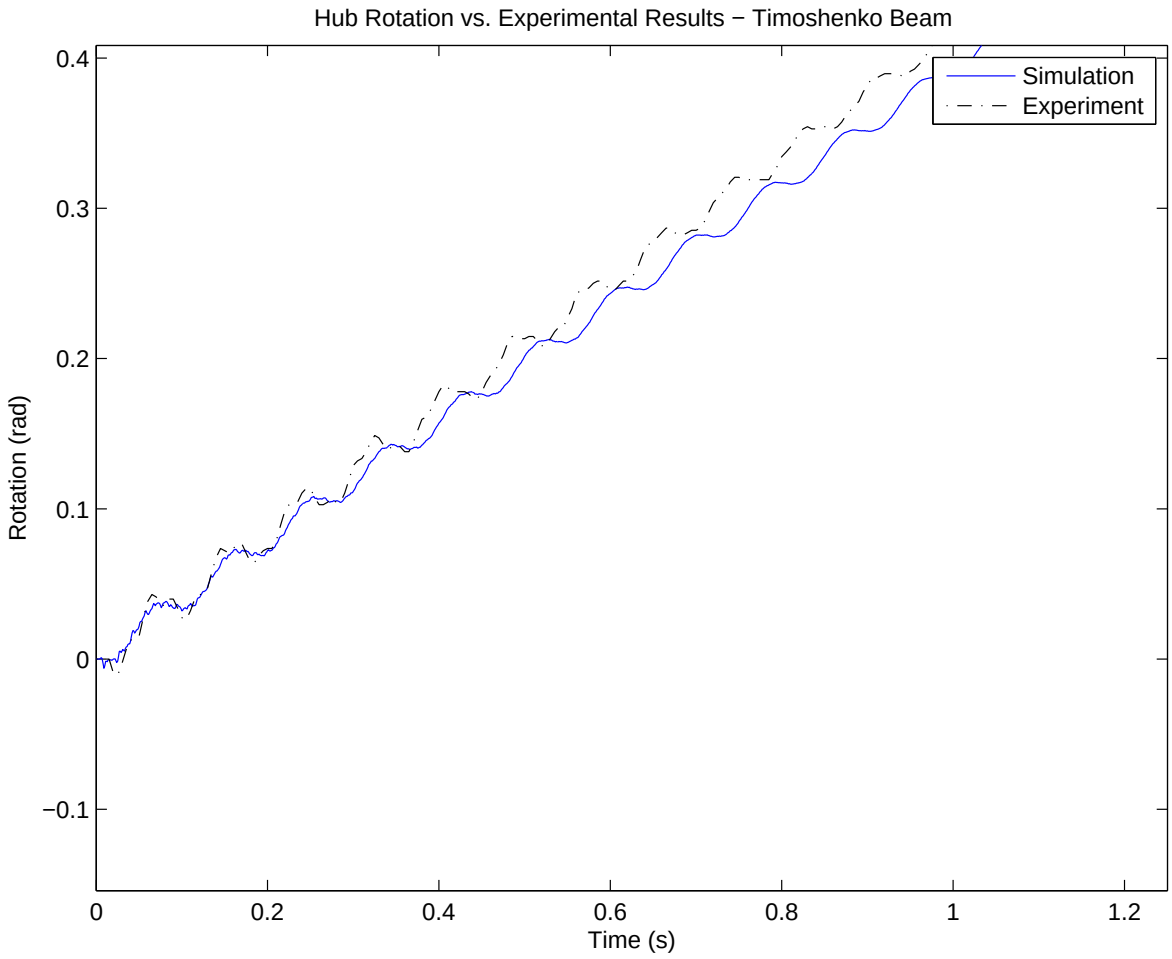

Figure 7.26: 2D Timoshenko Beam Hub Rotation (Minimal Damping - Initial 1.2s)

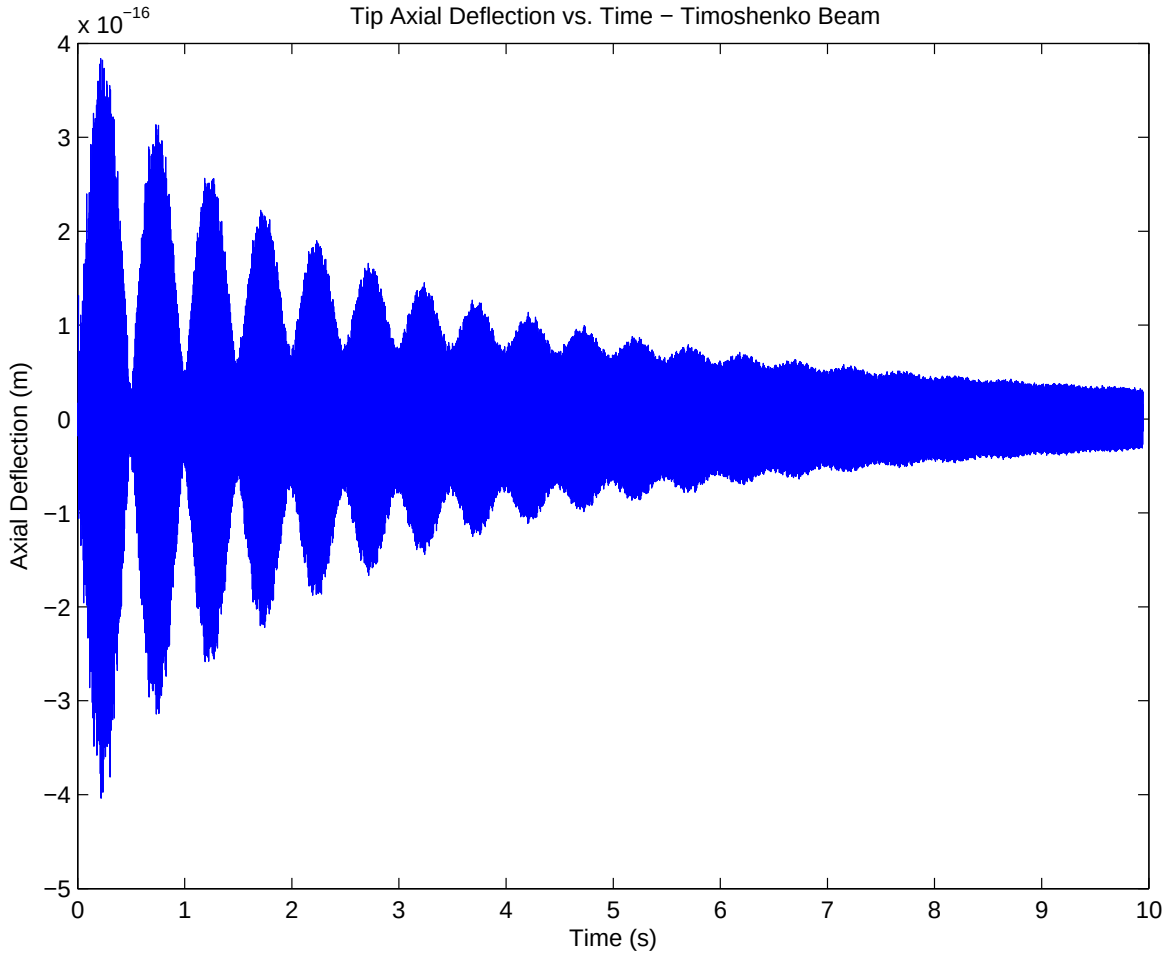

Figure 7.27: 2D Timoshenko Beam Tip Axial Deflection vs. Time

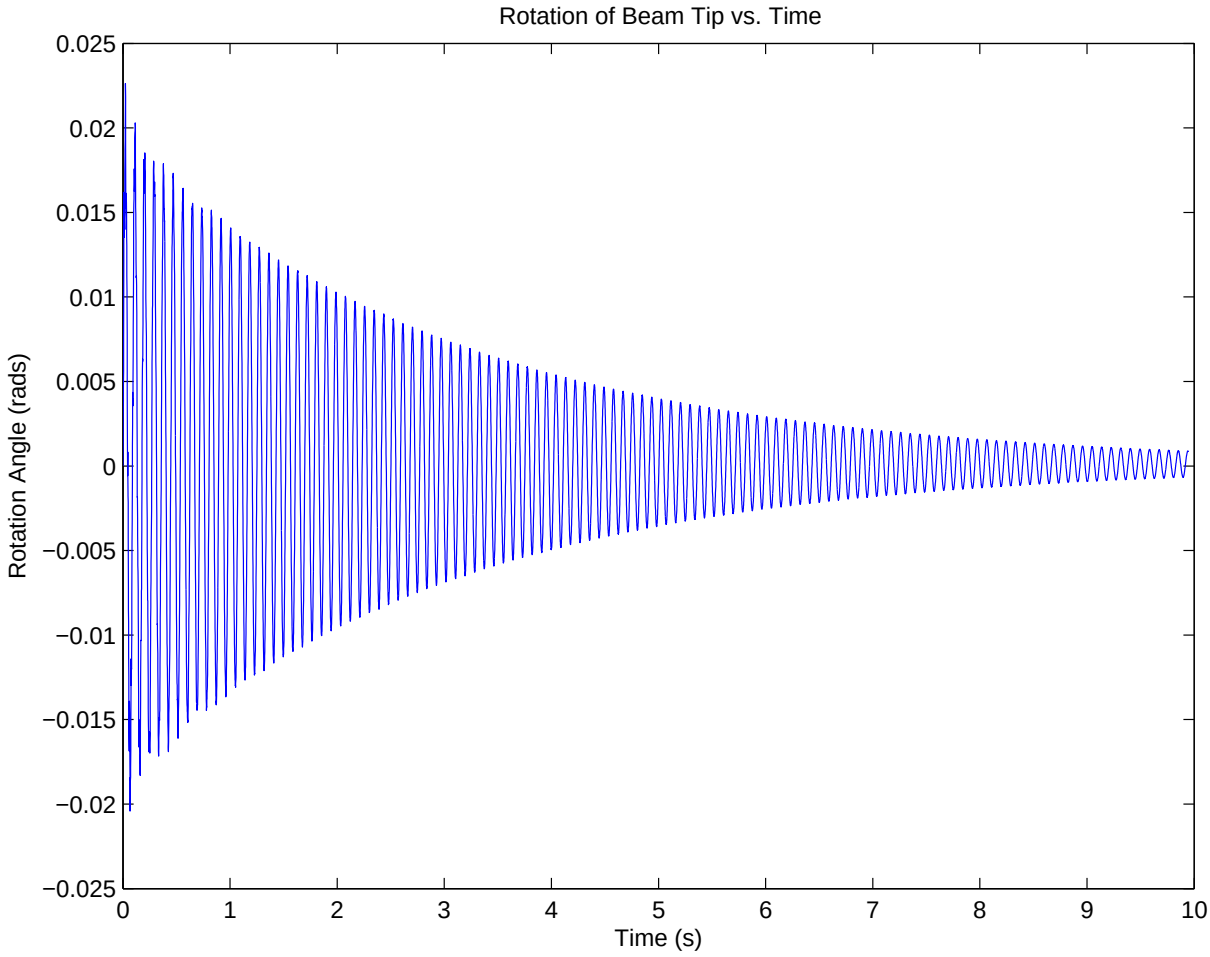

Figure 7.28: 2D Timoshenko Beam Tip Rotation vs. Time

7.6 3D Timoshenko Beam Model Results

The tip deflection for the 3D Timoshenko beam model (Figures 7.29 and 7.30) is essentially the same as the 2D case. The only difference is due to differences in the system damping.

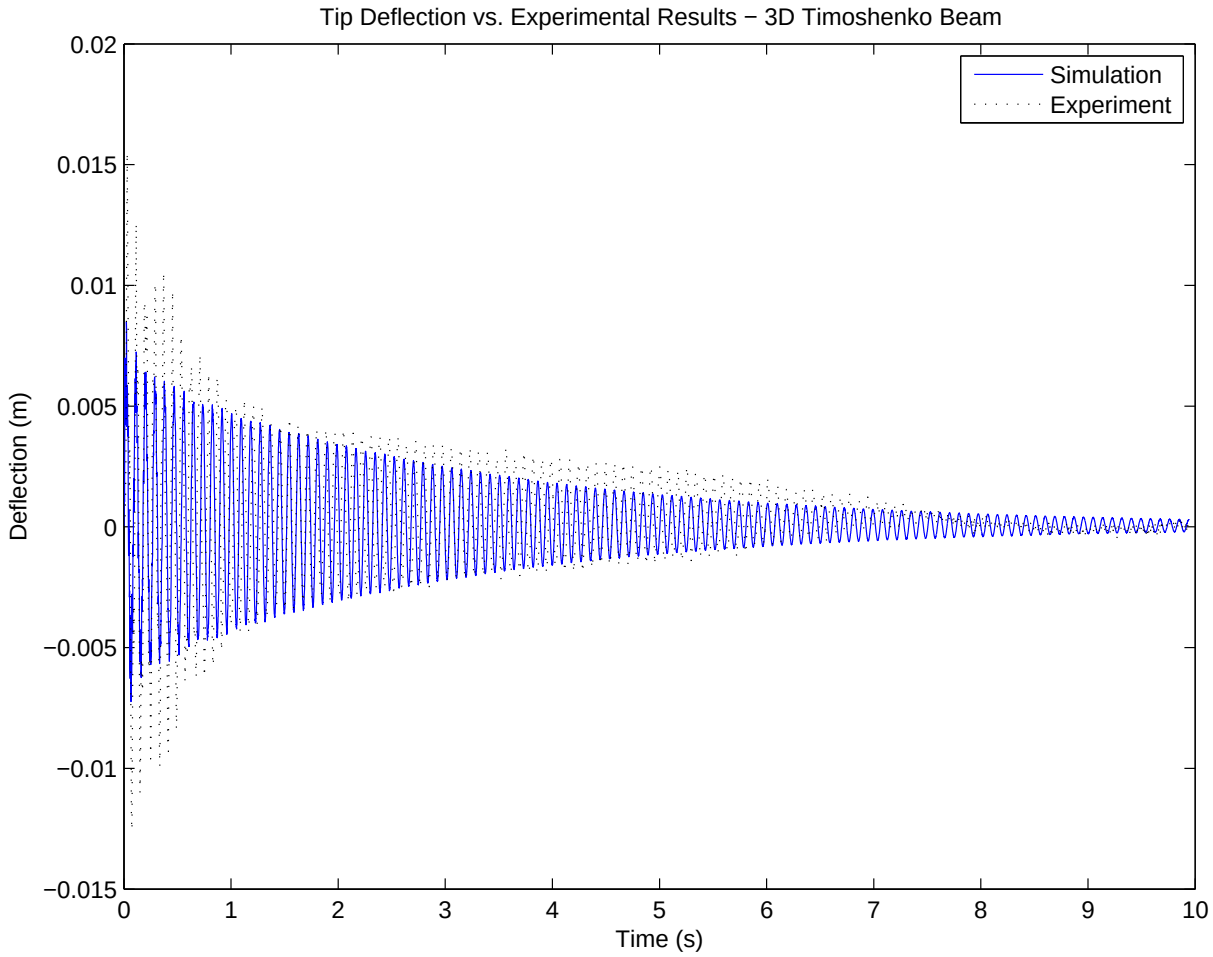

Figure 7.29: 3D Timoshenko Beam Tip Deflection vs. Experiment

Only the first elastic mode of the system (along with the rigid body mode) is significant, since most of the elastic modes are either damped out or very small (see Figure 7.31). Only the modes 36 Hz and 77 Hz are at all visible aside from the rigid body mode and the first elastic mode.

The hub rotation behaviour (Figures 7.32–7.36) is consistent with the 2D Timoshenko model, as is the tip axial deflection (Figure 7.27) and the tip in-plane rotation (Figure 7.38).

The out-of-plane deflection of the tip (Figure 7.39) is extremely small as is the out-of-plane rotation (Figure 7.40). The angle of twist of the tip (Figure 7.41) is a couple of orders of magnitude larger than than the out-of-plane rotation/deflection, but is still very small. Also, Rhody [1] did not full document the design of the end-effector so it was not possible

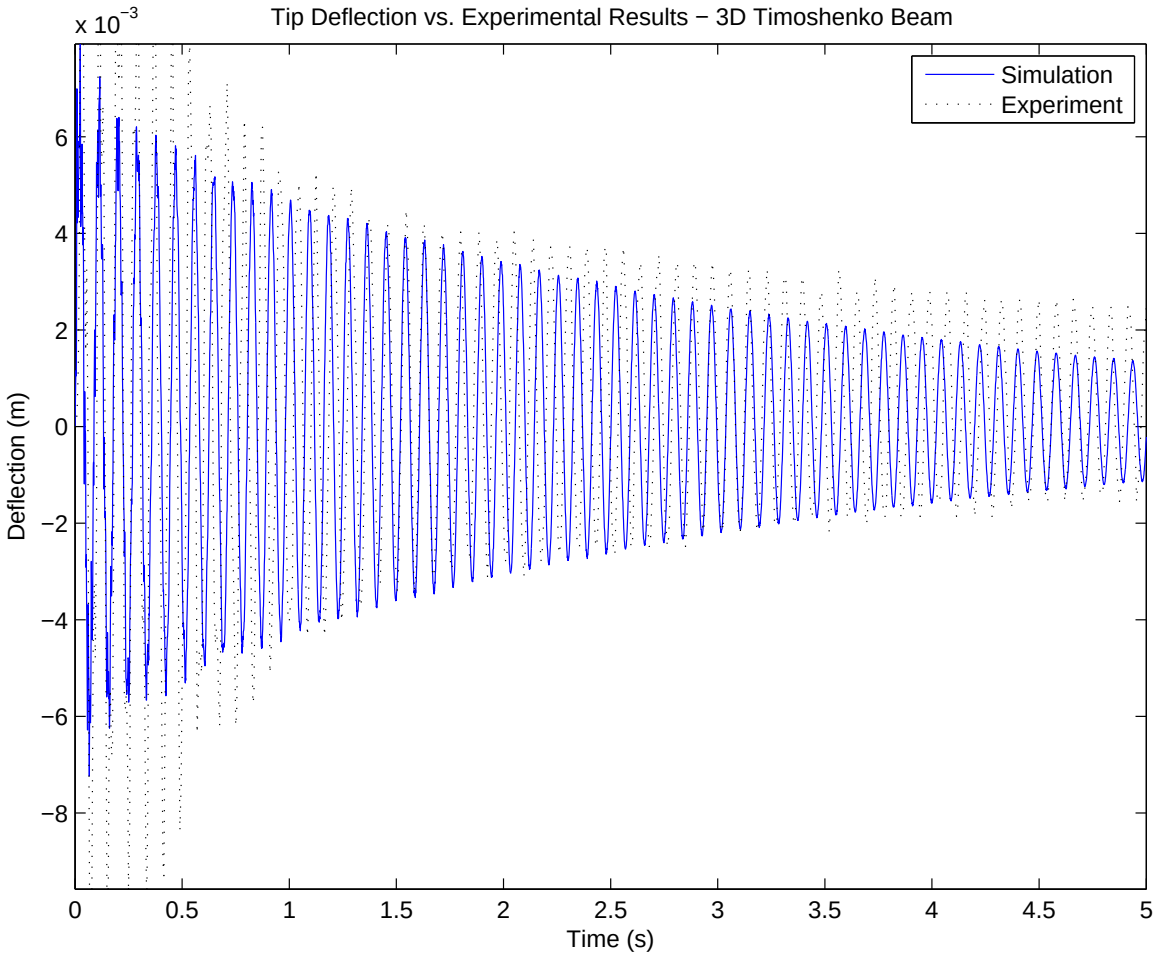

Figure 7.30: 3D Timoshenko Beam Tip Deflection vs. Experiment (initial 5s)

to determine the inertia terms J_{exx}, J_{eyy}, or J_{exy}. As such, their contribution to the out-of-plane deflection/rotation and the angle of twist is missing. That said, it is unlikely that the addition of those would scale the results to the same order of magnitude as the other deflection/rotations.

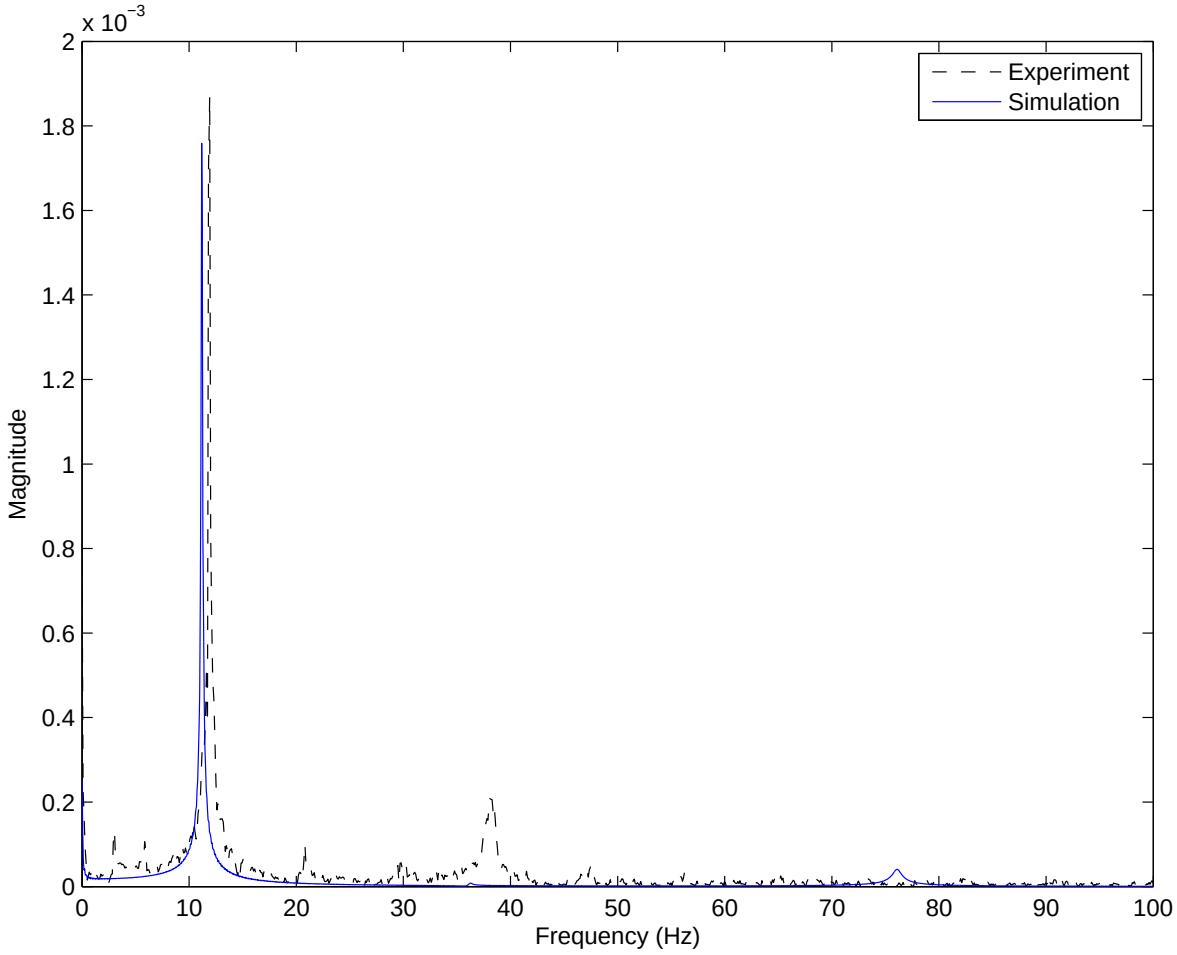

Figure 7.31: 3D Timoshenko Beam FFT Simulation vs. Experiment

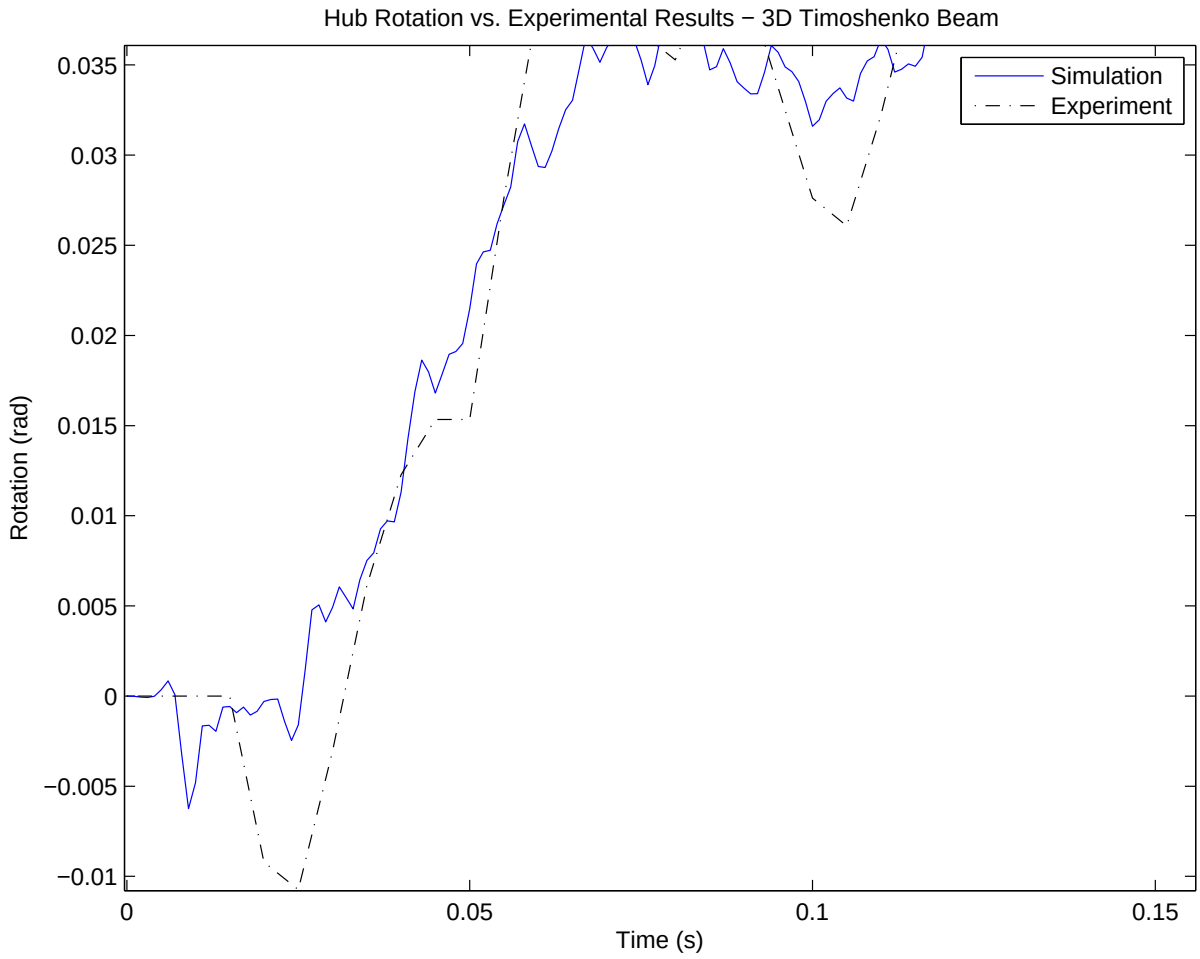

Figure 7.32: 3D Timoshenko Beam Hub Rotation vs. Experiment (initial 0.15s)

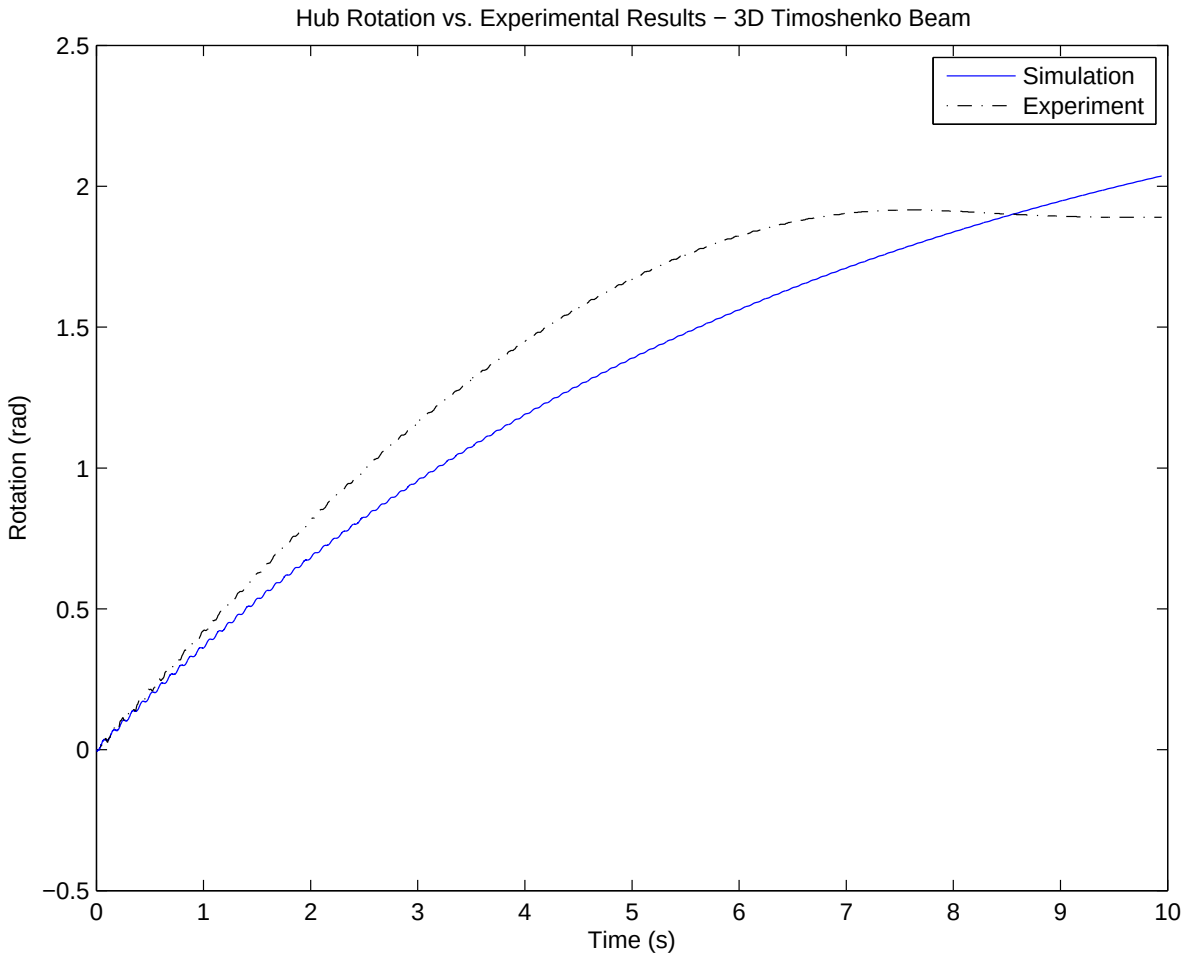

Figure 7.33: 3D Timoshenko Beam Hub Rotation vs. Experiment

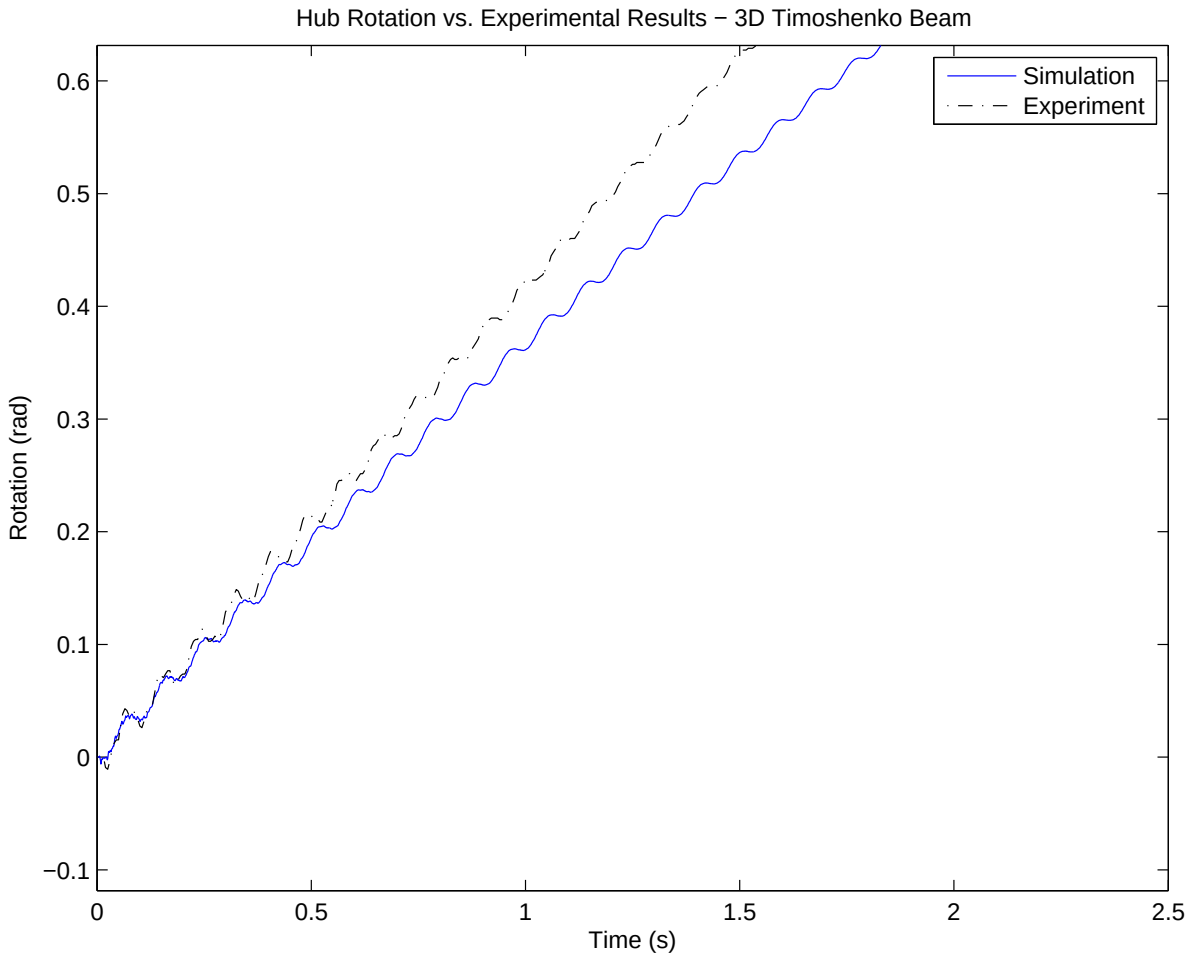

Figure 7.34: 3D Timoshenko Beam Hub Rotation vs. Experiment (initial 2.5s)

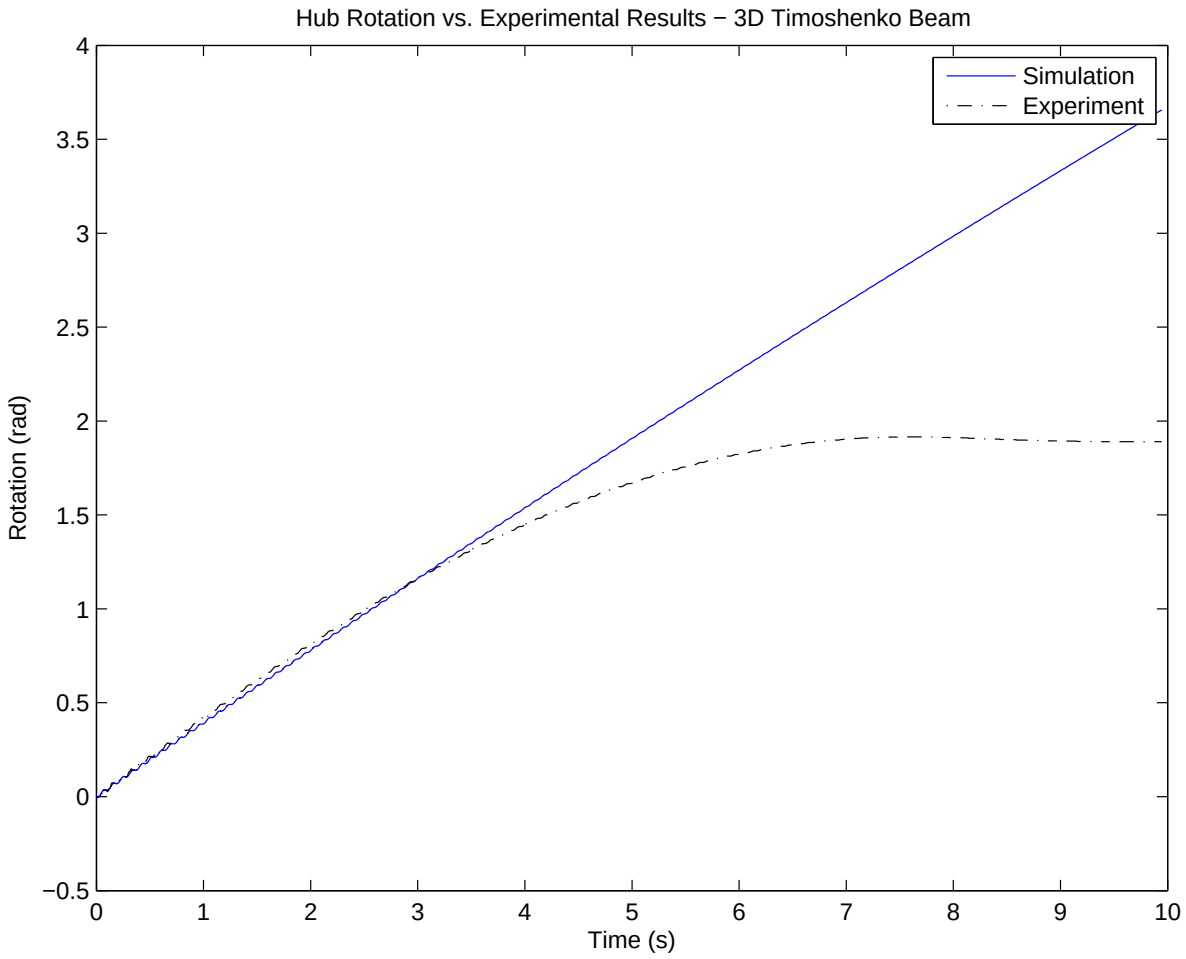

Figure 7.35: 3D Timoshenko Beam Hub Rotation (Minimal Damping)

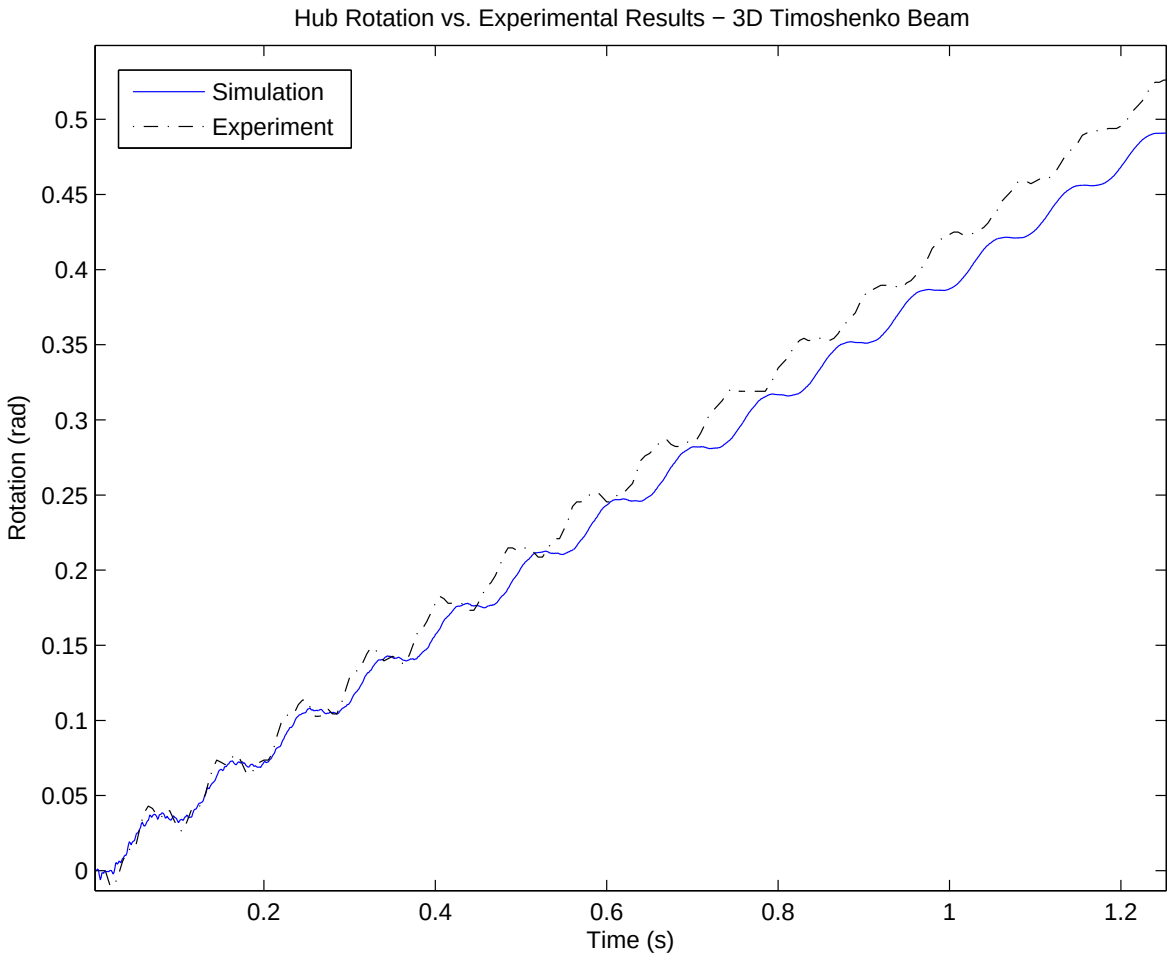

Figure 7.36: 3D Timoshenko Beam Hub Rotation (Minimal Damping - Initial 1.2s)

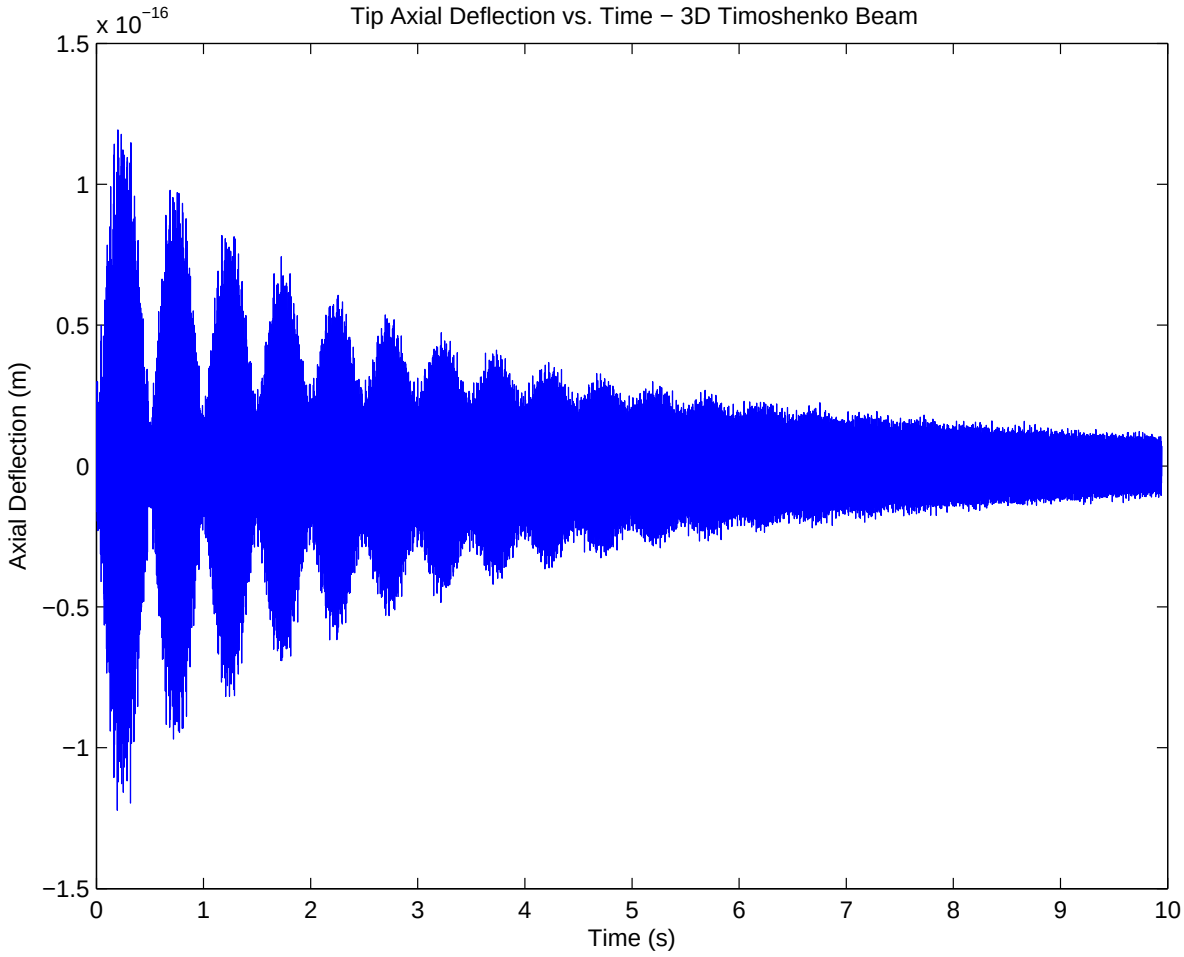

Figure 7.37: 3D Timoshenko Beam Tip Axial Deflection vs. Time

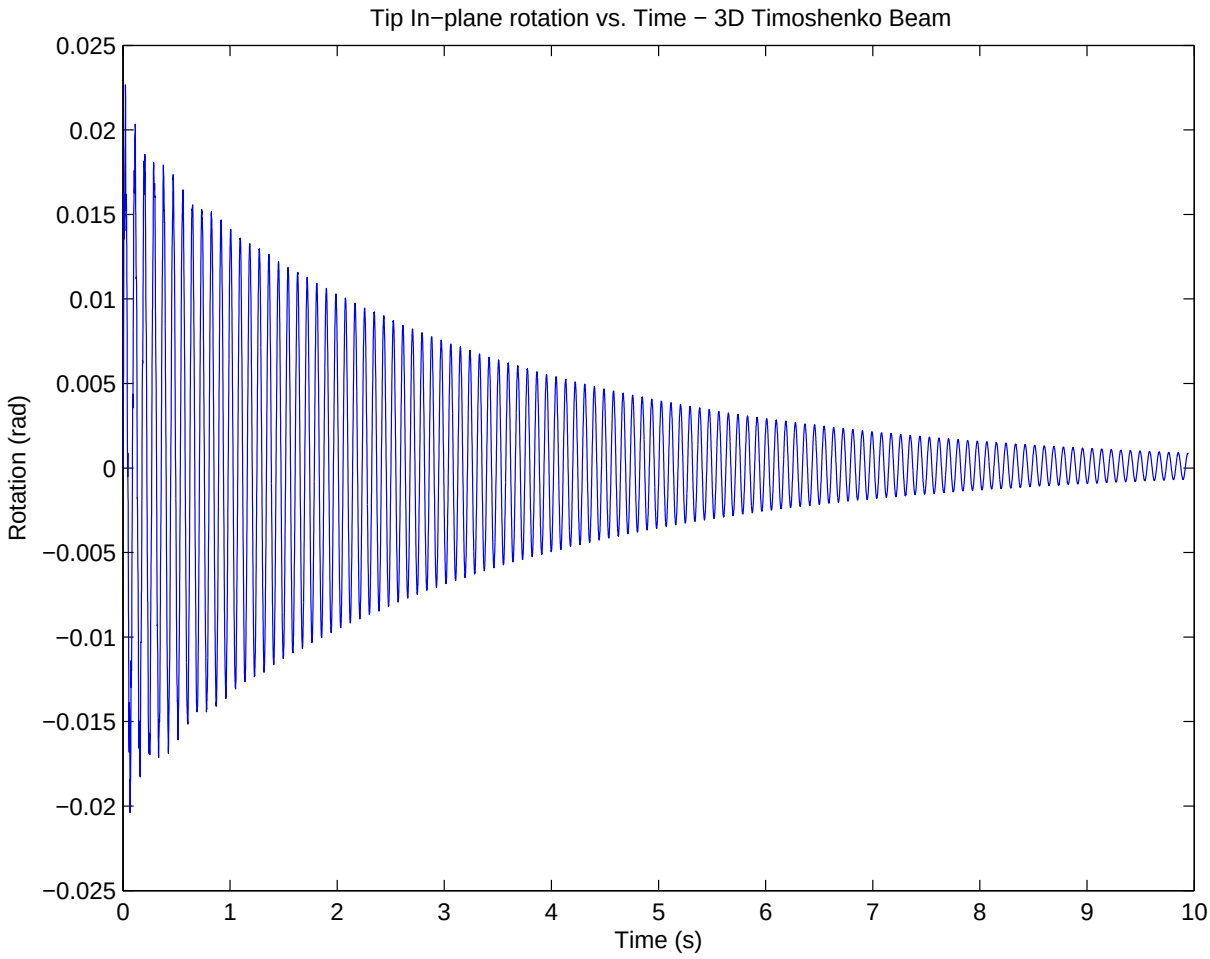

Figure 7.38: 3D Timoshenko Beam Tip In-Plane Rotation vs. Time

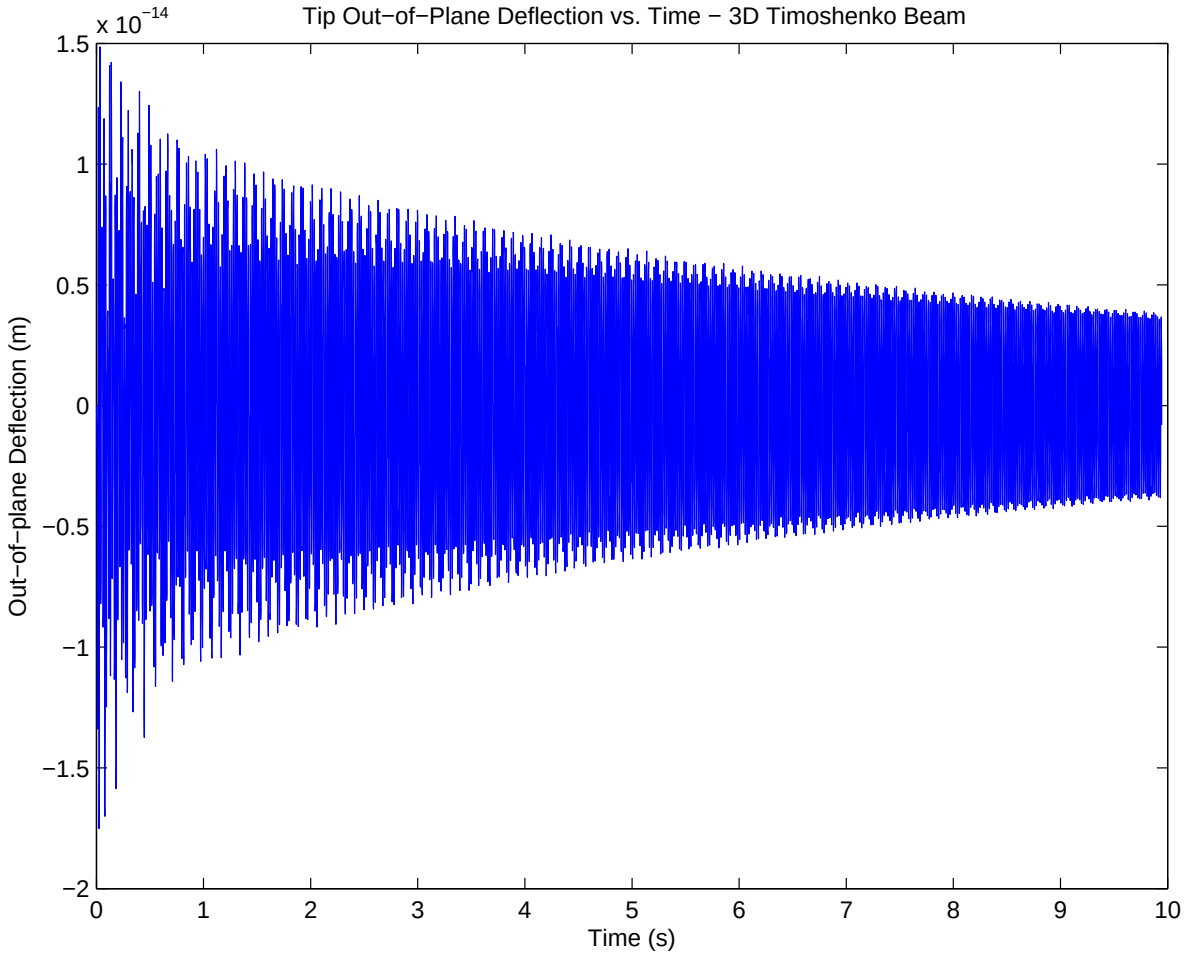

Figure 7.39: 3D Timoshenko Beam Tip Out-of-Plane Deflection vs. Time

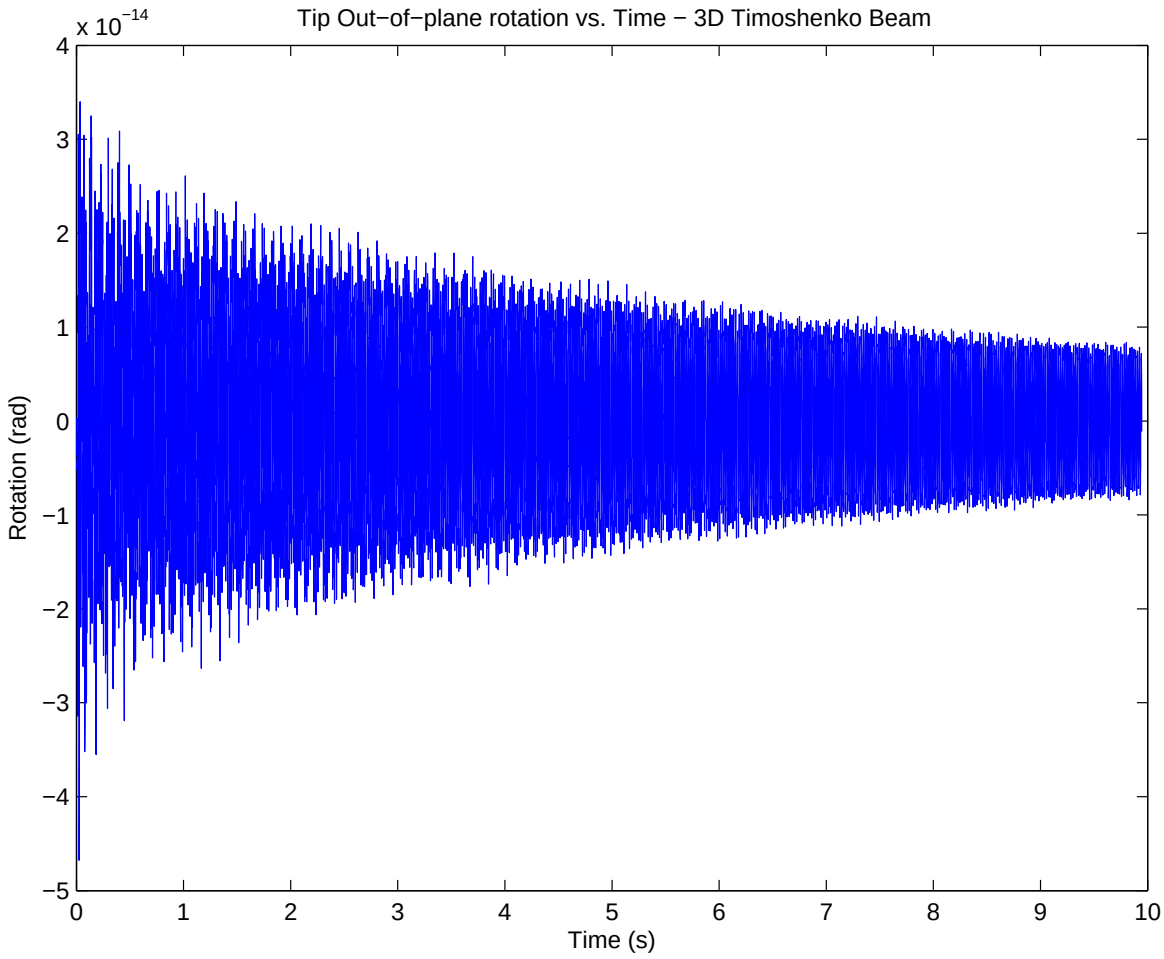

Figure 7.40: 3D Timoshenko Beam Tip Out-of-Plane Rotation vs. Time

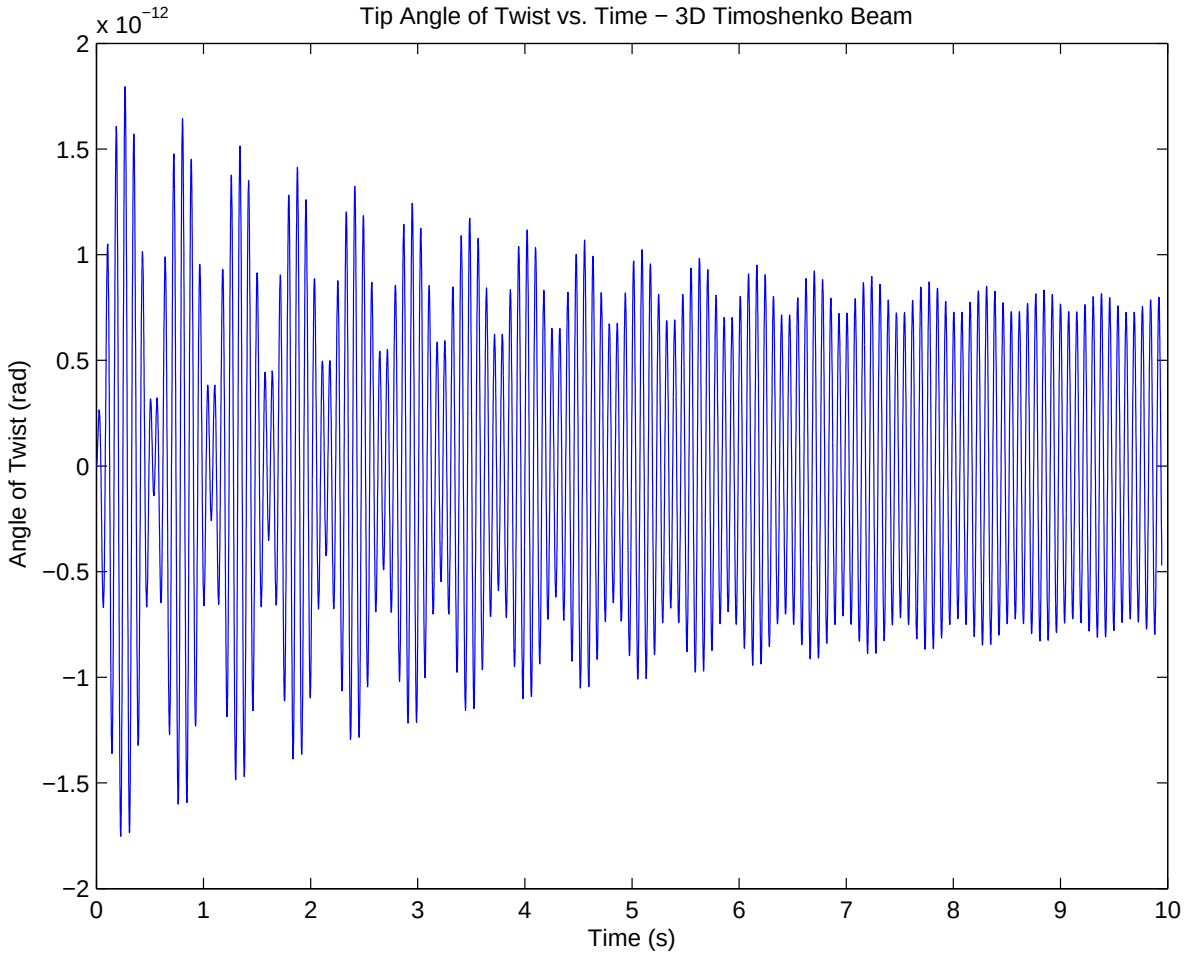

Figure 7.41: 3D Timoshenko Beam Tip Angle of Twist vs. Time

7.7 Investigation Of An Offset Capture

Here we only consider the 3D Timoshenko beam since both the 2D models assume that the captures are coincident. If we consider that the capture of the target mass did not occur directly at the centre of mass of the end-effector, it could be off in the x-direction (which is along the neutral axis) or it could be off in the z-direction (out of the plane of the neutral axis). A capture offset in the y-direction would only occur if the location of either centre of mass is incorrect, since an increase in y would be into the end-effector (which is rigid) and a negative change in y would mean that the target is not touching the end-effector.

Adding a positive 1 mm x-offset makes only minor changes to the final results and as such are not shown, but a positive 1 mm z-offset increases the angle of twist from the order 10^{-12} to 10^{-4} as shown in Figure 7.42. However, the hub rotation and the in-plane tip deflection show only minor changes. The measurement of the tip deflection in this experiment was with an infrared sensor on the beam tip. If the beam is twisting in addition to deflecting, this will lead to some measurement error. For a 1 mm offset this is not significant, but it might be for larger offsets. Also note that this is with J_{exx}, J_{eyy}, or J_{exy} all zero since Rhody did not provide the necessary information to compute this. These terms are all more significant in both the capture equations and in simulation for an offset capture.

Note that an x-offset capture results in a change to $\dot{\overline{v}}_L^+$ and gives a small value to $\dot{\psi}_{zL}^+$. A z-offset capture gives a negative value to $\dot{\theta}_{xL}^+$ and no change to $\dot{\overline{v}}_L^+$.

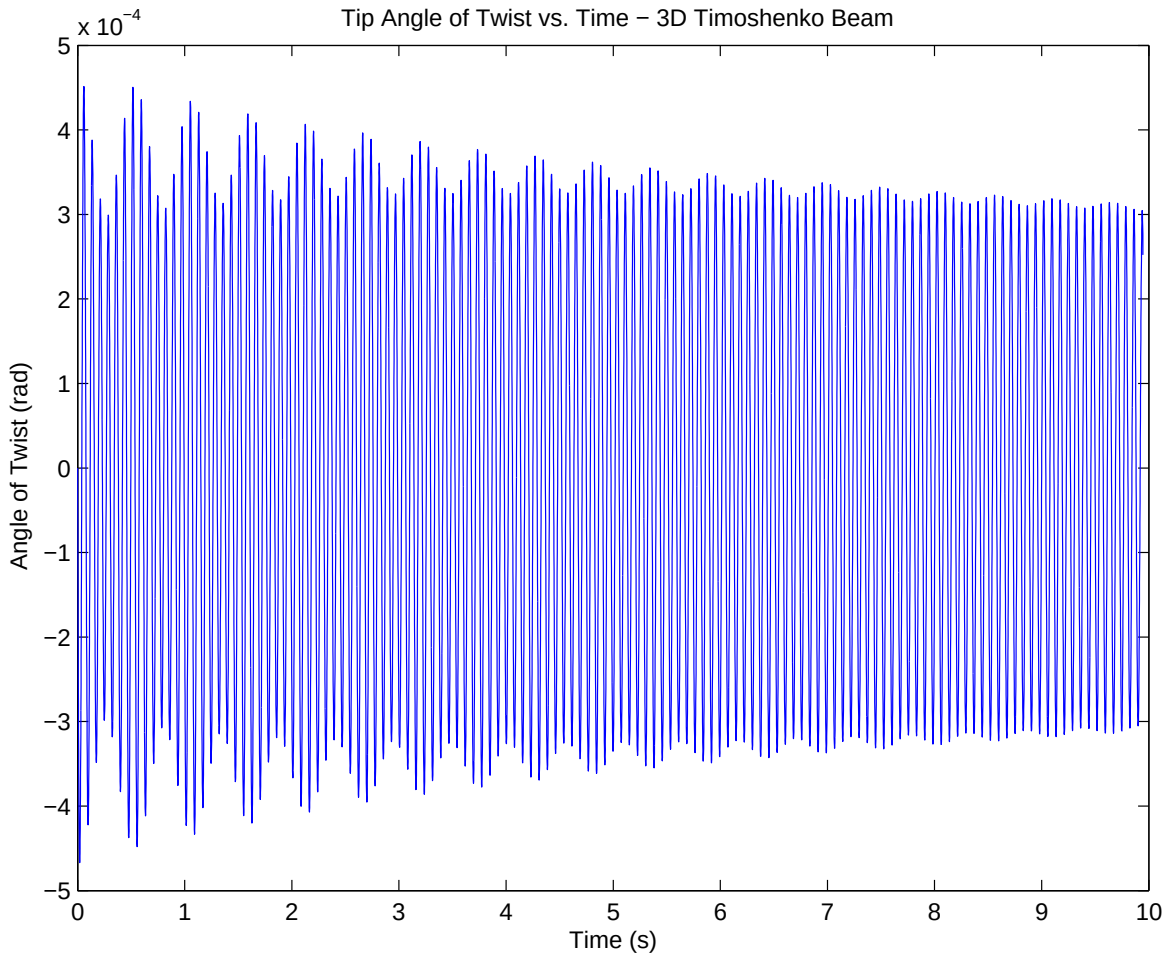

Figure 7.42: 3D Timoshenko Beam Tip Angle of Twist vs. Time (1 mm z-offset)

7.8 Discussion

The experiment that Ben Rhody designed [1] (and is used in this chapter) was designed to examine the control of a beam during capture. His beam model was a simple 2D Euler-Bernoulli beam and as such, he tried to minimize the other possible contributions (*e.g.,* torsion). So, he designed his end-effector such that it would not undergo torsion as a result. Also, the capture occurs such that the centre of mass of the end-effector and the target are coincident. Since the experiment was designed with a 2D Euler-Bernoulli beam in mind, it is not surprising that the 2D or 3D Timoshenko models do not yield better results, or that the ignored terms (*i.e.,* out-of-plane effects, torsion, and extension) are small.

By having the capture occur at the centre of mass, many of the terms in the capture equations (and mass matrix) are eliminated (in addition to eliminating torsional effects). For this experiment, the capture equations mostly were of the form,

$$\dot{\overline{v}}_L^+ = \frac{m_t \dot{y}_t^-}{(m_t + m_e)} \tag{7.2}$$

which is just a simple transfer of linear momentum.

If friction could be properly characterized, the system damping used here could be reduced which would properly allow one to see the effects of the higher modes in the Timoshenko models since they are nearly all damped out of the system.

CHAPTER

8 Discussion, Summary, Conclusions, and Future Work

This chapter presents a comparison to previous work, summary of the work done in the thesis, conclusions, and suggestions for directions of future work.

8.1 Discussion

The work of Chapnik *et al.* [21, 22] was used to verify terms in the 2D Euler-Bernoulli beam kinetic energy derived in Chapter 3. However, Chapnik *et al.* neglect the centripetal and Coriolis effects. Specifically, they define the position of a point on the beam in inertial space as (converting to consistent notation):

$$r = x\theta + \overline{v}(x,t) \tag{8.1}$$

which leads to a velocity of

$$\dot{s} = x\dot{\theta} + \dot{\overline{v}}(x,t) \tag{8.2}$$

which gives a kinetic energy for the beam of

$$T_b = \frac{1}{2}\int_0^L \rho A(x^2\dot{\theta}^2 + 2x\dot{\theta}\dot{\overline{v}} + \dot{\overline{v}}^2)\mathrm{d}x \tag{8.3}$$

comparing this to the beam kinetic energy derived in Chapter 3 (Equation (3.23)):

$$T_b = \frac{1}{2}\int_0^L \rho A(x^2\dot{\theta}^2 + 2x\dot{\theta}\dot{\overline{v}} + \dot{\overline{v}}^2 + \dot{\theta}^2\overline{v}^2)\mathrm{d}x + \frac{1}{2}\int_0^L \rho I_{yy}\dot{\theta}^2\mathrm{d}x \tag{8.4}$$

we see that we have additional terms that are not present in Chapnik's derivation. Similarly, for the end effector (*i.e.,* tip mass), Chapnik presents the kinetic energy (once again in a consistent notation) as

$$T_e = \frac{1}{2}m_e(L^2\dot{\theta}^2 + 2L\dot{\theta}\dot{\overline{v}}_L + \dot{\overline{v}}_L^2) \tag{8.5}$$

where our kinetic energy from Equation (3.67) is given as

$$T_e = \frac{1}{2} m_e \left((\dot{\overline{v}}_L + \dot{\overline{v}}'_L d_{e1}) + (L + d_{e1})\dot{\theta} \right)^2 + \frac{1}{2} m_e (\overline{v}_L + \overline{v}'_L d_{e1})^2 \dot{\theta}^2 \tag{8.6}$$

Once again, we have additional terms that are not in Chapnik's analysis. However, the strain energy and the kinetic energy due to the motor inertia are equivalent.

Chapnik *et al.* do model an additional factor that is not included in the model in this thesis. Friction was not included in the models used in this thesis because the experiment used [1] did not provide enough data to properly characterize the friction model.

The work of Rhody [1] covers modelling the dynamics and control of Class II problems (See Chapter 1 for details on the classes). His approach includes a simple stick-slip friction model of the motor friction but the approach is limited in its application as pre-determination of the impact force is required. For the type of problems in Class II this may be appropriate but the difficulty will increase for the remaining classes. His approach does achieve better agreement with experiment (likely due to inclusion of a simple friction model), but the models presented in this thesis cover Classes II through VII.

Kövecses *et al.* [3, 4] present specifics on the equations describing the transition between the pre- and post-capture systems, but neglect to provide the details on the equations of motion for those systems, whereas this thesis presents the equations of motion for the pre- and post-capture regions, as well as the equations that describe the transition. In another paper, Kövecses *et al.*[26] presents the form of all of the equations, but not the specific details.

The approach taken in Kövecses *et al.* [3, 4] is to take the variation of the constraint equations and substitute the resulting velocity variation equations into the Jourdain variational equations to eliminate the variations relating to the constraints. It is not clear that this is a mathematically rigorous method for handling the problem. The constraint equations derived are only valid for the post-capture system, where the variations apply to the transition region between the pre- and post-capture systems. In this particular case, the approaches may be equivalent but it is unclear.

The constraint embedding approach used in this thesis has an additional advantage over the velocity variation approach. Bahar [29] outlines a method to derive the impulses due to the impact when the constraint embedding approach is used to solve impact problems. Note that Kövecses and Fenton [4] extended their approach to calculate the constraint impulses.

Lastly, comparing the results derived in Chapter 5 relating the pre- and post-capture velocities to the results from Kövecses *et al.* [3] we see that while our equation relating the beam deflection velocities matches, the results for the tip deflection velocities and angular velocities do not. Comparing the results, the angular velocity relation in Kövecses *et al.* [3] is incorrect as a there are some problems with consistency of units on terms that are to be added together. That is, some terms that add together have different units. However, the

results derived herein do concur with the results from Kövecses and Cleghorn's newer paper [4] (if one ignores the additional effects included in our model).

All the previous work discussed here that relates to dynamic mass capture are system models that only use 2D Euler-Bernoulli beam models whereas this thesis includes system models that support both 2D and 3D Timoshenko beam models (including out-of-plane effects and torsion). This allows for the capture equations to be extended to include classes VI and VII in addition to edge cases of classes IV and V (where the capture may induce torsion or the target is not translating in the plane of the beam).

8.2 Summary of Work

Using the classification system proposed in the Introduction, investigations into dynamic mass capture to date have been restricted to classes I through III. This thesis includes a more complete model for classes II and III (that includes the end-effector offset from the end of the beam). It also includes centripedal and Coriolis effects. A 2D Timoshenko beam model supports classes IV and V, while a 3D Timoshenko model is used for classes IV through VII (Chapter 5 and Appendix F). Only class VIII is not covered by the models in this thesis.

To support this work, two new models for torsion have been derived (Chapter 2 and section A.3) and new results on difficulties with some existing torsion models (section A.2). Software has been developed to derive Finite Element models from first principles and solve the resulting system of equations (Chapter 4 and Appendix D). The system was verified by examining the convergence of a fixed-free beam in pure torsion (Section 4.5). Finally, a method for determining the system damping has been presented (Chapter 6).

Models of 2D Euler-Bernoulli beam (with point mass end-effector and target), a 2D Timoshenko beam (with rigid body end-effector and target moving in the plane of the beam), and a complete 3D Timoshenko beam that includes torsion and rigid bodies for the end-effector and target that support a full range of motion were done. This last model also supports an eccentric end-effector as well as eccentric capture of the target. Comparisons of these models was done with respect to an experiment by Rhody [1]. In addition, simulations of eccentric capture were done by considering an offset of the capture of the payload in the x and z directions (the y case was not done because of the nature of the capture). It was shown that even a small offset (1 mm) in the z-direction leads to an increase by several orders of magnitude in the angle of twist, to the point where it is close to being significant.

8.3 Conclusions

While none of the three models accurately modelled the chosen experiment [1], as previously stated, this is likely due to the omission of a friction model. Unfortunately, the experiment did not provide enough information to properly characterize a friction model. The design of the experiment is such that it is unable to show the effect of many different terms in the capture equations and Lagrangians.

This thesis presents a variety of different models based upon the situation. For the experiment examined, it is clear that a 2D Euler-Bernoulli model is sufficient, but for other situations one of the Timoshenko models may be more appropriate. For 2D cases, it's likely that the Timoshenko model is more appropriate for the capture equations since the momentum transferred by the capture is localized to the end-effector whereas the Euler-Bernoulli beam model has the possibility of transferring momentum directly to the hub.

If the capture of the target and end-effector is not at the centre of mass of each of the bodies, even a small offset can introduce a significant in the angle of twist of the beam and in that case, the 3D Timoshenko model becomes important. So, if the point of capture is uncertain, a shift to the 3D model should be considered even for what appears to be plane motion (and capture).

For a general end-effector and target, the 3D Timoshenko beam model would be most appropriate since a general end-effector and target may lead to the eccentric capture case as shown in Chapter 2 and torsion results as shown in 7.7.

The inclusion of friction in the system would likely not affect the capture equations since the capture happens instantaneously and as such the frictional impulse will be zero. While there is no change in the capture equations, the inclusion of friction would affect the simulations.

8.4 Future Work

While not modelled, one model of friction that could possibly be implemented is that of Bliman and Sorine [80, 81, 82, 83] which provides a differential equation model of both dynamic and static friction. This has the advantage of only a few parameters to identify. However, if one is spending the time to properly characterize the hub/motor the LuGre model is preferable [84, 85, 86, 87].

Since the assumed displacement torsion model discussed in Chapter 2 suffers from the same problem as the Reissner torsion model (see section A.2) some comparison of the assumed stress model (section A.3) to the assumed displacement model should be done. Since the assumed stress model is more complex, the assumed displacement model is

preferred if its accuracy can be shown. In addition to comparisons between the models, experiments to compare both models can be done. This is viewed as a second step after direct comparisons between the models is done. How does the comparison change based upon the the cross-section of the beam? If the assumed displacement model is sufficient, are there other approaches to modelling the warping function? Can either work be extended to handle a varying cross-section?

Since the experiment used in this thesis only covered classes II and IV, more experiments are necessary to cover classes III, V, VI, and VII. This requires a beam with strain gauges along the length attached to a motor. This would allow one to move the beam prior to capture and to find the shape of the beam. The end-effector can be simplified to use rare earth magnets instead of an electromagnet. Some method of launching the target that could possibly impart spin would be necessary to handle classes VI and VII. That said, if the target is only translating, classes IV and V would be covered and would show most of the effects from the 2D and 3D Timoshenko capture equations.

Now that the basic model exists, we can start to look at applying to to design a controller for a flexible beam that captures a target. It could also be used in the design of a flexible beam itself. In addition, the model can be used for prediction purposes for existing beams/targets. If a manipulator on the International space station is going to be used to grab a particular payload (*e.g.,* the SpaceX Dragon capsule), what will happen to be beam? Can the motor and controller properly compensate for various situations?

Appendices

APPENDIX

A Torsion of Uniform Cross-section Beams

This appendix discusses modelling of torsion of constant cross-section beams. The first section presents the derivation of uniform torsion, the second illustrates problems with Reissner torsion and the third derivation of a new model non-uniform torsion.

A.1 Derivation of St. Venant Warping Function

This section discusses the uniform torsion of constant cross-section beams, in particular torsion of rectangular beams. It is divided into 5 subsections. The first subsection begins the derivation of the general uniform torsion problem for beams of an arbitrary cross-section. The second continues the derivation for a rectangular cross-section. These two subsections are based upon the work of Sokolnikoff [31] but omit unnecessary details and add additional explanations. The third subsection derives the torsional inertia of a rectangular beam while the fourth derives the torsional kinetic energy of a rectangular beam. Lastly, the final subsection does a convergence analysis of the torsional inertia expression to discover an adequate approximation and compares this result to some other expressions for the torsional inertia.

General Cross-Section Problem Definition

Restating Equations (2.15)–(2.17),

$$u = \alpha\phi(y,z) \tag{A.1}$$

$$v = -\alpha xz \tag{A.2}$$

$$w = \alpha xy \tag{A.3}$$

The warping function $\phi(y,z)$ has to be determined to satisfy the differential equations of equilibrium,

$$\frac{\partial}{\partial y}\sigma_{xy}(x,y,z)+\frac{\partial}{\partial z}\sigma_{zx}(x,y,z)+\frac{\partial}{\partial x}\sigma_{xx}(x,y,z) = -F_x \tag{A.4}$$

$$\frac{\partial}{\partial y}\sigma_{yy}(x,y,z)+\frac{\partial}{\partial z}\sigma_{yz}(x,y,z)+\frac{\partial}{\partial x}\sigma_{xy}(x,y,z) = -F_y \tag{A.5}$$

$$\frac{\partial}{\partial y}\sigma_{yz}(x,y,z)+\frac{\partial}{\partial z}\sigma_{zz}(x,y,z)+\frac{\partial}{\partial x}\sigma_{zx}(x,y,z) = -F_z \tag{A.6}$$

and the boundary equations,

$$\sigma_{yy}(x,y,z)n_y+\sigma_{yz}(x,y,z)n_z = 0 \tag{A.7}$$

$$\sigma_{yz}(x,y,z)n_y+\sigma_{zz}(x,y,z)n_z = 0 \tag{A.8}$$

$$\sigma_{xy}(x,y,z)n_y+\sigma_{xz}(x,y,z)n_z = 0 \tag{A.9}$$

where $\underset{\sim}{n}$ is the outward normal unit vector at the boundary,

$$\underset{\sim}{n} = \underset{\sim}{\mathscr{F}}_a^T \begin{bmatrix} 0 \\ n_y \\ n_z \end{bmatrix} \tag{A.10}$$

All normal stresses in this situation will be zero since for this case,

$$\frac{\partial u}{\partial x}=0 = \frac{1}{E}\left(\sigma_{xx}-\nu\left(\sigma_{yy}+\sigma_{zz}\right)\right) \tag{A.11}$$

$$\frac{\partial v}{\partial y}=0 = \frac{1}{E}\left(\sigma_{yy}-\nu\left(\sigma_{xx}+\sigma_{yy}\right)\right) \tag{A.12}$$

$$\frac{\partial w}{\partial z}=0 = \frac{1}{E}\left(\sigma_{zz}-\nu\left(\sigma_{xx}+\sigma_{zz}\right)\right) \tag{A.13}$$

and the only way for these equations to be satisfied is when all the normal stresses are zero. Note that E is Young's modulus for the material, ν is Poisson's ratio and both are assumed to be constant throughout the beam. The shear stresses in terms of the displacements are,

$$\sigma_{xy} = G\left(\frac{\partial v}{\partial x}+\frac{\partial w}{\partial y}\right) \tag{A.14}$$

$$\sigma_{xz} = G\left(\frac{\partial w}{\partial z}+\frac{\partial v}{\partial x}\right) \tag{A.15}$$

$$\sigma_{yz} = G\left(\frac{\partial v}{\partial y}+\frac{\partial u}{\partial z}\right) \tag{A.16}$$

where G is the shear modulus of the material and is also constant in the beam. Substituting the assumed displacements (given in Equations (A.1)-(A.3)) into these equations we get,

$$\sigma_{xy} = -G\alpha\left(z - \frac{\partial}{\partial y}\phi(y,z)\right) \tag{A.17}$$

$$\sigma_{xz} = G\alpha\left(\frac{\partial}{\partial z}\phi(y,z) + y\right) \tag{A.18}$$

$$\sigma_{yz} = 0 \tag{A.19}$$

Note that there are no applied forces to the system so F_x, F_y, and F_z are all zero. Substituting this and the stresses given in Equations (A.17)-(A.19) into Equations (A.4)-(A.6), only Equation (A.4) remains,

$$G\alpha\left(\frac{\partial^2}{\partial y^2}\phi(y,z) + \frac{\partial^2}{\partial z^2}\phi(y,z)\right) = 0 \tag{A.20}$$

Now that we are reduced to the single partial differential equation, simplify it by dividing out G which cannot be zero since it is a material property and α which should not be zero at the cross-section of interest, to obtain

$$\frac{\partial^2}{\partial y^2}\phi(y,z) + \frac{\partial^2}{\partial z^2}\phi(y,z) = 0 \tag{A.21}$$

Similarly, for the boundary conditions, we have only Equation (A.9) remaining, which becomes

$$n_y z - n_y\frac{\partial}{\partial y}\phi(y,z) - n_z\frac{\partial}{\partial z}\phi(y,z) - n_z y = 0 \tag{A.22}$$

But, we can collect the $\phi(y,z)$ terms using,

$$\frac{\partial}{\partial n}\phi(y,z) = n_y\frac{\partial}{\partial y}\phi(y,z) + n_z\frac{\partial}{\partial z}\phi(y,z) \tag{A.23}$$

which is the derivative of the warping function in the direction of the boundary normal $\underset{\rightarrow}{n}$ on the boundary C (See Figure A.1). Substituting that result into the boundary condition (A.22) gives a new form of the boundary condition as

$$\frac{\partial}{\partial n}\phi(y,z) = n_y z - n_z y \tag{A.24}$$

Since the boundary condition for this problem is complicated, let us reformulate this problem as a simpler one. It follows from Equation (A.21) that $\phi(y,z)$ must be a harmonic function throughout the region bounded by the curve C (which is the boundary of our cross-section) with the normal derivative of this function satisfying the boundary condition given in Equation (A.24). Since the warping function is harmonic throughout the cross-section of the beam, we can construct an analytic function $\phi(y,z) + j\psi(y,z)$ of the complex variable

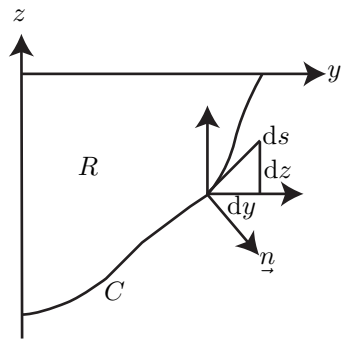

Figure A.1: General Cross-Section Boundary Relations

$y+\mathrm{j}z$ [88]. For the derivative of the analytic function to be continuous, $\psi(y,z)$ must be related to $\phi(y,z)$ by the Cauchy-Riemann equations,

$$\frac{\partial}{\partial y}\phi(y,z) = \frac{\partial}{\partial z}\psi(y,z) \tag{A.25}$$

$$\frac{\partial}{\partial z}\phi(y,z) = -\frac{\partial}{\partial y}\psi(y,z) \tag{A.26}$$

Differentiating the first Cauchy-Riemann equation with respect to z,

$$\frac{\partial^2}{\partial y \partial z}\phi(y,z) = \frac{\partial^2}{\partial z^2}\psi(y,z) \tag{A.27}$$

and the second with respect to y,

$$\frac{\partial^2}{\partial y \partial z}\phi(y,z) = -\frac{\partial^2}{\partial y^2}\psi(y,z) \tag{A.28}$$

and then subtracting Equation (A.27) from Equation (A.28), yields

$$\frac{\partial^2}{\partial y^2}\psi(y,z) + \frac{\partial^2}{\partial z^2}\psi(y,z) = 0 \tag{A.29}$$

which means that $\psi(y,z)$ must be a harmonic function as well. To find the boundary conditions for this new PDE, let us first return to Equation (A.23), and redefine n_y and n_z in terms of an element of boundary arclength $\mathrm{d}s$ (See Figure A.1) as,

$$n_y = \frac{\mathrm{d}z}{\mathrm{d}s} \tag{A.30}$$

$$n_z = -\frac{\mathrm{d}y}{\mathrm{d}s} \tag{A.31}$$

Substituting these results into Equation (A.23),

$$\left(\frac{\mathrm{d}z}{\mathrm{d}s}\right)\frac{\partial}{\partial y}\phi(y,z) - \left(\frac{\mathrm{d}y}{\mathrm{d}s}\right)\frac{\partial}{\partial z}\phi(y,z) = \frac{\partial}{\partial n}\phi(y,z) \tag{A.32}$$

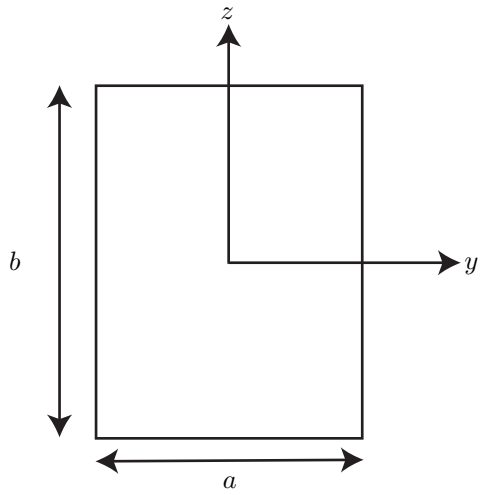

Figure A.2: Rectangular Cross-section

and making use of the Cauchy-Riemann equations,

$$\left(\frac{\mathrm{d}z}{\mathrm{d}s}\right)\frac{\partial}{\partial z}\psi(y,z)+\left(\frac{\mathrm{d}y}{\mathrm{d}s}\right)\frac{\partial}{\partial y}\psi(y,z)=\frac{\partial}{\partial n}\phi(y,z) \tag{A.33}$$

Note that the left-hand side of this equation is the definition of the derivative of $\psi(y,z)$ with respect to s, so this equation becomes,

$$\frac{\mathrm{d}}{\mathrm{d}s}\psi(y,z)=\frac{\mathrm{d}}{\mathrm{d}n}\phi(y,z) \tag{A.34}$$

Substituting this result as well as Equations (A.30) and (A.31) into the original boundary condition Equation (A.24),

$$\frac{\mathrm{d}}{\mathrm{d}s}\psi(y,z)=\frac{\mathrm{d}z}{\mathrm{d}s}z+\frac{\mathrm{d}y}{\mathrm{d}s}y \tag{A.35}$$

and solving, we get the following relation for any arbitrary boundary C,

$$\psi(y,z)=\frac{1}{2}\left(z^2+y^2\right) \tag{A.36}$$

which is only true for y and z on the boundary.

Rectangular Beam of Constant Cross-section

While the work in the previous section is for an arbitrary cross-section, we are concerned with rectangular beams. So, now consider a cross-section as shown in Figure A.2. Considering a boundary C that is a box of dimensions $a \times b$ where $b \geq a$, we get the following relation on the top and bottom boundaries $(y, \pm\frac{b}{2})$,

$$\psi(y,\pm\frac{b}{2})=\frac{1}{8}b^2+\frac{1}{2}y^2 \tag{A.37}$$

and similarly for the left and right boundaries $(\pm\frac{a}{2}, z)$,

$$\psi(\pm\frac{a}{2}, z) = \frac{1}{2}z^2 + \frac{1}{8}a^2 \tag{A.38}$$

To simplify the boundary conditions, introduce a new function $f(y,z)$ which is related to $\psi(y,z)$ in the following manner,

$$\frac{\partial^2}{\partial y^2}\psi(y,z) + 1 = f(y,z) \tag{A.39}$$

The function $f(y,z)$ is a harmonic function since $\psi(y,z)$ satisfies Equation (A.29) and we can also get the following relation for $f(y,z)$,

$$f(y,z) = 1 - \frac{\partial^2}{\partial z^2}\psi(y,z) \tag{A.40}$$

By differentiating Equation (A.37) we can get the second derivative of the boundary condition with respect to y for the top and bottom boundaries,

$$\frac{\partial^2}{\partial y^2}\psi(y,z)\Big|_{(y,\pm\frac{b}{2})} = 1 \tag{A.41}$$

We can also get the second derivative with respect to z of the boundary condition on the left and right boundaries from Equation (A.38),

$$\frac{\partial^2}{\partial y^2}\psi(y,z)|_{(\pm\frac{a}{2},z)} = 1 \tag{A.42}$$

Therefore, the boundary condition for $f(y,z)$ on the top and bottom boundaries is,

$$f(y,\pm\frac{b}{2}) = 2 \tag{A.43}$$

and for the left and right boundaries,

$$f(\pm\frac{a}{2}, z) = 0 \tag{A.44}$$

The function $f(y,z)$ is harmonic so it satisfies the PDE,

$$\frac{\partial^2}{\partial y^2}f(y,z) + \frac{\partial^2}{\partial z^2}f(y,z) = 0 \tag{A.45}$$

Note that we have non-homogeneous boundary conditions on the z boundaries. This can be solved by separation of variables in two steps. Separate $f(y,z)$ according to

$$f(y,z) = f_2(y,z) + f_3(y,z) \tag{A.46}$$

where

$$\nabla^2 f_2(y,z) = 0 \quad \text{and} \quad \nabla^2 f_3(y,z) = 0 \tag{A.47}$$

with the boundary conditions

$$\begin{aligned} f_2\left(-\frac{a}{2},z\right) &= 0 & f_3\left(-\frac{a}{2},z\right) &= 0 \\ f_2\left(\frac{a}{2},z\right) &= 0 & f_3\left(\frac{a}{2},z\right) &= 0 \\ f_2\left(y,-\frac{b}{2}\right) &= 2 & f_3\left(y,-\frac{b}{2}\right) &= 0 \\ f_2\left(y,\frac{b}{2}\right) &= 0 & f_3\left(y,\frac{b}{2}\right) &= 2 \end{aligned}$$

So, we have a set of two PDEs where only one boundary condition is non-zero. First, solving the equation for $f_2(y,z)$

$$\nabla^2 f_2(y,z) = 0, \qquad y \in \left[-\frac{a}{2},\frac{a}{2}\right] \quad z \in \left[-\frac{b}{2},\frac{b}{2}\right] \tag{A.48}$$

subject to the boundary conditions

$$f_2\left(-\frac{a}{2},z\right) = 0 \tag{A.49}$$

$$f_2\left(\frac{a}{2},z\right) = 0 \tag{A.50}$$

$$f_2\left(y,-\frac{b}{2}\right) = 2 \tag{A.51}$$

$$f_2\left(y,\frac{b}{2}\right) = 0 \tag{A.52}$$

This can be solved by separation of variables according to

$$f_2(y,z) = Y_2(y)Z_2(z) \tag{A.53}$$

Substitute (A.53) into (A.48) to find

$$\nabla^2 Y_2(y)Z_2(z) = 0 \quad \text{which may be written as} \quad \frac{Y_{2,yy}}{Y_2} = -\frac{Z_{2,zz}}{Z_2} = -\lambda_2^2 \tag{A.54}$$

where λ_2 is a constant to be determined. Equation (A.54) leads to two differential equations

$$Y_{2,zz} + \lambda_2^2 Y_2 = 0 \tag{A.55}$$

$$Z_{2,zz} - \lambda_2^2 Z_2 = 0 \tag{A.56}$$

Because of the homogeneous boundary conditions (A.49)-(A.50) only (A.55) is an eigenvalue problem. The solution to (A.55) must be of the form

$$Y_2(y) = A_2 \cos\left(\lambda_2\left(y+\frac{a}{2}\right)\right) + B_2 \sin\left(\lambda_2\left(y+\frac{a}{2}\right)\right) \tag{A.57}$$

Note that incorporating the translation transformation to y does not change the validity of proposed solution because it still satisfies (A.55). Evaluate (A.57) on the y-boundaries to find

$$\begin{bmatrix} 1 & 0 \\ \cos(\lambda_2 a) & \sin(\lambda_2 a) \end{bmatrix} \begin{bmatrix} A_2 \\ B_2 \end{bmatrix} = 0 \tag{A.58}$$

which has the characteristic equation

$$\Delta_2 = \sin(\lambda_2 a) = 0 \tag{A.59}$$

which leads to the eigenvalues

$$\lambda_2 = \frac{n\pi}{a} \quad n \text{ an integer} \tag{A.60}$$

and the eigenfunctions

$$Y_{2n}(y) = B_2 \sin\left(\lambda_2 \left(y + \frac{a}{2}\right)\right) = B_2 \sin\left(\frac{n\pi}{a}\left(y + \frac{a}{2}\right)\right) \tag{A.61}$$

The solution to (A.56) is of the form

$$Z_2(z) = C_2 \cosh\left(\lambda_2 \left(z - \frac{b}{2}\right)\right) + D_2 \sinh\left(\lambda_2 \left(z - \frac{b}{2}\right)\right) \tag{A.62}$$

As with y, incorporating the translation transformation to z does not change the validity of proposed solution because it still satisfies (A.56). Evaluate (A.62) on the z-boundary $z = \frac{b}{2}$ to find

$$Z_2\left(\frac{b}{2}\right) = C_2 = 0 \tag{A.63}$$

Therefore, Equation (A.62) becomes

$$Z_2(z) = D_2 \sinh\left(\frac{n\pi}{a}\left(z - \frac{b}{2}\right)\right) \tag{A.64}$$

and $f_2(y,z)$ is of the form

$$f_2(y,z) = \sum_{n=1}^{\infty} F_{2n} Y_{2n}(y) Z_2(z) \tag{A.65}$$

$$= \sum_{n=1}^{\infty} F_{2n} \sin\left(\frac{n\pi}{a}\left(y + \frac{a}{2}\right)\right) \sinh\left(\frac{n\pi}{a}\left(z - \frac{b}{2}\right)\right) \tag{A.66}$$

From Equation (A.51)

$$f_2\left(y, -\frac{b}{2}\right) = \sum_{n=1}^{\infty} -F_{2n} \sin\left(\frac{n\pi}{a}\left(y + \frac{a}{2}\right)\right) \sinh\left(n\pi \frac{b}{a}\right) = 2 \tag{A.67}$$

Noting that

$$\int_{-\frac{a}{2}}^{\frac{a}{2}} \sin\left(\frac{n\pi}{a}\left(y + \frac{a}{2}\right)\right) \sin\left(\frac{m\pi}{a}\left(y + \frac{a}{2}\right)\right) dy = \begin{cases} 0 & m \neq n \\ \frac{a}{2} & m = n \end{cases}$$

take the inner product of Equation (A.67) with respect to

$$\sin\left(\frac{n\pi}{a}\left(y+\frac{a}{2}\right)\right)$$

to find

$$-F_{2n}\frac{a}{2}\sinh\left(n\pi\frac{b}{a}\right)=\frac{2a}{n\pi}\left(1+(-1)^{n+1}\right) \tag{A.68}$$

Which allows us to solve for F_{2n} as

$$F_{2n}=-\frac{4}{n\pi}\frac{\left(1+(-1)^{n+1}\right)}{\sinh\left(n\pi\frac{b}{a}\right)} \tag{A.69}$$

F_{2n} can also be written as,

$$F_{2n}=\begin{cases}0 & n \text{ even}\\ -\frac{8}{n\pi}\frac{1}{\sinh\left(n\pi\frac{b}{a}\right)} & n \text{ odd}\end{cases} \tag{A.70}$$

then $f_2(y,z)$ is,

$$f_2(y,z)=\sum_{n=1,3,5,\cdots}^{\infty}-\frac{8}{n\pi}\sin\left(\frac{n\pi}{a}\left(y+\frac{a}{2}\right)\right)\frac{\sinh\left(\frac{n\pi}{a}\left(z-\frac{b}{2}\right)\right)}{\sinh\left(n\pi\frac{b}{a}\right)} \tag{A.71}$$

$$=\sum_{j=1}^{\infty}-\frac{8}{(2j-1)\pi}\sin\left(\frac{(2j-1)\pi}{a}\left(y+\frac{a}{2}\right)\right)\frac{\sinh\left(\frac{(2j-1)\pi}{a}\left(z-\frac{b}{2}\right)\right)}{\sinh\left((2j-1)\pi\frac{b}{a}\right)} \tag{A.72}$$

Now, solving the equation for $f_3(y,z)$,

$$\nabla^2 f_3(y,z)=0,\qquad y\in\left[-\frac{a}{2},\frac{a}{2}\right]\quad z\in\left[-\frac{b}{2},\frac{b}{2}\right] \tag{A.73}$$

subject to the boundary conditions

$$f_3\left(-\frac{a}{2},z\right)=0 \tag{A.74}$$

$$f_3\left(\frac{a}{2},z\right)=0 \tag{A.75}$$

$$f_3\left(y,-\frac{b}{2}\right)=0 \tag{A.76}$$

$$f_3\left(y,\frac{b}{2}\right)=2 \tag{A.77}$$

As before, this can be solved by separation of variables according to

$$f_3(y,z)=Y_3(y)Z_3(z) \tag{A.78}$$

Substitute (A.78) into (A.73) to find

$$\nabla^2 Y_3(y)Z_3(z) = 0 \quad \text{which may be written as} \quad \frac{Y_{3,yy}}{Y_3} = -\frac{Z_{3,zz}}{Z_3} = -\lambda_3^2 \tag{A.79}$$

where λ_3 is a constant to be determined. Equation (A.79) leads to two differential equations

$$Y_{3,zz} + \lambda_3^2 Y_3 = 0 \tag{A.80}$$

$$Z_{3,zz} - \lambda_3^2 Z_3 = 0 \tag{A.81}$$

Because of the homogeneous boundary conditions (A.74)-(A.75) only (A.80) is an eigenvalue problem. The solution to (A.80) must be of the form

$$Y_3(y) = A_3 \cos\left(\lambda_3\left(y + \frac{a}{2}\right)\right) + B_3 \sin\left(\lambda_3\left(y + \frac{a}{2}\right)\right) \tag{A.82}$$

The translation transformation to y does not change the validity of proposed solution because it still satisfies (A.80). Evaluate (A.82) on the y-boundaries to find

$$\begin{bmatrix} 1 & 0 \\ \cos(\lambda_3 a) & \sin(\lambda_3 a) \end{bmatrix} \begin{bmatrix} A_3 \\ B_3 \end{bmatrix} = 0 \tag{A.83}$$

which has the characteristic equation

$$\Delta_3 = \sin(\lambda_3 a) = 0 \tag{A.84}$$

which leads to the eigenvalues

$$\lambda_3 = \frac{n\pi}{a} \quad n \text{ an integer} \tag{A.85}$$

and the eigenfunctions

$$Y_{3n}(y) = B_3 \sin\left(\lambda_3\left(y + \frac{a}{2}\right)\right) = B_3 \sin\left(\frac{n\pi}{a}\left(y + \frac{a}{2}\right)\right) \tag{A.86}$$

The solution to (A.81) is of the form

$$Z_3(z) = C_3 \cosh\left(\lambda_3\left(z + \frac{b}{2}\right)\right) + D_3 \sinh\left(\lambda_3\left(z + \frac{b}{2}\right)\right) \tag{A.87}$$

The translation transformation to z does not change the validity of proposed solution because it still satisfies (A.81). Evaluate (A.87) on the z-boundary $z = -\frac{b}{2}$ to find

$$Z_3\left(-\frac{b}{2}\right) = C_3 = 0 \tag{A.88}$$

Therefore Equation (A.81) becomes

$$Z_3(z) = D_3 \sinh\left(\frac{n\pi}{a}\left(z + \frac{b}{2}\right)\right) \tag{A.89}$$

and $f_3(y,z)$ is of the form,

$$f_3(y,z) = \sum_{n=1}^{\infty} F_{3n} Y_{3n}(y) Z_3(z) \tag{A.90}$$

$$= \sum_{n=1}^{\infty} F_{3n} \sin\left(\frac{n\pi}{a}\left(y+\frac{a}{2}\right)\right) \sinh\left(\frac{n\pi}{a}\left(z+\frac{b}{2}\right)\right) \tag{A.91}$$

From (A.77)

$$f_3\left(y,\frac{b}{2}\right) = \sum_{n=1}^{\infty} F_{3n} \sin\left(\frac{n\pi}{a}\left(y+\frac{a}{2}\right)\right) \sinh\left(n\pi\frac{b}{a}\right) = 2 \tag{A.92}$$

Noting that

$$\int_{-\frac{a}{2}}^{\frac{a}{2}} \sin\left(\frac{n\pi}{a}\left(y+\frac{a}{2}\right)\right) \sin\left(\frac{m\pi}{a}\left(y+\frac{a}{2}\right)\right) dy = \begin{cases} 0 & m \\ \frac{a}{2} & m=n \end{cases}$$

take the inner product of (A.92) with respect to

$$\sin\left(\frac{n\pi}{a}\left(y+\frac{a}{2}\right)\right)$$

to find

$$F_{3n}\frac{a}{2}\sinh\left(n\pi\frac{b}{a}\right) = \frac{2a}{n\pi}\left(1+(-1)^{n+1}\right) \tag{A.93}$$

Which allows us to solve for F_{3n} as

$$F_{3n} = \frac{4}{n\pi}\frac{\left(1+(-1)^{n+1}\right)}{\sinh\left(n\pi\frac{b}{a}\right)} \tag{A.94}$$

which can also be written as

$$F_{3n} = \begin{cases} 0 & n \text{ even} \\ \frac{8}{n\pi}\frac{1}{\sinh\left(n\pi\frac{b}{a}\right)} & n \text{ odd} \end{cases} \tag{A.95}$$

then we get that $f_3(y,z)$ is,

$$f_3(y,z) = \sum_{n=1,3,5,\ldots}^{\infty} \frac{8}{n\pi}\sin\left(\frac{n\pi}{a}\left(y+\frac{a}{2}\right)\right)\frac{\sinh\left(\frac{n\pi}{a}\left(z+\frac{b}{2}\right)\right)}{\sinh\left(n\pi\frac{b}{a}\right)} \tag{A.96}$$

$$= \sum_{j=1}^{\infty} \frac{8}{(2j-1)\pi}\sin\left(\frac{(2j-1)\pi}{a}\left(y+\frac{a}{2}\right)\right)\frac{\sinh\left(\frac{(2j-1)\pi}{a}\left(z+\frac{b}{2}\right)\right)}{\sinh\left((2j-1)\pi\frac{b}{a}\right)} \tag{A.97}$$

Now, we combine the two solutions. Using Equations (A.72) and (A.97) to form $f(y,z)$ we get

$$f(y,z) = \sum_{j=1}^{\infty} -\frac{8}{(2j-1)\pi}\sin\left(\frac{(2j-1)\pi}{a}\left(y+\frac{a}{2}\right)\right)\frac{\sinh\left(\frac{(2j-1)\pi}{a}\left(z-\frac{b}{2}\right)\right)}{\sinh\left((2j-1)\pi\frac{b}{a}\right)}$$
$$\frac{8}{(2j-1)\pi}\sin\left(\frac{(2j-1)\pi}{a}\left(y+\frac{a}{2}\right)\right)\frac{\sinh\left(\frac{(2j-1)\pi}{a}\left(z+\frac{b}{2}\right)\right)}{\sinh\left((2j-1)\pi\frac{b}{a}\right)} \tag{A.98}$$

$$= \sum_{j=1}^{\infty}\frac{8}{(2j-1)\pi}\sin\left(\frac{(2j-1)\pi}{a}\left(y+\frac{a}{2}\right)\right)\times$$
$$+\left(\frac{\sinh\left(\frac{(2j-1)\pi}{a}\left(z+\frac{b}{2}\right)\right)}{\sinh\left((2j-1)\pi\frac{b}{a}\right)}-\frac{\sinh\left(\frac{(2j-1)\pi}{a}\left(z-\frac{b}{2}\right)\right)}{\sinh\left((2j-1)\pi\frac{b}{a}\right)}\right) \tag{A.99}$$

$$= \sum_{j=1}^{\infty}\frac{8}{(2j-1)\pi}\sin\left(\frac{(2j-1)\pi}{a}\left(y+\frac{a}{2}\right)\right)\times$$
$$\left(\frac{\sinh\left(\frac{(2j-1)\pi}{a}\left(z+\frac{b}{2}\right)\right)-\sinh\left(\frac{(2j-1)\pi}{a}\left(z-\frac{b}{2}\right)\right)}{\sinh\left((2j-1)\pi\frac{b}{a}\right)}\right) \tag{A.100}$$

However, we can simplify this further. The first hyperbolic term in the numerator expands to,

$$\sinh\left(\frac{(2j-1)\pi z}{a}\right)\cosh\left(\frac{(2j-1)\pi b}{2a}\right)+\cosh\left(\frac{(2j-1)\pi z}{a}\right)\sinh\left(\frac{(2j-1)\pi b}{2a}\right)$$

similarly, the second hyperbolic term in the numerator is,

$$\sinh\left(\frac{(2j-1)\pi z}{a}\right)\cosh\left(\frac{(2j-1)\pi b}{2a}\right)-\cosh\left(\frac{(2j-1)\pi z}{a}\right)\sinh\left(\frac{(2j-1)\pi b}{2a}\right)$$

So, subtracting these two terms we get,

$$\sinh\left(\frac{(2j-1)\pi}{a}\left(z+\frac{b}{2}\right)\right)-\sinh\left(\frac{(2j-1)\pi}{a}\left(z-\frac{b}{2}\right)\right)=2\cosh\left(\frac{(2j-1)\pi z}{a}\right)\sinh\left(\frac{(2j-1)\pi b}{2a}\right) \tag{A.101}$$

The half-angle expansion of the denominator is,

$$\sinh\left((2j-1)\pi\frac{b}{a}\right)=2\sinh\left((2j-1)\pi\frac{b}{2a}\right)\cosh\left((2j-1)\pi\frac{b}{2a}\right) \tag{A.102}$$

When we combine Equations (A.101) and (A.102), the hyperbolic sine terms cancel. So, using this in Equation (A.100),

$$f(y,z)=\sum_{j=1}^{\infty}\frac{8}{(2j-1)\pi}\left(\frac{\sin\left(\frac{(2j-1)\pi}{a}\left(y+\frac{a}{2}\right)\right)\cosh\left(\frac{(2j-1)\pi z}{a}\right)}{\cosh\left(\frac{(2j-1)\pi b}{2a}\right)}\right) \tag{A.103}$$

Now, letting $j = n+1$, we get,

$$f(y,z) = \sum_{n=0}^{\infty} \frac{8}{(2n+1)\pi} \left(\frac{\sin\left(\frac{(2n+1)\pi}{a}\left(y+\frac{a}{2}\right)\right)\cosh\left(\frac{(2n+1)\pi z}{a}\right)}{\cosh\left((2n+1)\pi\frac{b}{2a}\right)} \right) \tag{A.104}$$

Examining just the sine term, we expand it to get

$$\sin\left(\frac{(2n+1)\pi}{a}\left(y+\frac{a}{2}\right)\right) = \sin\left(\frac{(2n+1)\pi y}{a} + \pi n + \frac{\pi}{2}\right) \tag{A.105}$$

$$= \cos\left(\frac{(2n+1)\pi y}{a} + \pi n\right) \tag{A.106}$$

Now, expanding this,

$$\cos\left(\frac{(2n+1)\pi y}{a} + \pi n\right) = \cos\left(\frac{(2n+1)\pi y}{a}\right)\cos(\pi n) - \sin\left(\frac{(2n+1)\pi y}{a}\right)\sin(\pi n) \tag{A.107}$$

However, since $\sin(\pi n) = 0$ the second term is zero, leading to,

$$\cos\left(\frac{(2n+1)\pi y}{a} + \pi n\right) = \cos\left(\frac{(2n+1)\pi y}{a}\right)\cos(\pi n) \tag{A.108}$$

$$= (-1)^n \cos\left(\frac{(2n+1)\pi y}{a}\right) \tag{A.109}$$

since $\cos(\pi n) = (-1)^n$. Therefore, we have,

$$\sin\left(\frac{(2n+1)\pi}{a}\left(y+\frac{a}{2}\right)\right) = (-1)^n \cos\left(\frac{(2n+1)\pi y}{a}\right) \tag{A.110}$$

Using this in Equation (A.104) to replace the sine term we get the formal series solution for $f(y,z)$,

$$f(y,z) = \sum_{n=0}^{\infty} \frac{8(-1)^n \cos\left(\frac{(2n+1)\pi y}{a}\right)\cosh\left(\frac{(2n+1)\pi z}{a}\right)}{(2n+1)\pi\cosh\left(\frac{(2n+1)\pi b}{2a}\right)} \tag{A.111}$$

Using this formula for $f(y,z)$ in Equation (A.39) we get,

$$\frac{\partial^2}{\partial y^2}\psi(y,z) + 1 = \sum_{n=0}^{\infty} \frac{8(-1)^n \cos\left(\frac{(2n+1)\pi y}{a}\right)\cosh\left(\frac{(2n+1)\pi z}{a}\right)}{(2n+1)\pi\cosh\left(\frac{1}{2}\frac{(2n+1)\pi b}{a}\right)} \tag{A.112}$$

and in Equation (A.40),

$$\frac{\partial^2}{\partial z^2}\psi(y,z) = 1 - \sum_{n=0}^{\infty} \frac{8(-1)^n \cos\left(\frac{(2n+1)\pi y}{a}\right)\cosh\left(\frac{(2n+1)\pi z}{a}\right)}{(2n+1)\pi\cosh\left(\frac{1}{2}\frac{(2n+1)\pi b}{a}\right)} \tag{A.113}$$

Integrating Equation (A.112) with respect to y, yields

$$\frac{\partial}{\partial y}\psi(y,z) = \sum_{n=0}^{\infty} \frac{8(-1)^n \sin\left(\frac{(2n+1)\pi y}{a}\right)\cosh\left(\frac{(2n+1)\pi z}{a}\right)}{(2n+1)^2\pi^2 \cosh\left(\frac{1}{2}\frac{(2n+1)\pi b}{a}\right)} - y + k_1(z) \tag{A.114}$$

and integrating Equation (A.113) with respect to z, yields

$$\frac{\partial}{\partial z}\psi(y,z) = z - \sum_{n=0}^{\infty} \frac{8(-1)^n \cos\left(\frac{(2n+1)\pi y}{a}\right)\sinh\left(\frac{(2n+1)\pi z}{a}\right)}{(2n+1)^2\pi^2 \cosh\left(\frac{1}{2}\frac{(2n+1)\pi b}{a}\right)} + k_2(y) \tag{A.115}$$

Making use of the Cauchy-Riemann equations, we can rewrite these equations in terms of the warping function function $\phi(y,z)$. Using Equation (A.26) in Equation (A.114) we get,

$$\frac{\partial}{\partial z}\phi(y,z) = -\sum_{n=0}^{\infty} \frac{8a(-1)^n \sin\left(\frac{(2n+1)\pi y}{a}\right)\cosh\left(\frac{(2n+1)\pi z}{a}\right)}{(2n+1)^2\pi^2 \cosh\left(\frac{1}{2}\frac{(2n+1)\pi b}{a}\right)} + y - k_1(z) \tag{A.116}$$

and using Equation (A.25) in Equation (A.115), gives

$$\frac{\partial}{\partial y}\phi(y,z) = z - \sum_{n=0}^{\infty} \frac{8a(-1)^n \cos\left(\frac{(2n+1)\pi y}{a}\right)\sinh\left(\frac{(2n+1)\pi z}{a}\right)}{(2n+1)^2\pi^2 \cosh\left(\frac{1}{2}\frac{(2n+1)\pi b}{a}\right)} + k_2(y) \tag{A.117}$$

To find the integration functions $k_1(z)$ and $k_2(y)$, rewrite these equations in terms of the shear stresses by using Equations (A.18) and (A.17) respectively. Since it will be easier to solve for $k_2(y)$, we will start by using Equation (A.17) in Equation (A.117) to find

$$\frac{\sigma_{xy}}{G\alpha} + z = z - \sum_{n=0}^{\infty} \frac{8a(-1)^n \cos\left(\frac{(2n+1)\pi y}{a}\right)\sinh\left(\frac{(2n+1)\pi z}{a}\right)}{(2n+1)^2\pi^2 \cosh\left(\frac{1}{2}\frac{(2n+1)\pi b}{a}\right)} + k_2(y) \tag{A.118}$$

On either the left or the right boundary the shear stress σ_{xy} should be zero. Making these substitutions, we get,

$$z = z + k_2\left(\pm\frac{1}{2}a\right) \tag{A.119}$$

which means that $k_2(y) = 0$ is a simple solution that satisfies these conditions. Using Equation (A.17) in Equation (A.116),

$$\frac{\sigma_{zx}}{G\alpha} - y = -\sum_{n=0}^{\infty} \frac{8a(-1)^n \sin\left(\frac{(2n+1)\pi y}{a}\right)\cosh\left(\frac{(2n+1)\pi z}{a}\right)}{(2n+1)^2\pi^2 \cosh\left(\frac{1}{2}\frac{(2n+1)\pi b}{a}\right)} + y - k_1(z) \tag{A.120}$$

On the top and bottom boundaries ($z = \pm\frac{b}{2}$) the shear stress σ_{xz} must be zero. This gives,

$$y = \sum_{n=0}^{\infty} \frac{8(-1)^n \sin\left(\frac{(2n+1)\pi y}{a}\right)}{(2n+1)^2\pi^2} - y + k_1(\pm\frac{b}{2}) \tag{A.121}$$

and isolating $k_1(\pm\frac{b}{2})$,

$$k_1(\pm\frac{b}{2}) = 2y - \sum_{n=0}^{\infty} \frac{8a(-1)^n \sin\left(\frac{(2n+1)\pi y}{a}\right)}{(2n+1)^2\pi^2} \tag{A.122}$$

Since $k_1(z)$ is constant with respect to y, the only way this can be satisfied is if the right hand side is zero for all y. To prove this, let us make use of generalized Fourier series again by finding a series expansion of $2y$ using $\sin\left(\frac{(2n+1)\pi y}{a}\right)$. That is, we would like to find,

$$2y = \sum_{n=0}^{\infty} d_n \sin\left(\frac{(2n+1)\pi y}{a}\right) \tag{A.123}$$

Now taking the inner product of Equation (A.123) with its right-hand side sine terms leads to

$$\sum_{m=0}^{\infty} \int_{\frac{-a}{2}}^{\frac{a}{2}} 2y \sin\left(\frac{(2m+1)\pi y}{a}\right) \mathrm{d}y = \sum_{m=0}^{\infty}\sum_{n=0}^{\infty} \int_{\frac{-a}{2}}^{\frac{a}{2}} \sin\left(\frac{(2m+1)\pi y}{a}\right) d_n \sin\left(\frac{(2n+1)\pi y}{a}\right) \mathrm{d}y \tag{A.124}$$

The integral on the right hand side is only non-zero if $m = n$. Therefore, after carrying out the integration and equating terms,

$$\frac{(-1)^m a^2}{\pi^2(2m+1)^2} = \frac{1}{2} d_m a \tag{A.125}$$

and isolating d_m produces

$$d_m = \frac{8a(-1)^m}{(2m+1)^2\pi^2} \tag{A.126}$$

Using this in Equation (A.123), Equation (A.122) becomes

$$k_1(\pm\frac{b}{2}) = \sum_{m=0}^{\infty} \frac{8a(-1)^m}{(2m+1)^2\pi^2} \sin\left(\frac{(2m+1)\pi y}{a}\right) - \sum_{n=0}^{\infty} \frac{8a(-1)^n \sin\left(\frac{(2n+1)\pi y}{a}\right)}{(2n+1)^2\pi^2} \tag{A.127}$$

which means that $k_1(\pm\frac{b}{2}) = 0$. As before, the simplest solution that satisfies this is if $k_1(z) = 0$. However, before we make a decision on the values of $k_1(z)$ and $k_2(y)$ let us first integrate Equations (A.116) and (A.117) to solve for $\phi(y,z)$.

$$\phi(y,z) = yz - \sum_{n=0}^{\infty} \frac{8a^2(-1)^n \sin\left(\frac{(2n+1)\pi y}{a}\right) \sinh\left(\frac{(2n+1)\pi z}{a}\right)}{(2n+1)^3\pi^3 \cosh\left(\frac{1}{2}\frac{(2n+1)\pi b}{a}\right)} - k_1(z)z + k_3(y) \tag{A.128}$$

$$\phi(y,z) = yz - \sum_{n=0}^{\infty} \frac{8a^2(-1)^n \sin\left(\frac{(2n+1)\pi y}{a}\right) \sinh\left(\frac{(2n+1)\pi z}{a}\right)}{(2n+1)^3\pi^3 \cosh\left(\frac{1}{2}\frac{(2n+1)\pi b}{a}\right)} + k_2(y)y + k_4(z) \tag{A.129}$$

For these to be equivalent and satisfy the earlier boundary conditions on $k_1(z)$ and $k_2(y)$, it is necessary that both $k_1(z)$ and $k_2(y)$ be zero. But for $k_3(y)$ and $k_4(z)$ all that is necessary is

that they are the same constant. The effect of this constant is to shift the warping function such that the origin of the frame (i.e., the centre of the cross-section) is no longer in the original plane. To keep the origin in the original plane, we choose to set this constant to zero. Therefore, the warping function is,

$$\phi(y,z) = yz - \sum_{n=0}^{\infty} \frac{8a^2(-1)^n \sin\left(\frac{(2n+1)\pi y}{a}\right)\sinh\left(\frac{(2n+1)\pi z}{a}\right)}{(2n+1)^3\pi^3\cosh\left(\frac{1}{2}\frac{(2n+1)\pi b}{a}\right)} \tag{A.130}$$

Derivation of Torsional Inertia

Using the warping function we can get a new definition for the torsional inertia of the beam, commonly denoted as J. There are two different ways we can derive the formula for J. The first, which is the technique used by Rivello [33] and Sokolnikoff [31], is to define it in terms of the torsional couple created by the shear stresses. The second which is mentioned by Baruh [30] (but only done for the non-warping case) derives J based upon the potential energy. Both methods are shown here to illustrate that either method results in the same definition of J.

Derivation of J based upon the resultant moment

The torsional moment experienced at a cross-section is,

$$M_x = \int_A \left(\sigma_{zx}y - \sigma_{xy}z\right) \mathrm{d}A \tag{A.131}$$

where σ_{zx} is as defined in Equation (A.18) and σ_{xy} is as defined in Equation (A.17). Substituting these definitions into M_x we get,

$$M_x = \int_A G\alpha\left(z^2 - z\frac{\partial}{\partial y}\phi(y,z) + y^2 + y\frac{\partial}{\partial z}\phi(y,z)\right) \mathrm{d}A \tag{A.132}$$

Since G and α don't vary over the cross-section,

$$M_x = G\alpha\int_A\left(z^2 - z\frac{\partial}{\partial y}\phi(y,z) + y^2 + y\frac{\partial}{\partial z}\phi(y,z)\right) \mathrm{d}A \tag{A.133}$$

Traditionally, the torsional moment is related to the twist rate through the formula,

$$M_x = GJ\alpha \tag{A.134}$$

Therefore, we can define J as,

$$J = \int_A \left(y^2 + z^2\right)\mathrm{d}A + \int_A\left(y\frac{\partial}{\partial z}\phi(y,z) - z\frac{\partial}{\partial y}\phi(y,z)\right)\mathrm{d}A \tag{A.135}$$

which can be written as,

$$J = J_g + J_w \tag{A.136}$$

where J_g is the geometric torsional inertia and J_w is the warping correction factor. We have already calculated the partial derivatives of the warping function in Equations (A.116) and (A.117). Restating those equations,

$$\frac{\partial}{\partial y}\phi(y,z) = z - \sum_{n=0}^{\infty} \frac{8a(-1)^n \cos\left(\frac{(2n+1)\pi y}{a}\right)\sinh\left(\frac{(2n+1)\pi z}{a}\right)}{(2n+1)^2\pi^2 \cosh\left(\frac{1}{2}\frac{(2n+1)\pi b}{a}\right)} \tag{A.137}$$

$$\frac{\partial}{\partial z}\phi(y,z) = y - \sum_{n=0}^{\infty} \frac{8a(-1)^n \sin\left(\frac{(2n+1)\pi y}{a}\right)\cosh\left(\frac{(2n+1)\pi z}{a}\right)}{(2n+1)^2\pi^2 \cosh\left(\frac{1}{2}\frac{(2n+1)\pi b}{a}\right)} \tag{A.138}$$

To facilitate the manipulations we will write these equations as,

$$\frac{\partial}{\partial z}\phi(y,z) = y + S_1(y,z) \tag{A.139}$$

$$\frac{\partial}{\partial y}\phi(y,z) = z + S_2(y,z) \tag{A.140}$$

Substituting these into the equation for J_w, results in

$$J = \int_A \left(2y^2 + y\,S_1(y,z) - z\,S_2(y,z)\right) \mathrm{d}A \tag{A.141}$$

which when combined with J_g leads to,

$$J = \int_{\frac{-b}{2}}^{\frac{b}{2}}\int_{\frac{-a}{2}}^{\frac{a}{2}} 2y^2\,\mathrm{d}y\,\mathrm{d}z + \int_{\frac{-b}{2}}^{\frac{b}{2}}\int_{\frac{-a}{2}}^{\frac{a}{2}} y\,S_1(y,z)\,\mathrm{d}y\,\mathrm{d}z - \int_{\frac{-b}{2}}^{\frac{b}{2}}\int_{\frac{-a}{2}}^{\frac{a}{2}} z\,S_2(y,z)\,\mathrm{d}y\,\mathrm{d}z \tag{A.142}$$

We will integrate just one term at a time. So, integrating the first term we get,

$$J = \frac{1}{6}a^3 b + \int_{\frac{-b}{2}}^{\frac{b}{2}}\int_{\frac{-a}{2}}^{\frac{a}{2}} y\,S_1(y,z)\,\mathrm{d}y\,\mathrm{d}z - \int_{\frac{-b}{2}}^{\frac{b}{2}}\int_{\frac{-a}{2}}^{\frac{a}{2}} z\,S_2(y,z)\,\mathrm{d}y\,\mathrm{d}z \tag{A.143}$$

Now expanding the second term,

$$\begin{aligned} J = \frac{1}{6}a^3 b - \frac{8a}{\pi^2}\sum_{n=0}^{\infty}\int_{\frac{-b}{2}}^{\frac{b}{2}}\int_{\frac{-a}{2}}^{\frac{a}{2}} \frac{y(-1)^n \cosh\left(\frac{(2n+1)\pi z}{a}\right)\sin\left(\frac{(2n+1)\pi y}{a}\right)}{(2n+1)^2 \cosh\left(\frac{1}{2}\frac{(2n+1)\pi b}{a}\right)}\,\mathrm{d}y\,\mathrm{d}z \\ - \int_{\frac{-b}{2}}^{\frac{b}{2}}\int_{\frac{-a}{2}}^{\frac{a}{2}} z\,S_2(y,z)\,\mathrm{d}y\,\mathrm{d}z \end{aligned} \tag{A.144}$$

and then carrying out the integration with respect to y, produces

$$\begin{aligned} J = \frac{1}{6}a^3 b - \frac{16a^3}{\pi^4}\sum_{n=0}^{\infty}\int_{\frac{-b}{2}}^{\frac{b}{2}} \frac{\cosh\left(\frac{(2n+1)\pi z}{a}\right)}{(2n+1)^4 \cosh\left(\frac{1}{2}\frac{(2n+1)\pi b}{a}\right)}\,\mathrm{d}z \\ - \int_{\frac{-b}{2}}^{\frac{b}{2}}\int_{\frac{-a}{2}}^{\frac{a}{2}} z\,S_2(y,z)\,\mathrm{d}y\,\mathrm{d}z \end{aligned} \tag{A.145}$$

Integrating the second term with respect to z, reduces this to

$$J = \frac{1}{6}a^3 b - \frac{32a^4}{\pi^5}\sum_{n=0}^{\infty}\frac{\sinh\left(\frac{1}{2}\frac{(2n+1)\pi b}{a}\right)}{(2n+1)^5\cosh\left(\frac{1}{2}\frac{(2n+1)\pi b}{a}\right)} - \int_{\frac{-b}{2}}^{\frac{b}{2}}\int_{\frac{-a}{2}}^{\frac{a}{2}} z\,S_2(y,z)\,\mathrm{d}y\,\mathrm{d}z \tag{A.146}$$

which can be written as,

$$J = \frac{1}{6}a^3 b - \frac{32a^4}{\pi^5}\sum_{n=0}^{\infty}\frac{\tanh\left(\frac{1}{2}\frac{(2n+1)\pi b}{a}\right)}{(2n+1)^5} - \int_{\frac{-b}{2}}^{\frac{b}{2}}\int_{\frac{-a}{2}}^{\frac{a}{2}} z\,S_2(y,z)\,\mathrm{d}y\,\mathrm{d}z \tag{A.147}$$

Considering the final term we have,

$$\begin{aligned} J = {} & \frac{1}{6}a^3 b - \frac{32a^4}{\pi^5}\sum_{n=0}^{\infty}\frac{\tanh\left(\frac{1}{2}\frac{(2n+1)\pi b}{a}\right)}{(2n+1)^5} \\ & + \frac{8a}{\pi^2}\sum_{n=0}^{\infty}\int_{\frac{-b}{2}}^{\frac{b}{2}}\int_{\frac{-a}{2}}^{\frac{a}{2}}\frac{z(-1)^n\cos\left(\frac{(2n+1)\pi y}{a}\right)\sinh\left(\frac{(2n+1)\pi z}{a}\right)}{(2n+1)^2\cosh\left(\frac{1}{2}\frac{(2n+1)\pi b}{a}\right)}\,\mathrm{d}y\,\mathrm{d}z \end{aligned} \tag{A.148}$$

Integrating with respect to y, gives

$$J = \frac{1}{6}a^3 b - \frac{32a^4}{\pi^5}\sum_{n=0}^{\infty}\frac{\tanh\left(\frac{1}{2}\frac{(2n+1)\pi b}{a}\right)}{(2n+1)^5} + \frac{16a^2}{\pi^3}\sum_{n=0}^{\infty}\int_{\frac{-b}{2}}^{\frac{b}{2}}\frac{z\sinh\left(\frac{(2n+1)\pi z}{a}\right)}{(2n+1)^3\cosh\left(\frac{1}{2}\frac{(2n+1)\pi b}{a}\right)}\,\mathrm{d}z \tag{A.149}$$

and then integrating with respect to z, gives

$$J = \frac{1}{6}a^3 b - \frac{32a^4}{\pi^5}\sum_{n=0}^{\infty}\frac{\tanh\left(\frac{1}{2}\frac{(2n+1)\pi b}{a}\right)}{(2n+1)^5} + \frac{16a^3 b}{\pi^4}\sum_{n=0}^{\infty}\frac{1}{(2n+1)^4} - \frac{32a^4}{\pi^5}\sum_{n=0}^{\infty}\frac{\tanh\left(\frac{1}{2}\frac{(2n+1)\pi b}{a}\right)}{(2n+1)^5} \tag{A.150}$$

which can be simplified to,

$$J = \frac{1}{3}a^3 b - \frac{64a^4}{\pi^5}\sum_{n=0}^{\infty}\frac{\tanh\left(\frac{1}{2}\frac{(2n+1)\pi b}{a}\right)}{(2n+1)^5} \tag{A.151}$$

which cannot be simplified further since the series does not have a known closed form expression.

Derivation of J using potential energy

Start with the definition of the shear strains,

$$\gamma_{yx} = \frac{\partial v}{\partial x} + \frac{\partial u}{\partial y} \tag{A.152}$$

$$\gamma_{zx} = \frac{\partial u}{\partial z} + \frac{\partial w}{\partial x} \tag{A.153}$$

$$\gamma_{yz} = \frac{\partial w}{\partial y} + \frac{\partial v}{\partial z} \tag{A.154}$$

Substituting the displacements from Equations (A.1)-(A.3) into the shear strains, produces

$$\gamma_{yx} = \alpha\left(\frac{\partial}{\partial y}\phi(y,z) - z\right) \tag{A.155}$$

$$\gamma_{zx} = \alpha\left(\frac{\partial}{\partial z}\phi(y,z) + y\right) \tag{A.156}$$

$$\gamma_{yz} = 0 \tag{A.157}$$

The potential energy due to shear is in general,

$$U = \int_V G\left(\gamma_{yx}^2 + \gamma_{zx}^2 + \gamma_{yz}^2\right) \mathrm{d}V \tag{A.158}$$

which after substituting the shear strains in terms of the warping function $\phi(y,z)$ becomes,

$$U = \int_V G\left(z^2 + y^2 + \left(\frac{\partial}{\partial y}\phi(y,z)\right)^2 + \left(\frac{\partial}{\partial z}\phi(y,z)\right)^2 + 2y\frac{\partial}{\partial z}\phi(y,z) - 2z\frac{\partial}{\partial y}\phi(y,z)\right)\alpha^2 \mathrm{d}V \tag{A.159}$$

which we will write as,

$$U = \int_x GJ\alpha^2 \mathrm{d}x \tag{A.160}$$

where J is defined as,

$$J = \int_A \left(z^2 + y^2 + \left(\frac{\partial}{\partial y}\phi(y,z)\right)^2 + \left(\frac{\partial}{\partial z}\phi(y,z)\right)^2 + 2y\frac{\partial}{\partial z}\phi(y,z) - 2z\frac{\partial}{\partial y}\phi(y,z)\right) \mathrm{d}A \tag{A.161}$$

Note that this definition is different than our definition of J in the previous subsection. However, we will show that this definition results in the same final expression for J. As before, we will use Equations (A.139) and (A.140) in Equation (A.161) to facilitate manipulation. After substitution we have,

$$\begin{aligned} J = \int_A \big(z^2 + y^2 + (S_1(y,z) + y)^2 + (S_2(y,z) + z)^2 + 2y(S_1(y,z) + y) \\ -2z(S_2(y,z) + z)\big) \mathrm{d}A \end{aligned} \tag{A.162}$$

which after simplifying becomes,

$$J = \int_A \left(4y^2 + S_2(y,z)^2 + S_1(y,z)^2 + 4yS_1(y,z)\right) \mathrm{d}A \tag{A.163}$$

Of note that for each of the summations $S_1(y,z)$ and $S_2(y,z)$ because of the orthogonal nature of the trigonmetric functions when we integrate the squared terms we can move the sum outside the integral and square each term since the integral of mismatched terms will be zero. Expanding the integral Equation (A.163) gives

$$\begin{aligned} J = \int_{\frac{-b}{2}}^{\frac{b}{2}}\int_{\frac{-a}{2}}^{\frac{a}{2}} 4y^2 \mathrm{d}y\mathrm{d}z + \int_{\frac{-b}{2}}^{\frac{b}{2}}\int_{\frac{-a}{2}}^{\frac{a}{2}} S_2(y,z)^2 \mathrm{d}y\mathrm{d}z + \int_{\frac{-b}{2}}^{\frac{b}{2}}\int_{\frac{-a}{2}}^{\frac{a}{2}} S_1(y,z)^2 \mathrm{d}y\mathrm{d}z \\ + \int_{\frac{-b}{2}}^{\frac{b}{2}}\int_{\frac{-a}{2}}^{\frac{a}{2}} 4yS_1(y,z) \mathrm{d}y\mathrm{d}z \end{aligned} \tag{A.164}$$

As before, we will consider one term at a time. Integrating the first term gives,

$$J = \frac{1}{3}a^3 b + \int_{\frac{-b}{2}}^{\frac{b}{2}}\int_{\frac{-a}{2}}^{\frac{a}{2}} S_2(y,z)^2\,\mathrm{d}y\,\mathrm{d}z + \int_{\frac{-b}{2}}^{\frac{b}{2}}\int_{\frac{-a}{2}}^{\frac{a}{2}} S_1(y,z)^2\,\mathrm{d}y\,\mathrm{d}z + \int_{\frac{-b}{2}}^{\frac{b}{2}}\int_{\frac{-a}{2}}^{\frac{a}{2}} 4yS_1(y,z)\,\mathrm{d}y\,\mathrm{d}z \tag{A.165}$$

Substituting for $S_2(y,z)$ from Equations (A.137) and (A.140) into the second term results in

$$J = \frac{1}{3}a^3 b + \frac{64a^2}{\pi^4}\sum_{n=0}^{\infty}\int_{\frac{-b}{2}}^{\frac{b}{2}}\int_{\frac{-a}{2}}^{\frac{a}{2}} \frac{\cos\left(\frac{(2n+1)\pi y}{a}\right)^2 \sinh\left(\frac{(2n+1)\pi z}{a}\right)^2}{(2n+1)^4\cosh\left(\frac{1}{2}\frac{(2n+1)\pi b}{a}\right)^2}\,\mathrm{d}y\,\mathrm{d}z + \int_{\frac{-b}{2}}^{\frac{b}{2}}\int_{\frac{-a}{2}}^{\frac{a}{2}} S_1(y,z)^2\,\mathrm{d}y\,\mathrm{d}z + \int_{\frac{-b}{2}}^{\frac{b}{2}}\int_{\frac{-a}{2}}^{\frac{a}{2}} 4yS_1(y,z)\,\mathrm{d}y\,\mathrm{d}z \tag{A.166}$$

and integrating the second term with respect to y, produces

$$J = \frac{1}{3}a^3 b + \frac{32a^3}{\pi^4}\sum_{n=0}^{\infty}\int_{\frac{-b}{2}}^{\frac{b}{2}} \frac{\sinh\left(\frac{(2n+1)\pi z}{a}\right)^2}{(2n+1)^4\cosh\left(\frac{1}{2}\frac{(2n+1)\pi b}{a}\right)^2}\,\mathrm{d}z + \int_{\frac{-b}{2}}^{\frac{b}{2}}\int_{\frac{-a}{2}}^{\frac{a}{2}} S_1(y,z)^2\,\mathrm{d}y\,\mathrm{d}z + \int_{\frac{-b}{2}}^{\frac{b}{2}}\int_{\frac{-a}{2}}^{\frac{a}{2}} 4yS_1(y,z)\,\mathrm{d}y\,\mathrm{d}z \tag{A.167}$$

and after integrating with respect to z, we get

$$J = \frac{1}{3}a^3 b + \frac{16a^3}{\pi^5}\sum_{n=0}^{\infty} \frac{a\sinh\left(\frac{(2n+1)\pi b}{a}\right) - \pi b(2n+1)}{(2n+1)^5\cosh\left(\frac{1}{2}\frac{(2n+1)\pi b}{a}\right)^2} + \int_{\frac{-b}{2}}^{\frac{b}{2}}\int_{\frac{-a}{2}}^{\frac{a}{2}} S_1(y,z)^2\,\mathrm{d}y\,\mathrm{d}z + \int_{\frac{-b}{2}}^{\frac{b}{2}}\int_{\frac{-a}{2}}^{\frac{a}{2}} 4yS_1(y,z)\,\mathrm{d}y\,\mathrm{d}z \tag{A.168}$$

Substituting for $S_1(y,z)$ from Equations (A.138) and (A.139) in the third term we have,

$$J = \frac{1}{3}a^3 b + \frac{16a^3}{\pi^5}\sum_{n=0}^{\infty} \frac{a\sinh\left(\frac{(2n+1)\pi b}{a}\right) - \pi b(2n+1)}{(2n+1)^5\cosh\left(\frac{1}{2}\frac{(2n+1)\pi b}{a}\right)^2} + \frac{64a^2}{\pi^4}\sum_{n=0}^{\infty}\int_{\frac{-b}{2}}^{\frac{b}{2}}\int_{\frac{-a}{2}}^{\frac{a}{2}} \frac{\cosh\left(\frac{(2n+1)\pi z}{a}\right)^2 \sin\left(\frac{(2n+1)\pi y}{a}\right)^2}{(2n+1)^4\cosh\left(\frac{1}{2}\frac{(2n+1)\pi b}{a}\right)^2}\,\mathrm{d}y\,\mathrm{d}z + \int_{\frac{-b}{2}}^{\frac{b}{2}}\int_{\frac{-a}{2}}^{\frac{a}{2}} 4yS_1(y,z)\,\mathrm{d}y\,\mathrm{d}z \tag{A.169}$$

Integrating the third term with respect to y, yields

$$\begin{aligned} J = \frac{1}{3}a^3 b + \frac{16a^3}{\pi^5}\sum_{n=0}^{\infty}\frac{a\sinh\left(\frac{(2n+1)\pi b}{a}\right)-\pi b(2n+1)}{(2n+1)^5\cosh\left(\frac{1}{2}\frac{(2n+1)\pi b}{a}\right)^2} \\ +\frac{32a^3}{\pi^4}\sum_{n=0}^{\infty}\int_{\frac{-b}{2}}^{\frac{b}{2}}\frac{\cosh\left(\frac{(2n+1)\pi z}{a}\right)^2}{(2n+1)^4\cosh\left(\frac{1}{2}\frac{(2n+1)\pi b}{a}\right)^2}\,\mathrm{d}z \\ +\int_{\frac{-b}{2}}^{\frac{b}{2}}\int_{\frac{-a}{2}}^{\frac{a}{2}} 4yS_1(y,z)\,\mathrm{d}y\,\mathrm{d}z \end{aligned} \tag{A.170}$$

and then integrating with respect to z, results in

$$\begin{aligned} J = \frac{1}{3}a^3 b + \frac{16a^3}{\pi^5}\sum_{n=0}^{\infty}\frac{a\sinh\left(\frac{(2n+1)\pi b}{a}\right)-\pi b(2n+1)}{(2n+1)^5\cosh\left(\frac{1}{2}\frac{(2n+1)\pi b}{a}\right)^2} \\ +\frac{16a^3}{\pi^5}\sum_{n=0}^{\infty}\frac{a\sinh\left(\frac{(2n+1)\pi b}{a}\right)+\pi b(2n+1)}{(2n+1)^5\cosh\left(\frac{1}{2}\frac{(2n+1)\pi b}{a}\right)^2}+\int_{\frac{-b}{2}}^{\frac{b}{2}}\int_{\frac{-a}{2}}^{\frac{a}{2}} 4yS_1(y,z)\,\mathrm{d}y\,\mathrm{d}z \end{aligned} \tag{A.171}$$

which can be simplified to the form

$$\begin{aligned} J = \frac{1}{3}a^3 b + \frac{32a^4}{\pi^5}\sum_{n=0}^{\infty}\frac{\sinh\left(\frac{(2n+1)\pi b}{a}\right)}{(2n+1)^5\cosh\left(\frac{1}{2}\frac{(2n+1)\pi b}{a}\right)^2} \\ +\int_{\frac{-b}{2}}^{\frac{b}{2}}\int_{\frac{-a}{2}}^{\frac{a}{2}} 4yS_1(y,z)\,\mathrm{d}y\,\mathrm{d}z \end{aligned} \tag{A.172}$$

Substituting for $S_1(y,z)$ in the last term, leads to

$$\begin{aligned} J = \frac{1}{3}a^3 b + \frac{32a^4}{\pi^5}\sum_{n=0}^{\infty}\frac{\sinh\left(\frac{(2n+1)\pi b}{a}\right)}{(2n+1)^5\cosh\left(\frac{1}{2}\frac{(2n+1)\pi b}{a}\right)^2} \\ -\frac{32a}{\pi^2}\sum_{n=0}^{\infty}\int_{\frac{-b}{2}}^{\frac{b}{2}}\int_{\frac{-a}{2}}^{\frac{a}{2}}\frac{(-1)^n y\cosh\left(\frac{(2n+1)\pi z}{a}\right)\sin\left(\frac{(2n+1)\pi y}{a}\right)}{(2n+1)^2\cosh\left(\frac{1}{2}\frac{(2n+1)\pi b}{a}\right)}\,\mathrm{d}y\,\mathrm{d}z \end{aligned} \tag{A.173}$$

after carrying out the integration with respect to y, we have

$$\begin{aligned} J = \frac{1}{3}a^3 b + \frac{32a^4}{\pi^5}\sum_{n=0}^{\infty}\frac{\sinh\left(\frac{(2n+1)\pi b}{a}\right)}{(2n+1)^5\cosh\left(\frac{1}{2}\frac{(2n+1)\pi b}{a}\right)^2} \\ -\frac{64a^3}{\pi^4}\sum_{n=0}^{\infty}\int_{\frac{-b}{2}}^{\frac{b}{2}}\frac{\cosh\left(\frac{(2n+1)\pi z}{a}\right)}{(2n+1)^4\cosh\left(\frac{1}{2}\frac{(2n+1)\pi b}{a}\right)}\,\mathrm{d}z \end{aligned} \tag{A.174}$$

and then integrating with respect to z, produces

$$J = \frac{1}{3}a^3 b + \frac{32a^4}{\pi^5}\sum_{n=0}^{\infty}\frac{\sinh\left(\frac{(2n+1)\pi b}{a}\right)}{(2n+1)^5\cosh\left(\frac{1}{2}\frac{(2n+1)\pi b}{a}\right)^2} - \frac{128a^4}{\pi^5}\sum_{n=0}^{\infty}\frac{\sinh\left(\frac{1}{2}\frac{(2n+1)\pi b}{a}\right)}{(2n+1)^5\cosh\left(\frac{1}{2}\frac{(2n+1)\pi b}{a}\right)} \tag{A.175}$$

Combining terms in Equation (A.175) allows us to write

$$J = \frac{1}{3}a^3 b - \frac{32a^4}{\pi^5}\sum_{n=0}^{\infty}\frac{\sinh\left(\frac{(2n+1)\pi b}{a}\right)}{(2n+1)^5\cosh\left(\frac{1}{2}\frac{(2n+1)\pi b}{a}\right)^2} \tag{A.176}$$

which can be rewritten as,

$$J = \frac{1}{3}a^3 b - \frac{64a^4}{\pi^5}\sum_{n=0}^{\infty}\frac{\sinh\left(\frac{1}{2}\frac{(2n+1)\pi b}{a}\right)}{(2n+1)^5\cosh\left(\frac{1}{2}\frac{(2n+1)\pi b}{a}\right)} \tag{A.177}$$

or alternatively as,

$$J = \frac{1}{3}a^3 b - \frac{64a^4}{\pi^5}\sum_{n=0}^{\infty}\frac{\tanh\left(\frac{1}{2}\frac{(2n+1)\pi b}{a}\right)}{(2n+1)^5} \tag{A.178}$$

which is the same as what we found in the previous section.

Torsional Kinetic Energy

Revisiting the displacements, now we consider that α is now a function of time. Therefore,

$$v = -\alpha(t)xz \tag{A.179}$$

$$w = \alpha(t)xy \tag{A.180}$$

$$u = \alpha(t)\phi(y,z) \tag{A.181}$$

The kinetic energy of the beam due to shear is in general,

$$T = \frac{1}{2}\int_V \rho\left(\dot{u}^2 + \dot{v}^2 + \dot{w}^2\right)\mathrm{d}V \tag{A.182}$$

which after substitution of the displacements is,

$$T = \frac{1}{2}\int_V \rho x^2\left(z^2+y^2\right)\dot{\alpha}(t)^2\,\mathrm{d}V + \frac{1}{2}\int_V \rho\phi(y,z)^2\dot{\alpha}(t)^2\,\mathrm{d}V \tag{A.183}$$

Which can be written as,

$$T = \frac{1}{2}\int_x \rho J_g x^2\dot{\alpha}(t)^2\,\mathrm{d}x + \frac{1}{2}\int_V \rho\phi(y,z)^2\dot{\alpha}(t)^2\,\mathrm{d}V \tag{A.184}$$

using the definition of J_g from Equation (A.136).

Convergence Analysis of J

The formula for J includes an infinite series with no closed form solution. So it is important to know how many terms in the series are needed to get a "good" approximation to J. First, let us perform a change of variables to facilitate the analysis. Let $b = a\beta$ where β is the ratio of height to width of the cross-section. After substitution into J we get,

$$J = \frac{1}{3}a^4\beta - \frac{64a^4}{\pi^5}\sum_{n=0}^{\infty}\frac{\tanh\left(\frac{1}{2}(2n+1)\pi\beta\right)}{(2n+1)^5} \tag{A.185}$$

Factoring out the a^4,

$$J = a^4\left(\frac{1}{3}\beta - \frac{64}{\pi^5}\sum_{n=0}^{\infty}\frac{\tanh\left(\frac{1}{2}(2n+1)\pi\beta\right)}{(2n+1)^5}\right) \tag{A.186}$$

Now, add and subtract 1 inside the sum giving,

$$J = a^4\left(\frac{1}{3}\beta - \frac{64}{\pi^5}\sum_{n=0}^{\infty}\frac{1-1+\tanh\left(\frac{1}{2}(2n+1)\pi\beta\right)}{(2n+1)^5}\right) \tag{A.187}$$

which can be re-written as,

$$\frac{J}{a^4} = \frac{1}{3}\beta - \frac{64}{\pi^5}\left(\sum_{n=0}^{\infty}\frac{1}{(2n+1)^5} - \sum_{n=0}^{\infty}\frac{1-\tanh\left(\frac{1}{2}(2n+1)\pi\beta\right)}{(2n+1)^5}\right) \tag{A.188}$$

Now, we can use the Riemann Zeta function to simplify the first sum. Using the identity [89],

$$\sum_{n=0}^{\infty}\frac{1}{(2n+1)^m} = (-1+2^{-m})(-\zeta(m)) \tag{A.189}$$

we get,

$$\frac{J}{a^4} = \frac{1}{3}\beta - \frac{64}{\pi^5}\left(\frac{31}{32}\zeta(5) - \sum_{n=0}^{\infty}\frac{1-\tanh\left(\frac{1}{2}(2n+1)\pi\beta\right)}{(2n+1)^5}\right) \tag{A.190}$$

Therefore, the right hand side is now only a function of two variables, N which determines the number of terms to use and β the ratio of height to width. Since the leading term won't affect the convergence we will just consider the series when plotting. Note that our assumption during the warping function derivation is that β is greater than or equal to 1. Since tanh in the last sum rapidly approaches 1, each term quickly becomes zero. If we consider the worst geometric case ($\beta = 1$), we see convergence of the series terms (including ζ) as in Figure A.3. So, even in the worse case, the correction sum contributes little to the final result past the first term.

To see the effectiveness of this approach consider an alternate approximation by letting the original series in Equation (A.186) range up to N terms,

$$J \approx a^4\left(\frac{1}{3}\beta - \frac{64}{\pi^5}\sum_{n=0}^{N}\frac{\tanh\left(\frac{1}{2}(2n+1)\pi\beta\right)}{(2n+1)^5}\right) \tag{A.191}$$

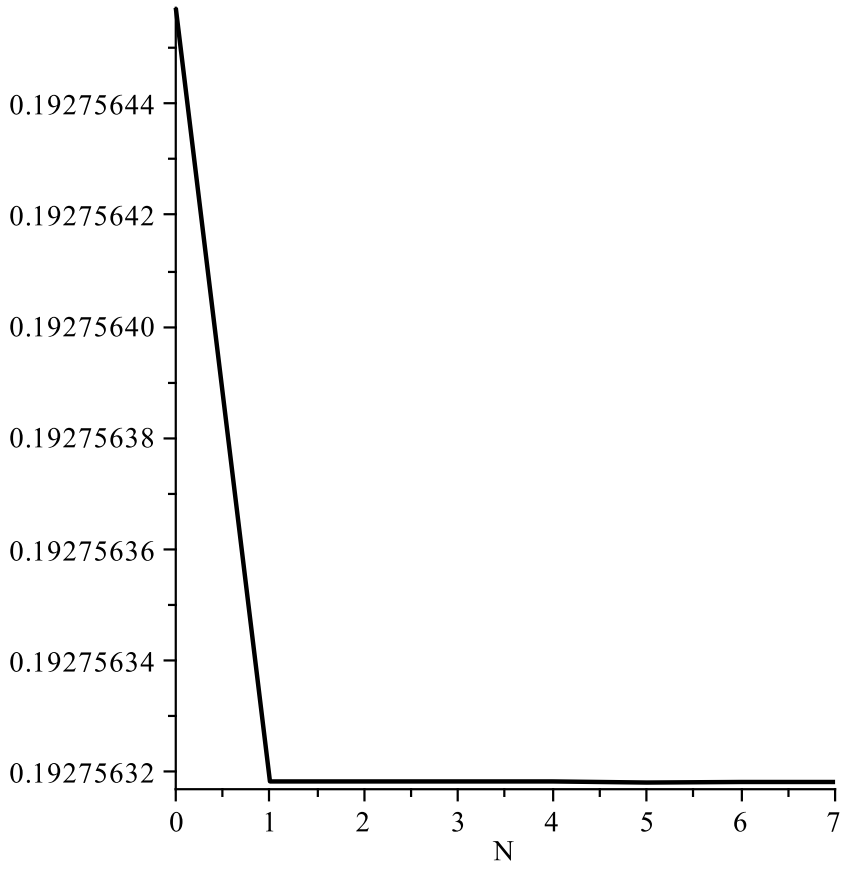

Figure A.3: Series Contribution to J vs. N ($\beta = 1$)

Dividing through by the a^4,

$$\frac{J}{a^4} \approx \frac{1}{3}\beta - \frac{64}{\pi^5}\sum_{n=0}^{N}\frac{\tanh\left(\frac{1}{2}(2n+1)\pi\beta\right)}{(2n+1)^5} \tag{A.192}$$

Comparing the series contribution of this equation versus the zeta approximation (plus correction series), we get Figure A.4.

Plotting the β vs. N for the standard approximation (since it converges more slowly) in a three-dimensional plot we get Figure A.5. Note that the solution is insensitive to N since the result does not change much due to N. Also, once β is not much greater than 1, there is also very little change. Investigating the rapid convergence further for a cross-section where $a = 1$ mm and $b = 30$ mm. Using just a single term ($N = 0$) in the zeta approximation, Equation (A.190) we get,

$$J_0 \approx 9.7899 \text{ mm}^4 \tag{A.193}$$

If we ignore the correction sum term, we also get,

$$J_\zeta \approx 9.7899 \text{ mm}^4 \tag{A.194}$$

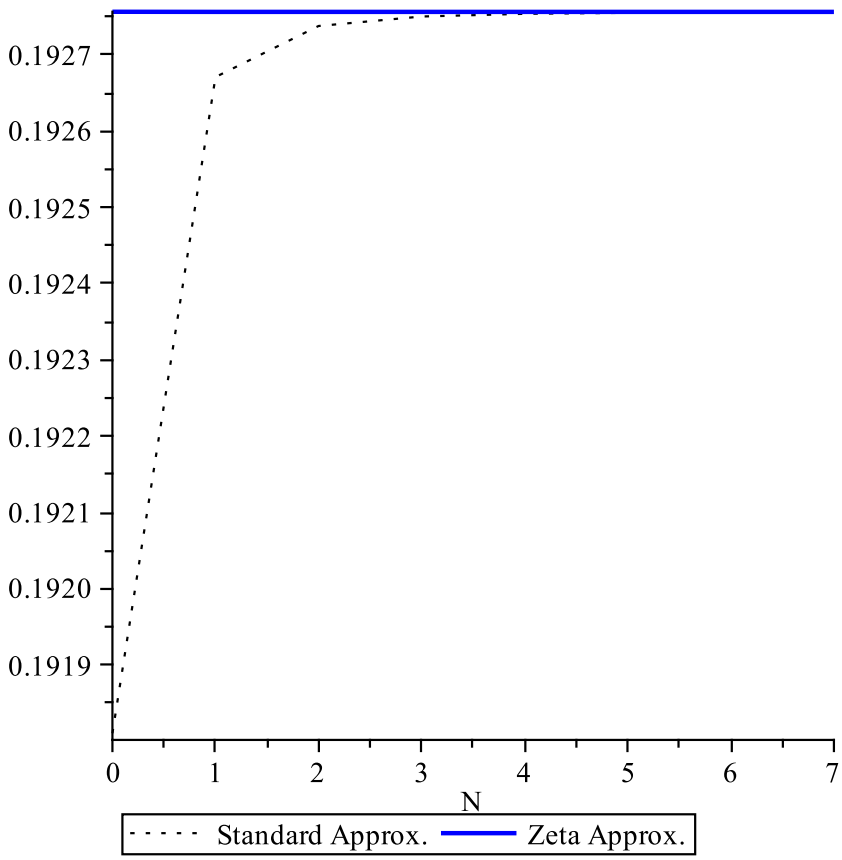

Figure A.4: Comparing Approximation of the Series Contribution to J vs. N ($\beta = 1$)

Therefore, we can safely use the approximation

$$J \approx \frac{1}{3}a^3 b - \frac{62a^4}{\pi^5}\zeta(5) \tag{A.195}$$

for larger values of β. Note that we had assumed that there was no warping in the cross-section the formula for J would be,

$$J_{\phi=0} = \frac{1}{12}ab\left(a^2 + b^2\right) \tag{A.196}$$

which for the numerical example above would give,

$$J_{\phi=0} = 2,252 \text{ mm}^4 \tag{A.197}$$

and using a single term in Rivello's series approximation to J [33],

$$J_R = 7.9795739217 \text{ mm}^4 \tag{A.198}$$

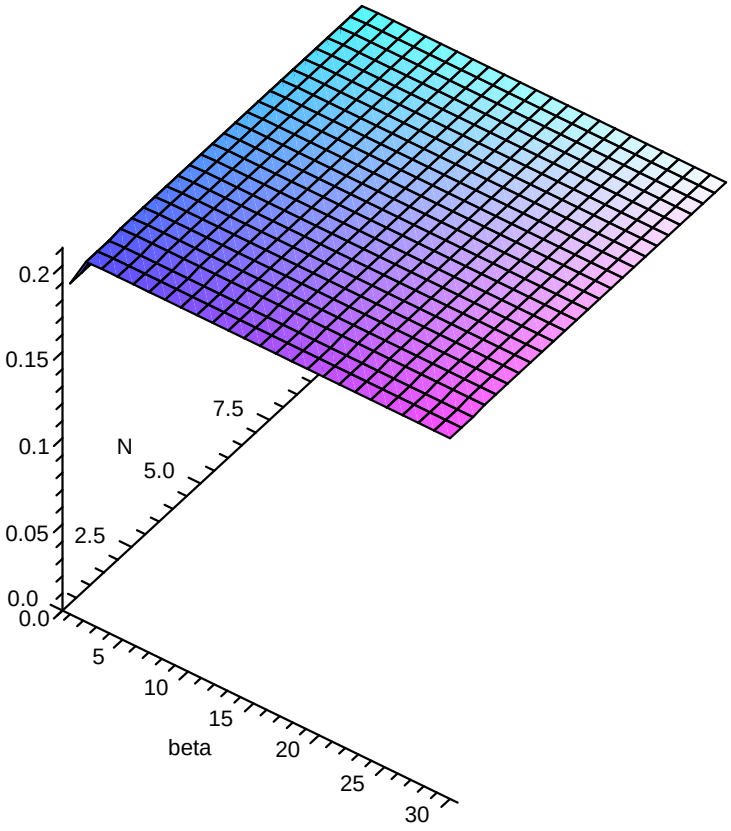

Figure A.5: Series Contribution to J for β vs. N

Therefore, a single term approximation using Rivello's formula has an error of

$$E_R = 18.5\,\% \tag{A.199}$$

Although, it should converge to the correct solution. The error for the no-warping assumption is,

$$E_{\phi=0} = 22,903\,\% \tag{A.200}$$

A.2 ϕ Dependence in Reissner Torsion

For simplicity's sake, in this section we will focus on the original static model as proposed by Reissner. Reissner's assumptions for the deflection due to torsion are,

$$u(x,y,z) = \psi(x)\phi(y,z) \tag{A.201}$$

$$v(x,y,z) = -\theta(x)z \tag{A.202}$$

$$w(x,y,z) = \theta(x)y \tag{A.203}$$

To ensure that there is no warping at the fixed end of the beam ($x = 0$),

$$\psi(0) = 0 \tag{A.204}$$

The differential equations he derives are as follows (using consistent constants with Chapter 2),

$$G\left(L_c\theta_{,x} + K\psi\right) - EP\psi_{,xx} = 0 \tag{A.205}$$

$$G\left(J_g\theta_{,x} + L_c\psi\right) = M \tag{A.206}$$

where M is the applied torque and the other constants are from Equations (2.23)–(2.26). To understand the equations further, let us derive the equations using a different method than that of Reissner. The potential strain energy is,

$$U = \frac{1}{2}\int_V \left(\sigma_{xx}\epsilon_{xx} + \tau_{xy}\gamma_{xy} + \tau_{xz}\gamma_{xz}\right) \mathrm{d}V \tag{A.207}$$

since those are the only non-zero stress-strain combinations due to the displacement and stress assumptions. In general, this becomes,

$$U = \frac{1}{2}\int_V \left(Eu_{,x}^2 + G\left(u_{,y} + v_{,x}\right)^2 + G\left(u_{,z} + w_{,x}\right)^2\right) \mathrm{d}V \tag{A.208}$$

and with our definitions for the deflections,

$$U = \frac{1}{2}\int_V \left(E\psi_{,x}^2\phi^2 + G\left(\psi\phi_{,y} - z\theta_{,x}\right)^2 + G\left(\psi\phi_{,z} + y\theta_{,x}\right)^2\right) \mathrm{d}V \tag{A.209}$$

Note that we need to be concerned with variations with respect to $\phi(y,z)$, $\psi(x)$, and $\theta(x)$. Carrying out the variation with respect to ϕ,

$$\int_V \left(E\phi\psi_{,x}^2\delta\phi + G\psi\left(\phi_{,y}\psi - z\theta_{,x}\right)\delta\phi_{,y} + G\psi\left(\phi_{,z}\psi + y\theta_{,x}\right)\delta\phi_{,z}\right) \mathrm{d}V = 0 \tag{A.210}$$

and the variation with respect to ψ,

$$\int_V \left(E\phi^2\psi_{,x}\delta\psi_{,x} + G\left(\phi_{,y}^2\psi - z\phi_{,y}\theta_{,x} + \phi_{,z}^2\psi + y\phi_{,z}\theta_{,x}\right)\delta\psi\right) \mathrm{d}V = 0 \tag{A.211}$$

Finally, the variation with respect to θ,

$$\int_V G\left(\left(y\phi_{,z} - z\phi_{,y}\right)\psi + (z^2 + y^2)\theta_{,x}\right)\delta\theta_{,x}\mathrm{d}V = 0 \tag{A.212}$$

Integrating Equation (A.210), by parts using Gauss' Theorem,

$$\int_S G\psi\left(\left(\phi_{,y}\mathrm{n}_y + \phi_{,z}\mathrm{n}_z\right)\psi + (y\mathrm{n}_z - z\mathrm{n}_y)\theta_{,x}\right)\delta\phi\mathrm{d}S + \int_V \left(E\phi\psi_{,x}^2 - G\psi^2\left(\phi_{,yy} + \phi_{,zz}\right)\right)\delta\phi\mathrm{d}V = 0 \tag{A.213}$$

where n_y is the y component of the surface normal and n_z is the z component of the surface normal. Integrating Equation (A.211) by parts,

$$\int_{A_c} E\phi^2\psi_{,x}\delta\psi \mathrm{d}A_c\Big|_0^l + \int_V \left(-E\phi^2\psi_{,xx} + G\left(\phi_{,y}^2+\phi_{,z}^2\right)\psi + G\left(y\phi_{,z}-z\phi_{,y}\right)\theta_{,x}\right)\delta\psi \,\mathrm{d}V = 0 \tag{A.214}$$

Note that neither ψ or $\delta\psi$ vary over the cross-section. Assuming that the material properties are constant for the cross-section and making use of Equations (2.23)-(2.26), this becomes,

$$EP\psi_{,x}\delta\psi\big|_0^l + \int_0^L \left(-EP\psi_{,xx} + G\left(K\psi + L\theta_{,x}\right)\right)\delta\psi \,\mathrm{d}x = 0 \tag{A.215}$$

Similarly, integrating Equation (A.212) by parts,

$$\int_{A_c} G\left(\left(y\phi_{,z}-z\phi_{,y}\right)\psi + (z^2+y^2)\theta_{,x}\right)\delta\theta \mathrm{d}A_c\Big|_0^l - \int_V G\left(\left(y\phi_{,z}-z\phi_{,y}\right)\psi_{,x} + (z^2+y^2)\theta_{,xx}\right)\delta\theta \mathrm{d}V = 0 \tag{A.216}$$

Once again, using the same set of assumptions along with Equations (2.23) and (2.26),

$$G\left(L\psi + J_g\theta_{,x}\right)\delta\theta\big|_0^l - \int_0^l G\left(L\psi_{,x} + J_g\theta_{,xx}\right)\delta\theta \mathrm{d}x = 0 \tag{A.217}$$

This gives us the following equations of equilibrium,

$$\begin{aligned} E\phi\psi_{,x}^2 - G\psi^2\left(\phi_{,yy}+\phi_{,zz}\right) &= 0 && \text{(A.218)}\\ G\left(K\psi + L_c\theta_{,x}\right) - EP\psi_{,xx} &= 0 && \text{(A.219)}\\ J_g\theta_{,xx} + L_c\psi_{,x} &= 0 && \text{(A.220)} \end{aligned}$$

and the boundary conditions,

$$\begin{aligned} \int_S \psi\left(\left(\phi_{,y}\mathrm{n}_y + \phi_{,z}\mathrm{n}_z\right)\psi + (y\mathrm{n}_z - z\mathrm{n}_y)\theta_{,x}\right)\delta\phi \mathrm{d}S &= 0 && \text{(A.221)}\\ \psi_{,x}\delta\psi\big|_0^l &= 0 && \text{(A.222)}\\ \left(-D^*\psi + J_g\theta_{,x}\right)\delta\theta\big|_0^l &= 0 && \text{(A.223)} \end{aligned}$$

If we consider $x = 0$ to be fixed and $x = l$ to be free, the boundary conditions become,

$$\begin{aligned} \int_S \psi\left(\left(\phi_{,y}\mathrm{n}_y + \phi_{,z}\mathrm{n}_z\right)\psi + (y\mathrm{n}_z - z\mathrm{n}_y)\theta_{,x}\right)\delta\phi \mathrm{d}S &= 0 && \text{(A.224)}\\ \psi(0) &= 0 && \text{(A.225)}\\ \psi_{,x}(l) &= 0 && \text{(A.226)}\\ \theta(0) &= 0 && \text{(A.227)}\\ J_g\theta_{,x}(l) &= D^*\psi(l) && \text{(A.228)} \end{aligned}$$

We can re-arrange Equation (A.218) to get,

$$G\psi^2\left(\phi_{,yy}+\phi_{,zz}\right)=E\phi\psi_{,x}^2 \tag{A.229}$$

which can be written as,

$$\frac{G}{E}\frac{\phi_{,yy}+\phi_{,zz}}{\phi}=\left(\frac{\psi_{,x}}{\psi}\right)^2 \tag{A.230}$$

We will assume that the each side is equal to a positive constant since the only way it could be negative is if the ratio inside the square is a complex number. This gives,

$$\frac{G}{E}\left(\phi_{,yy}+\phi_{,zz}\right)-\lambda^2\phi = 0 \tag{A.231}$$

$$\psi_{,x}^2-\lambda^2\psi^2 = 0 \tag{A.232}$$

The second equation can be simplified to,

$$\psi_{,x}-\lambda\psi=0 \tag{A.233}$$

which gives us four differential equations to describe 3 variables. Also, when combined with our boundary condition that $\psi(0)=0$, this would mean that there is no warping of the cross-section.

A.3 Modelling Torsion including Shear and Poisson Effects

In this model, we are only using the stress assumptions as given in Equations (2.50) and (2.51). This means that Equations (2.44)–(2.46) become,

$$\sigma_{xx} = E\epsilon_{xx} \tag{A.234}$$

$$\epsilon_{yy} = -\nu\epsilon_{xx} \tag{A.235}$$

$$\epsilon_{zz} = -\nu\epsilon_{xx} \tag{A.236}$$

From Equations (A.235) and (A.236) one can see that the normal strains in the y and z directions are now dependent upon the axial deformation. Therefore, assume displacements of the form

$$u = u(x,y,z,t) \tag{A.237}$$

$$v = v(x,y,z,t) \tag{A.238}$$

$$w = w(x,y,z,t) \tag{A.239}$$

which means that Equations (A.234)–(A.236) become,

$$\sigma_{xx} = E\,u_{,x}(x,y,z,t) \tag{A.240}$$

$$v_{,y}(x,y,z,t) = -\nu\,u_{,x}(x,y,z,t) \tag{A.241}$$

$$w_{,z}(x,y,z,t) = -\nu\,u_{,x}(x,y,z,t) \tag{A.242}$$

and the shear strains from Equations (2.35)–(2.37) become,

$$\gamma_{yz} = v_{,z}(x,y,z,t) + w_{,y}(x,y,z,t) \tag{A.243}$$
$$\gamma_{zx} = u_{,z}(x,y,z,t) + w_{,x}(x,y,z,t) \tag{A.244}$$
$$\gamma_{xy} = u_{,y}(x,y,z,t) + v_{,x}(x,y,z,t) \tag{A.245}$$

and the resulting shear stresses are,

$$\tau_{yz} = G\left[v_{,z}(x,y,z,t) + w_{,y}(x,y,z,t)\right] \tag{A.246}$$
$$\tau_{zx} = G\left[u_{,z}(x,y,z,t) + w_{,x}(x,y,z,t)\right] \tag{A.247}$$
$$\tau_{xy} = G\left[u_{,y}(x,y,z,t) + v_{,x}(x,y,z,t)\right] \tag{A.248}$$

Note that we can combine Equations (A.241) and (A.242) to get,

$$v_{,y}(x,y,z,t) = w_{,z}(x,y,z,t) \tag{A.249}$$

The torsional strain energy has as an additional term not in Equation (2.56) which now has the form

$$U = \frac{1}{2}\int_V \left(\sigma_{xx}\epsilon_{xx} + \tau_{xy}\gamma_{xy} + \tau_{zx}\gamma_{zx} + \tau_{yz}\gamma_{yz}\right) \mathrm{d}V \tag{A.250}$$

which, after substitution from Equation (A.240) and Equations (A.243)–(A.248), yields

$$\begin{aligned} U = \frac{1}{2}\int_V \Big[& E\,u_{,x}(x,y,z,t)^2 + G\left(u_{,y}(x,y,z,t) + v_{,x}(x,y,z,t)\right)^2 \\ & + G\left(u_{,z}(x,y,z,t) + w_{,x}(x,y,z,t)\right)^2 + G\left(v_{,z}(x,y,z,t) + w_{,y}(x,y,z,t)\right)^2 \Big] \mathrm{d}V \end{aligned} \tag{A.251}$$

and the kinetic energy as given in Equation (2.60) becomes,

$$T = \frac{1}{2}\int_V \rho\left[\dot{u}(x,y,z,t)^2 + \dot{v}(x,y,z,t)^2 + \dot{w}(x,y,z,t)^2\right] \mathrm{d}V \tag{A.252}$$

Using Hamilton's Principle as given in Equation (2.63) and taking the variation with respect to $u(x,y,z,t)$, we get

$$\delta\mathscr{A}_1 = \int_{t_1}^{t_2}\int_V [\rho\,\dot{u}\delta\dot{u} - \mathbf{d_u}\cdot\nabla\delta u]\mathrm{d}V\mathrm{d}t \tag{A.253}$$

where $\mathbf{d_u}$ is given as,

$$\mathbf{d_u} = \begin{bmatrix} Eu_{,x} & G\left(v_{,x} + u_{,y}\right) & G\left(w_{,x} + u_{,z}\right) \end{bmatrix}^T \tag{A.254}$$

Taking the variation with respect to $v(x,y,z,t)$ yields

$$\delta\mathscr{A}_2 = \int_{t_1}^{t_2}\int_V \left[\rho\,\dot{v}\delta\dot{v} - \mathbf{d_v}\cdot\nabla\delta v\right] \mathrm{d}V\mathrm{d}t \tag{A.255}$$

where $\mathbf{d_v}$ is given as,

$$\mathbf{d_v} = \begin{bmatrix} G\left(u_{,y} + v_{,x}\right) & 0 & G\left(v_{,z} + w_{,y}\right) \end{bmatrix}^T \tag{A.256}$$

and lastly, taking the variation with respect to $w(x,y,z,t)$ gives

$$\delta\mathscr{A}_3 = \int_{t_1}^{t_2}\int_V \left[\rho\dot{w}\delta\dot{w} - \mathbf{d_w}\cdot\nabla\delta w\right] \mathrm{d}V\,\mathrm{d}t \tag{A.257}$$

where $\mathbf{d_w}$ is given as,

$$\mathbf{d_w} = \begin{bmatrix} G\left(u_{,z} + w_{,x}\right) & G\left(v_{,z} + w_{,y}\right) & 0 \end{bmatrix}^T \tag{A.258}$$

Each of these variations are independent so they must go to zero independently. We can make use of the results in Appendix B to integrate these equations. First integrating Equation (A.253),

$$\left[\int_V \rho\dot{u}\delta u \mathrm{d}V\right]_{t_1}^{t_2} - \int_{t_1}^{t_2}\int_S \mathbf{d_u}\cdot\mathbf{n}\delta u\,\mathrm{d}S\mathrm{d}t - \int_{t_1}^{t_2}\int_V \left[\rho\ddot{u} - (\nabla\cdot\mathbf{d_u})\right]\delta u\,\mathrm{d}V\mathrm{d}t = 0 \tag{A.259}$$

If we consider that $\mathbf{n}$ has the form,

$$\mathbf{n} = \begin{bmatrix} n_x & n_y & n_z \end{bmatrix}^T \tag{A.260}$$

then Equation (A.259) can be written as,

$$\begin{aligned}\left[\int_V \rho\dot{u}\delta u \mathrm{d}V\right]_{t_1}^{t_2} - \int_{t_1}^{t_2}\int_S \left[Eu_{,x}n_x + G[\left(v_{,x}+u_{,y}\right)n_y + \left(w_{,x}+u_{,z}\right)n_z]\right]\delta u\,\mathrm{d}S\mathrm{d}t \\ - \int_{t_1}^{t_2}\int_V \left[\rho\ddot{u} - Eu_{,xx} - G\left(v_{,xy}+u_{,yy}\right) - G\left(w_{,xz}+u_{,zz}\right)\right]\delta u\,\mathrm{d}V\mathrm{d}t = 0\end{aligned} \tag{A.261}$$

n_x is perpendicular to the cross-section so this can be written as

$$\begin{aligned}\left[\int_V \rho\dot{u}\delta u \mathrm{d}V\right]_{t_1}^{t_2} - \left[\int_{t_1}^{t_2}\int_A \delta u\,\mathrm{d}A\mathrm{d}t\right]_0^l \\ - \int_{t_1}^{t_2}\int_S G\left[\left(v_{,x}+u_{,y}\right)n_y + \left(w_{,x}+u_{,z}\right)n_z\right]\delta u\,\mathrm{d}S\mathrm{d}t \\ - \int_{t_1}^{t_2}\int_V \left[\rho\ddot{u} - Eu_{,xx} - G\left(v_{,xy}+u_{,yy}\right) - G\left(w_{,xz}+u_{,zz}\right)\right]\delta u\,\mathrm{d}V\mathrm{d}t = 0\end{aligned} \tag{A.262}$$

We can make use of Equations (A.241) and (A.242) to get,

$$\begin{aligned}\left[\int_V \rho\dot{u}\delta u \mathrm{d}V\right]_{t_1}^{t_2} - \left[\int_{t_1}^{t_2}\int_A Eu_{,x}\delta u\,\mathrm{d}A\mathrm{d}t\right]_0^l \\ - \int_{t_1}^{t_2}\int_S G\left[\left(v_{,x}+u_{,y}\right)n_y + \left(w_{,x}+u_{,z}\right)n_z\right]\delta u\,\mathrm{d}S\mathrm{d}t \\ - \int_{t_1}^{t_2}\int_V \left[\rho\ddot{u} - (E-2G\nu)u_{,xx} - G(u_{,yy}+u_{,zz})\right]\delta u\,\mathrm{d}V\mathrm{d}t = 0\end{aligned} \tag{A.263}$$

Next, integrating Equation (A.255) leads to

$$\left[\int_V \rho\dot{v}\delta v \mathrm{d}V\right]_{t_1}^{t_2} - \int_{t_1}^{t_2}\int_S \mathbf{d_v}\cdot\mathbf{n}\delta v \mathrm{d}S\mathrm{d}t - \int_{t_1}^{t_2}\int_V \left[\rho\ddot{v} - (\nabla\cdot\mathbf{d_v})\right]\delta v \mathrm{d}V\mathrm{d}t = 0 \tag{A.264}$$

and similarly, integrating Equation (A.257) produces

$$\left[\int_V \rho\dot{w}\delta w \mathrm{d}V\right]_{t_1}^{t_2} - \int_{t_1}^{t_2}\int_S \mathbf{d_w}\cdot\mathbf{n}\delta w \mathrm{d}S\mathrm{d}t - \int_{t_1}^{t_2}\int_V \left[\rho\ddot{w} - (\nabla\cdot\mathbf{d_w})\right]\delta w \mathrm{d}V\mathrm{d}t = 0 \tag{A.265}$$

Substituting for $\mathbf{d_v}$ and $\mathbf{n}$ in Equation (A.264) produces

$$\begin{aligned}\left[\int_V \rho\dot{v}\delta v \mathrm{d}V\right]_{t_1}^{t_2} - \int_{t_1}^{t_2}\int_S G[(u_{,y}+v_{,x})n_x + (v_{,z}+w_{,y})n_z]\delta v \mathrm{d}S\mathrm{d}t \\ - \int_{t_1}^{t_2}\int_V \left[\rho\ddot{v} - G(u_{,yx} + v_{,xx} + v_{,zz} + w_{,yz})\right]\delta v \mathrm{d}V\mathrm{d}t = 0\end{aligned} \tag{A.266}$$

and we can make use of Equations (A.241) and (A.249) in the above to get,

$$\begin{aligned}\left[\int_V \rho\dot{v}\delta v \mathrm{d}V\right]_{t_1}^{t_2} - \int_{t_1}^{t_2}\int_S G[(u_{,y}+v_{,x})n_x + (v_{,z}+w_{,y})n_z]\delta v \mathrm{d}S\mathrm{d}t \\ - \int_{t_1}^{t_2}\int_V \left[\rho\ddot{v} - G(v_{,xx} + v_{,zz} + (1-\frac{1}{\nu})v_{,yy})\right]\delta v \mathrm{d}V\mathrm{d}t = 0\end{aligned} \tag{A.267}$$

and similarly, for Equation (A.265), we get,

$$\begin{aligned}\left[\int_V \rho\dot{w}\delta w \mathrm{d}V\right]_{t_1}^{t_2} - \int_{t_1}^{t_2}\int_S G[(u_{,z}+w_{,x})n_x + (v_{,z}+w_{,y})n_y]\delta w \mathrm{d}S\mathrm{d}t \\ - \int_{t_1}^{t_2}\int_V \left[\rho\ddot{w} - G(w_{,xx} + w_{,yy} + (1-\frac{1}{\nu})w_{,zz})\right]\delta w \mathrm{d}V\mathrm{d}t = 0\end{aligned} \tag{A.268}$$

In summary, the governing equations are,

$$\rho\ddot{u} - (E-2G\nu)u_{,xx} - G(u_{,yy}+u_{,zz}) = 0 \tag{A.269}$$

$$\rho\ddot{v} - G(v_{,xx} + v_{,zz} + (1-\frac{1}{\nu})v_{,yy}) = 0 \tag{A.270}$$

$$\rho\ddot{w} - G(w_{,xx} + w_{,yy} + (1-\frac{1}{\nu})w_{,zz}) = 0 \tag{A.271}$$

The boundary conditions arising from the variations are,

$$\int_{t_1}^{t_2}\int_A Eu_{,x}\delta u \mathrm{d}A\mathrm{d}t\Big|_0^l = 0 \tag{A.272}$$

$$\int_{t_1}^{t_2}\int_S G\left[\left(v_{,x}+u_{,y}\right)n_y + \left(w_{,x}+u_{,z}\right)n_z\right]\delta u \mathrm{d}S\mathrm{d}t = 0 \tag{A.273}$$

$$\int_{t_1}^{t_2}\int_S G[(u_{,y}+v_{,x})n_x + (v_{,z}+w_{,y})n_z]\delta v \mathrm{d}S\mathrm{d}t = 0 \tag{A.274}$$

$$\int_{t_1}^{t_2}\int_S G[(u_{,z}+w_{,x})n_x + (v_{,z}+w_{,y})n_y]\delta w \mathrm{d}S\mathrm{d}t = 0 \tag{A.275}$$

and the initial conditions are deduced from,

$$\int_V \rho \ddot{u} \delta u \mathrm{d}V \Big|_{t_1}^{t_2} = 0 \tag{A.276}$$

$$\int_V \rho \ddot{v} \delta v \mathrm{d}V \Big|_{t_1}^{t_2} = 0 \tag{A.277}$$

$$\int_V \rho \ddot{w} \delta w \mathrm{d}V \Big|_{t_1}^{t_2} = 0 \tag{A.278}$$

APPENDIX

B Volume Integration of Variational Gradients

From Harris and Stocker [90], we have that

$$\nabla \cdot (s\mathbf{a}) = (\nabla s) \cdot \mathbf{a} + s\,(\nabla \cdot \mathbf{a}) \tag{B.1}$$

where s is a scalar field and $\mathbf{a}$ is a vector field. If we consider the scalar field to be $\delta\Phi$ we get,

$$\nabla \cdot (\mathbf{a}\delta\Phi) = (\nabla\delta\Phi) \cdot \mathbf{a} + (\nabla \cdot \mathbf{a})\,\delta\Phi \tag{B.2}$$

and integrating over the volume,

$$\int_V \nabla \cdot (\mathbf{a}\delta\Phi)\,\mathrm{d}V = \int_V (\nabla\delta\Phi) \cdot \mathbf{a}\,\mathrm{d}V + \int_V (\nabla \cdot \mathbf{a})\,\delta\Phi\,\mathrm{d}V \tag{B.3}$$

Using the divergence theorem, we can replace the left hand side with an integration over the surface S to get,

$$\int_S \mathbf{a} \cdot \mathbf{n}\delta\Phi\,\mathrm{d}S = \int_V (\nabla\delta\Phi) \cdot \mathbf{a}\,\mathrm{d}V + \int_V (\nabla \cdot \mathbf{a})\,\delta\Phi\,\mathrm{d}V \tag{B.4}$$

where $\mathbf{n}$ is the normal to the surface. Re-arranging terms, we get,

$$\int_V (\nabla\delta\Phi) \cdot \mathbf{a}\,\mathrm{d}V = \int_S \mathbf{a} \cdot \mathbf{n}\delta\Phi\,\mathrm{d}S - \int_V (\nabla \cdot \mathbf{a})\,\delta\Phi\,\mathrm{d}V \tag{B.5}$$

or alternatively,

$$\int_V \mathbf{a} \cdot (\nabla\delta\Phi)\,\mathrm{d}V = \int_S \mathbf{a} \cdot \mathbf{n}\delta\Phi\,\mathrm{d}S - \int_V (\nabla \cdot \mathbf{a})\,\delta\Phi\,\mathrm{d}V \tag{B.6}$$

APPENDIX

C Integration of ϕ over the cross-section

Recall from chapter 2, there are a number of equations involving ϕ given in Equations (2.23)–(2.25). These are,

$$P = \int_A \phi(y,z)^2 \mathrm{d}A \tag{C.1}$$

$$K = \int_A \left(\phi_{,y}(y,z)^2 + \phi_{,z}(y,z)^2\right) \mathrm{d}A \tag{C.2}$$

$$L_c = \int_A \left(y\phi_{,z}(y,z) - z\phi_{,y}(y,z)\right) \mathrm{d}A \tag{C.3}$$

In this appendix, we look at the integration of these over a rectangular cross-section. For a rectangular cross-section, if we assume a St. Venant warping function for ϕ, we get the equation given in Equation (A.130), which is restated below for convenience.

$$\phi(y,z) = yz - \sum_{n=0}^{\infty} \frac{8a^2(-1)^n \sin\left(\frac{(2n+1)\pi y}{a}\right) \sinh\left(\frac{(2n+1)\pi z}{a}\right)}{(2n+1)^3\pi^3 \cosh\left(\frac{1}{2}\frac{(2n+1)\pi b}{a}\right)} \tag{C.4}$$

Alternatively, this could be written as,

$$\phi(y,z) = yz - \sum_{n=0}^{\infty} C(n) f(n,y) g(n,z) \tag{C.5}$$

where,

$$C(n) = \frac{8a^2(-1)^n}{(2n+1)^3\pi^3 \cosh\left(\frac{1}{2}\frac{(2n+1)\pi b}{a}\right)} \tag{C.6}$$

$$f(n,y) = \sin\left(\frac{(2n+1)\pi y}{a}\right) \tag{C.7}$$

$$g(n,z) = \sinh\left(\frac{(2n+1)\pi z}{a}\right) \tag{C.8}$$

Therefore, $\phi_{,y}$ and $\phi_{,z}$ become,

$$\phi_{,y}(y,z) = z - \sum_{n=0}^{\infty} C(n) f_{,y}(n,y) g(n,z) \tag{C.9}$$

$$\phi_{,z}(y,z) = y - \sum_{n=0}^{\infty} C(n) f(n,y) g_{,z}(n,z) \tag{C.10}$$

and the derivatives of $f(n,y)$ and $g(n,z)$ are,

$$f_{,y}(n,y) = \frac{(2n+1)\pi}{a} \cos\left(\frac{(2n+1)\pi y}{a}\right) \tag{C.11}$$

$$g_{,z}(n,z) = \frac{(2n+1)\pi}{a} \cosh\left(\frac{(2n+1)\pi z}{a}\right) \tag{C.12}$$

C.1 Calculation of the P integral

Looking at the P integral in Equation (C.1) after substitution of Equation (C.5),

$$P = \int_{-b/2}^{b/2}\int_{-a/2}^{a/2} (yz - \sum_{n=0}^{\infty} C(n) f(n,y) g(n,z))^2 \mathrm{d}y\mathrm{d}z \tag{C.13}$$

$$= \int_{-b/2}^{b/2}\int_{-a/2}^{a/2} \left(y^2 z^2 - 2yz \sum_{n=0}^{\infty} C(n) f(n,y) g(n,z) + \sum_{n=0}^{\infty}\sum_{m=0}^{\infty} C(n)C(m) f(n,y) f(m,y) g(n,z) g(m,z) \right) \mathrm{d}y\mathrm{d}z \tag{C.14}$$

We can pull the sums and C factors out of the integral giving,

$$P = \int_{-b/2}^{b/2}\int_{-a/2}^{a/2} y^2 z^2 \mathrm{d}y\mathrm{d}z - 2\sum_{n=0}^{\infty} C(n) \int_{-b/2}^{b/2}\int_{-a/2}^{a/2} yz f(n,y) g(n,z) \mathrm{d}y\mathrm{d}z + \sum_{n=0}^{\infty}\sum_{m=0}^{\infty} C(n)C(m) \int_{-b/2}^{b/2}\int_{-a/2}^{a/2} f(n,y) f(m,y) g(n,z) g(m,z) \mathrm{d}y\mathrm{d}z \tag{C.15}$$

which can be written as,

$$P = \int_{-b/2}^{b/2} z^2 \int_{-a/2}^{a/2} y^2 \mathrm{d}y\mathrm{d}z - 2\sum_{n=0}^{\infty} C(n) \int_{-b/2}^{b/2} z g(n,z) \int_{-a/2}^{a/2} y f(n,y) \mathrm{d}y\mathrm{d}z + \sum_{n=0}^{\infty}\sum_{m=0}^{\infty} C(n)C(m) \int_{-b/2}^{b/2} g(n,z) g(m,z) \int_{-a/2}^{a/2} f(n,y) f(m,y) \mathrm{d}y\mathrm{d}z \tag{C.16}$$

Note that,

$$\int_{-a/2}^{a/2} f(n,y) f(m,y) \mathrm{d}y = 0 \quad \forall m \neq n \tag{C.17}$$

which allows us to simplify the integral for P to,

$$P = \int_{-b/2}^{b/2} z^2 \int_{-a/2}^{a/2} y^2 \mathrm{d}y\mathrm{d}z - 2\sum_{n=0}^{\infty} C(n) \int_{-b/2}^{b/2} z g(n,z) \int_{-a/2}^{a/2} y f(n,y) \mathrm{d}y\mathrm{d}z + \sum_{n=0}^{\infty} C(n)^2 \int_{-b/2}^{b/2} g(n,z)^2 \int_{-a/2}^{a/2} f(n,y)^2 \mathrm{d}y\mathrm{d}z \tag{C.18}$$

or alternatively (since f and g are independent of z and y respectively),

$$P = \int_{-b/2}^{b/2} z^2 \mathrm{d}z \int_{-a/2}^{a/2} y^2 \mathrm{d}y - 2\sum_{n=0}^{\infty} C(n) \int_{-b/2}^{b/2} z g(n,z) \mathrm{d}z \int_{-a/2}^{a/2} y f(n,y) \mathrm{d}y + \sum_{n=0}^{\infty} C(n)^2 \int_{-b/2}^{b/2} g(n,z)^2 \mathrm{d}z \int_{-a/2}^{a/2} f(n,y)^2 \mathrm{d}y \tag{C.19}$$

Since the individual integrals will reoccur in the other constants K and L_c, we will write this as,

$$P = P_1 - 2\sum_{n=0}^{\infty} C(n) G_{z1}(n) F_{y1}(n) + \sum_{n=0}^{\infty} C(n)^2 G_2(n) F_2(n) \tag{C.20}$$

where the individual constants/functions are,

$$P_1 = \int_{-b/2}^{b/2} z^2 \mathrm{d}z \int_{-a/2}^{a/2} y^2 \mathrm{d}y \tag{C.21}$$

$$G_{z1} = \int_{-b/2}^{b/2} z g(n,z) \mathrm{d}z \tag{C.22}$$

$$F_{y1} = \int_{-a/2}^{a/2} y f(n,y) \mathrm{d}y \tag{C.23}$$

$$G_2 = \int_{-b/2}^{b/2} g(n,z)^2 \mathrm{d}z \tag{C.24}$$

$$F_2 = \int_{-a/2}^{a/2} f(n,y)^2 \mathrm{d}y \tag{C.25}$$

The constant P_1 is,

$$P_1 = \int_{-b/2}^{b/2} z^2 \int_{-a/2}^{a/2} y^2 \mathrm{d}y \mathrm{d}z = \frac{a^3 b^3}{144} \tag{C.26}$$

Calculating the integral G_{z1},

$$G_{z1}(n) = \int_{-b/2}^{b/2} z g(n,z) \mathrm{d}z \tag{C.27}$$

$$= \frac{a}{(2n+1)^2 \pi^2} \left((2n+1)\pi b \cosh\left(\frac{1}{2} \frac{(2n+1)\pi b}{a} \right) - 2a \sinh\left(\frac{1}{2} \frac{(2n+1)\pi b}{a} \right) \right) \tag{C.28}$$

and the integral F_{y1},

$$F_{y1}(n) = \int_{-a/2}^{a/2} y f(n,y) \mathrm{d}y = \frac{2(-1)^n a^2}{\pi^2 (2n+1)^2} \tag{C.29}$$

The integral G_2 becomes,

$$G_2 = \int_{-b/2}^{b/2} g(n,z)^2 \mathrm{d}z \tag{C.30}$$

$$= \frac{1}{2(2n+1)\pi} \left(2a \cosh\left(\frac{1}{2} \frac{(2n+1)\pi b}{a} \right) \sinh\left(\frac{1}{2} \frac{(2n+1)\pi b}{a} \right) - \pi b (2n+1) \right) \tag{C.31}$$

and lastly, the integral $F_2(n)$ is,

$$F_2(n) = \int_{-a/2}^{a/2} f(n,y)^2 \mathrm{d}y = \frac{a}{2} \tag{C.32}$$

$$F_2 = \frac{a}{2} \tag{C.33}$$

which we note does not depend upon n. Finally, calculating $C(n)^2$,

$$C(n)^2 = \frac{64a^4}{(2n+1)^6\pi^6 \cosh^2\left(\frac{1}{2}\frac{(2n+1)\pi b}{a}\right)} \tag{C.34}$$

Now that all the functions of n are known, we can start substitution of their values into the individual terms of P. The second term of Equation (C.20) becomes,

$$-2\sum_{n=0}^{\infty} C(n)\frac{2(-1)^n a^3}{\pi^4(2n+1)^4}\left((2n+1)\pi b\cosh\left(\frac{1}{2}\frac{(2n+1)\pi b}{a}\right) - 2a\sinh\left(\frac{1}{2}\frac{(2n+1)\pi b}{a}\right)\right) \tag{C.35}$$

and after substitution of $C(n)$ from Equation (C.6),

$$-2\sum_{n=0}^{\infty} C(n)G_{z1}(n)F_{y1}(n) = -2\sum_{n=0}^{\infty}\frac{16(-1)^{2n}a^5}{\pi^7(2n+1)^7}\left((2n+1)\pi b - 2a\tanh\left(\frac{1}{2}\frac{(2n+1)\pi b}{a}\right)\right) \tag{C.36}$$

and since $(-1)^2 = 1$, this becomes,

$$-2\sum_{n=0}^{\infty} C(n)G_{z1}(n)F_{y1}(n) = -\frac{32a^5}{\pi^7}\sum_{n=0}^{\infty}\frac{1}{(2n+1)^7}\left((2n+1)\pi b - 2a\tanh\left(\frac{1}{2}\frac{(2n+1)\pi b}{a}\right)\right) \tag{C.37}$$

and the last term of Equation (C.20) is,

$$C(n)^2\frac{a}{4(2n+1)\pi}\left(2a\cosh\left(\frac{1}{2}\frac{(2n+1)\pi b}{a}\right)\sinh\left(\frac{1}{2}\frac{(2n+1)\pi b}{a}\right) - \pi b(2n+1)\right) \tag{C.38}$$

Substituting $C(n)^2$ from Equation (C.34),

$$\sum_{n=0}^{\infty} C(n)^2 G_2(n)F_2(n) = \frac{16a^5}{(2n+1)^7\pi^7}\left(2a\tanh\left(\frac{1}{2}\frac{(2n+1)\pi b}{a}\right) - \pi b(2n+1)\operatorname{sech}^2\left(\frac{1}{2}\frac{(2n+1)\pi b}{a}\right)\right) \tag{C.39}$$

Therefore, Equation (C.20) becomes,

$$\begin{aligned} P = \frac{a^3b^3}{144} &+ \frac{16a^5}{\pi^7}\sum_{n=0}^{\infty}\frac{2}{(2n+1)^7}\left(2a\tanh\left(\frac{1}{2}\frac{(2n+1)\pi b}{a}\right) - (2n+1)\pi b\right) \\ &+ \frac{1}{(2n+1)^7}\left(2a\tanh\left(\frac{1}{2}\frac{(2n+1)\pi b}{a}\right) - (2n+1)\pi b\operatorname{sech}^2\left(\frac{1}{2}\frac{(2n+1)\pi b}{a}\right)\right) \end{aligned} \tag{C.40}$$

after combining terms,

$$P = \frac{a^3b^3}{144} + \frac{16a^5}{\pi^7}\sum_{n=0}^{\infty}\frac{1}{(2n+1)^7}\left(6a\tanh\left(\frac{1}{2}\frac{(2n+1)\pi b}{a}\right) - (2n+1)\pi b\left(2 + \operatorname{sech}^2\left(\frac{1}{2}\frac{(2n+1)\pi b}{a}\right)\right)\right) \tag{C.41}$$

and expanding,

$$\boxed{P = \frac{a^3b^3}{144} + \frac{16a^5}{\pi^7}\left(\sum_{n=0}^{\infty}\frac{6a\tanh\left(\frac{1}{2}\frac{(2n+1)\pi b}{a}\right)}{(2n+1)^7} - 2\pi b\left(\sum_{n=0}^{\infty}\frac{1}{(2n+1)^6} - \sum_{n=0}^{\infty}\frac{\operatorname{sech}^2\left(\frac{1}{2}\frac{(2n+1)\pi b}{a}\right)}{(2n+1)^6}\right)\right)} \tag{C.42}$$

C.2 Calculation of the K integral

After substitution of Equation (C.5) into Equation (C.2),

$$\begin{aligned} K = &\int_A (y^2+z^2)\mathrm{d}A - 2\int_A \sum_{n=0}^{\infty} C(n)\left(z f_{,y}(n,y)g(n,z) + y f(n,y)g_{,z}(n,z)\right)\mathrm{d}A \\ &+ \int_A \sum_{n=0}^{\infty}\sum_{m=0}^{\infty} C(n)C(m)\left(f_{,y}(n,y)f_{,y}(m,y)g(n,z)g(m,z) + f(n,y)f(m,y)g_{,z}(n,z)g_{,z}(m,z)\right)\mathrm{d}A \end{aligned} \tag{C.43}$$

After factoring,

$$\begin{aligned} K = J_g &- 2\sum_{n=0}^{\infty} C(n)\left(\int_{-b/2}^{b/2} z g(n,z)\int_{-a/2}^{a/2} f_{,y}(n,y)\mathrm{d}y\mathrm{d}z + \int_{-b/2}^{b/2} g_{,z}(n,z)\int_{-a/2}^{a/2} y f(n,y)\mathrm{d}y\mathrm{d}z\right) \\ &+ \sum_{n=0}^{\infty}\sum_{m=0}^{\infty} C(n)C(m)\left(\int_{-b/2}^{b/2} g(n,z)g(m,z)\int_{-a/2}^{a/2} f_{,y}(n,y)f_{,y}(m,y)\mathrm{d}y\mathrm{d}z\right. \\ &\left.+ \int_{-b/2}^{b/2} g_{,z}(n,z)g_{,z}(m,z)\int_{-a/2}^{a/2} f(n,y)f(m,y)\mathrm{d}y\mathrm{d}z\right) \end{aligned} \tag{C.44}$$

Note that we have several integrals that have already been calculated. We can simplify this because,

$$\int_{-a/2}^{a/2} f_{,y}(n,y)f_{,y}(m,y)\mathrm{d}y = 0 \quad \forall m \neq n \tag{C.45}$$

Along with Equation (C.17), this allows us to reduce the integral to,

$$\begin{aligned} K = J_g &- 2\sum_{n=0}^{\infty} C(n)\left(\int_{-b/2}^{b/2} z g(n,z)\mathrm{d}z\int_{-a/2}^{a/2} f_{,y}(n,y)\mathrm{d}y + \int_{-b/2}^{b/2} g_{,z}(n,z)\mathrm{d}z\int_{-a/2}^{a/2} y f(n,y)\mathrm{d}y\right) \\ &+ \sum_{n=0}^{\infty} C(n)^2\left(\int_{-b/2}^{b/2} g(n,z)^2\mathrm{d}z\int_{-a/2}^{a/2} f_{,y}(n,y)^2\mathrm{d}y + \int_{-b/2}^{b/2} g_{,z}(n,z)^2\mathrm{d}z\int_{-a/2}^{a/2} f(n,y)^2\mathrm{d}y\right) \end{aligned} \tag{C.46}$$

Using the functions from before, this becomes,

$$K = J_g - 2\sum_{n=0}^{\infty} C(n)\left(G_{z1}(n)F_{y2}(n) + G_{z2}(n)F_{y1}(n)\right) + \sum_{n=0}^{\infty} C(n)^2\left(G_2(n)F_{2y}(n) + G_{2z}(n)F_2\right) \tag{C.47}$$

where the other functions are as follows,

$$F_{y2}(n) = \int_{-a/2}^{a/2} f_{,y}(n,y)\mathrm{d}y \tag{C.48}$$

$$G_{z2}(n) = \int_{-b/2}^{b/2} g_{,z}(n,z)\mathrm{d}z \tag{C.49}$$

$$F_{2y}(n) = \int_{-a/2}^{a/2} f_{,y}(n,y)^2\mathrm{d}y \tag{C.50}$$

$$G_{2y}(n) = \int_{-b/2}^{b/2} g_{,z}(n,z)^2\mathrm{d}z \tag{C.51}$$

Calculating the $F_{y2}(n)$ integral we get,

$$F_{y2}(n) = \int_{-a/2}^{a/2} f_{,y}(n,y)\mathrm{d}y = 2(-1)^n \tag{C.52}$$

and calculating $G_{z2}(n)$ gives,

$$G_{z2}(n) = \int_{-b/2}^{b/2} g_{,z}(n,z)\mathrm{d}z = 2\sinh\left(\frac{1}{2}\frac{(2n+1)\pi b}{a}\right) \tag{C.53}$$

The $F_{2y}(n)$ integral is,

$$F_{2y}(n) = \int_{-a/2}^{a/2} f_{,y}(n,y)^2\mathrm{d}y = \frac{\pi^2(2n+1)^2}{2a} \tag{C.54}$$

and the $G_{2y}(n)$ integral is,

$$G_{2y}(n) = \int_{-b/2}^{b/2} g_{,z}(n,z)^2\mathrm{d}z \tag{C.55}$$

$$= \frac{(2n+1)\pi}{2a^2}\left(2a\cosh\left(\frac{1}{2}\frac{(2n+1)\pi b}{a}\right)\sinh\left(\frac{1}{2}\frac{(2n+1)\pi b}{a}\right) + \pi b(2n+1)\right) \tag{C.56}$$

The first term in the first series of Equation (C.47) is,

$$G_{z1}(n)F_{y2}(n) = \frac{2a(-1)^n}{(2n+1)^2\pi^2}\left((2n+1)b\pi\cosh\left(\frac{1}{2}\frac{(2n+1)\pi b}{a}\right) - 2a\sinh\left(\frac{1}{2}\frac{(2n+1)\pi b}{a}\right)\right) \tag{C.57}$$

and the second term of that series is,

$$G_{z2}(n)F_{y1}(n) = \frac{4a^2(-1)^n\sinh\left(\frac{1}{2}\frac{(2n+1)\pi b}{a}\right)}{(2n+1)^2\pi^2} \tag{C.58}$$

Therefore, the first series is,

$$-2\sum_{n=0}^{\infty} C(n)\frac{2ab(-1)^n \cosh\left(\frac{1}{2}\frac{(2n+1)\pi b}{a}\right)}{(2n+1)\pi} \tag{C.59}$$

and after substitution of $C(n)$ Equation (C.59) becomes,

$$-\frac{32a^3b}{\pi^4}\sum_{n=0}^{\infty}\frac{1}{(2n+1)^4} \tag{C.60}$$

The first term in the second series of Equation (C.47) is,

$$G_2(n)F_{2y}(n) = \frac{(2n+1)\pi\left(2a\cosh\left(\frac{1}{2}\frac{(2n+1)\pi b}{a}\right)\sinh\left(\frac{1}{2}\frac{(2n+1)\pi b}{a}\right) - \pi b(2n+1)\right)}{4a} \tag{C.61}$$

and the second term in that series is,

$$G_{2z}(n)F_2(n) = \frac{(2n+1)\pi\left(2a\cosh\left(\frac{1}{2}\frac{(2n+1)\pi b}{a}\right)\sinh\left(\frac{1}{2}\frac{(2n+1)\pi b}{a}\right) + \pi b(2n+1)\right)}{4a} \tag{C.62}$$

Therefore, the second series of Equation (C.47) is,

$$\sum_{n=0}^{\infty} C(n)^2(2n+1)\pi\cosh\left(\frac{1}{2}\frac{(2n+1)\pi b}{a}\right)\sinh\left(\frac{1}{2}\frac{(2n+1)\pi b}{a}\right) \tag{C.63}$$

and after substitution for $C(n)^2$,

$$\frac{64a^4}{\pi^5}\sum_{n=0}^{\infty}\frac{\tanh\left(\frac{1}{2}\frac{(2n+1)\pi b}{a}\right)}{(2n+1)^5} \tag{C.64}$$

Therefore, K is,

$$\boxed{K = J_g - \frac{32a^3b}{\pi^4}\sum_{n=0}^{\infty}\frac{1}{(2n+1)^4} + \frac{64a^4}{\pi^5}\sum_{n=0}^{\infty}\frac{\tanh\left(\frac{1}{2}\frac{(2n+1)\pi b}{a}\right)}{(2n+1)^5}} \tag{C.65}$$

C.3 Calculation of the L_c integral

Lastly, when we substitute Equation (C.5) into Equation (C.3) we get,

$$L_c = \int_A \left((y^2-z^2) - \sum_{n=0}^{\infty} C(n)\left(yf(n,y)g_{,z}(n,z) - zf_{,y}(n,y)g(n,z)\right)\right)\mathrm{d}A \tag{C.66}$$

which upon expansion gives,

$$L_c = \int_A (y^2-z^2)\mathrm{d}A - \sum_{n=0}^{\infty} C(n)\left(\int_A yf(n,y)g_{,z}(n,z)\mathrm{d}A - \int_A zf_{,y}(n,y)g(n,z)\mathrm{d}A\right) \tag{C.67}$$

which can be expanded to,

$$L_c = \int_{-b/2}^{b/2}\int_{-a/2}^{a/2}(y^2-z^2)\mathrm{d}y\mathrm{d}z - \sum_{n=0}^{\infty} C(n)\left(\int_{-b/2}^{b/2} g_{,z}(n,z)\int_{-a/2}^{a/2} yf(n,y)\mathrm{d}y\mathrm{d}z \right.$$
$$\left. - \int_{-b/2}^{b/2} zg(n,z)\mathrm{d}z\int_{-a/2}^{a/2} f_{,y}(n,y)\mathrm{d}y\right) \tag{C.68}$$
$$= \int_{-b/2}^{b/2}\int_{-a/2}^{a/2}(y^2-z^2)\mathrm{d}y\mathrm{d}z - \sum_{n=0}^{\infty} C(n)\left(\int_{-b/2}^{b/2} g_{,z}(n,z)\mathrm{d}z\int_{-a/2}^{a/2} yf(n,y)\mathrm{d}y \right.$$
$$\left. - \int_{-b/2}^{b/2} zg(n,z)\mathrm{d}z\int_{-a/2}^{a/2} f_{,y}(n,y)\mathrm{d}y\right) \tag{C.69}$$

using the functions as defined earlier this becomes,

$$L_c = L_{c1} - \sum_{n=0}^{\infty} C(n)\left(G_{z2}(n)F_{y1}(n) - G_{z1}(n)F_{y2}(n)\right) \tag{C.70}$$

where L_{c1} is,

$$L_{c1} = \int_{-b/2}^{b/2}\int_{-a/2}^{a/2}(y^2-z^2)\mathrm{d}y\mathrm{d}z = \frac{ab(a^2-b^2)}{12} \tag{C.71}$$

and all the functions inside the series have been previously calculated. Therefore, L_c is,

$$L_c = \frac{ab(a^2-b^2)}{12} - \frac{2a}{\pi^2}\sum_{n=0}^{\infty} C(n)\frac{(-1)^n\left(4a\sinh\left(\frac{1}{2}\frac{(2n+1)\pi b}{a}\right) - \pi b(2n+1)\cosh\left(\frac{1}{2}\frac{(2n+1)\pi b}{a}\right)\right)}{(2n+1)^2} \tag{C.72}$$

and after substitution of $C(n)$ and simplification,

$$L_c = \frac{ab(a^2-b^2)}{12} - \frac{16a^3}{\pi^5}\sum_{n=0}^{\infty}\frac{4a\tanh\left(\frac{1}{2}\frac{(2n+1)\pi b}{a}\right) - \pi b(2n+1)}{(2n+1)^5} \tag{C.73}$$

and expanding,

$$\boxed{L_c = \frac{ab(a^2-b^2)}{12} + \frac{16a^3}{\pi^5}\left(\pi b\sum_{n=0}^{\infty}\frac{1}{(2n+1)^4} - 4a\sum_{n=0}^{\infty}\frac{\tanh\left(\frac{1}{2}\frac{(2n+1)\pi b}{a}\right)}{(2n+1)^5}\right)} \tag{C.74}$$

C.4 Convergence analysis of the integrals

From Equations (C.42), (C.65), and (C.74) we have the following solutions to the integrals,

$$P = \frac{a^3b^3}{144} + \frac{16a^5}{\pi^7}\left(\sum_{n=0}^{\infty}\frac{6a\tanh\left(\frac{1}{2}\frac{(2n+1)\pi b}{a}\right)}{(2n+1)^7} - 2\pi b\left(\sum_{n=0}^{\infty}\frac{1}{(2n+1)^6} - \sum_{n=0}^{\infty}\frac{\operatorname{sech}^2\left(\frac{1}{2}\frac{(2n+1)\pi b}{a}\right)}{(2n+1)^6}\right)\right) \tag{C.75}$$

$$K = J_g - \frac{32a^3b}{\pi^4}\sum_{n=0}^{\infty}\frac{1}{(2n+1)^4} + \frac{64a^4}{\pi^5}\sum_{n=0}^{\infty}\frac{\tanh\left(\frac{1}{2}\frac{(2n+1)\pi b}{a}\right)}{(2n+1)^5} \tag{C.76}$$

$$L_c = \frac{ab(a^2-b^2)}{12} + \frac{16a^3}{\pi^5}\left(\pi b\sum_{n=0}^{\infty}\frac{1}{(2n+1)^4} - 4a\sum_{n=0}^{\infty}\frac{\tanh\left(\frac{1}{2}\frac{(2n+1)\pi b}{a}\right)}{(2n+1)^5}\right) \tag{C.77}$$

Examining the tanh factor, we can write it as,

$$\tanh\left(\frac{1}{2}\frac{(2n+1)\pi b}{a}\right) = \tanh\left(\frac{1}{2}(2n+1)\pi\beta\right) \tag{C.78}$$

where $\beta = \frac{b}{a}$ which is the ratio of the height to the width of the cross-section. When $n = 0$ (part of the first term in the series) this becomes,

$$\tanh\left(\frac{\pi\beta}{2}\right) \tag{C.79}$$

and plotting we get Figures C.1 and C.2. Note that even for fairly low values of β this approaches 1. From the dimensions in Table 7.1 we get that $\beta \approx 31.46$ which leads to,

$$\tanh\left(\frac{\pi\beta}{2}\right) \approx 1 \tag{C.80}$$

to a high degree of precision.

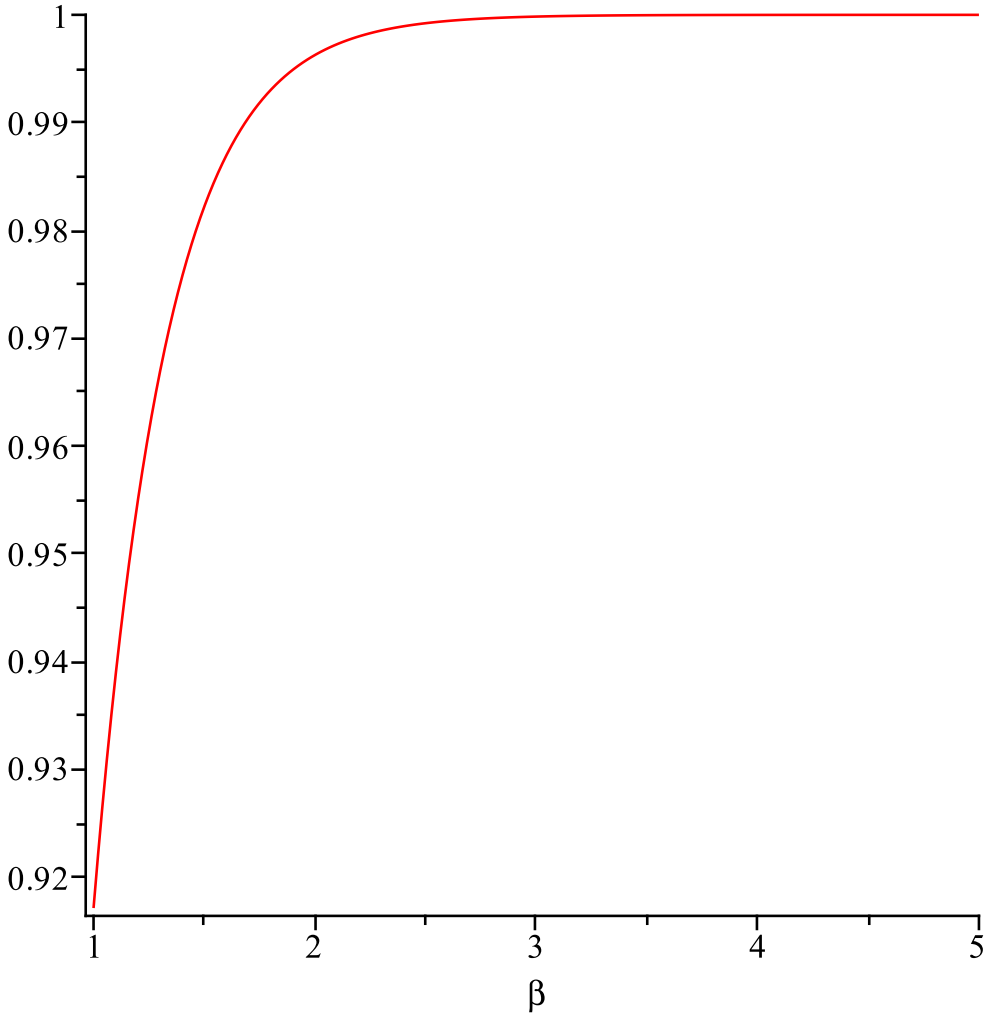

Figure C.1: tanh vs. β (β from 1 to 5)

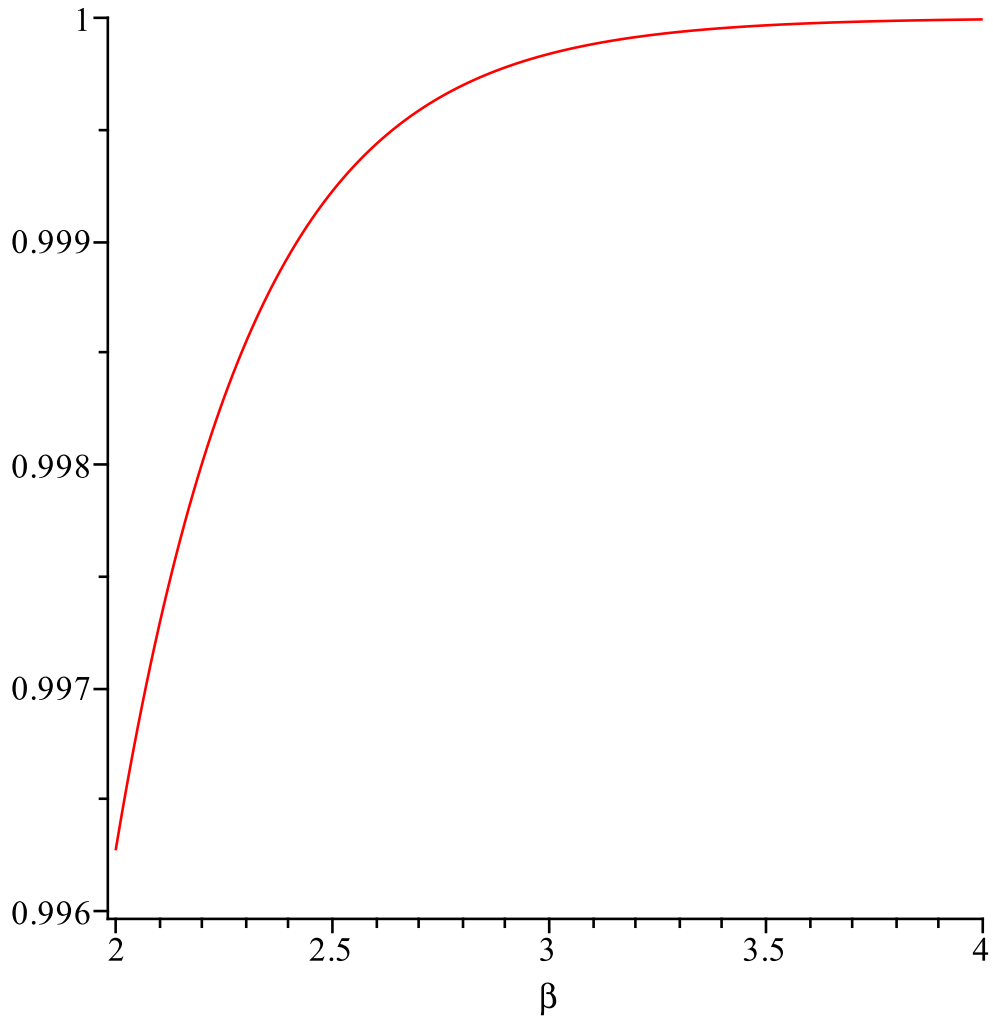

Figure C.2: tanh vs. β (β from 2 to 4)

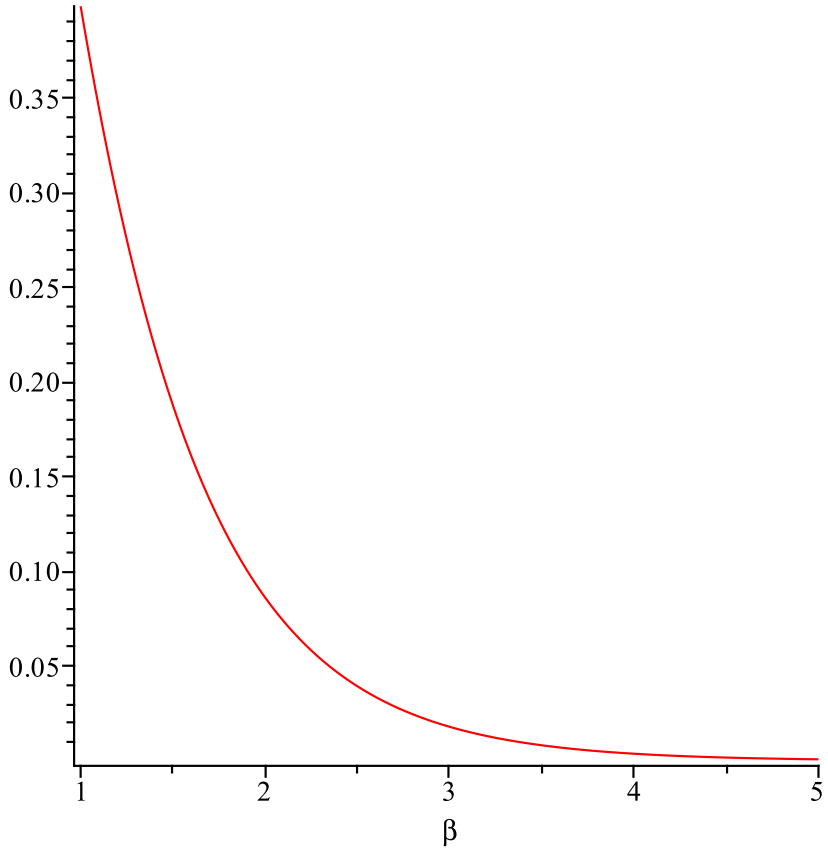

Figure C.3: sech^2 vs. β (β from 1 to 5)

Examining the sech^2 term,

$$\text{sech}^2\left(\frac{1}{2}\frac{(2n+1)\pi b}{a}\right) = \text{sech}^2\left(\frac{1}{2}(2n+1)\pi\beta\right) \tag{C.81}$$

and when $n = 0$,

$$\text{sech}^2\left(\frac{\pi\beta}{2}\right) \tag{C.82}$$

and plotting we get Figures C.3 and C.4.

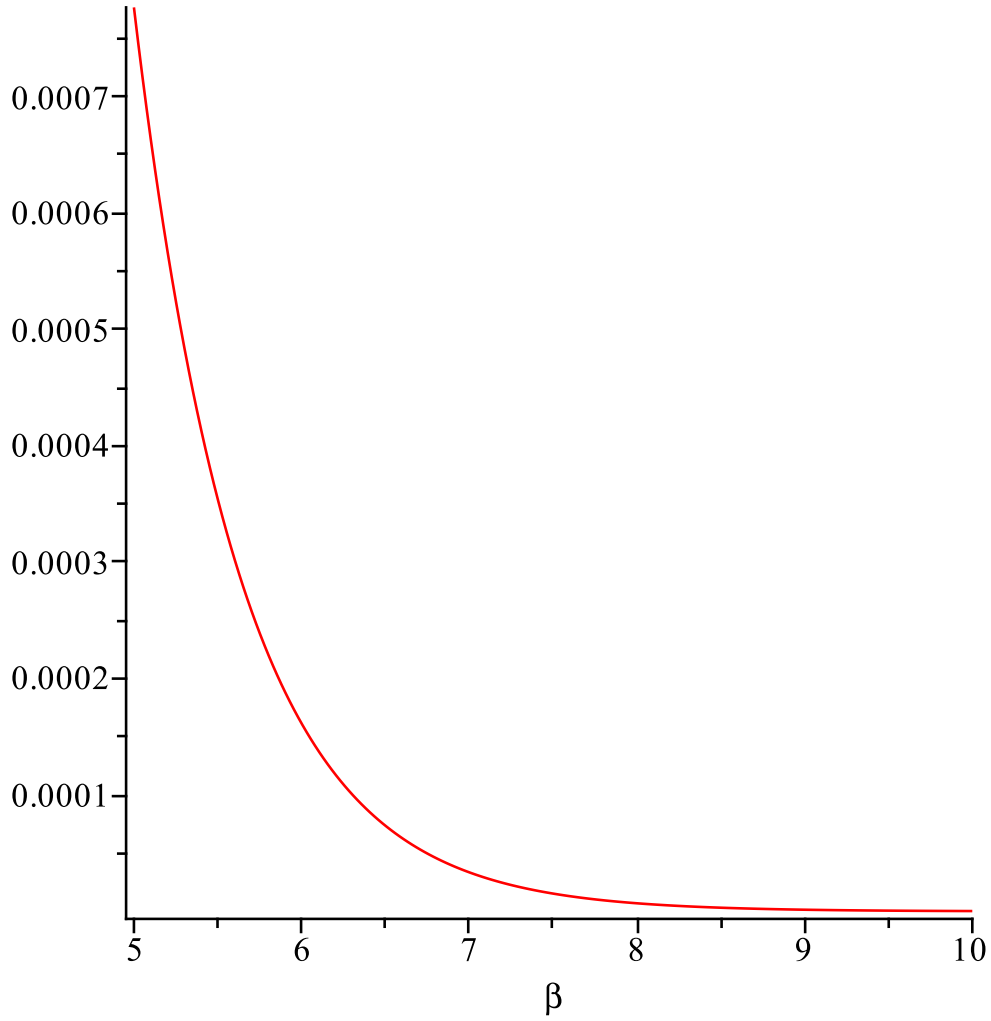

Figure C.4: sech^2 vs. β (β from 5 to 10)

We can see that it approaches 0 relatively quickly. For our given β, this becomes,

$$\operatorname{sech}^2\left(\frac{\pi\beta}{2}\right) \approx 0 \tag{C.83}$$

also to a high degree of precision. Therefore, that term can be safely eliminated from the series. So, making use of these results for tanh and sech^2, the solutions become,

$$P = \frac{a^3b^3}{144} + \frac{16a^5}{\pi^7}\left(6a\sum_{n=0}^{\infty}\frac{1}{(2n+1)^7} - 2\pi b\sum_{n=0}^{\infty}\frac{1}{(2n+1)^6}\right) \tag{C.84}$$

$$K = J_g - \frac{32a^3b}{\pi^4}\sum_{n=0}^{\infty}\frac{1}{(2n+1)^4} + \frac{64a^4}{\pi^5}\sum_{n=0}^{\infty}\frac{1}{(2n+1)^5} \tag{C.85}$$

$$L_c = \frac{ab(a^2-b^2)}{12} + \frac{16a^3}{\pi^5}\left(\pi b\sum_{n=0}^{\infty}\frac{1}{(2n+1)^4} - 4a\sum_{n=0}^{\infty}\frac{1}{(2n+1)^5}\right) \tag{C.86}$$

Recall from Equation (A.189) [89],

$$\sum_{n=0}^{\infty}\frac{1}{(2n+1)^m} = (-1+2^{-m})(-\zeta(m)) \tag{C.87}$$

where $\zeta(m)$ is the Riemann zeta function. Or alternatively,

$$\sum_{n=0}^{\infty}\frac{1}{(2n+1)^m} = \zeta(m)(1-2^{-m}) \tag{C.88}$$

This allows us to get analytical solutions for all the series (for cases when β is sufficiently large). Therefore, the solutions become,

$$P = \frac{a^3b^3}{144} + \frac{16a^5}{\pi^7}\left(6a\,\zeta(7)(1-2^{-7}) - 2\pi b\,\zeta(6)(1-2^{-6})\right) \tag{C.89}$$

$$K = J_g - \frac{32a^3b}{\pi^4}\,\zeta(4)(1-2^{-4}) + \frac{64a^4}{\pi^5}\,\zeta(5)(1-2^{-5}) \tag{C.90}$$

$$L_c = \frac{ab(a^2-b^2)}{12} + \frac{16a^3}{\pi^5}\left(\pi b\,\zeta(4)(1-2^4) - 4a\,\zeta(5)(1-2^{-5})\right) \tag{C.91}$$

For all cases where,

$$\tanh\left(\frac{\pi\beta}{2}\right) \approx 1, \qquad \operatorname{sech}^2\left(\frac{\pi\beta}{2}\right) \approx 0 \tag{C.92}$$

Therefore, these become,

$$P = \frac{a^3b^3}{144} + \frac{16a^5}{\pi^7}\left(6a\frac{127}{128}\,\zeta(7) - 2\pi b\frac{63}{64}\,\zeta(6)\right) \tag{C.93}$$

$$K = J_g - \frac{32a^3b}{\pi^4}\frac{15}{16}\,\zeta(4) + \frac{64a^4}{\pi^5}\frac{31}{32}\,\zeta(5) \tag{C.94}$$

$$L_c = \frac{ab(a^2-b^2)}{12} + \frac{16a^3}{\pi^5}\left(\pi b\frac{15}{16}\,\zeta(4) - 4a\frac{31}{32}\,\zeta(5)\right) \tag{C.95}$$

and simplifying,

$$P = \frac{a^3 b^3}{144} + \frac{a^5}{4\pi^7}\left(381 a\,\zeta(7) - 126\pi b\,\zeta(6)\right) \tag{C.96}$$

$$K = J_g + \frac{2a^3}{\pi^5}\left(31 a\,\zeta(5) - 15\pi b\,\zeta(4)\right) \tag{C.97}$$

$$L_c = \frac{ab(a^2 - b^2)}{12} + \frac{a^3}{\pi^5}\left(15\pi b\,\zeta(4) - 62 a\,\zeta(5)\right) \tag{C.98}$$

and for our particular values of a and b (from Table 7.1),

$$J_g = \frac{ab(a^2 + b^2)}{12} \approx 2.646 \times 10^{-7}\,\mathrm{m}^4 \tag{C.99}$$

$$P = \frac{a^3 b^3}{144} + \frac{a^5}{4\pi^7}\left(381 a\,\zeta(7) - 126\pi b\,\zeta(6)\right) \approx 2.212 \times 10^{-13}\,\mathrm{m}^4 \tag{C.100}$$

$$K = J_g + \frac{2a^3}{\pi^5}\left(31 a\,\zeta(5) - 15\pi b\,\zeta(4)\right) \approx 2.635 \times 10^{-7}\,\mathrm{m}^4 \tag{C.101}$$

$$L_c = \frac{ab(a^2 - b^2)}{12} + \frac{a^3}{\pi^5}\left(15\pi b\,\zeta(4) - 62 a\,\zeta(5)\right) \approx -2.635 \times 10^{-7}\,\mathrm{m}^4 \tag{C.102}$$

APPENDIX

D Example use of Symbolic-Numeric Finite Element Package

D.1 A Rotating 3D Timoshenko beam with a rigid body end-effector

Here we consider the specific case of the our system of interest which is a planar flexible single link with an end-effector. The basic configuration of the system is shown in Figure 3.3. The beam is modelled under the assumptions of Timoshenko beam theory, the torsion model as described in section 2.4, small strains, small deflections, and linear elastic materials.

Symbolic Computation Steps

We begin by loading the LinearAlgebra package, the SFEM package, and some utility functions.

```
restart; interface(imaginaryunit=_j): with(LinearAlgebra): with(SFEM):
read("tjlTools.mpl");
```

Next, we define a number of variables as shortcuts for various functions of the beam. These are used to simplify the writing of the kinetic and strain energies.

```
udot := diff(u(x,t),t):
vdot := diff(v(x,t),t):
wdot := diff(w(x,t),t):
dpsiz := diff(psi_z(x,t),t):
dpsix := diff(psi_x(x,t),t):
dpsiy := diff(psi_y(x,t),t):
dthetax := diff(theta_x(x,t),t):}
```

Now, defining end-effector variables,

```
ul := u(l,t):
vl := v(l,t):
wl := w(l,t):
psizl := psi_z(l,t):
psiyl := psi_y(l,t):
thetaxl := theta_x(l,t):
dthetaxl := diff(thetaxl,t):
dul := diff(ul,t):
dvl := diff(vl,t):
dwl := diff(wl,t):
dpsiyl := diff(psiyl,t):
dpsizl := diff(psizl,t):
```

and the angular velocity of the beam,

```
dtheta := diff(theta(t),t):
```

Definition of Lagrangian

From the previous chapter, the kinetic and strain energies are known for all parts of the system. Starting with the rotational kinetic energy of the end-effector,

```
Tre := 1/2*(Jexx*dthetaxl^2 + Jeyy*dpsiyl^2 + Jezz*(dpsizl+dtheta)^2)
+dthetaxl*(Jexy*dpsiyl + Jexz*(dtheta+dpsizl)) + Jeyz*dpsiyl(dtheta+dpsizl):
```

and the kinetic energy due to translation,

```
Kve1 := dul − dtheta*(vl+ de2 + psizl*de1 − thetaxl*de3) + dpsiyl*de3
− dpsizl*de2:
Kve2 := dvl + dpsizl*de1 − dthetaxl*de3 + dtheta*(l + ul + de1 − psizl*de2
+ psiyl*de3):
Kve3 := dwl − dpsiyl*de1 + dthetaxl*de2:
Tte := 1/2*(me+mt)*(Kve1^2+Kve2^2+Kve3^2):
```

Next, the kinetic energy of the beam due to extension, bending, and shear,

```
Txb := simplify(Int(1/2*(rhoA*((vdot+dtheta*(x+u(x,t)))^2
+(udot−dtheta*v(x,t))^2+wdot^2)
+rhoIyy*((dtheta+dpsiz)^2+dtheta^2*psi_z(x,t)^2)
+rhoIzz*(dpsiy^2+ dtheta^2*psi_y(x,t))),x)):
```

and the kinetic energy due to torsion,

```
Txt := simplify(1/2*Int(dtheta^2*(rhoP*psi_x(x,t)^2 + rhoIzz*theta(t)^2)
+rhoJg*dthetax^2+rhoP*dpsix^2,x)):
```

The kinetic energy of the motor is given by,

```
Tm := 1/2*Jm*diff(theta(t),t)^2:
```

Thus, the total kinetic energy is the sum of all three,

```
T_total := simplify(Tte + Tre + Txb + Txt + Tm):
```

The strain energy of the beam due to torsion is given as,

```
Uxt := 1/2*Int(E*P*diff(psi_x(x,t),x)^2 + G*(K*psi_x(x,t)^2
+2*Lc*diff(theta_x(x,t),x)*psi_x(x,t) + Jg*diff(theta_x(x,t),x)^2),x):
```

and the strain energy due to extension, bending, and shear,

```
Uxb := 1/2*Int(E*(A*diff(u(x,t),x)^2 + Iyy*diff(psi_z(x,t),x)^2
+ Izz*diff(psi_y(x,t),x)^2) +kGA*((diff(v(x,t),x)-psi_z(x,t))^2
+ (diff(w(x,t),x)-psi_y(x,t))^2),x):
```

Approximation

The functions to be approximated are as follows, $u(x,t)$, $v(x,t)$, $w(x,t)$, $\psi_x(x,t)$, $\psi_y(x,t)$, $\psi_z(x,t)$ and $\theta_x(x,t)$. We need C^0 functions for all functions. Since this is a beam, the variables v, w and ψ are best modelled with cubic basis functions and to prevent shear locking we will use cubic basis functions for u and θ_x as well.

```
approx_subs := map2(C0_Cubic_approx, phi,
[u(x,t),v(x,t),w(x,t), psi_x(x,t),psi_y(x,t),psi_z(x,t),theta_x(x,t)]):
```

The system variables for the approximations are,

```
approx_list := get_node_list(map(rhs,approx_subs)):
```

Defining the basis functions from x_1 to x_1+l_e, where l_e is the length of the element.

```
phi_bases := C0_Cubic_basis(phi,[x1,x1+1/3*l_e,x1+2/3*l_e,x1+l_e]):
```

Since both the first derivative of the basis functions will appear in the Lagrangian, we will calculate it.

```
dphi_bases := map(diff,phi_bases,x):
```

Therefore, the complete substitution list for the basis functions is,

```
full_phi_bases := [op(dphi_bases),op(phi_bases)]:
```

Euler-Lagrange Calculations

It is necessary to define the complete list of variables used in the problem. The augmented variables are the variables related to the coupling of the end effector and rotation. Since the theta equation is coupled directly to the spatial degrees of freedom (the elements), we place it last so we can easily separate the resulting mass and stiffness matrices into element matrices and a matrix of variables that only contribute once to the overall matrices.

```
augment_variables := [ul, vl, wl, psiyl, psizl, thetaxl, theta(t)]:
```

The complete set of all system variables is,

```
variables := ListTools[FlattenOnce](augment_variables,approx_list]):
```

Substitute the approximations into the Lagrangian,

```
Lagrange_subs := subs(approx_subs,Lagrangian):
```

The system accelerations are,

```
accel_var := map(diff,variables,t$2):
```

now we calculate the terms in the Euler-Lagrange equation.

```
(M_contrib, K_contrib) := EulerLagrange(Lagrange_subs,variables):
```

Simplification Procedures

Begin by using the small deflection assumption to eliminate the non-linear terms,

```
M_eq1 := map(update_integral_terms,M_contrib):
M_eq1 := map(update_integral_terms,M_eq1):
M_eq2 := map(linearize_expr,M_eq1):
K_eq1 := map(update_integral_terms,K_contrib):
K_eq1 := map(update_integral_terms,K_eq1):
K_eq2 := map(linearize_expr,K_eq1):
```

Note that `update_integral_terms` is called twice because sometimes new terms to be linearized are only found after the expansion. This is because sometimes Maple will create new integrals when expanding and sometimes not. Next, we eliminate all integrals with a zero integrand (since Maple doesn't eliminate inert integrals).

```
M_eq4 := map(replace_zero_integral,M_eq3):
K_eq3 := map(replace_zero_integral,K_eq2):
```

Evaluation of Integrals

Setting the bounds on the integrals, substitute for the basis functions and calculate the integrals. Note that material substitutions are an empty set. Since there are integrals that don't contain basis functions (*e.g.,* inertia of the beam) so they span the entire domain from 0 to L where L is the length of the beam.

```
mat_subs := []:

(M_expr,K_expr) := calculate_MK(M_eq4, K_eq3, full_phi_subs, mat_subs,
[x1, x1+l_e], [0,l]):
```

Note that some integrals will be just 1, so we simplify things by replacing them with L.

```
M_expr2 := map2(algsubs,Int(1, x)=l,M_expr):
K_expr2 := map2(algsubs,Int(1, x)=l,K_expr):
```

Formation of Element Matrices

Lastly, we can form the final element mass and stiffness matrices.

```
(M,b1) := GenerateMatrix(M_expr2,accel_var,outputoptions=[shape=symmetric]):
(K,b2) := GenerateMatrix(-K_expr2,variables,outputoptions=[shape=symmetric]):
```

The `b1` and `b2` vectors are all zero if the system is linear. These can be used to verify the linearization steps.

The first rows of both **M** and **K** do not depend upon the basis functions and don't need to be calculated on a per-element basis because they correspond to the augmented variables of the end-effector and the beam's angular rotation. So, we can separate each **M** and **K** matrix into two parts, one that only has to be calculated once and one that will be recalculated for each element. First, we determine the number of augmented variables,

```
naug := nops(augment_variables):
```

and the total number of variables,

```
nvars := nops(variables):
```

Therefore, the element mass matrix is,

```
M_reduced := SubMatrix(M, [naug...nvars],[naug...nvars]):
M_reduced[1,1] := 0:
```

and the contributions to the overall mass matrix due to the end-effector,

```
M_endconditions := SubMatrix(M,[1..naug],[1..naug]):
```

Similarly, we perform the same operations on the stiffness matrix, splitting it into element and global contributions.

```
K_reduced := SubMatrix(K, [naug...nvars],[naug...nvars]):
K_reduced[1,1] := 0:
K_endconditions := SubMatrix(K,[1..naug],[1..naug]):
```

We can now export the matrices to MATLAB, beginning with the element matrices.

```
matrix_to_MATLAB(M_reduced,M_elem,"M_elem.m");
matrix_to_MATLAB(K_reduced,K_elem,"K_elem.m");
```

Next, we export the auxiliary matrices,

```
matrix_to_MATLAB(M_endconditions,M_end,"M_end.m");
matrix_to_MATLAB(K_endconditions,K_end,"K_end.m");
```

The exported functions can now be called in Matlab by a global matrix assembly routine.

Numerical Computation Steps

There are three main stages to the numerical computation. First, the element mesh is defined and the software currently includes routines for setting up the necessary data structures for beams. Next, the global matrices for **M** and **K** are assembled as sparse matrices. Any boundary conditions are also applied at this stage. Lastly, the resulting ODE system is solved.

Definition of Element Mesh

We begin by setting up the basic data for the problem which means we need the number of nodes per element (`elem_nodes`), the number of degrees of freedom (DOF) per node (`node_dof`), the number of elements (`num_elem`), and the number of constrained nodes (`fixed_node`).

```
elem_nodes = 4;
node_dof = 7;
num_elem = 20;
fixed_node = 2;
```

Since we have an additional DOF (θ) that isn't directly associated with an individual element, we have an an "auxiliary node", that is associated with all elements. In our case, there is one auxiliary node (`aux_nodes`) and one variable (`aux_var`) per node.

```
aux_var = 1;
aux_nodes = 1;
aux_data = [aux_var,aux_nodes];
```

Now we can set up the element data structure (using `beam_elem_list`), and the nodal data (using `beam_node_list`). The `node_list` is a matrix of the nodal x coordinates and the number of DOF for that node. The `dof_list` is a column matrix containing the the starting DOF for that node which will aid in the assembly process. Note that the `beam_dimension` contains the starting and ending global x coordinates for the beam $(0, L)$.

```
elem_list = beam_elem_list(num_elem,elem_nodes,aux_nodes);
beam_dimension = [0, l];
[node_list,dof_list] = beam_node_list(elem_list, node_dof, ...
                                      beam_dimension, aux_data);
```

Matrix Assembly

The functions `K_elem` and `M_elem` are the functions to create the element stiffness and mass matrices respectively. They are the output of the symbolic steps. However, since the parameters vary depending upon the particular problem, these two lines are particular to that problem. They are called by the assembly routine for each element. Any parameters that are unique to a particular element are part of `elem_param` and these are then evaluated and passed to the element matrix routines during the assembly process.

```
Kfunc = 'K_elem(A, E, G, Iyy, Izz, Jg, Kt, Lc, P, kGA, l_e)';
Mfunc = 'M_elem(l_e, rhoA, rhoIyy, rhoIzz, rhoJg, rhoP, x1)';
elem_param = {'x1 = elem(2,1);' 'l_e = elem(end,1)-x1;'};
[K,M] = fe_assembly(elem_list, node_list, dof_list, ...
                    aux_nodes, Kfunc, Mfunc, elem_param);
```

Next, we augment the **K** and **M** matrices with the contributions from the end-effector. In this case, there are only contributions to the **M** matrix.

```
theta_dof = 1;
last_node = elem_list(end,end);
psiy_dof = dof_list(last_node)+1;
psiz_dof = psiy_dof+1;
thetax_dof = psiz_dof+1;
u_dof = thetax_dof+1;
v_dof = u_dof+1;
w_dof = v_dof+1;
aug_list = [u_dof,v_dof,w_dof,psiy_dof,psiz_dof,thetax_dof,theta_dof];
M_aug = M_end(Jexx, Jexy, Jexz, Jeyy, Jezz, Jm, Jtxx, Jtyy, Jtzz,
del, l, me, mt, rhoA, rhoIyy);
```

```
for i = 1:length(aug_list)
        f_r = aug_list(i);
        for j = 1:length(aug_list)
                f_c = aug_list(j);
                M(f_r,f_c) = M(f_r,f_c) + M_aug(i,j);
        end
end
```

Lastly, we apply any constraints to the system. In this case, we have that the beam is clamped at the motor $x = 0$ which fixes the first two nodes. Then, we create a new node list without these nodes.

```
[K,M] = constrain_node(fixed_node,dof_list,node_list,K,M);
node_list_new = node_list;
node_list_new(fixed_node,:) = [];
dof_list_new = ones(length(dof_list)-1,1);
dof_list_new(2:end) = cumsum(node_list_new(:,end))+1;
```

ODE System Solution

Once the **K** and **M** matrices have been determined, we then need to find the damping matrix (and the applied force vector). Since this is a second order system of ODEs and all the matrices are constant in time, we can solve the resulting system by using a Newmark-Beta method. This is considerably faster than using a solver like Matlab's `ode15s`.

```
[t,u,v,a] = newmark_beta(M,K,C,R,beta,gamma,tstart,tstop, ...
                                        u0,v0,accel0,h);
```

Full details on the determination of the damping matrix are in Chapter 6 and details on the Newmark-Beta method are found in Chapter 4.

APPENDIX

E Jourdain's Variational Principle and Impact

Examining Jourdain's Variational Principle (JVP) [28] for impact problems as done in Bahar [29] we have,

$$\sum_{i=1}^{n}\left[\frac{\mathrm{d}}{\mathrm{d}t}\left(\frac{\partial T}{\partial \dot{q}_i}\right)-\frac{\partial T}{\partial q_i}-Q_i\right]\delta\dot{q}_i=0 \tag{E.1}$$

For impact problems, we are looking at an instant in time since this is an impulsive process. We will denote t^- as the time right before impact and t^+ as the time right after impact. These are assumed to be infinitesimally close to each other. Bahar [29] states,

> "The integral with respect to time of the second term of equation (1) can be shown to vanish through the use of the mean value theorem of integral calculus. This result is also obvious on physical grounds, as the gradient of the kinetic energy with respect to configurational coordinates that remain constant during the impulsive process is zero."

where equation (1) that Bahar refers to is Equation (E.1). However, for rotating frames it is possible to have kinetic energy terms where a velocity (*i.e.*, $\dot{\theta}$) is multiplied by a displacement (*e.g.*, $\overline{v}$). For example, even in the simplest model of the end effector (2D Point Mass), we get the kinetic energy as given in Equation (3.67),

$$T_e=\frac{1}{2}m_e\left((\dot{\overline{v}}_L+\dot{\overline{v}}'_L d_{e1})+(L+d_{e1})\dot{\theta}\right)^2+\frac{1}{2}m_e(\overline{v}_L+\overline{v}'_L d_{e1})^2\dot{\theta}^2 \tag{E.2}$$

Note the last term includes $\frac{1}{2}m_e\dot{\theta}^2\overline{v}_L^2$ which will not have a zero gradient. Therefore, the second sentence in the above quotation is incorrect. So, let us check Bahar's work for the first sentence of the quotation. Given Equation (E.1) and integrate it over an impulse interval $[t^-,t^+]$ to find

$$\int_{t^-}^{t^+}\sum_{i}^{n}\left[\frac{\mathrm{d}}{\mathrm{d}t}\left(\frac{\partial T}{\partial \dot{q}_i}\right)-\frac{\partial T}{\partial q_i}-Q_i\right]\delta\dot{q}_i\mathrm{d}t=0 \tag{E.3}$$

Taking each term separately,

$$\int_{t^-}^{t^+} \sum_i^n \left[\frac{\mathrm{d}}{\mathrm{d}t} \left(\frac{\partial T}{\partial \dot{q}_i} \right) \right] \delta \dot{q}_i \mathrm{d}t = \sum_i^n \int_{t^-}^{t^+} \mathrm{d} \left(\frac{\partial T}{\partial \dot{q}_i} \right) \delta \dot{q}_i \tag{E.4}$$

$$= \sum_i^n \left(p^+ - p^- \right) \delta \dot{q}_i \tag{E.5}$$

which is the change in momentum over $[t^-, t^+]$. For the second term

$$- \int_{t^-}^{t^+} \sum_i^n \left[\frac{\partial T}{\partial q_i} \right] \delta \dot{q}_i \mathrm{d}t = - \sum_i^n \int_{t^-}^{t^+} \left[\frac{\partial T}{\partial q_i} \right] \mathrm{d}t \, \delta \dot{q}_i \tag{E.6}$$

we note that under the assumptions of a Jourdain variation $\delta q_i = 0$ or the configuration variables are assumed to be held constant so $\partial q_i = 0$ and because $\partial T \nrightarrow \infty$ the Mean Value Theorem of integral calculus yields

$$- \sum_i^n \int_{t^-}^{t^+} \left[\frac{\partial T}{\partial q_i} \right] \mathrm{d}t \delta \dot{q}_i = - \sum_i^n \underbrace{(t^+ - t^-)}_{\to 0} \underbrace{\left[\frac{\partial T}{\partial q_i} \right]_{t_0}}_{constant} \delta \dot{q}_i \tag{E.7}$$

$$= - \sum_i^n (0) \delta \dot{q}_i \tag{E.8}$$

where t_0 is a point in the time interval $[t^-, t^+]$. In the case of the last term it's easiest to see if we re-write it using an impulse function and the total impulse $\hat{Q}_i = \int_{t^-}^{t^+} Q_i \mathrm{d}t$ supplied by the external force Q_i

$$- \int_{t^-}^{t^+} \sum_i^n \left[Q_i \right] \delta \dot{q}_i \mathrm{d}t = - \sum_i^n \int_{t^-}^{t^+} Q_i \mathrm{d}t \delta \dot{q}_i \tag{E.9}$$

$$= - \sum_i^n \int_{t^-}^{t^+} \hat{Q}_i \delta (t - t_0) \mathrm{d}t \, \delta \dot{q}_i \tag{E.10}$$

$$= - \sum_i^n \hat{Q}_i \, \delta \dot{q}_i \tag{E.11}$$

So, no assumption about the q_i or $\dot{q}_i$ dependence of T is necessary for the second term to integrate to zero. Note that it also doesn't require that the gradient with respect to configurational coordinates to be zero.

APPENDIX

F Capture Dynamics of a 2D Euler-Bernoulli Beam

F.1 Post-Capture Velocity Constraint

Modelling the capture process as a plastic collision, from Section 5.1, we get that the velocities before and after impact must be equivalent. Therefore, our velocity constraint is that after capture the target velocity and end effector velocities have to match. The target velocity is given in equation (3.4) as

$$\underset{\sim}{v}_t = \underset{\sim}{\mathcal{F}}_a^T \begin{bmatrix} \dot{x}_t \\ \dot{y}_t \\ 0 \end{bmatrix} \tag{F.1}$$

and the end effector velocity is given in equation (3.66) as

$$\underset{\sim}{v}_e = \underset{\sim}{\mathcal{F}}_a^T \begin{bmatrix} -\dot{\theta}(\overline{v}_L + \overline{v}'_L d_{e1})\cos\theta - \left(\dot{\overline{v}}_L + d_{e1}\dot{\overline{v}}'_L + \dot{\theta}(L+d_{e1})\right)\sin\theta \\ \left(\dot{\overline{v}}_L + d_{e1}\dot{\overline{v}}'_L + \dot{\theta}(L+d_{e1})\right)\cos\theta - \dot{\theta}(\overline{v}_L + \overline{v}'_L d_{e1})\sin\theta \\ 0 \end{bmatrix} \tag{F.2}$$

Since they are both defined in the same frame, we can equate components resulting in the following constraints.

$$\dot{x}_t + \dot{\theta}(\overline{v}_L + \overline{v}'_L d_{e1})\cos\theta + \left(\dot{\overline{v}}_L + d_{e1}\dot{\overline{v}}'_L + \dot{\theta}(L+d_{e1})\right)\sin\theta = 0 \tag{F.3}$$

$$\dot{y}_t - \left(\dot{\overline{v}}_L + d_{e1}\dot{\overline{v}}'_L + \dot{\theta}(L+d_{e1})\right)\cos\theta + \dot{\theta}(\overline{v}_L + \overline{v}'_L d_{e1})\sin\theta = 0 \tag{F.4}$$

Since we are considering the impact duration to be infinitesimal, all position variables can be replaced with their value at impact ($\theta = \theta(t_1)$, $\overline{v}_L = \overline{v}_L(t_1)$, $\overline{v}'_L = \overline{v}'_L(t_1)$) which we will denote as θ_0, $\overline{v}_{L0}$, and $\overline{v}'_{L0}$ respectively. Hence, equations (F.3) and (F.4) become

$$\dot{x}_t + \dot{\theta}(\overline{v}_{L0} + \overline{v}'_{L0} d_{e1})\cos\theta_0 + \left(\dot{\overline{v}}_L + d_{e1}\dot{\overline{v}}'_L + \dot{\theta}(L+d_{e1})\right)\sin\theta_0 = 0 \tag{F.5}$$

$$\dot{y}_t - \left(\dot{\overline{v}}_L + d_{e1}\dot{\overline{v}}'_L + \dot{\theta}(L+d_{e1})\right)\cos\theta_0 + \dot{\theta}(\overline{v}_{L0} + \overline{v}'_{L0} d_{e1})\sin\theta_0 = 0 \tag{F.6}$$

F.2 Quasi-Velocities

We convert the velocities ($\dot{\overline{v}}_L$, $\dot{\overline{v}}'_L$, $\dot{\overline{v}}(x,t)$, $\dot{x}_t$, $\dot{y}_t$) to quasi-velocities $\dot{\mathcal{Q}}_i$. The quasi-velocities $\dot{\mathcal{Q}}_5$ and $\dot{\mathcal{Q}}_6$ are defined by the left hand side of Equations (F.5) and (F.6) respectively, *i.e.,*

$$\dot{\mathcal{Q}}_5 = \dot{x}_t + \dot{\theta}(\overline{v}_{L0} + \overline{v}'_{L0} d_{e1})\cos\theta_0 + \left(\dot{\overline{v}}_L + d_{e1}\dot{\overline{v}}'_L + \dot{\theta}(L + d_{e1})\right)\sin\theta_0 \tag{F.7}$$

$$\dot{\mathcal{Q}}_6 = \dot{y}_t - \left(\dot{\overline{v}}_L + d_{e1}\dot{\overline{v}}'_L + \dot{\theta}(L + d_{e1})\right)\cos\theta_0 + \dot{\theta}(\overline{v}_{L0} + \overline{v}'_{L0} d_{e1})\sin\theta_0 \tag{F.8}$$

The remaining quasi-velocities are set equal to the Lagrangian velocities as shown in Equations (F.9) through (F.12).

$$\dot{\mathcal{Q}}_1 = \quad \dot{\overline{v}}_L \tag{F.9}$$

$$\dot{\mathcal{Q}}_2 = \quad \dot{\overline{v}}'_L \tag{F.10}$$

$$\dot{\mathcal{Q}}_3 = \quad \dot{\overline{v}}(x,t) \tag{F.11}$$

$$\dot{\mathcal{Q}}_4 = \quad \dot{\theta} \tag{F.12}$$

We then substitute these quasi-velocities into Equations (F.7) and (F.8) to get the constraint quasi-velocties, $\dot{\mathcal{Q}}_5$ and $\dot{\mathcal{Q}}_6$ strictly in terms of $\dot{x}_t$, $\dot{y}_t$, and $\dot{\mathcal{Q}}_{i=1,2,3,4}$.

$$\dot{\mathcal{Q}}_5 = \dot{x}_t + \dot{\mathcal{Q}}_4(\overline{v}_{L0} + \overline{v}'_{L0} d_{e1})\cos\theta_0 + \left(\dot{\mathcal{Q}}_1 + d_{e1}\dot{\mathcal{Q}}_2 + \dot{\mathcal{Q}}_4(L + d_{e1})\right)\sin\theta_0 \tag{F.13}$$

$$\dot{\mathcal{Q}}_6 = \dot{y}_t - \left(\dot{\mathcal{Q}}_1 + d_{e1}\dot{\mathcal{Q}}_2 + \dot{\mathcal{Q}}_4(L + d_{e1})\right)\cos\theta_0 + \dot{\mathcal{Q}}_4(\overline{v}_{L0} + \overline{v}'_{L0} d_{e1})\sin\theta_0 \tag{F.14}$$

F.3 Quasi-Kinetic Energy

Since we know that the velocity of the target mass is given by:

$$\underline{v}_t = \underline{\underline{\mathcal{F}}}_a^T \begin{bmatrix} \dot{x}_t \\ \dot{y}_t \\ 0 \end{bmatrix} \tag{F.15}$$

we need to rewrite Equations (F.13) and (F.14) to isolate $\dot{x}_t$ and $\dot{y}_t$.

$$\dot{x}_t = \dot{\mathcal{Q}}_5 - \dot{\mathcal{Q}}_4(\overline{v}_{L0} + \overline{v}'_{L0} d_{e1})\cos\theta_0 - \left(\dot{\mathcal{Q}}_1 + d_{e1}\dot{\mathcal{Q}}_2 + \dot{\mathcal{Q}}_4(L + d_{e1})\right)\sin\theta_0 \tag{F.16}$$

$$\dot{y}_t = \dot{\mathcal{Q}}_6 + \left(\dot{\mathcal{Q}}_1 + d_{e1}\dot{\mathcal{Q}}_2 - \dot{\mathcal{Q}}_4(L + d_{e1})\right)\cos\theta_0 - \dot{\mathcal{Q}}_4(\overline{v}_{L0} + \overline{v}'_{L0} d_{e1})\sin\theta_0 \tag{F.17}$$

The kinetic energy for the target becomes

$$\begin{aligned} T_t^* \quad &= \quad \frac{1}{2} m_t \left(\dot{\mathcal{Q}}_5 - \dot{\mathcal{Q}}_4(\overline{v}_{L0} + \overline{v}'_{L0} d_{e1})\cos\theta_0 - \left(\dot{\mathcal{Q}}_1 + d_{e1}\dot{\mathcal{Q}}_2 + \dot{\mathcal{Q}}_4(L + d_{e1})\right)\sin\theta_0\right)^2 \\ &+ \quad \frac{1}{2} m_t \left(\dot{\mathcal{Q}}_6 + \left(\dot{\mathcal{Q}}_1 + d_{e1}\dot{\mathcal{Q}}_2 + \dot{\mathcal{Q}}_4(L + d_{e1})\right)\cos\theta_0 - \dot{\mathcal{Q}}_4(\overline{v}_{L0} + \overline{v}'_{L0} d_{e1})\sin\theta_0\right)^2 \end{aligned} \tag{F.18}$$

The velocity of the end effector mass (in terms of quasi-velocities) is

$$\underset{\sim}{v}_e = \underset{\rightarrow}{\mathscr{F}}_a^T \begin{bmatrix} -\dot{\mathscr{Q}}_4(\overline{v}_{L0} + \overline{v}'_{L0} d_{e1})\cos\theta_0 - \left(\dot{\mathscr{Q}}_1 + d_{e1}\dot{\mathscr{Q}}_2 + \dot{\mathscr{Q}}_4(L+d_{e1})\right)\sin\theta_0 \\ \left(\dot{\mathscr{Q}}_1 + d_{e1}\dot{\mathscr{Q}}_2 + \dot{\mathscr{Q}}_4(L+d_{e1})\right)\cos\theta_0 - \dot{\mathscr{Q}}_4(\overline{v}_{L0} + \overline{v}'_{L0} d_{e1})\sin\theta_0 \\ 0 \end{bmatrix} \tag{F.19}$$

leading to the following for the kinetic energy of the end effector mass

$$\begin{aligned} T_e^* &= \frac{1}{2} m_e \left(-\dot{\mathscr{Q}}_4(\overline{v}_{L0} + \overline{v}'_{L0} d_{e1})\cos\theta_0 - \left(\dot{\mathscr{Q}}_1 + d_{e1}\dot{\mathscr{Q}}_2 + \dot{\mathscr{Q}}_4(L+d_{e1})\right)\sin\theta_0\right)^2 \\ &+ \frac{1}{2} m_e \left(\left(\dot{\mathscr{Q}}_1 + d_{e1}\dot{\mathscr{Q}}_2 - \dot{\mathscr{Q}}_4(L+d_{e1})\right)\cos\theta_0 - \dot{\mathscr{Q}}_4(\overline{v}_{L0} + \overline{v}'_{L0} d_{e1})\sin\theta_0\right)^2 \end{aligned} \tag{F.20}$$

Calculating the kinetic energy due to flexibility of the beam,

$$T_b^* = \frac{1}{2}\int_0^L \rho A(\underset{\sim}{v}_x \cdot \underset{\sim}{v}_x)\mathrm{d}x \tag{F.21}$$

where $\underset{\sim}{v}_x$ is given by,

$$\underset{\sim}{v}_x = \underset{\rightarrow}{\mathscr{F}}_a^T \begin{bmatrix} -\left(\dot{\mathscr{Q}}_3 + x\dot{\mathscr{Q}}_4\right)\sin\theta_0 - \dot{\mathscr{Q}}_4(y + \overline{v}_0)\cos\theta_0 \\ \left(\dot{\mathscr{Q}}_3 + x\dot{\mathscr{Q}}_4\right)\cos\theta_0 - \dot{\mathscr{Q}}_4(y + \overline{v}_0)\sin\theta_0 \\ 0 \end{bmatrix} \tag{F.22}$$

which is simplified from Equation (3.19) since the $\overline{v}'$ terms are ignored the kinetic energy of an Euler-Bernoulli beam. Which, when substituted into equation (F.21), results in

$$T_b^* = \frac{1}{2}\int_0^L \rho A(x^2\dot{\mathscr{Q}}_4^2 + 2x\dot{\mathscr{Q}}_4\dot{\mathscr{Q}}_3 + \dot{\mathscr{Q}}_3^2 + \dot{\mathscr{Q}}_4^2\overline{v}_0^2)\mathrm{d}x + \frac{1}{2}\int_0^L \rho I_{yy}\dot{\mathscr{Q}}_4^2\mathrm{d}x \tag{F.23}$$

The only remaining term in the kinetic energy of the system is due to the inertia of the motor:

$$T_r^* = \frac{1}{2} J_m \dot{\mathscr{Q}}_4^2 \tag{F.24}$$

Adding the kinetic energy contributions from Equations (F.18), (F.20), (F.23), and (F.24) leads to the total kinetic energy of the system.

$$\begin{aligned} T^* = &\frac{1}{2} J_m \dot{\mathscr{Q}}_4^2 + \frac{1}{2}\int_0^L \rho A(x^2\dot{\mathscr{Q}}_4^2 + 2x\dot{\mathscr{Q}}_4\dot{\mathscr{Q}}_3 + \dot{\mathscr{Q}}_3^2 + \dot{\mathscr{Q}}_4^2\overline{v}_0^2)\mathrm{d}x + \frac{1}{2}\int_0^L \rho I_{yy}\dot{\mathscr{Q}}_4^2\mathrm{d}x \\ &+ \frac{1}{2} m_t \left(\dot{\mathscr{Q}}_5 - \dot{\mathscr{Q}}_4(\overline{v}_{L0} + \overline{v}'_{L0} d_{e1})\cos\theta_0 - \left(\dot{\mathscr{Q}}_1 + d_{e1}\dot{\mathscr{Q}}_2 + \dot{\mathscr{Q}}_4(L+d_{e1})\right)\sin\theta_0\right)^2 \\ &+ \frac{1}{2} m_t \left(\dot{\mathscr{Q}}_6 + \left(\dot{\mathscr{Q}}_1 + d_{e1}\dot{\mathscr{Q}}_2 + \dot{\mathscr{Q}}_4(L+d_{e1})\right)\cos\theta_0 - \dot{\mathscr{Q}}_4(\overline{v}_{L0} + \overline{v}'_{L0} d_{e1})\sin\theta_0\right)^2 \\ &+ \frac{1}{2} m_e \left(-\dot{\mathscr{Q}}_4(\overline{v}_{L0} + \overline{v}'_{L0} d_{e1})\cos\theta_0 - \left(\dot{\mathscr{Q}}_1 + d_{e1}\dot{\mathscr{Q}}_2 + \dot{\mathscr{Q}}_4(L+d_{e1})\right)\sin\theta_0\right)^2 \\ &+ \frac{1}{2} m_e \left(\left(\dot{\mathscr{Q}}_1 + d_{e1}\dot{\mathscr{Q}}_2 + \dot{\mathscr{Q}}_4(L+d_{e1})\right)\cos\theta_0 - \dot{\mathscr{Q}}_4(\overline{v}_{L0} + \overline{v}'_{L0} d_{e1})\sin\theta_0\right)^2 \end{aligned} \tag{F.25}$$

F.4 Generalised Quasi-Momenta

To form the variational equation, we need the derivatives of the kinetic energy with respect to each of the quasi-velocities. The derivative of the kinetic energy with respect to $\dot{\mathcal{Q}}_1$ (the generalised quasi-momentum of $\dot{\mathcal{Q}}_1$) is

$$\frac{\partial T^*}{\partial \dot{\mathcal{Q}}_1} = (m_t + m_e)\left(\dot{\mathcal{Q}}_1 + \dot{\mathcal{Q}}_4(L + d_{e1}) + \dot{\mathcal{Q}}_2 d_{e1}\right) + m_t(\dot{\mathcal{Q}}_6 \cos\theta_0 - \dot{\mathcal{Q}}_5 \sin\theta_0) \tag{F.26}$$

The $\dot{\mathcal{Q}}_2$ generalised quasi-momentum is

$$\frac{\partial T^*}{\partial \dot{\mathcal{Q}}_2} = d_{e1}\left((m_t + m_e)\left(\dot{\mathcal{Q}}_1 + \dot{\mathcal{Q}}_4(L + d_{e1}) + \dot{\mathcal{Q}}_2 d_{e1}\right) + m_t\left(\dot{\mathcal{Q}}_6 \cos\theta_0 - \dot{\mathcal{Q}}_5 \sin\theta_0\right)\right) \tag{F.27}$$

and the $\dot{\mathcal{Q}}_3$ quasi-momentum is

$$\frac{\partial T^*}{\partial \dot{\mathcal{Q}}_3} = \int_0^L \rho A\left(\dot{\mathcal{Q}}_3 + x\dot{\mathcal{Q}}_4\right) \mathrm{d}x \tag{F.28}$$

The $\dot{\mathcal{Q}}_4$ generalised quasi-momentum is given by

$$\begin{aligned}
\frac{\partial T^*}{\partial \dot{\mathcal{Q}}_4} &= (m_t + m_e)\left(\dot{\mathcal{Q}}_4\left((L + d_{e1})^2 + (\overline{v}'_{L0} d_{e1} + \overline{v}_{L0})^2\right) + \dot{\mathcal{Q}}_1(L + d_{e1}) + \dot{\mathcal{Q}}_2(L d_{e1} + d_{e1}^2)\right) \\
&+ J_m \dot{\mathcal{Q}}_4 + \int_0^L \rho A\left((x^2 + \overline{v}_0(x)^2)\dot{\mathcal{Q}}_4 + x\dot{\mathcal{Q}}_3\right) \mathrm{d}x + \int_0^L \rho I_{yy} \dot{\mathcal{Q}}_4 \mathrm{d}x \\
&+ m_t\left(\dot{\mathcal{Q}}_6\left((L + d_{e1})\cos\theta_0 - (\overline{v}'_{L0} d_{e1} + \overline{v}_{L0})\sin\theta_0\right)\right. \\
&- \left.\dot{\mathcal{Q}}_5\left((\overline{v}'_{L0} d_{e1} + \overline{v}_{L0})\cos\theta_0 + (L + d_{e1})\sin\theta_0\right)\right)
\end{aligned} \tag{F.29}$$

The quasi-velocities $\dot{\mathcal{Q}}_5$ and $\dot{\mathcal{Q}}_6$ are constrained and as such, these quasi-momenta do not need to be calculated.

F.5 Velocity Relations

The results from Equations (F.26) through (F.29) are used in the equation

$$\sum_{i=1}^{6}\left(\frac{\partial T}{\partial \dot{\mathcal{Q}}_i}^{+} - \frac{\partial T}{\partial \dot{\mathcal{Q}}_i}^{-}\right)\delta\dot{\mathcal{Q}}_i = 0 \tag{F.30}$$

which relates the post-impact quasi-velocities to the pre-impact quasi-velocities. Note that no quasi-impulse is shown since the impulse due to the applied moment will be zero (because the impact is instantaneous). As discussed in chapter 5, the variations with respect to the constrained quasi-velocities will be zero whereas the other variations must be non-zero. Therefore, we are left with equations for $\dot{\mathcal{Q}}_1$, $\dot{\mathcal{Q}}_2$, $\dot{\mathcal{Q}}_3$, and $\dot{\mathcal{Q}}_4$. The equation arising from $\dot{\mathcal{Q}}_1$ (tip deflection rate) is

$$\begin{aligned}
(m_t + m_e)\left(\dot{\mathcal{Q}}_1^+ + \dot{\mathcal{Q}}_4^+(L + d_{e1}) + \dot{\mathcal{Q}}_2^+ d_{e1}\right) = &(m_t + m_e)\left(\dot{\mathcal{Q}}_1^- + \dot{\mathcal{Q}}_4^-(L + d_{e1}) + \dot{\mathcal{Q}}_2^- d_{e1}\right) \\
&+ m_t\left(\dot{\mathcal{Q}}_6^- \cos\theta_0 - \dot{\mathcal{Q}}_5^- \sin\theta_0\right)
\end{aligned} \tag{F.31}$$

Note that $\dot{\mathcal{Q}}_5^-$ and $\dot{\mathcal{Q}}_6^-$ are calculated by evaluating Equations (F.13) and (F.14) at the time instant before impact. The equation arising from $\dot{\mathcal{Q}}_2$ (tip rotation rate) is

$$\begin{aligned} d_{e1}(m_t+m_e)\left(\dot{\mathcal{Q}}_1^+ + \dot{\mathcal{Q}}_4^+(L+d_{e1}) + \dot{\mathcal{Q}}_2^+ d_{e1}\right) = & d_{e1}(m_t+m_e)\left(\dot{\mathcal{Q}}_1^- + \dot{\mathcal{Q}}_4^-(L+d_{e1}) + \dot{\mathcal{Q}}_2^- d_{e1}\right) \\ & + d_{e1} m_t\left(\dot{\mathcal{Q}}_6^- \cos\theta_0 - \dot{\mathcal{Q}}_5^- \sin\theta_0\right) \end{aligned} \tag{F.32}$$

Note that these two equations are only different by a factor of d_{e1}. Therefore, they are not independent and we can find that,

$$\dot{\mathcal{Q}}_2^+ = \frac{\dot{\mathcal{Q}}_1^+}{d_{e1}} \tag{F.33}$$

The equation arising from $\dot{\mathcal{Q}}_3$ (beam deflection rate) is

$$\int_0^L \rho A\left(\dot{\mathcal{Q}}_3^+ + x\dot{\mathcal{Q}}_4^+\right)\mathrm{d}x = \int_0^L \rho A\left(\dot{\mathcal{Q}}_3^- + x\dot{\mathcal{Q}}_4^-\right)\mathrm{d}x \tag{F.34}$$

and the equation arising from $\dot{\mathcal{Q}}_4$ (beam rotation rate) is,

$$\begin{aligned} & J_m\dot{\mathcal{Q}}_4^+ + (m_t+m_e)\left(\left((\overline{v}'_{L0}d_{e1}+\overline{v}_{L0})^2 + (L+d_{e1})^2\right)\dot{\mathcal{Q}}_4^+ + (L+d_{e1})\dot{\mathcal{Q}}_1^+ + (d_{e1}^2+Ld_{e1})\dot{\mathcal{Q}}_2^+\right) \\ & + \int_0^L \rho A\left((x^2+\overline{v}_0(x)^2)\dot{\mathcal{Q}}_4^+ + x\dot{\mathcal{Q}}_3^+\right)\mathrm{d}x + \int_0^L \rho I_{yy}\dot{\mathcal{Q}}_4^+\mathrm{d}x \\ & = J_m\dot{\mathcal{Q}}_4^- + (m_t+m_e)\left(\left((\overline{v}'_{L0}d_{e1}+\overline{v}_{L0})^2 + (L+d_{e1})^2\right)\dot{\mathcal{Q}}_4^- + (L+d_{e1})\dot{\mathcal{Q}}_1^- + (d_{e1}^2+Ld_{e1})\dot{\mathcal{Q}}_2^-\right) \\ & + \int_0^L \rho A\left((x^2+\overline{v}_0(x)^2)\dot{\mathcal{Q}}_4^- + x\dot{\mathcal{Q}}_3^-\right)\mathrm{d}x + \int_0^L \rho I_{yy}\dot{\mathcal{Q}}_4^-\mathrm{d}x \\ & + m_t\left(\left((L+d_{e1})\cos\theta_0 - (\overline{v}_{L0}+d_{e1}\overline{v}'_{L0})\sin\theta_0\right)\dot{\mathcal{Q}}_6^- - \left((\overline{v}_{L0}+d_{e1}\overline{v}'_{L0})\cos\theta_0 + (L+d_{e1})\sin\theta_0\right)\dot{\mathcal{Q}}_5^-\right) \end{aligned} \tag{F.35}$$

Substituting the pre-impact constraint relations into Equations (F.31) through (F.35) leads to the following equations (after converting to true velocities).

$$(m_t+m_e)\left(\dot{\overline{v}}_L^+ + (L+d_{e1})\dot{\theta}^+ + d_{e1}\dot{\overline{v}}'^+_L\right) = m_e\left(\dot{\overline{v}}_L^- + (L+d_{e1})\dot{\theta}^- + d_{e1}\dot{\overline{v}}'^-_L\right) + m_t\left(\dot{y}_t^-\cos\theta_0 - \dot{x}_t^-\sin\theta_0\right) \tag{F.36}$$

$$\dot{\overline{v}}'^+_L = \frac{\dot{\overline{v}}_L^+}{d_{e1}} \tag{F.37}$$

$$\int_0^L \rho A\left(\dot{\overline{v}}^+ + x\dot{\theta}^+\right)\mathrm{d}x = \int_0^L \rho A\left(\dot{\overline{v}}^- + x\dot{\theta}^-\right)\mathrm{d}x \tag{F.38}$$

$$\begin{aligned} & J_m\dot{\theta}^+ + (m_t+m_e)\left(\left((\overline{v}'_{L0}d_{e1}+\overline{v}_{L0})^2 + (L+d_{e1})^2\right)\dot{\theta}^+ + (L+d_{e1})\dot{\overline{v}}_L^+ + (Ld_{e1}+d_{e1}^2)\dot{\overline{v}}'^+_L\right) \\ & + \int_0^L \rho\left(A\left((\overline{v}_0(x)^2+x^2)\dot{\theta}^+ + x\dot{\overline{v}}^+\right) + I_{yy}\dot{\theta}^+\right)\mathrm{d}x \\ & = J_m\dot{\theta}^- + m_e\left(\left((\overline{v}'_{L0}d_{e1}+\overline{v}_{L0})^2 + (L+d_{e1})^2\right)\dot{\theta}^- + (L+d_{e1})\dot{\overline{v}}_L^- + (Ld_{e1}+d_{e1}^2)\dot{\overline{v}}'^-_L\right) \\ & + \int_0^L \rho\left(A\left((x^2+\overline{v}_0(x)^2)\dot{\theta}^- + x\dot{\overline{v}}^-\right) + I_{yy}\dot{\theta}^-\right)\mathrm{d}x \\ & + m_t\left(\left((L+d_{e1})\cos\theta_0 - (\overline{v}_{L0}+\overline{v}'_{L0}d_{e1})\sin\theta_0\right)\dot{y}_t^- - \left((\overline{v}_{L0}+\overline{v}'_{L0}d_{e1})\cos\theta_0 + (L+d_{e1})\sin\theta_0\right)\dot{x}_t^-\right) \end{aligned} \tag{F.39}$$

The integrals in Equation (F.38) are both over the same domain so we can equate the integrands and isolate $\dot{\overline{v}}(x)^+$ to get the relation between the beam deflection rate before and after impact.

$$\dot{\overline{v}}(x)^+ = \dot{\overline{v}}(x)^- + x(\dot{\theta}^+ - \dot{\theta}^-) \tag{F.40}$$

Substituting this relation into the angular velocity relation (Equation (F.39)) results in the elimination of a number of terms inside the integrals,

$$\begin{aligned}
&J_m\dot{\theta}^+ + (m_t + m_e)\left(\left(\overline{v}'_{L0}d_{e1} + \overline{v}_{L0}\right)^2 + \left(L + d_{e1}\right)^2\right)\dot{\theta}^+ + \left(L + d_{e1}\right)\dot{\overline{v}}_L^+ + \left(Ld_{e1} + d_{e1}^2\right)\dot{\overline{v}}'^+_L\Big) \\
&+ \int_0^L \rho\left(A\overline{v}_0(x)^2 + I_{yy}\right)\dot{\theta}^+ \mathrm{d}x \\
&= J_m\dot{\theta}^- + m_e\Big(\left(\overline{v}'_{L0}d_{e1} + \overline{v}_{L0}\right)^2 + \left(L + d_{e1}\right)^2\Big)\dot{\theta}^- + \left(L + d_{e1}\right)\dot{\overline{v}}_L^- + \left(Ld_{e1} + d_{e1}^2\right)\dot{\overline{v}}'^-_L\Big) \\
&+ \int_0^L \rho\left(A\overline{v}_0(x)^2 + I_{yy}\right)\dot{\theta}^- \mathrm{d}x + m_t\Big(\left(\left(L + d_{e1}\right)\cos\theta_0 - \left(\overline{v}_{L0} + \overline{v}'_{L0}d_{e1}\right)\sin\theta_0\right)\dot{y}_t^- \\
&- \left(\left(\overline{v}_{L0} + \overline{v}'_{L0}d_{e1}\right)\cos\theta_0 + \left(L + d_{e1}\right)\sin\theta_0\right)\dot{x}_t^-\Big)
\end{aligned} \tag{F.41}$$

Isolating $\dot{\overline{v}}_L^+$ in Equation (F.36) leads to the following equation.

$$\dot{\overline{v}}_L^+ = \frac{m_e\left(\dot{\overline{v}}_L^- + \left(L + d_{e1}\right)\dot{\theta}^- + d_{e1}\dot{\overline{v}}'^-_L\right) + m_t\left(\dot{y}_t^-\cos\theta_0 - \dot{x}_t^-\sin\theta_0\right) - \left(m_e + m_t\right)\left(L + d_{e1}\right)\dot{\theta}^+}{2\left(m_t + m_e\right)} \tag{F.42}$$

Since the angular velocity relation and the tip deflection relation are coupled, solve the linear system of equations (F.42) and (F.41) to decouple $\dot{\theta}^+$. This yields

$$\dot{\theta}^+ = \frac{\left(J_m + m_e(\overline{v}'_{L0}d_{e1} + \overline{v}_{L0})^2 + \int_0^L \rho\left(A\overline{v}_0(x)^2 + I_{yy}\right)\mathrm{d}x\right)\dot{\theta}^- - m_t(\overline{v}'_{L0}d_{e1} + \overline{v}_{L0})(\dot{x}_t^-\cos\theta_0 + \dot{y}_t^-\sin\theta_0)}{J_m + (m_e + m_t)(\overline{v}'_{L0}d_{e1} + \overline{v}_{L0})^2 + \int_0^L \rho\left(A\overline{v}_0(x)^2 + I_{yy}\right)\mathrm{d}x} \tag{F.43}$$

The result of this equation can then be used in Equations (F.42), (F.37), and (F.40) to solve for the new system velocities.

Bibliography

[1] Rhody, B. J., 1992. "Dynamics and control of mass capture by a single-link flexible arm robot". Master's thesis, Systems Design Engineering, University of Waterloo.

[2] Ewins, D. J., 1986. *Modal Testing: Theory and Practice*. No. 2 in Engineering Dynamics Series. Research Studies Press Ltd., Taunton, Somerset, England.

[3] Kövecses, J., Fenton, R., and Cleghorn, W., 1998. "Impulsive motion of a single flexible robot link". In Proceedings of the IASTED International Conference on Robotics and Manufacturing, M. Hamza, ed., pp. 38–40.

[4] Kövecses, J., and Cleghorn, W. L., 2003. "Finite and impulsive motion of constrained mechanical systems via Jourdain's principle: discrete and hybrid parameter models". *International Journal of Non-Linear Mechanics,* ***38***, pp. 935–956.

[5] Yoshida, K., Kurazume, R., Sashida, N., and Umetani, Y., 1992. "Modeling of collision dynamics for space free-floating links with extended generalized inertia tensor". In Proc. IEEE Conf. on Robotics & Automation, pp. 899–904.

[6] Yoshida, K., 1993. "Space structure capturing and assembling by experimental free-floating robot satellite simulators". In Proc. 2nd Intl. Conf. on Dynamics & Control of Structures in Space, pp. 141–160.

[7] Bellezza, F., Lanari, L., and Ulivi, G., 1990. "Exact modeling of the flexible slewing link". In Proc. IEEE Int. Conf. on Robotics and Automation.

[8] Bruch, J., and Mitchell, T., 1987. "Vibrations of a mass-loaded clamped-free Timoshenko beam". *Journal of Sound and Vibration,* ***114***(2), pp. 341–345.

[9] Goldsmith, W., 1960. *Impact: The Theory and Physical Behaviour of Colliding Solids*. Edward Arnold, London.

[10] Lee, E., 1940. "The impact of a mass striking a beam". *Journal of Applied Mechanics*, December, pp. A–129–A–137.

[11] Yigit, A., 1994. "The effect of flexibility on the impact response of a two-link rigid-flexible manipulator". *Journal of Sound and Vibration*, pp. 349–361.

[12] Gau, W., and Shabana, A., 1995. "Use of the finite element method in the analysis of impact-induced longitudinal waves in constrained elastic systems". *Journal of Mechanical Design,* ***117***(2), pp. 336–342.

[13] Shabana, A. A., 1993. "Propagation of impact-induced longitudinal waves in mechanical systems with variable kinematic structure". *Journal of Vibration and Acoustics,* ***115***(1), pp. 1–8.

[14] Rismantab-Sany, J., and Shabana, A., 1990. "On the use of the momentum balance in the impact analysis of constrained elastic systems". *Journal of Vibration and Acoustics,* ***112***, January, pp. 119–126.

[15] Rismantab-Sany, J., and Shabana, A., 1988. "Impulsive motion of non-holonomic deformable multibody systems part i: Kinematic and dynamic equations". *Journal of Sound and Vibration,* ***127***(2), pp. 193–204.

[16] Shabana, A. A., 1988. "Impulsive motion of non-holonomic deformable multibody systems part ii: Impact analysis". *Journal of Sound and Vibration,* ***127***(2), pp. 205–219.

[17] Hsu, W. C., and Shabana, A. A., 1993. "Finite element analysis of impact-induced transverse waves in rotating beams". *Journal of Sound and Vibration,* ***168***(2), pp. 355–369.

[18] Palas, H., Hsu, W. C., and Shabana, A., 1992. "On the use of momentum balance and the assumed modes method in transverse impact problems". *Journal of Vibration and Acoustics,* ***114***(3), pp. 364–373.

[19] Hwang, K., and Shabana, A., 1995. "Effect of mass capture on the propagation of transverse waves in rotating beams". *Journal of Sound and Vibration,* ***186***(3), pp. 495–525.

[20] Yoshida, K., and Sashida, N., 1993. "Modeling of impact dynamics and impulse minimization for space robots". In Proc. IEEE/RSJ Conf. on Intel. Robots & Systems, pp. 2064–2069.

[21] Chapnik, B., Heppler, G., and Aplevich, J., 1990. "Controlling the impact response of a one-link robotic arm". In Proceedings of the 1990 IEEE International Conference on Robotics and Automation, IEEE, pp. 1444–1449.

[22] Chapnik, B., Heppler, G., and Aplevich, J., 1991. "Modeling impact on a one-link flexible robotic arm". *IEEE Transactions on Robotics and Automation,* ***7***(4), August, pp. 479–488.

[23] Kövecses, J., Fenton, R., and Cleghorn, W. L., 1997. "A dynamic analysis for robotic interception of a moving target". In 8th International Conference on Advanced Robotics, IEEE, pp. 493–498.

[24] Kövecses, J., Fenton, R., and Cleghorn, W. L., 1997. "Effects of robotic interception of a moving target considering manipulator flexibility". In Proceedings The Second World Congress on Intelligent Manufacturing, L. Monostori, ed., pp. 497–508.

[25] Kövecses, J., Fenton, R., and Cleghorn, W., 1997. "Dynamic simulation of a structurally flexible manipulator intercepting and capturing a moving object". In Fifth Applied Mechanisms and Robotics Conference.

[26] Kövecses, J., Fenton, R., and Cleghorn, W., 1999. "Dynamic modeling and analysis of a robot manipulator intercepting and capturing a moving object, with the consideration of structural flexibility". *Multibody Systems Dynamics,* ***3***, pp. 137–162.

[27] Kövecses, J., Fenton, R., and Cleghorn, W., 1999. "A dynamic performance evaluation model for target capture by robot mechanisms, with the consideration of structural flexibility". In Proceedings of the 1999 ASME Design Engineering Technical Conference, ASME, pp. 1–12.

[28] Jourdain, P. E., 1909. "Note on an analogue of Gauss' principle of least constraint". *Quarterly Journal of Pure and Applied Mathematics,* ***40***, pp. 153–157.

[29] Bahar, L. Y., 1994. "On The Use of Quasi-Velocities In Impulsive Motion". *International Journal of Engineering Science,* ***32***(11), pp. 1669–1686.

[30] Baruh, H., 1999. *Analytical Dynamics.* Mc-Graw Hill, New York.

[31] Sokolnikoff, I. S., 1956. *Mathematical Theory of Elasticity.* McGraw-Hill, New York.

[32] Timoshenko, S., 1958. *Strength of Materials Part II Advanced Theory and Problems*, 3rd ed. Van Nostrand Reinhold Company, New York.

[33] Rivello, R. M., 1969. *Theory and Analysis of Flight Structures.* McGraw-Hill, New York.

[34] Carnegie, W., 1959. "Vibrations of pre-twisted cantilever blading". *Proceedings of the Institution of Mechanical Engineers,* ***173***(12), pp. 343–374.

[35] Carnegie, W., 1962. "Vibrations of pre-twisted cantilever blading: An additional effect due to torsion". *Proceedings of the Institution of Mechanical Engineers,* ***176***(13), pp. 315–322.

[36] Carnegie, W., 1964. "Vibrations of pre-twisted cantilever blading allowing for rotary inertia and shear deflection". *Journal of Mechanical Engineering Science,* ***6***(2), pp. 105–109.

[37] Carnegie, W., and Thomas, J., 1972. "The effects of shear deformation and rotary inertia on the lateral frequencies of cantilever beams in bending". *Journal of Engineering for Industry,* ***94***(1), February, pp. 267–278.

[38] Dokumaci, E., 1987. "An exact solution for coupled bending and torsion vibrations of uniform beams having single cross-sectional symmetry". *Journal of Sound and Vibration,* ***119***(3), pp. 443–449.

[39] Banerjee, J. R., 2000. "Explicit modal analysis of an axially loaded timoshenko beam with bending-torsion coupling". *Journal of Applied Mechanics,* ***67***, June, pp. 307–313.

[40] Reissner, E., 1952. "On non-uniform torsion of cylindrical rods". *Journal of Mathematics and Physics,* ***XXXI***, pp. 214–221.

[41] Barr, A. D. S., 1962. "Torsional waves in uniform rods of non-circular cross-section". *Journal of Mechanical Engineering Science,* ***4***(2), pp. 127–135.

[42] Ritchie, S. J. K., and Leevers, P. S., 1999. "Non-uniform and dynamic torsion of elastic beams part 1: governing equations and particular solutions". *Journal of Strain Analysis,* ***34***(5), September, pp. 303–311.

[43] Ritchie, S. J. K., and Leevers, P. S., 1999. "Non-uniform and dynamic torsion of elastic beams part 2: the double torsion test". *Journal of Strain Analysis,* ***34***(5), pp. 313–322.

[44] Martinez, F., and Ségura, J.-M., 2000. "Effects of non uniform torsion in homogeneous or composite beams". In Proceedings of the Fourteenth International Symposium of Mathematical Theory of Networks and Systems MTNS 2000.

[45] Bishop, R. E. D., Cannon, S. M., and Miao, S., 1989. "On coupled bending and torsional vibration of uniform beams". *Journal of Sound and Vibration,* ***131***(3), pp. 457–464.

[46] Eslimy-Isfanany, S. H. R., Banerjee, J. R., and Sobey, A. J., 1996. "Response of bending-torsion coupled beam to deterministic and random loads". *Journal of Sound and Vibration,* ***195***(2), pp. 267–283.

[47] Banerjee, J. R., Guo, S., and Howson, W. P., 1996. "Exact dynamic stiffness matrix of a bending-torsion coupled beam including warping". *Computers & Structures,* ***59***(4), pp. 613–621.

[48] Banerjee, J. R., 1999. "Explicit frequency equation and mode shapes of a cantilever beam coupled in bending and torsion". *Journal of Sound and Vibration,* ***224***(2), pp. 267–281.

[49] Fichera, G., Lacagnina, M., and Petrone, F., 2004. "Modelling of torsion beam rear suspension by using multi-body method". *Multibody System Dynamics,* ***12***, pp. 303–316.

[50] Wang, K., Inman, D. J., and Farrar, C. R., 2005. "Modeling and analysis of cracked composite cantilever beam vibrating in coupled bending and torsion". *Journal of Sound and Vibration,* ***284***, pp. 23–49.

[51] Klinkel, S., and Govindjee, S., 2003. "Anisotropic bending-torsion coupling for warping in a non-linear beam". *Computational Mechanics,* ***31***, pp. 78–87.

[52] Lanczos, C., 1986. *The Variational Principles of Mechanics*, 4th ed. Dover, New York.

[53] Liu, Y., Pilkey, D., Antes, H., and Rubenchik, V., 1993. "Direct integration of the integral equations of the beam torsion problem". *Computers & Structures,* ***48***(4), pp. 647–652.

[54] Reissner, E., 1956. "Note on torsion with variable twist". *Journal of Applied Mechanics,* ***23***(2), pp. 315–316.

[55] Reissner, E., 1979. "Some considerations on the problem of torsion and flexure of prismatical beams". *International Journal of Solids and Structures,* ***15***, pp. 41–53.

[56] van Erp, G. M., Menken, C. M., and Veldpaus, F. E., 1988. "The non-linear flexural-torsional behaviour of straight slender elastic beams with arbitrary cross sections". *Thin-Walled Structures,* ***6***(5), January, pp. 385–404.

[57] Meirovitch, L., 2003. *Methods of Analytical Dynamics*. Dover, Mineola, New York.

[58] Lahey, T., and Heppler, G., 2005. "Symbolic Derivation of Finite Element Mass and Stiffness Matrices". In Maple Conference 2005 Proceedings, I. S. Kotsireas, ed., Maplesoft, pp. 340–354.

[59] Beltzer, A., 1990. *Variational and Finite Element Methods*. Springer-Verlag.

[60] Portela, A., and Charafi, A., 2002. *Finite Elements Using Maple*. Springer.

[61] Wang, P., Chang, T., and van Hulzen, J., 1984. "Code generation and optimization for finite element analysis". In *EUROSAM '84 International Symposium on Symbolic and Algebraic Computation Proceedings*, J. Fitch, ed., Vol. 174 of *Lecture Notes in Computer Science*. Springer-Verlag, pp. 237–247.

[62] Wang, P., Tan, H., Saleeb, A., and Chang, T., 1986. "Code generation for hybrid mixed mode formulation in finite element analysis". In Proceedings of the 1986 Symposium on Symbolic and Algebraic Computation Symsac '86, B. W. Char, ed., ACM, pp. 45–52.

[63] Wang, P., 1986. "FINGER: a symbolic system for automatic generation of numerical programs in finite element analysis". *Journal of Symbolic Computation,* ***2***, pp. 305–316.

[64] Sharma, N., and Wang, P., 1988. "Symbolic derivation and automatic generation of parallel routines for finite element analysis". In *Proceedings of the Symbolic and Algebraic Computation International Symposium ISSAC '88*, P. Gianni, ed., Vol. 358 of *Lecture Notes in Computer Science*. Springer-Verlag, Rome, Italy, July 4–8, pp. 33–56.

[65] Amberg, G., Tönhardt, R., and Winkler, C., 1999. "Finite element simulations using symbolic computing". *Mathematics and Computers in Simulation*, pp. 257–274.

[66] Bathe, K.-J., and Wilson, E. L., 1976. *Numerical Methods in Finite Element Analysis*. Prentice Hall, Englewood Cliffs, New Jersey.

[67] Heppler, G. R., and Hansen, J. S., 1983. "Time integration of the equations of motion of a structural system including damping". *AIAA Journal,* ***21***(9), September, pp. 1301–1309.

[68] Inman, D. J., 1994. *Engineering Vibration*. Prentice Hall, Englewood Cliffs, New Jersey.

[69] Brach, R. M., 1991. *Mechanical Impact Dynamics: Rigid Body Collisions*. John Wiley and Sons, New York.

[70] Adhikari, S., 2000. "Damping models for structural vibration". PhD thesis, Cambridge University Engineering Department, Trinity College, Cambridge, September.

[71] Adhikari, S., 2006. "Damping modelling using generalized proportional damping". *Journal of Sound and Vibration,* ***293***, pp. 156–170.

[72] Ljung, L., 1999. *System Identification: Theory for the User*. PTR Prentice Hall, Upper Saddle River, New Jersey.

[73] Rorres, C., and Romano, D. G., 1997. "Finding the Center of a Circular Starting Line in an Ancient Greek Stadium". *SIAM Review,* ***39***(4), December, pp. 745–754.

[74] Björck, A., and Hammarling, S., 1983. "A Schur method for the square root of a matrix". *Linear Algebra and its Applications,* ***52-53***, pp. 127–140.

[75] Higham, N. J., 1987. "Computing real square roots of a real matrix". *Linear Algebra and its Applications,* ***88-89***, pp. 405–430.

[76] Davies, P. I., and Higham, N. J., 2003. "A Schur-Parlett algorithm for computing matrix functions". *SIAM Journal on Matrix Analysis and Applications,* ***25***(2), pp. 464–485.

[77] Golub, G. H., and Van Loan, C. F., 1996. *Matrix Computation*, 3rd ed. Johns Hopkins University Press.

[78] Moler, C. B., and Van Loan, C. F., 2003. "Nineteen dubious ways to compute the exponential of a matrix, twenty-five years later". *SIAM Review,* ***45***(1), pp. 1–47.

[79] Vermuelen, A. H., and Heppler, G. R., 1998. "Predicting and avoiding shear locking in beam vibration problems using the b-spline field approximation method". *Computer Methods in Applied Mechanics and Engineering,* ***158***(3–4), June, pp. 311–327.

[80] Bliman, P., and Sorine, M., 1993. "Friction modeling by hysteresis operators. Application to Dahl, stickton, and Stribeck effects". In *Models of Hysteresis*. Longman Scientific and Technical.

[81] Bliman, P., and Sorine, M., 1995. "Easy-to-use realistic dry friction models for automatic control". In Proceedings of the 3rd European Control Conference, pp. 3788–3794.

[82] Bliman, P., and Sorine, M., 1993. "A System-Theoretic Approach of Systems with Hysteresis. Application to Friction Modelling and Compensation". In Proceedings of the 2nd European Control Conference, pp. 1844–1849.

[83] Lahey, T., 2002. "Modelling Hysteresis in the Bending of Fabrics". Master's thesis, Systems Design Engineering, University of Waterloo.

[84] C. Canadas de Wit, Olsson, H., Åström, K. J., and Lischinsky, P., 1995. "A new model for control of systems with friction". *IEE Transactions on Automatic Control,* ***40***(3), pp. 419–425.

[85] C. Canadas de Wit, and Lischinsky, P., 1997. "Adaptive friction compensation with partially known dynamic friction model". *International Journal of Adaptive Control and Signal Processing,* ***11***, pp. 65–80.

[86] Gäfvert, M., 1997. "Comparisons of two dynamic friction models". In Proc. Sixth IEEE Conference on Control Applications (CCA).

[87] Waiboer, R. R., Aarts, R. G. K. M., and Jonker, J. B., 2003. "Closed-loop dynamic simulation of robotic manipulators with joint friction using a perturbation method". In Multibody Dynamics 2003, J. A. Ambrósio, ed.

[88] Sokolnikoff, I. S., and Sokolnikoff, E. S., 1941. *Higher Mathematics for Engineers and Physicists*. McGraw-Hill, New York.

[89] NIST, 2012. *Digital Library of Mathematical Functions*. National Institute of Standards and Technology, March. See http://dlmf.nist.gov/25.2.ii.

[90] Harris, J. W., and Stocker, H., 1998. *Handbook of Mathematics and Computational Science*. Springer, New York.

Nomenclature

A	Cross-sectional area of the beam	11
$\mathbf{A}$	Set of unconstrained quasi-velocities	42
$\mathscr{A}$	Hamilton's action integral	15
a_i	Damping parameters for $\hat{f}$	72
α	Rate of change of angle of twist	9
$\dot{\alpha}$	Angular velocity of the target about the x-axis	20
b_1	Mass damping coefficient for viscous damping	62
b_2	Stiffness damping coefficient for viscous damping	62
$\dot{\beta}$	Angular velocity of the target about the y-axis	20
b_i	Decay coefficents for $\hat{f}$	72
$\mathbf{C}$	System Damping matrix	63
$\mathbf{C}_{ab}$	Rotation matrix from frame B to frame A	21
$\mathbf{C}_{bc}$	Infinitesimal rotation matrix from frame C to frame B	27
CoM	Centre of mass	27
$\mathbf{d}_b$	Displacement matrix (3x1) excluding torsion	24
$\mathbf{d}_t$	Displacement matrix (3x1) due to torsion	24
d_{e1}	Axial offset of the end-effector CoM from the end of the beam	26
d_{e2}	y-offset of the end-effector CoM from the end of the beam	30
d_{e3}	z-offset of the end-effector CoM from the end of the beam	30
$\delta_\Delta(t)$	Dirac delta function	65
Δp_i	Increment in the generalised momentum of coordinate i	41
$\delta \dot{q}_i$	Variation with respect to velocity $\dot{q}_i$	41
δq_i	Variation with respect to q_i	41
δt	Variation with respect to time t	41
$\Delta\theta_i$	Infinitesimal rotation of the frame about axis i	27
$\mathrm{d}m$	Differential mass element of the beam ($\rho \mathrm{d}V$)	18
$\underset{\sim}{d}$	Offset vector of the end-effector CoM from the end of the beam	30
E	Young's modulus	11

$()'$	Derivative with respect to x-coordinate	21
ζ_i	Damping factor for mode j	63
$\dot{z}_t$	Velocity of the target in the z-direction	20